

# Evaluation of the Thermal Conditions and Smoke Obscuration of Live Fire Training Fuel Packages

Jack Regan  
Robin Zevotek

UL Firefighter Safety Research Institute  
Columbia, MD 21045







# Evaluation of the Thermal Conditions and Smoke Obscuration of Live Fire Training Fuel Packages

Jack Regan  
Robin Zevotek

UL Firefighter Safety Research Institute  
Columbia, MD 21045

March 21, 2019



UL Firefighter Safety Research Institute  
*Stephen Kerber, Director*

In no event shall UL be responsible to anyone for whatever use or non-use is made of the information contained in this Report and in no event shall UL, its employees, or its agents incur any obligation or liability for damages including, but not limited to, consequential damage arising out of or in connection with the use or inability to use the information contained in this Report. Information conveyed by this Report applies only to the specimens actually involved in these tests. UL has not established a factory Follow-Up Service Program to determine the conformance of subsequently produced material, nor has any provision been made to apply any registered mark of UL to such material. The issuance of this Report in no way implies Listing, Classification or Recognition by UL and does not authorize the use of UL Listing, Classification or Recognition Marks or other reference to UL on or in connection with the product or system.

# Acknowledgments

The authors would like to thank the UL FSRI staff, particularly Steve Kerber, Craig Weinschenk, Sarah Huffman, Dan Madrzykowski, Keith Stakes, Joseph Willi, Mike Alt, and Josh Crandall, for their help in the planning, execution, and analysis of these experiments. Additionally, Roy McLane of Thermal Fabrication was invaluable with his assistance with the fabrication and installation of instrumentation. Thanks to Kerby Kerber and his staff of the Delaware County Emergency Service Training Center for allowing for the use of his facilities for the experiments and his assistance with the planning and logistics of the experiments. Their generous help ensured that the experiments went safely and smoothly.

The authors would additionally like to thank Kelly Opert and the UL LLC technical support staff for their support in conducting the HRR characterization experiments.

This work was funded through a grant from the Department of Homeland Security's Assistance to Firefighters Grant Program under the Fire Prevention & Safety Research & Development Grant EMW-2014-FP-00471-001. Without this critical funding and support, this vital fire service research would not be possible.



To assist the design and implementation of the experiments for the Training Fires study, fire service experts from across the world with knowledge in firefighter training, specifically in the areas of live fire evolutions, were brought together. The individuals below provided direction for the project, assisted in planning the experiments, witnessed the testing, and developed concrete conclusions. Their tireless support and effort make this project relevant to the fire service across the world.

#### Fire Service Technical Panel

---

Name	Affiliation
Derek Alkonis	County of Los Angeles Fire Department
Brian Arnold	Oklahoma City Fire Department
Charles Bailey	Montgomery County (MD) Fire & Rescue Services
John Ceriello	Fire Department of New York
Sean DeCrane	Cleveland Fire Department
James Dominick	Northeastern Illinois Public Safety Training Academy
Steve Edwards	Maryland Fire and Rescue Institute
Kenny Fent	National Institute for Occupational Safety and Health
Michael Gagliano	Seattle Fire Department
Sean Gray	Cobb County Fire Department
Bobby Halton	Fire Engineering Magazine
Todd Harms	Phoenix Fire Department
Ed Hartin	Central Whidbey Island Fire & Rescue
George Healy	Fire Department of New York
Gavin Horn	University of Illinois Fire Service Institute
David Rhodes	Atlanta Fire Department
Allan Rice	Alabama Fire College; North American Fire Training Directors
Ken Richards	Old Mystic Fire Department; NFPA 1403
Erich Roden	Milwaukee Fire Department
Tim Sendelbach	Firehouse Magazine (ret.)
Dan Shaw	Fairfax County Fire Rescue/NFPA 1403
Denise Smith	Skidmore College
Jens Stiegel	Frankfurt am Main Fire & Rescue Services
Stefan Svensson	Lund University, Department of Fire Safety Engineering
Adam Thiel	Philadelphia Fire Department
Peter Van Dorpe	Algonquin-Lake In the Hills Fire Department
Devon Wells	International Society of Fire Service Instructors

---

# Contents

<b>Contents</b>	<b>iv</b>
<b>List of Figures</b>	<b>vii</b>
<b>List of Tables</b>	<b>x</b>
<b>List of Acronyms</b>	<b>xi</b>
<b>1 Background</b>	<b>2</b>
<b>2 Introduction</b>	<b>3</b>
2.1 Scope . . . . .	4
<b>3 Literature Review</b>	<b>5</b>
3.1 Standards . . . . .	5
3.2 Line of Duty Deaths and Injuries . . . . .	6
3.3 Previous Research . . . . .	8
<b>4 Fuel Load Characterization Experiments</b>	<b>14</b>
4.1 Free Burn HRR Experiments . . . . .	14
4.1.1 Methodology . . . . .	14
4.1.2 Fuel Packages Contents and Arrangement . . . . .	15
4.1.3 Results . . . . .	23
4.1.4 Discussion . . . . .	25
4.1.5 Training Fuel Packages vs. Furnishings . . . . .	44
4.1.6 Free Burn HRR Limitations . . . . .	49
4.2 Compartment HRR Experiments . . . . .	50
4.2.1 Results . . . . .	51
4.2.2 Discussion . . . . .	53
4.2.3 Compartment HRR Limitations . . . . .	55
<b>5 Training Prop Experiments</b>	<b>57</b>
5.1 Methodology . . . . .	57
5.2 Structure . . . . .	57
5.3 Instrumentation & Measurement Uncertainty . . . . .	59
5.4 Training Prop Experiment Description . . . . .	62
5.5 Results . . . . .	67

5.6	Discussion . . . . .	70
5.6.1	Effect of Geometry & Quantity . . . . .	70
5.6.2	Effect of Additional Pallets . . . . .	74
5.6.3	Comparison of Engineered Lumber to Dimensional Lumber . . . . .	80
5.6.4	Use of Smoke Barrels . . . . .	82
5.6.5	Use of Synthetic Materials in Training Fuel Packages . . . . .	86
5.6.6	Hay vs. Straw . . . . .	90
5.6.7	Fuel Outside the Fire Room . . . . .	91
5.6.8	Pallets in Place of Other Wood Fuels . . . . .	96
5.6.9	Flashover in Training Fuel Loads . . . . .	100
5.7	Training Prop Experiment Limitations . . . . .	103
<b>6</b>	<b>Training Considerations</b>	<b>104</b>
6.1	Fuel Package Design Can Take Advantage of <i>NFPA 1403</i> Compliant Fuels . . . . .	104
6.2	Training Fuel Packages Do Not Need To Be Tended During Evolutions . . . . .	106
6.3	Obscuration Can Be Increased Without Using Synthetic Fuels . . . . .	107
6.4	When using NFPA 1403 compliant wood-based fuels, orientation and quantity are important for predicting fire size . . . . .	112
6.5	Select the Fuel Package for the Intended Lesson . . . . .	115
6.6	Wood-based training fuels can create hazardous conditions without transitioning to flashover . . . . .	123
<b>7</b>	<b>Future Research Needs</b>	<b>127</b>
<b>8</b>	<b>Summary</b>	<b>128</b>
	<b>References</b>	<b>129</b>
	<b>Appendices</b>	<b>133</b>
<b>A</b>	<b>Free Burn Heat Release Rate Results</b>	<b>134</b>
A.1	Training Fuel Packages . . . . .	134
A.2	Comparison Fuel Packages . . . . .	142
A.3	Comparison Room Burns . . . . .	147
<b>B</b>	<b>Container Burn Results</b>	<b>148</b>
B.1	Experiment 1 Results . . . . .	148
B.2	Experiment 2 Results . . . . .	150
B.3	Experiment 3 Results . . . . .	151
B.4	Experiment 4 Results . . . . .	153
B.5	Experiment 5 Results . . . . .	154
B.6	Experiment 6 Results . . . . .	156
B.7	Experiment 7 Results . . . . .	157
B.8	Experiment 8 Results . . . . .	159
B.9	Experiment 9 Results . . . . .	160
B.10	Experiment 10 Results . . . . .	161

B.11	Experiment 11 Results	162
B.12	Experiment 12 Results	164
B.13	Experiment 13 Results	165
B.14	Experiment 14 Results	167
B.15	Experiment 15 Results	168
B.16	Experiment 16 Results	170
B.17	Experiment 17 Results	171
B.18	Experiment 18 Results	172
B.19	Experiment 19 Results	173
B.20	Experiment 20 Results	174
B.21	Experiment 21 Results	176
B.22	Experiment 22 Results	177
B.23	Experiment 23 Results	178
B.24	Experiment 24 Results	180
B.25	Experiment 25 Results	181

# List of Figures

3.1	Utech’s Thermal Exposure Conditions . . . . .	11
3.2	Modern PPE Performance Comparison with Utech Thermal Classes . . . . .	13
4.1	Fuel Racks for Training Fuel HRR Characterization . . . . .	16
4.2	Images of Pallets, Excelsior, and Straw Used for HRR Experiments . . . . .	16
4.3	Representative Images of Training Fuel Loads . . . . .	17
4.4	Images of Comparison Fuel Packages . . . . .	23
4.5	Average HRR (kW) versus Average MLR (kg/s) Over the Peak Burning Period . . . . .	27
4.6	Total Energy (MJ) vs. Total Mass Burned (kg) . . . . .	28
4.7	Peak HRR (MW vs. Initial Fuel Mass (kg) . . . . .	29
4.8	Images of Straw and Excelsior Fuel Packages . . . . .	30
4.9	HRR vs. Time for Straw and Excelsior Fuel Packages . . . . .	30
4.10	Images of Peak HRR for Straw and Excelsior Fuels . . . . .	31
4.11	3 Pallet Triangle Replicate Fuel Loads . . . . .	32
4.12	Images of Lean-to Fuel Packages . . . . .	33
4.13	Effect of Pallet Count on HRR . . . . .	34
4.14	Images of Peak HRR for Lean-to Pallet Fuel Packages . . . . .	35
4.15	HRR (kW) vs. Time for 3 Pallet Configurations . . . . .	36
4.16	Images of Peak HRR for 3 Pallet fuel packages . . . . .	36
4.17	Innovative Fuel Rack . . . . .	37
4.18	HRR (kW) vs. Time for 3 Pallet Configurations . . . . .	38
4.19	6 Pallet Fuel Packages . . . . .	39
4.20	HRR (kW) vs. Time for Straw and Excelsior Tests . . . . .	40
4.21	Images of Peak HRR for 6 Pallet Fuels . . . . .	41
4.22	OSB, MDF, and 1 in. x 6 in. Dimensional Lumber Fuel Packages . . . . .	42
4.23	Comparison of HRR for OSB, MDF, and 1 in. x 6 in. Dimensional Lumber . . . . .	43
4.24	Images of Two Sofas . . . . .	44
4.25	Peak HRR - Sofa and Comparable Training Fuel Packages . . . . .	45
4.26	Images of Peak HRR for Upholstered Sofas and Wood-Based Training Fuels of Comparable Magnitude . . . . .	46
4.27	Peak HRR - Chairs and Comparable Training Fuel Packages . . . . .	47
4.28	Peak HRR - Beds and Comparable Training Fuel Packages . . . . .	48
4.29	Average HRR (kW) vs. Average MLR (kg/s) Over the Peak Burning Period . . . . .	49
4.30	Training Fuel Load Position for Compartment HRR Experiments . . . . .	50
4.31	HRR for Compartment Burn Experiments . . . . .	51
4.32	Total Energy for Compartment Burn Experiments . . . . .	52



4.33	Comparison of Free Burn vs. Compartment HRR for Training Fuel Loads . . . . .	54
4.34	Compartment HRR Experiment Comparison . . . . .	55
5.1	Metal Prop exterior . . . . .	58
5.2	Metal Prop Instrumentation . . . . .	59
5.3	3 Pallet Experiment Orientations . . . . .	70
5.4	Comparison of 3 Pallet Container Experiments . . . . .	71
5.5	Smoke Opacity for Horizontal and Vertical Pallet Configurations . . . . .	73
5.6	Minimum Obscuration for Experiment 10 . . . . .	74
5.7	3 and 6 pallet Fuel Packages . . . . .	75
5.8	HGL Temperature and Hall Heat Flux for 6 Pallet Orientations . . . . .	76
5.9	Comparison of Hallway Thermal Conditions With 3 and 6 Vertically Stacked Pallets . . . . .	78
5.10	Smoke Opacity for 3 and 6 Pallet Lean-to Fuel Loads . . . . .	79
5.11	Heat Flux for Alternative Wood Fuels . . . . .	80
5.12	Hallway Temperatures for Alternative Wood Fuels . . . . .	81
5.13	Burning in Hallway for Experiment 19 . . . . .	81
5.14	Smoke Opacity for OSB, MDF, and Dimensional Lumber Fuel Packages . . . . .	82
5.15	Smoke Barrel Contents . . . . .	83
5.16	Fire dynamics of 3 Pallet triangle With and Without Smoke Barrels . . . . .	83
5.17	Smoke Opacity for Smoke Barrel Experiment Without Increased Airflow . . . . .	84
5.18	Smoke Opacity for Smoke Barrel Experiments With Increased Airflow . . . . .	85
5.19	Smoke Opacity Comparison for Smoke Barrel Experiments . . . . .	86
5.20	3 Pallet Fuel Packages with Synthetic Additions . . . . .	87
5.21	Comparison of Heat Flux With Addition of Synthetic Fuels . . . . .	88
5.22	Hallway HGL Temperatures With Addition of Synthetic Fuels . . . . .	88
5.23	Smoke Opacity for Pallets and Straw with Tar Paper and Sofa Cushion . . . . .	89
5.24	Visibility Conditions in Hallway for Furnished Room Experiment . . . . .	90
5.25	Hallway HGL Temperatures and Heat Flux for Pallets and Straw/Hay . . . . .	91
5.26	OSB on Hallway Ceiling for Experiment 3 . . . . .	92
5.27	Heat Flux for OSB Fuel Package With and Without OSB On the Hallway Ceiling . . . . .	93
5.28	OSB on Hallway Walls for Experiment 4 . . . . .	94
5.29	Hallway Thermal Conditions - Addition of OSB to Hallway Wall and Floor . . . . .	95
5.30	OSB on Hallway Walls for Experiment 4 . . . . .	96
5.31	Pallets on Wall vs. OSB on Wall . . . . .	97
5.32	Hallway Thermal Conditions - OSB and Pallets on Wall . . . . .	98
5.33	Image of Pallets on Floor . . . . .	99
5.34	Hallway Thermal Conditions - Addition of OSB to Hallway Wall and Ceiling . . . . .	100
5.35	Fire Room Temperatures for Fuel Packages at Flashover Threshold . . . . .	102
6.1	Common Training Fuel Packages . . . . .	104
6.2	Orientation & Heat Release Rate . . . . .	105
6.3	Hallway Heat Flux for Large Wood Fuel Packages . . . . .	107
6.4	Effect of Synthetic MAterials on Fire Dynamics in Training Prop . . . . .	108
6.5	Horizontal vs. Vertical Pallet Timing . . . . .	113
6.6	Total Energy Exposure vs. Fuel Weight for End Hall Heat Flux Gauge . . . . .	114

6.7	Examples of Candle Demonstrations . . . . .	115
6.8	Examples of Scaled House Demonstrations . . . . .	116
6.9	Comparisons of Structure Volume vs Energy Needed to Consume Oxygen . . . . .	117
6.10	Example Evaluation of Fuel and Compartment Size . . . . .	118
6.11	Effect of igniting primary fuel package on obscuration from smoke barrels. . . . .	119
6.12	Effect of Additional Fuel on Hallway Heat Flux . . . . .	121
6.13	Hallway Camera View with and without OSB on ceiling . . . . .	122
6.14	Effect of Additional OSB in Hall . . . . .	122
6.15	Fire Room Flashover Criteria - Training Fuels . . . . .	124
6.16	Floor Plan of L Shape Training Prop Used . . . . .	125
6.17	Modern PPE Performance Comparison with Exposure at End of Hall . . . . .	126

# List of Tables

3.1	NIST Thermal Classes . . . . .	10
4.1	Training Fuel Package Descriptions for HRR Characterization . . . . .	18
4.2	Comparison Fuel Package Descriptions for HRR Characterization . . . . .	22
4.3	Training Fuel Package HRR Characterization Results . . . . .	24
4.4	Comparison Fuel Package HRR Characterization Results . . . . .	25
4.5	Effective Heat of Combustion Results . . . . .	26
4.6	Three Pallet Triangle Replicate Experiments Results . . . . .	32
4.7	Lean-to Fuel Package Experiments Results . . . . .	34
4.8	Fuel Loads Used with Pallets and Straw or Excelsior . . . . .	35
4.9	Fuel Loads Used with three pallet Configuration . . . . .	37
4.10	Furnished Room Contents . . . . .	51
4.11	Peak HRR and Total Energy Released for HRR Characterization Experiments . . . . .	52
5.1	Fuel Package Descriptions with Door Open at Ignition . . . . .	63
5.2	Fuel Package Descriptions with Door Open at 6 Minutes . . . . .	65
5.3	Fuel Package Descriptions with Door Closed, Window Open at 6 Minutes . . . . .	66
5.4	Container Experiments Results Summary . . . . .	68
5.5	Extra Pallet Comparison Tests . . . . .	75
5.6	Peak Thermal Conditions for Experiments 7, 8, and 24 . . . . .	77
5.7	Peak Thermal Conditions for Experiments 1, 2, and 21 . . . . .	89
5.8	Free Burn HRR and Compartment Thermal Conditions . . . . .	101
6.1	Peak Obscuration for Non-NFPA 1403 Compliant Fuel Packages . . . . .	110

# List of Acronyms

AFG	Assistance to Firefighters Grant program
DHS	U.S Department of Homeland Security
FEMA	Federal Emergency Management Agency
HRR	Heat release rate
MDF	Medium density fiberboard
MLR	Mass loss rate
NFPA	National Fire Protection Association
OSB	Oriented strand board
HGL	Hot gas layer
UL FSRI	Underwriters Laboratories Firefighter Safety Research Institute
IECC	International Energy Conservation Code

# Abstract

Firefighters routinely conduct live fire training in an effort to prepare themselves for the challenges of the fire ground. While conducting realistic live fire training is important, it also carries inherent risks. This is highlighted by several live fire training incidents in which an inappropriate fuel load contributed to the death of participants. *NFPA 1403: Standard on Live Fire Training Evolutions* was first established in response to a live fire training incident in which several firefighters died. Among the stipulations in *NFPA 1403* is that the fuel load shall be composed of wood-based fuels. The challenge of balancing safety with fidelity [1] has led instructors to explore a variety of different methods to create more realistic training conditions. A series of experiments was conducted in order to characterize common training fuels, compare these training fuels to furnishings, and examine the performance of these training fuels in a metal container prop. Heat release rate (HRR) characterization of training fuels indicated that wood-based training fuels had a constant effective heat of combustion ( $\Delta h_{c,eff}$ ). Depending on the method used, this value was between 13.6 and 13.9 MJ/kg. This indicates that, even in engineered wood products, wood is the primary material responsible for combustion. In order to further explore the conclusions from the HRR testing, additional experiments were conducted in an L-shaped metal training prop. The results of these experiments highlighted a number of considerations for firefighter training. Thermal conditions consistent with “realistic fires” could be produced using NFPA 1403 compliant fuels, and in fact the thermal conditions produced by larger wood-based fuel packages were more severe than those produced by fuel packages with a small amount of synthetic fuel. The fuel package used in training evolutions should reflect the training prop or building being used, the available ventilation, and the intended lesson. Fuel load weight and orientation are both important considerations when designing a fuel package. The training considerations drawn from this report will help to increase firefighters’ understanding of fire dynamics, and help instructors better understand fuel packages and the fire dynamics that they produce.

# 1 Background

A shift in the makeup of home furnishings and building construction techniques has resulted in residential fires characterized by a potential for rapid fire spread [2]. Due to the fact that residential structures contain products that support rapid fire growth, there is an increased likelihood that the fire may be underventilated by the time the fire department arrives. Several line-of-duty deaths and injuries [3–7] have highlighted the hazards associated with these fires, and have emphasized the importance of firefighters having a good understanding of fire dynamics. An important part of developing this understanding is useful, realistic live fire training.

Despite the emphasis on fire dynamics understanding, a gap has been identified between the fire dynamics observed on fire incidents and the fire dynamics observed in the live fire training environment. A key component of the fire dynamics observed in live fire training is the fuel package, which is often blamed for this gap. In order to quantify this gap, research is needed to develop data to characterize common fire training fuels and compare them to the furniture found in today's residential occupancies.

It is important to characterize these fuel packages both in a laboratory setting and in practical training situations, to quantify the fire dynamics to which students and instructors may be exposed. This project addresses these needs by evaluating the ability of different fuel packages and “innovative” methods for fuel arrangement, combined with fuel quantity, to produce the fire dynamics consistent with those observed in residential structure fires.

## 2 Introduction

Firefighter training commonly includes participation in live fire training evolutions in preparation for the real-world fire ground and situations that the firefighter will face in the field. Fire department instructors attempt to create training fires with fire behavior and visual effects similar to fires in residential structures while knowing that both the training structure and fuel packages often limit their ability to do so. Some instructors have explored innovative methods and training fuel packages in an effort to create training evolutions that are more representative of a ventilation limited house fire. These methods can come in the form of modifications to the available training structure in addition to utilizing non-traditional and sometimes prohibited fuel loads. For example, some training instructors incorporate synthetic materials such as tar paper or polyurethane foam into the fuel package in order to accelerate fire growth and create more realistic smoke conditions. These fuel loads are not permitted for live fire training by the *National Fire Protection Association (NFPA) 1403* [8] training standard; however, could be useful as a demonstration with students located outside of the structure. These examples, in addition to many others, have been developed and adjusted based on trial and error by fire training instructors. The goal of this series of experiments is to collect innovative ideas that are being used and characterize the fire dynamics of each fuel package. Any use of materials utilized in this study that are not permitted by NFPA 1403 should be considered a demonstration and not a live fire training exercise. These demonstrations can be used to show flashover, flow paths, other fire dynamics principles, without placing a student or instructor in the prop.

This report is part of a larger project looking at the safety, fidelity, and exposure of training fires with the goal of quantifying the fire dynamics of three common types of live fire training structures. The three other parts of this study are listed below.

- Acquired Structures Training Experiments.
- Concrete Training Building Experiments [9].
- Metal Container Prop Experiments [10].

The acquired structure training fire experiments provided a comparison of training fuels to home furnishings experiments from previous research in fire service ventilation (horizontal, vertical, and positive pressure). The acquired structure training experiments utilized common training fuels within a structure similar in construction and configuration to the one-story ranch structure used in previous studies [11–13]. The concrete training building experiments studied the conditions within a concrete live fire training building, utilizing both common training fuel packages and a fuel package composed of furniture items with synthetic elements. Different ventilation configurations were studied to determine their effect on the fire environment as well as answer critical questions such as whether or not a ventilation-limited state can be reached by training fuel loads within a concrete training building. The metal container prop experiments studied the fire dynamics in

training props assembled from metal shipping containers. The experiments focused on the effects of wall lining materials, such as metal, insulated metal, and gypsum board and fiberglass insulation, along with a comparison of training fuels to furnishings with different ventilation configurations.

This report quantifies the fire dynamics and fidelity of common training fuels as well as innovative fuel packages and compares them to the fire dynamics produced by modern furnishings both in free burn and within a compartment. The free burn cases were conducted under an oxygen consumption calorimeter to compare heat release rate (HRR) and total energy released. The compartment burns were conducted in a metal container prop configured as a long hallway with a burn room at the far end. The results were analyzed to provide fire service instructors with a quantitative comparison of potential fuel loads for live fire training, along with considerations for improving the fire dynamics learning experience during live fire training and fire dynamics demonstrations. In order to design effective training evolutions, instructors should use these research results to complement personal experience from both the training ground and the fire ground. Although this report covers a significant number of fuel loads to provide clarification to the efficacy of different fuels used in the fire training environment, future research is still needed to identify and analyze the effectiveness of additional training methods, both those used as interactive as well as demonstrative.

## **2.1 Scope**

While the other reports in this project have focused on the fire dynamics produced in a particular type of fire service training prop, this report is intended to compare and contrast the fire dynamics produced by different training fuel packages in both a free burn environment, independent of compartment effects and in a training prop with a simple configuration. Thus, it is important to recognize that different structure types, lining materials, and ventilation configurations may all cause the fire dynamics of a particular fuel package to differ from those reported in these experiments.



# 3 Literature Review

## 3.1 Standards

*NFPA 1403: Standard on Live Fire Training Evolutions* outlines the minimum requirements for conducting live fire training in acquired and fixed facility training structures [8]. The document discusses the responsibilities of the instructors, safety officers, and participants, and also provides guidelines for the types of fuels that can be included in the fuel package. The standard defines acceptable fuels as “pine excelsior, wooden pallets, straw, hay, and other wood-based products” [8]. The standard specifically forbids treated wood products, rubber, plastic, polyurethane foam, upholstered furniture, and chemically treated straw as fuels. *NFPA 1403* additionally makes several specific recommendations for acquired structure training burns. The standard recommends against the use of low-density particleboard and unidentified materials found within the structure. Furthermore, the document mandates that combustible materials not included in the fuel load should be moved to an area of the structure remote from the fire room.

There have been several instances where firefighters have been killed or injured during live fire evolutions where the procedures and precautions of *NFPA 1403* were not followed. The National Institute of Occupational Safety and Health (NIOSH) investigated several of these incidents, which are described below. These incidents have resulted in a series of revisions to *NFPA 1403* since its initial release in 1986. The 2018 Edition of *NFPA 1403* lists a series of prerequisites that students must have prior to participating in live fire training. Among these prerequisites are training on the proper use of personal protective equipment (PPE), ventilation, and fire behavior. Specifically, students should have a proper understanding of fire dynamics, including heat transfer, basic chemistry, and compartment fire behavior; the components, capabilities, and limitations of their PPE; and nozzle techniques and door control.

*NFPA 1403* additionally provides guidelines for selecting an appropriate fuel load, and cautions that an excessive fuel load can result in a ventilation-controlled fire. Ventilation-controlled fires present a hazard because additional ventilation results in fire growth or flashover. It is important that firefighters understand the concept of ventilation-controlled fires, since many residential structure fires are ventilation-controlled. Prior to the 2018 version of *NFPA 1403*, the standard did not address ventilation in any substantive way. The 2018 version, however, includes a methodology for conducting controlled, ventilation-limited training fires. These scenarios are intended to teach fire behavior rather than firefighting skills such as line advancement or search and rescue. The document stipulates that students and instructors should be positioned in a “safe observation space,” outside of the fire room, at the same level or below the fire room, and removed from the exhaust portion of the flow path. The observation space must have a charged hose line capable of suppressing the fire and an unimpeded path of egress. When done safely and correctly, a demonstration of a ventilation-controlled fire behavior can be a useful tool for teaching fire behavior, which is one of job performance requirements identified in *NFPA 1001: Standard for Fire Fighter Professional*

*Qualifications* [14].

## 3.2 Line of Duty Deaths and Injuries

*NFPA 1403* was established in response to a 1982 incident in Colorado, in which two firefighters died and two more were injured during a training evolution in an abandoned storage shed. The building was an approximately 28 ft x 61 ft wood-framed building with a sloped roof and interior ceilings composed of low-density fiberboard. The building had originally been built as a chicken coop, but had also been used for automobile storage, and at the time of the incident had temporary dividers on the interior. The fuel load for the training evolution included crankcase oil, tires, and tar paper. Fuel packages were placed in each of the four rooms of the structure. Two scenarios were conducted in the structure, with the first scenario intended to be a smoke training drill where the students were instructed to find specific objects within the building. Following this drill, the training supervisor added more tires to each of the fuel loads, and the firefighters re-entered the building with a 30 GPM booster line. Conditions started to deteriorate rapidly as the combustible ceiling material began to burn. The training supervisor and two of the students were able to exit the building, while the other two students became disoriented and were unable to exit the building. An after action report identified several contributing factors to the incident, which included an inappropriate fuel load, the lack of an adequate water supply, the lack of an adequately sized hoseline, and the lack of additional manpower to staff a backup hoseline or a RIT team [15].

NIOSH led an investigation of a 2005 incident in Pennsylvania that resulted in the death of a 47-year-old fire instructor and attracted further studies into the hazards of the training fire environment. The instructor experienced a catastrophic failure of his facepiece lens during a live fire “train the trainer” course and died of thermal injuries two days after the event. The burn building was a two and a half story concrete block structure. Investigators attributed the facepiece failure to the high thermal conditions that were present in the basement during the evolution. The investigation emphasized the importance of using the minimum amount of fuel necessary to perform live fire training to maintain firefighter safety. Additionally, this incident demonstrated the dangers of repeated evolutions without allowing sufficient time between evolutions for the burn building and the instructor’s PPE to cool down [16].

In a 2007 incident, a probationary firefighter was killed during a training evolution in a vacant end-of-the-row townhouse in Maryland. The scenario used approximately 12 wooden pallets and 11 bales of excelsior as fuel, and featured fire sets on all three floors of the townhouse. Additionally, mattresses, tires, and other debris was not removed from the first floor of the townhouse, and contributed to the fuel load. The victim was on the nozzle of the first hoseline and was instructed to bypass the fires on the first and second floors and make an attack on the third floor fire. When the attack team reached the stairway between the second and third floors, they were overcome by high heat conditions. Two of the participants exited the structure through a window. The victim reached the window, but was unable to get the lower half of her body out of the window. While the instructor was trying to remove her from the fire room through the window, her mask became dislodged. She was finally removed when another instructor came up the stairs and helped her legs

through the window. The victim succumbed to thermal injuries and asphyxia. NIOSH attributed the outcome of the incident to several factors, including a lack of equipment, a lack of physical fitness performance requirements, and a failure to follow the requirements of *NFPA 1403* [17].

Two career firefighters were killed during a training fire in an acquired structure in Florida. The structure was a one story, single family house with three bedrooms, two bathrooms, and a kitchen. The fire was ignited in one of the bedrooms and had a fuel load of wooden pallets, straw, and a urethane foam mattress. Before ignition, other materials in the room, such as urethane foam padding, hollow core wood doors, and carpeting were not removed, and thus contributed to the fuel load. Four firefighters acted as interior safety officers throughout the duration of the incident. The victims entered the structure first and performed a primary search of the building. They were followed by the attack line. The victims passed the safety/ignition officer positioned outside of the fire room, who retreated to the living room to help the attack company while the victims proceeded to search the fire room. Before applying water, the fire room window was vented and dark, heavy smoke exited the window. The attack company began to apply water in short bursts, and one of the safety officers exited the structure, thinking that he had been “steamed.” The victims remained unaccounted for for several minutes. During this time, it is suspected that the fire room had transitioned to flashover. After the victims failed to acknowledge repeated attempts by the Incident Commander (IC) to contact them, the IC activated the rapid intervention team (RIT), who found the victims in the fire room. They were transported to a local hospital and pronounced dead. The investigation identified the fuel load and uncoordinated ventilation as contributing factors, noting that the use of fuel with unknown burning characteristics can lead to unexpected fire development and rapid fire progression [18].

In another line of duty death incident, a New York volunteer firefighter was killed during a simulated “mayday” scenario, where he and another firefighter were acting as the simulated victims. The victim had very little training prior to the incident, and had never worn a self-contained breathing apparatus (SCBA) under live fire conditions before. The training was conducted in a vacant two story duplex. The scenario called for two firefighters trapped in an upstairs bedroom in one half of the duplex, and involved the engine and rescue company making entry through the other half of the duplex, breaching a wall, and rescuing the downed firefighters. The intended fuel source was a burn barrel in one of the bedrooms, but an assistant chief ignited a foam mattress when the ignition firefighter had trouble igniting the burn barrels. The ignition of the mattress led to rapid fire growth and caused conditions throughout the duplex to deteriorate. The ignition firefighter attempted to help the two trapped firefighters, but in the process of doing so lost his gloves, received burns to his hands, and was forced to exit out of a second story window. When the engine and rescue companies arrived on scene, they both acted as RIT teams, and removed the trapped firefighters from the structure. One victim was transported to a local hospital where he was pronounced dead. The other firefighter that was removed from the structure and the ignition firefighter that jumped from the second floor were flown to a regional burn center. The investigation highlighted the importance of not using live victims during live fire training and ensuring that the fuels used in training burns are in accordance with *NFPA 1403* [19].

### 3.3 Previous Research

One common factor among the LODD incidents described in the previous section is the use of improper fuels or fuel loads. In several of the acquired structure burns, the addition of debris or fuels found around the house had the effect of increasing the fire size beyond what was manageable or expected. In an effort to better understand the training fuels that firefighters use, a series of research studies have aimed to quantify parts of the training fire environment.

Madrzykowski [20] investigated a pair of training fires in which firefighters had been killed. The first incident occurred during the previously mentioned incident in Florida, where two firefighters died while conducting a search when the fire room transitioned to flashover [18]. The National Institute of Standards and Technology (NIST) recreated the fire room and two adjacent spaces, and evaluated the thermal conditions produced by five different combinations of fuel load and ventilation conditions. The results indicated that flashover conditions were reached for each fuel load, including the experiment where only pallets, straw, wood molding, and a hollow core door were used. Furthermore, the temperatures exceeded 500°F (260°C), and the heat fluxes exceeded 20 kW/m<sup>2</sup> during each test, indicating that the thermal conditions in the fire room were unsurvivable for even a firefighter in full PPE. An additional experiment examined the peak HRR of the pallets and straw, which was found to be 2.8 MW [20]. The author compared this HRR to the theoretical HRR required for flashover in the room and found that the HRR was sufficient to cause flashover.

The second incident that was investigated was the one which occurred in Pennsylvania during a “train the trainer” class conducted in a concrete live fire training building. After the last burn of the day, an instructor was found lying face-down on the floor in the basement with damage to his facepiece. He later succumbed to his injuries. NIST instrumented the burn building where the incident occurred and attempted to recreate the thermal conditions that were present at the time of the instructor’s death. They first used a fuel load of pallets and excelsior to “pre-heat” the burn structure. Then, additional pallets and straw were added. When the fires peaked, the fire was suppressed with a hose stream and the compartment was hydraulically ventilated. Once the compartment was cleared, additional pallets were added to the embers, and the process was repeated. The ambient heat flux at 4.9 ft (1.5 m) from the ceiling before the last evolution was 6 kW/m<sup>2</sup>, and the ambient temperature in the burn structure was 302°F (150°C) at 5.02 ft (1.53 m) below the ceilings. The instructor was in the process of adding two additional pallets to the fire burning in the basement fire room and was overcome by hot gases from the existing fire, which resulted in the catastrophic failure of his SCBA facepiece. Based on the charring of some of the neoprene components of the facepiece, it was concluded that it was possibly exposed to temperatures of at least 647°F (342°C), well above the glass transition temperature and melting temperature of the high temperature polycarbonate facepiece [16]. The recreation of the fire conditions in the training building showed peak temperatures in excess of 932°F (500°C) and peak heat flux values in excess of 20 kW/m<sup>2</sup> at 5.00 ft (1.50 m) above the floor [20]. Laboratory experiments indicated that a fuel load consisting of six pallets and straw had a peak HRR of 4.5 MW.

In both fatal training fire incidents, the thermal conditions that resulted from the fuel loads ex-

ceeded the protective capabilities of the firefighters' PPE. This highlights the necessity of using discretion when determining the fuel load of training fires.

Willi et al [21] conducted a series of experiments to quantify the thermal exposure of firefighters in a concrete live fire training building. The authors constructed a portable data acquisition system capable of gathering heat flux and temperature data from a firefighter's immediate environment during live fire training exercises. The tests examined two types of firefighter training evolutions: scenarios conducted in concrete live fire training buildings, that used wooden pallets and straw as the fuel load and scenarios conducted in a metal container-based training prop known as a "flashover simulator", that had a fuel load consisting of pallets, straw, OSB, and medium density particleboard. The results indicated that routine training evolutions exhibited heat fluxes on the order of  $1 \text{ kW/m}^2$  and temperatures close to  $122^\circ\text{F}$  ( $50^\circ\text{C}$ ), whereas more severe exposures showed heat fluxes between  $3 \text{ kW/m}^2$  and  $6 \text{ kW/m}^2$  and temperatures between  $302^\circ\text{F}$  ( $150^\circ\text{C}$ ) and  $392^\circ\text{F}$  ( $200^\circ\text{C}$ ). Furthermore, the experiments showed that in some instances, the temperature data underpredicted the thermal hazard posed by the heat flux based on the NIST Thermal Classes, which are a method of classifying the thermal environment based on the performance of electronic equipment carried by first responders. The authors also noted that stationary temperatures located in training buildings underpredicted the overall thermal hazard encountered by the firefighters working in those buildings.

René Rossi [22] conducted a series of experiments in several types of firefighter training buildings in Switzerland to examine the effect of different thermal exposures on core temperature and sweat production. Heat flux and temperature measurements were also taken in the training buildings. Rather severe peak thermal conditions were observed during the tests, noting temperatures as high as  $532^\circ\text{F}$  ( $278^\circ\text{C}$ ) and heat fluxes as high as  $26 \text{ kW/m}^2$ . The more routine exposures contained temperatures between  $122^\circ\text{F}$  ( $50^\circ\text{C}$ ) and  $266^\circ\text{F}$  ( $130^\circ\text{C}$ ) and heat fluxes between and  $5 \text{ kW/m}^2$  and  $10 \text{ kW/m}^2$ . The results indicated that relatively high heat fluxes were observed for rather moderate temperatures.

While a number of studies have examined the thermal hazards that firefighter students and instructors are exposed to in the training fire environment, there is a gap in the literature regarding the fidelity of these training fires, that is, the degree of exactness that the training fires adhere to a fire that may be encountered on the fireground. Additionally, little research has focused on new training fuels, such as OSB, particleboard, and other engineered wood products, that some training academies and organizations have begun to incorporate into live fire training. This study will attempt to bridge the gap in understanding between training fuels and fuels that are representative of those found in residential structures. Additionally, this study will examine the relative thermal hazards and severity of conditions that may be developed when burning these fuels in the training environment.

Safety is a critical concern for live fire training scenarios. It is imperative that safety is not compromised in the pursuit of creating fire dynamics consistent with a ventilation-controlled residential fire. This means focusing on the minimization of training-related injuries and deaths from excessive thermal exposure. Additionally, thermal conditions in which equipment, such as facepieces, helmets, and electronic equipment, may be damaged are undesirable, as the replacement of such

equipment can unnecessarily burden a fire department.

Training fires are different from typical fires to which respond fire departments in that firefighters involved in suppression and search and rescue operations are not the only personnel inside the burn structure. Rather, support personnel such as instructors and stokers are actively involved in the training scenarios as well. Stokers are firefighters whose specific task is the construction and maintenance of fuel packages throughout the duration of the training evolution. In contrast to a residential fire, where the suppression team would likely mitigate conditions with a hoseline before entering areas with the most severe thermal conditions, these instructors and stokers are often tasked with maintaining the fire, and may be positioned in or close to the fire room, possibly for extended periods of time. Thus, the threat that thermal conditions in these areas pose to firefighters must be considered. Additionally, it is important for recruits to understand that although some areas are relatively safe for habitation in the training environment, the same areas in actual emergency incidents may quickly result in death or serious injury.

A variety of methods exist for evaluating the thermal conditions to which firefighters are exposed. In general, some methods divide the thermal environment into three or four classes, with the lowest class representing conditions only slightly more severe than ambient, and the highest class representing emergency conditions that are tenable for only a few seconds before equipment failure, injury, or death are imminent. Some of these methods, such as the NIST Thermal Classes proposed by Donnelly et al. [23] are used primarily for the purpose of evaluating electronic fire-fighting equipment. The NIST Thermal Classes specify four classes, based on criteria listed in Table 3.1. As these thermal classes are focused specifically on electronic equipment, particularly Personal Alert Safety System (PASS) alarms, they are not the most appropriate for evaluating the risk of thermal injury to firefighters in training fires. Additionally, heat flux and temperature are treated separately by the NIST Thermal Classes, and the consideration of only one value may give an incomplete picture of the thermal threat.

Table 3.1: NIST Thermal Classes

<b>Thermal Class</b>	<b>Maximum Time (min)</b>	<b>Maximum Temperature (°C)</b>	<b>Maximum Heat Flux (kW/m<sup>2</sup>)</b>
I	25	100	1
II	15	160	2
III	5	260	10
IV	≤1	≥260	≥10

A more appropriate method of characterizing a firefighter’s thermal environment involves using the thermal operating conditions outlined by Utech [24]. Utech uses the temperature at the firefighter’s height as an approximation of the convective heat transfer to the firefighter’s gear and the incident heat flux as an approximation of the radiative heat transfer to the firefighter’s gear from the surfaces of the room, the upper gas layer, and the fire itself. He combines these two quantities



to define three fields of thermal conditions: routine, ordinary, and emergency. According to Utech, routine conditions are defined as those with a surrounding temperature between 68°F (20°C) and 158°F (70°C) with an incident heat flux between 1 kW/m<sup>2</sup> and 2 kW/m<sup>2</sup>. He maintains that these conditions translate approximately to ambient conditions, such as those that would be present during the overhaul phase of a fire. As the heat flux and surrounding temperature both increase, the thermal environment crosses into the ordinary operating range. This ordinary range is defined by temperatures between 158°F (70°C) and 392°F (200°C) and heat fluxes between 2 kW/m<sup>2</sup> and 12 kW/m<sup>2</sup>. Ordinary operating conditions represent more serious fire conditions, such as those next to a post-flashover room. According to Utech, firefighters are likely able to function under ordinary operating conditions from 10-20 minutes at a time, or for the working duration of an SCBA cylinder. Utech considers ordinary operating conditions those that were typical of a house fire. It is important that Utech’s definition of the ordinary operating class is understood in the proper context. It is likely that a “typical fire” in the 1970’s, when the thermal classes were developed, may be different than a modern fire with synthetic fuels. The final classification is emergency operating conditions, which are thermal conditions exceeding heat fluxes of 12 kW/m<sup>2</sup> and temperatures of 392°F (200°C). These operating conditions are intended to be consistent with an environment dangerous to a firefighter in PPE, such as a firefighter trapped in a room that is flashing over. Utech describes the emergency zone as one in which a firefighter’s PPE is only able to withstand an exposure on the order of a few seconds. Figure 3.1 offers a visual chart of the three thermal operating classes, where the x-axis is heat flux, plotted on a logarithmic scale, in kW/m<sup>2</sup>, and the y-axis is temperature, also plotted on a logarithmic scale, in °F on the left and °C on the right .

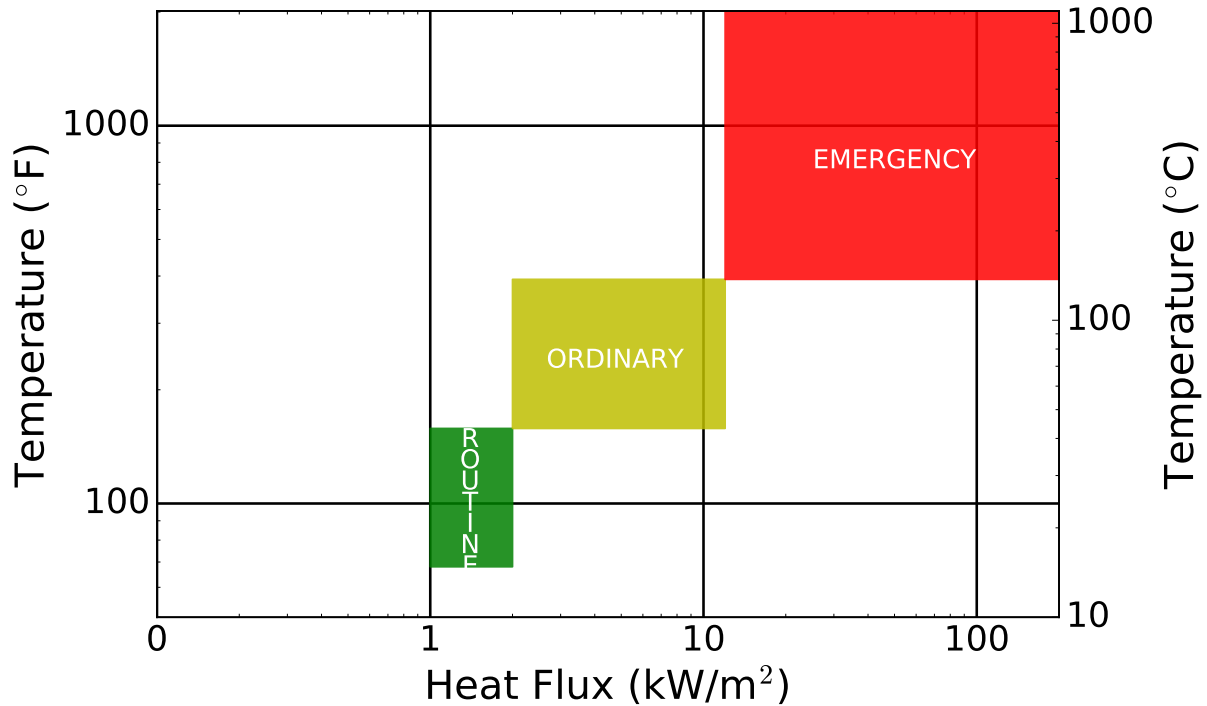
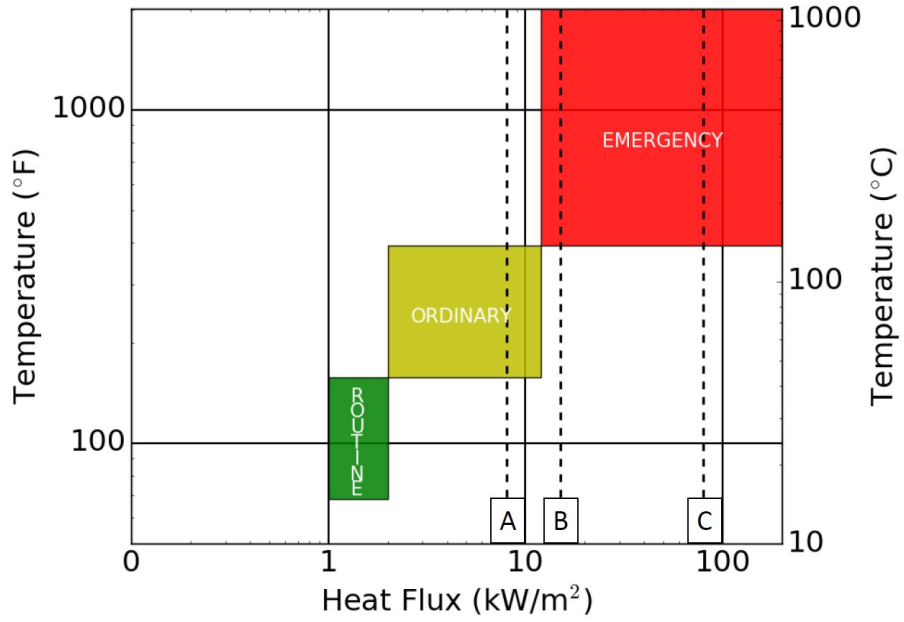


Figure 3.1: Utech’s Thermal Exposure Conditions

Rather than representing the threat to electronic firefighting equipment, as the NIST Thermal Classes are intended to do, Utech's thermal operating classes estimate the potential for thermal injury to a firefighter. Utech defined the three operating classes using the results of experiments that had been conducted on 1970s-era firefighter PPE. Firefighter PPE has improved significantly since 1973, when Utech introduced the thermal classes. Modern turnout gear is required to pass a battery of standard tests that establish minimum performance criteria [25, 26]. Putorti et al. [27] conducted an investigation in 2013 to quantify the performance of firefighter SCBA facepiece lens under radiant heat flux. The study indicated that hole formation was noted at heat fluxes as low as  $8 \text{ kW/m}^2$ . As the incident heat flux was increased, the time to hole formation decreased. Figure 3.2 shows these benchmarks, as well as the  $84 \text{ kW/m}^2$  heat flux that protective ensembles are exposed to during the thermal protective performance test [25], superimposed on the chart of Utech's thermal classes.

Comparison of Figures 3.1 and 3.2 show that the threshold between the ordinary and emergency operating classes falls between  $8 \text{ kW/m}^2$  and  $15 \text{ kW/m}^2$ , which is the range in which hole formation would occur in an SCBA facepiece lens after several minutes of constant exposure. Exposure criteria on the temperature axis and their relationship to PPE performance is currently a knowledge gap. Madrzykowski [28] conducted a literature review to compile previous research efforts to characterize the thermal operating environment of firefighters. The review highlighted that evaluating the operating environment of firefighters by pairing temperature and heat flux does not reflect the entire range of conditions to which firefighters may be exposed. Additionally, the thermal conditions within a structure can change from a safe level to conditions where firefighters would be in immediate danger quite rapidly. The report recommended future research should aim to improve the understanding of convective and radiative heat flux on firefighter PPE, particularly the effect of hot gas flows of various velocities on the heat transfer rate through firefighter gear. Thus, while the heat flux thresholds in Utech's thermal operating classes are representative of thermal conditions which would precipitate the failure of firefighters' PPE, there is clearly limitations to expressing the thermal exposure of firefighters by considering only the peak temperature and heat flux exposures to which a firefighter may be subjected.





- 
- A 8 kW/m<sup>2</sup> (Minimum heat flux exposure where hole formation in SCBA facepiece lens was noted in less than 20 minutes [27])
  - B 15 kW/m<sup>2</sup> (Hole formation in SCBA facepiece lens occurs between 1.5 and 4 minutes [27])
  - C 84 kW/m<sup>2</sup> (Heat flux which PPE ensemble is exposed to during Thermal Protection Performance Test (TPP) [25])
- 

Figure 3.2: Modern PPE Performance Comparison with Utech Thermal Classes

# 4 Fuel Load Characterization Experiments

The use of wood-based fuels in fire training is required by *NFPA 1403*, however, little data exists on the energy release rates from the most common fuel packages. To fill this knowledge gap, this project quantified the heat release rate (HRR) using a free burn configuration of 21 training fuel packages along with 12 pieces of furniture to provide a comparison to fuels found in a residential home. Three of these training fuel packages were replicates to evaluate the repeatability of a base fuel package. The fuels were selected by the fire service technical panel to be representative of the majority of the training fuels throughout the country. “Innovative” fuel packages were found in fire service literature and suggested by the technical panel to expand on the commonly used fuels.

Two representative training fuel packages were also used in a room configuration to compare to a furnished compartment. The results were analyzed to provide the fire service with general knowledge on the energy release from the combustion of wood-based fuels as compared to home furnishings.

## 4.1 Free Burn HRR Experiments

HRR characterization was performed on several of the fuel packages used in the metal container prop experiments. Additional fuel packages and orientations were also examined. The purpose of these experiments was to examine the free burn HRR characteristics, including the mass loss rate (MLR), the total energy released during the experiment, and the effective heat of combustion of various training fuels and compare these properties to similar fuels representative of furnishings in a residential house. These quantities are important to understand as they lend insight into the burning characteristics of fuels in an environment independent of compartmentation and ventilation. The energy content of the fuels themselves, as well as the rate at which that energy is released into an environment, can be used to predict the thermal conditions produced in a given training scenario. Additionally, understanding the difference between the energy release characteristics of training fuels and furnishings can help bridge the gap between the fire dynamics encountered in training and those encountered in residential structures.

### 4.1.1 Methodology

The results presented in this section were conducted in two groups, both of which were conducted in the UL’s Oxygen Consumption Calorimetry Lab in Northbrook, IL. The first set exclusively examined training fuel loads, and the second examined comparison fuel loads. The fuel packages tested in UL’s Calorimetry Lab also collected mass loss data using a load cell. Both HRR and mass data were sampled at a frequency of 1 Hz. Data was recorded until the HRR dropped below 100 kW.

Bryant and Mullholland [29] estimate the expanded relative uncertainty of oxygen consumption calorimeters measuring high HRR fires at  $\pm 11\%$ . They identify several sources of error within the calorimeter, but one of the primary sources is the uncertainty in the gas concentration measurements. The load cell had a range of 0 lb (0 kg) to 440 lb (200 kg) with a resolution of a 0.11 lb (0.05 kg) and a calibration uncertainty within 1 % [30]. The expanded uncertainty is estimated to be less than  $\pm 5\%$ . It should be noted that the listed uncertainty for the load cell is for static measurements, and is possible that the uncertainty for the dynamic mass loss measurements is greater.

Mass loss rate was calculated by finding the rate of change of mass between measurement increments. A five second moving average was applied to the measurement to account for variation in the signal. While this provided a smoother mass loss curve, it may also filter out some of the local peaks. The impact of this averaging is likely similar to the uncertainty of the load cell, since the second-to-second fluctuations are on the same order of magnitude as the resolution of the scale. In a similar manner, a five second moving average was applied to the HRR data to account for fluctuations. Total energy release was calculated by numerically integrating the HRR data using an Euler scheme. The effective heat of combustion was estimated for each of the experiments where mass loss data was available. The SFPE handbook [31] lists three methods for evaluating the effective heat of combustion ( $\Delta h_{c,eff}$ ) of a fuel, which are shown in Equations 4.1-4.3. Equation 4.1 shows the first method, which involves dividing the peak HRR by the peak MLR. Since the MLR is often quite noisy, it is convenient to take the average HRR over the peak burning period, that is, the period in which the HRR is at least 80% of the peak HRR, and dividing by the average MLR value during this period, as shown in Equation 4.2. The third method involves calculating the total amount of energy released and dividing by the total mass lost during the experiment. The methods shown in Equations 4.2 and 4.3 were used to evaluate the  $\Delta h_{c,eff}$  for the fuel packages in these experiments.

$$\Delta h_{c,eff} = \frac{\dot{Q}_{peak}}{\dot{m}_{peak}} = \Delta h_{c,eff,peak} \quad (4.1)$$

$$\Delta h_{c,eff} = \frac{\dot{Q}_{ave,peak}}{\dot{m}_{ave,peak}} = \Delta h_{c,eff,80\%} \quad (4.2)$$

$$\Delta h_{c,eff} = \frac{Q_{total}}{\Delta m_{total}} = \Delta h_{c,eff,tot} \quad (4.3)$$

### 4.1.2 Fuel Packages Contents and Arrangement

Most of the training fuel packages were placed on a burn rack consisting of four tubular steel legs supporting a frame, on top of which is laid a 4 ft x 4 ft (1.22 m x 1.22 m) 1/4 in x 18GA steel mesh, as shown in Figure 4.1. For five of the experiments, the tubular rack was not available and a makeshift rack was used, as shown in the left image of Figure 4.1. For both the tubular and makeshift racks, the frame supported the pallets so that they sit 1 ft (0.30 m) above the floor of the fire room. One of the training fuel packages was evaluated in a modified rack proposed by a

members of the project technical panel, shown in the middle image of Figure 4.17. The burn rack was placed on a load cell to capture mass data for each experiment.

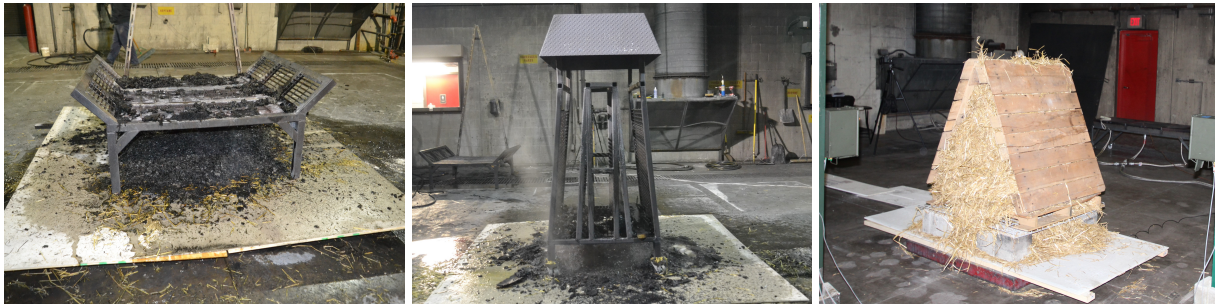


Figure 4.1: Training fuel racks used for HRR characterization experiments. Left image is the rack used for 15 of the 17 training fuel packages. Middle image is the modified rack used for the 3PR experiment. Right image is the makeshift rack.

The pallets, straw, and excelsior were purchased from the same supplier. The excelsior bales were nominally 75 lb (165 kg) standard bales, measuring 16 in x 18 in x 34 in (0.40 m x 0.45 m x 0.86 m) with 332 spur cut fibers. The pallets used for all of the experiments were three-runner wood pallets, nominally measuring 48 in. x 40 in. (1.22 m x 1.02 m). The average weight of the pallets used in the HRR characterization experiments was  $39.05 \pm 1.50$  lbs ( $17.71 \pm 0.68$  kg). The engineered wood boards and dimensional lumber were purchased from a local hardware distributor. The training fuel loads were not conditioned under a specific ambient temperature or relative humidity, but were stored in an indoor storage area prior to testing. The storage condition of the fuels is shown in Figure 4.2. This is similar to the way fuels may be stored at training academies, but also may introduce some variation between experiments as a result of environmental differences.



Figure 4.2: Images of straw (left), excelsior (middle), and pallets (right) used for HRR experiments.

The training fuel packages were configured by laboratory technicians for each of the experiments. Straw and excelsior were unbaled and “fluffed,” or pulled apart, prior to loading into the fuel package. Pallets and boards were secured in place using screws and wire. Each of the fuel packages was ignited with a butane torch in the center of the fuel package.

## Training Fuel Packages

HRR characterizations were conducted on 21 training fuel packages, three of which were replicates. Each of these fuel packages was wood-based and compliant with *NFPA 1403*. Table 4.1 gives descriptions of each fuel package evaluated, as well as the total weight of the fuel package. Additionally, pictures of each fuel package are given in Table 4.1.

It should be noted that the nomenclature used to describe the fuel packages in this document may vary regionally or from department to department. For example, the image on the left of Figure 4.3 may be referred to as a “teepee,” a “triangle,” or a “pyramid,” while the fuel package on the right may be referred to as a “lean-to,” or “stack,” among other names. The naming convention used in this report is not intended to endorse any particular name, but rather to provide consistency and clarity in talking about the geometric arrangement of the fuel packages themselves.

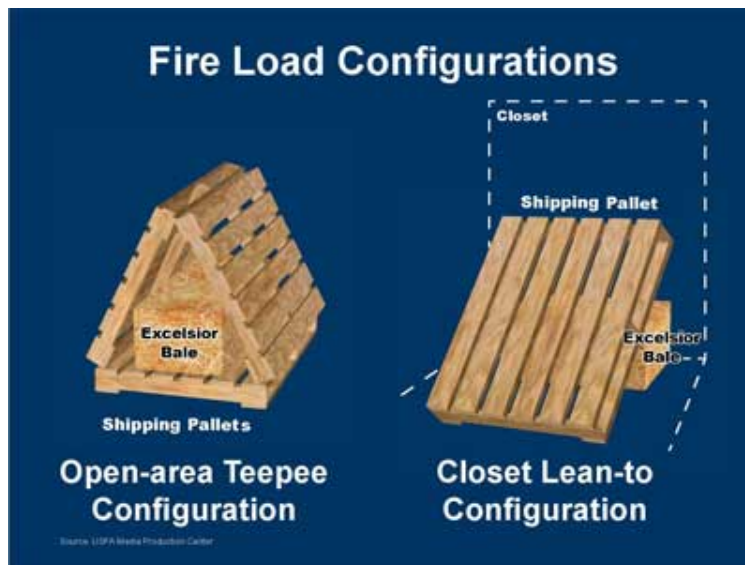









Figure 4.3: Images and nomenclature from NIOSH firefighter LODD report [17]


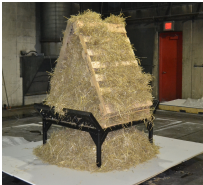






Table 4.1: Training Fuel Package Descriptions for HRR Characterization

Image	Label	Fuel Package	Total Weights lbs (kg)
	1S	1 bale of straw, fluffed	33.8 (15.3)
	2S	2 bales of straw, fluffed	64.2 (29.1)
	1E	1 bale of excelsior, fluffed	50.6 (23.0)
	2E	2 bales of excelsior, fluffed	119.8 (54.3)
	3P1S-1	3 pallets, arranged in a triangle, stuffed with 1 bale of straw (first replicate)	154.6 (70.1)
	3P1S-2	3 pallets, arranged in a triangle, stuffed with 1 bale of straw (second replicate)	152.9 (69.4)
	3P1S-3	3 pallets, arranged in a triangle, stuffed with 1 bale of straw (third replicate)	153.9 (69.8)

Legend:







# = Count	S = Straw	P = Pallets	M = MDF
E = excelsior	O = OSB	DL = Dim. Lumber	-Fi = Fisher Orientation
-Ga = Garcia Orientation	-V = Vertically Stacked	-H = Horizontally Stacked	-# = Replicate Number

Image	Label	Fuel Package	Total Weights lbs (kg)
	3P1S-H	3 pallets, arranged horizontally, stuffed with 2 bales of straw	153.8 (69.8)
	3P2S	3 pallets, arranged in a triangle, stuffed with 2 bales of straw	175.0 (79.4)
	3P1E	3 pallets, arranged in a triangle, stuffed with 1 bale of excelsior	168.0 (76.2)
	3P1SO	3 pallets, arranged in a triangle, stuffed with 1 bale of straw, with two vertical 4 ft x 8 ft sheets of OSB	244.9 (111.1)
	3P1SM	3 pallets, arranged in a triangle, stuffed with 1 bale of straw, with two vertical 4 ft x 8 ft sheets of MDF	266.2 (120.8)
	3P1SDL	3 pallets, arranged in a triangle, stuffed with 1 bale of straw, with 12 vertical 1 in. x 6 in. boards of dimensional lumber	221.6 (100.5)

\*3P1S fuel package was conducted during the same experimental series as the comparison fuel loads listed in Section 4.1.2. As such, the pallets and straw were not of the same stock as the rest of the training fuel experiments.

Legend:

# = Count	S = Straw	P = Pallets	M = MDF
E = excelsior	O = OSB	DL = Dim. Lumber	-Fi = Fisher Orientation
-Ga = Garcia Orientation	-V = Vertically Stacked	-H = Horizontally Stacked	-# = Replicate Number

Image	Label	Fuel Package	Total Weights lbs (kg)
	3P1S-V	3 pallets, arranged vertically, stuffed with 1 bale of straw	153.9 (69.8)
	4P1S-V	4 pallets, arranged vertically, stuffed with 1 bale of straw	189.1 (85.8)
	5P1S-V	5 pallets, arranged vertically, stuffed with 1 bale of straw	228.0 (103.4)
	6P1S-V	6 pallets, arranged vertically, stuffed with 1 bale of straw	266.9 (121.1)
	7P1S-V	7 pallets, arranged vertically, stuffed with 1 bale of straw	305.8 (138.7)
	3P1S-R	3 pallets, stuffed with 1 bale of straw, arranged in a metal rack with a hood	151.4 (68.7)

Legend:

# = Count

E = excelsior

-Ga = Garcia Orientation

S = Straw

O = OSB

-V = Vertically  
Stacked

P = Pallets

DL = Dim. Lumber



-H = Horizontally  
Stacked

M = MDF

-Fi = Fisher Orientation

-# = Replicate Number



Image	Label	Fuel Package	Total Weights lbs (kg)
	6P1S-Ga	6 pallets, stuffed with 1 bale of straw, with 3 pallets arranged into a triangle, one pallet placed on each end, and one over the top	267.4 (121.3)
	6P1S-Fi	6 pallets, stuffed with 1 bale of straw, with pallets stacked to the ceiling.	267.8 (121.5)
<b>Legend:</b>			
# = Count	S = Straw	P = Pallets	M = MDF
E = excelsior	O = OSB	DL = Dim. Lumber	Fi = Fisher Orientation
Ga = Garcia Orientation	-V = Vertically Stacked	-H = Horizontally Stacked	-# = Replicate Number

### Comparison Fuel Loads

In addition to the 17 training fuel loads, HRR characterization experiments were conducted on 12 furniture items to provide a comparison between a fuel load that may be found in a residential structure and training fuel loads such as those presented in the previous section. Table 4.2 lists the furniture item descriptions, their weights, and their labels. The furniture items that were evaluated included two types of sofas, three types of chairs, and a bed set.

Table 4.2: Comparison Fuel Package Descriptions for HRR Characterization

Label	Fuel Package	Total Weight lbs (kg)
SLI	Upholstered sofa with wood frame, polyurethane cushions, polyester batting, and polyester microfiber covering ignited in the left arm	101.0 (45.9)
SCI	Upholstered sofa with wood frame, polyurethane cushions, polyester batting, and polyester microfiber covering ignited in the center cushion	96.4 (43.8)
SRI	Upholstered sofa with wood frame, polyurethane cushions, polyester batting, and polyester microfiber covering ignited in the right arm	99.0 (45.0)
SC-1	Striped upholstered armchair with wood frame, polyurethane cushion, polyester batting, and cloth covering (first replicate)	62.4 (28.4)
SC-2	Striped upholstered armchair with wood frame, polyurethane cushion, polyester batting, and cloth covering (second replicate)	61.2 (27.8)
SC-3	Striped upholstered armchair with wood frame, polyurethane cushion, polyester batting, and cloth covering (third replicate)	62.4 (28.4)
YC-1	Yellow upholstered armchair with wood frame, polyurethane cushion, polyester batting, and cloth covering (first replicate)	54.6 (24.8)
YC-2	Yellow upholstered armchair with wood frame, polyurethane cushion, polyester batting, and cloth covering (second replicate)	57.0 (25.9)
B-1	Bed set consisting of metal stand, box spring, mattress, 4 in. foam pad, comforter, and pillows (first replicate)	229.0 (104.1)
B-2	Bed set consisting of metal stand, box spring, mattress, 4 in. foam pad, comforter, and pillows (second replicate)	231.2 (105.1)
BC-1	Barrel-type chair with a polyurethane foam cushion and an expanded polystyrene frame.	19.5 (8.7)
KS-1	Kit sofa with a wood frame and polyurethane upholstery.	111.3 (50.6)

Legend:

B = Bed	S = Upholstered Sofa	LI = Left ignition
CI = Center Ignition	RI = Right Ignition	SC = Striped Chair
BC = Barrel Chair	KS = Kit Sofa	YC = Yellow Chair
	-# = Replicate Number	



Figure 4.4: Images of comparison fuel packages. Images correspond with the order of items in Table 4.2, showing examples of the upholstered sofa (top left), striped chair (top middle), yellow chair (top right), barrel chair (bottom left), bed set (bottom middle), and kit sofa (bottom right).

The “kit sofa” differed from the other upholstered sofa in the sense that it required assembly prior to use. Additionally, the kit sofa weighed less than the other upholstered sofa. Only one replicate of the kit sofa was conducted, while three replicates of the upholstered sofa were conducted, although the ignition location was changed for each of the three experiments. The striped and yellow versions of the upholstered chair were comparable to each other in terms of composition and weight, and multiple replicates of each type of chair were conducted. The “barrel chair,” however, weighed significantly less than the upholstered chairs and had a frame composed of polystyrene, rather than wood.

### 4.1.3 Results

Tables 4.3 and Table 4.4 summarize the results of the HRR testing for the training fuel and comparison fuel packages, respectively. The table lists the Peak HRR, the peak mass loss rate, and the total energy release for each fuel package tested. The peak MLR reported in the tables is  $\Delta h_{c,eff,80\%}$ , defined by Equation 4.2.

The peak HRR for the fuel package reflects the peak rate at which energy is being released, and is a useful quantity for describing the growth of the fire. In a training fuel, high peak HRRs would correspond to higher temperatures and heat fluxes, particularly in areas closer to the seat of the fire. The total energy release reflects the amount of energy released by the fuel package over the duration of the experiment. The peak MLR is related to the peak HRR by the heat of combustion of the fuel, as discussed in Equations 4.1 and 4.2. The higher the MLR of the training fuel, the more surfaces of the fuel are producing flammable vapors. Fuels with a comparatively low peak MLR and comparatively high peak HRR, such as plastics, synthetic foams, and flammable liquids, are considered high energy fuels. Fuels with a comparatively higher peak MLR and a lower peak

HRR, such as wood-based fuels and other natural products, are lower energy fuels.

Table 4.3: Training Fuel Package HRR Characterization Results

Label	Peak HRR (MW)	Peak MLR* (kg/s)	Total Energy Release (MJ)
1S	1.04	0.10	207.01
2S	2.09	0.15	389.85
1E	1.69	0.13	325.33
2E	1.57	0.12	784.83
3P1S-1	1.91	0.15	854.14
3P1S-2	1.60	0.13	820.47
3P1S-3	2.05	0.15	880.86
3P1S-H	1.22	0.11	923.37
3P2S	2.45	0.17	1196.06
3P1E	3.04	0.20	1060.66
3P1SO	2.40	0.17	1547.87
3P1SM	2.73	0.19	1404.26
3P1SDL	2.44	0.17	1423.21
3P1S-V	2.00	0.15	814.17
4P1S-V	2.29	0.17	1025.26
5P1S-V	2.91	0.20	1341.55
6P1S-V	3.19	0.22	1575.49
7P1S-V	3.42	0.24	1815.34
3P1S-R	1.62	0.13	929.87
6P1S-Ga	3.64	0.25	1581.17
6P1S-Fi	3.8	0.27	1603.33

Legend:

# = count	S = straw	P = pallets	M = MDF
E = excelsior	O = OSB	DL = Dim. Lumber	-Fi = Fisher Orientation
-Ga = Garcia Orientation	-V = Vertically Stacked	-H = Horizontally Stacked	-# = Replicate Number

\*Peak MLR was evaluated by taking the average mass loss rate over the peak burning period, defined as 80% of the peak HRR

The time history plots used to develop Table 4.3 are located in Appendix A.1.

Table 4.4: Comparison Fuel Package HRR Characterization Results

Label	Peak HRR (MW)	Peak MLR* (kg/s)	Total Energy Release (MJ)
SLI	2.46	0.12	692.722
SCI	3.72	0.12	671.44
SRI	3.70	0.14	637.22
SC-1	1.61	0.08	215.5
SC-2	1.83	0.08	356.2
SC-3	1.82	0.07	455.78
YC-1	2.14	0.07	195.35
YC-2	1.94	0.06	226.22
B-1	2.23	0.10	936.21
B-2	1.85	0.08	994.93
BC-1	0.85	0.02	177.92
KS-1	1.82	0.09	569.62

Legend:

B = Bed

CI = Center Ignition

BC = Barrel Chair

S = Upholstered Sofa

RI = Right Ignition

KS = Kit Sofa

-# = Replicate Number

LI = Left ignition

SC = Striped Chair

YC = Yellow Chair

\*Peak MLR was evaluated by taking the average mass loss rate over the peak burning period, defined as 80% of the peak HRR.

The time history plots used to develop Table 4.4 are located in Appendix A.2.

#### 4.1.4 Discussion

##### Effective Heat of Combustion

The effective heat of combustion of each of the training fuel packages was evaluated using two methods: Equations 4.2 and 4.3. The resulting values for  $\Delta h_{c,eff}$  and the duration of the peak burning period (as defined in Equation 4.2) are shown in Table 4.5. The results show that for most of the fuels the predicted  $\Delta h_{c,eff,80\%}$  was lower than the predicted  $\Delta h_{c,eff,tot}$ . The difference between the two methods was most pronounced for the one bale of straw fuel package. It is possible that this large difference is due to the comparatively low total fuel weight. Most of the computed  $\Delta h_{c,eff}$  for the fuel packages fell between 10 and 15 MJ/kg, which is within the range commonly cited for wooden fuels [32].

Table 4.5: Effective Heat of Combustion Results

Label	$\Delta h_{c,eff}$ from Equation 4.2 (MJ/kg)	$\Delta h_{c,eff}$ from Equation 4.3 (MJ/kg)	Peak Burning Duration (s)
1S	9.84	16.43	61
2S	12.70	14.44	35
1E	11.38	14.18	90
2E	11.31	14.24	116
3P1S-1	11.38	12.36	132
3P1S-2	10.97	12.66	277
3P1S-3	12.35	13.07	75
3P1S-H	9.57	12.84	358
3P2S	12.28	15.45	140
3P1E	13.77	14.05	83
3P1SO	12.23	15.07	151
3P1SM	12.78	14.17	126
3P1SDL	12.52	15.74	239
3P1S-V	11.84	12.48	169
4P1S-V	11.99	13.30	180
5P1S-V	12.90	14.02	124
6P1S-V	12.82	13.95	185
7P1S-V	12.88	13.87	204
3P1S-R	11.15	14.62	294
6P1S-Ga	12.65	13.58	148
6P1S-Fi	12.61	14.39	215

Legend:			
# = count	S = straw	P = pallets	M = MDF
E = excelsior	O = OSB	DL = Dim. Lumber	-Fi = Fisher Orientation
-Ga = Garcia Orientation	-V = Vertically Stacked	-H = Horizontally Stacked	-# = Replicate Number

Figure 4.5 shows the average HRR during the peak burning period plotted against the MLR from the same period for each of the fuel packages. Applying a linear least-squares regression to the data in Table 4.3 results in a linear fit with a slope of 14.88 MJ/kg and a  $R^2$  value of 0.987. Because of the direct relationship between the average peak burning HRR and the corresponding average MLR, the slope of the linear fit represents the effective heat of combustion for the training fuel packages tested.

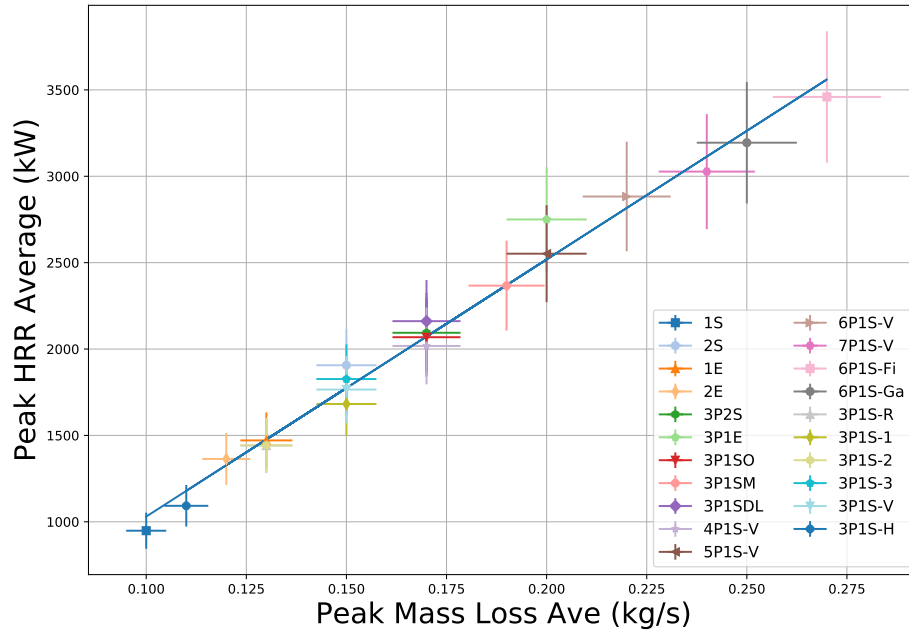


Figure 4.5: Average HRR (kW) versus average MLR (kg/s) over peak burning period. The peak burning period is taken to be the period in which the HRR is greater than or equal to 80% of the peak value. The error bars corresponding to each point indicate the uncertainty of the measurement.

A similar trend can be seen in Figure 4.6, which plots the total energy release computed for each training fuel against the total mass burned. Applying a similar least-squares regression to this dataset results in a linear fit with a slope of 14.21 MJ/kg and a  $R^2$  value of 0.980. Just as in Figure 4.5, the direct relationship between the total energy released and total mass burned indicates an approximately constant value for the wood-based training fuels tested in these experiments.

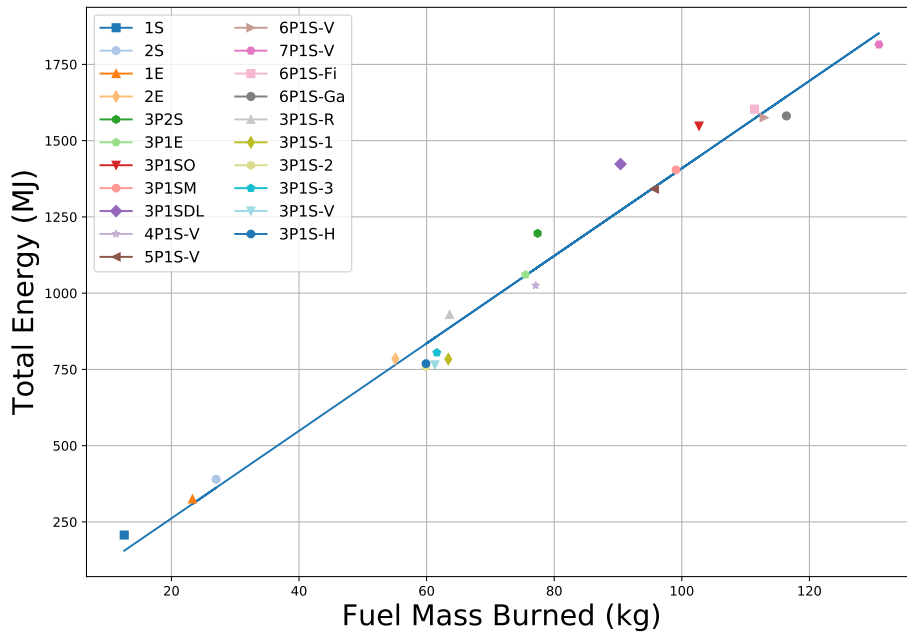


Figure 4.6: Total energy (MJ) vs. total mass burned (kg)

The  $R^2$  value, which describes the variability of the data about its mean, was high in each case, indicating the data is a good fit for the regression. This indicates that the variation in the  $\Delta h_{c,eff}$  is relatively small between the different wood-based fuel packages. The slopes of 14.88 and 14.34 MJ/kg, from Figures 4.5 and 4.6 respectively, fall within the range of  $\Delta h_{c,eff}$  values commonly cited for wood [33]. This indicates that all of the wood-based products tested have a similar combustion chemistry. While some of the wood-based fuels, specifically the engineered wood products, contain synthetic resins which may have environmental or health effects, the majority of the fuel weight is still wood and the HRR results reflect this.

Although the quantities of HRR, MLR, and total energy release are common measurements in the laboratory setting, most fire service organizations lack the equipment to measure the peak heat release rate for their individual fuel packages. However, predicting the peak heat release rate from a training fuel package is essential to predicting the “fire size” needed for a given lesson. A reliable field measurement of initial fuel weight is more achievable for training organizations looking to estimate the peak heat release rate from a given fuel package.

Figure 4.7 shows the peak heat release rate from the 17 *NFPA 1403* compliant fuel packages tested in the free-burn configuration plotted against their respective initial fuel weight. The black line represents a linear regression utilizing an ordinary least squares (OLS) regression model with a  $R^2$  value of 0.672. This represents a loose relationship between initial fuel weight and peak heat release rate when using *NFPA 1403* compliant wood-based fuels.



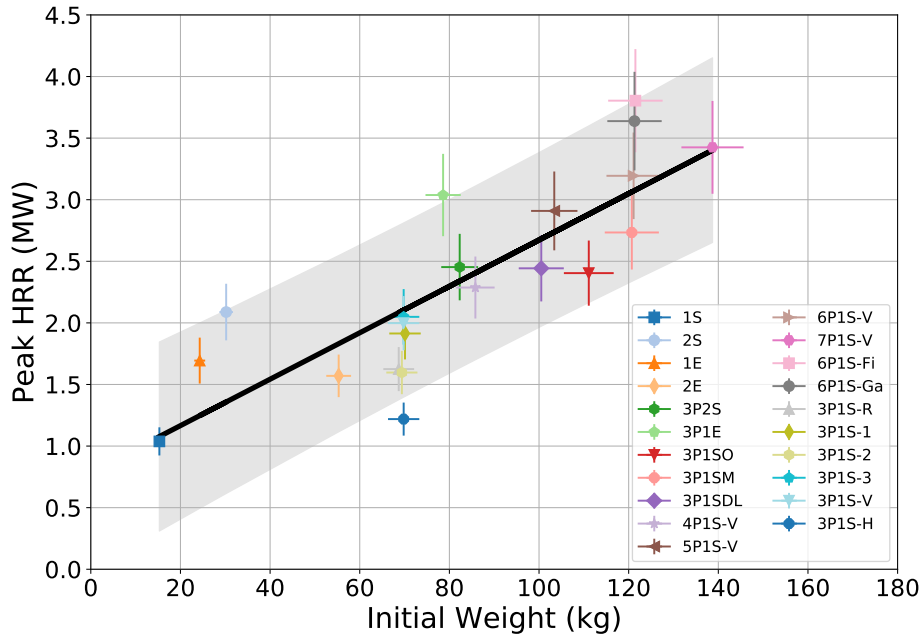


Figure 4.7: Peak heat release rate measured in megawatts as compared to initial fuel mass measured in kilograms for the 17 NFPA 1403 compliant fuel packages tested in a free-burn configuration. The black line represents an ordinary least squares regression with the gray area highlighting a  $\pm 95\%$  confidence interval. The error bars corresponding to each point indicate the uncertainty of the measurement.

Factors which complicate the use of initial weight to predict the peak heat release rate include the geometry of the fuels. In general if the fuel is located in a 4 ft x 4 ft x 4 ft (1.2 m x 1.2 m x 1.2 m) cube, as was the case for the majority of the fuel packages tested, and the baled material is sufficiently unbaled, the initial weight can be used to roughly approximate the range of peak heat release rates. A larger dataset will be needed to determine if a reliable scale factor can be identified for the use of estimating peak heat release rate from initial weight.

### Straw vs. Excelsior

Straw and excelsior are two common “kindling” materials in training fuel packages. Their high surface area to mass ratio facilitates ignition and fire spread, and because of this they are used in conjunction with other, more dense wood products. The straw or excelsior would be ignited first, to produce enough heat to ignite the more dense wood fuels. In some cases, excelsior may be used as a fuel by itself. The excelsior bales used in the HRR characterizations tests weighed approximately twice as much as a bale of straw. For both straw and excelsior, fuel packages consisting of one and two bales were compared. These four fuel packages are shown in Figure 4.8.



Figure 4.8: Images of fuel packages consisting of one (1S, top left) and two (2S, top right) bales of straw and one (1E, bottom left) and two (2E, bottom right) bales of excelsior.

Figure 4.9 shows the HRR time histories for the straw and excelsior fuel packages. The peak free burn HRR for one bale of straw was 1.04 MW. Adding an additional bale of straw increased the peak free burn HRR to 2.09 MW (101% increase). When this additional bale of straw was added, the duration of the peak burning period decreased from 61 seconds to 35 seconds. The peak HRR of one bale of excelsior fell between one and two bales of straw, at 1.69 MW. Adding an additional bale of excelsior resulted in a similar peak free burn HRR to the single bale of excelsior of 1.57 MW. The additional bale of excelsior increased the duration of the peak burning period from 90 seconds to 116 seconds. The addition of straw is advantageous for its rapid growth to a higher peak HRR, while excelsior does not reach as high of a peak HRR; it provides a longer peak burn time.

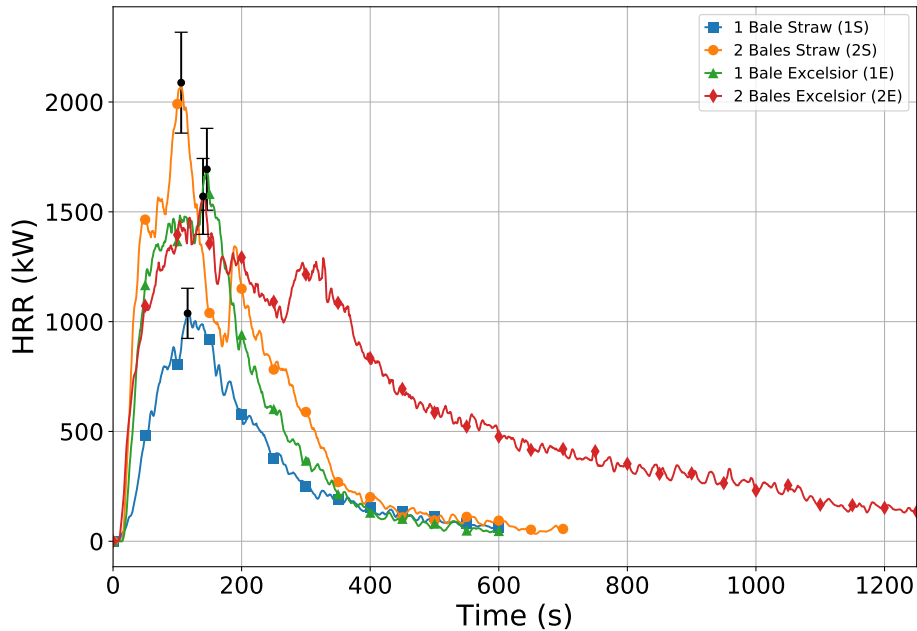


Figure 4.9: HRR (kW) vs. time for excelsior and straw fuel packages

Figure 4.10 shows each of the fuels at the time of their peak HRR. Visually, none of the four fuel packages produced smoke of a sufficient optical density to obscure the lighting in the laboratory. Under free burn conditions, the visual appearance of the burning fuel packages was relatively

similar. At the time of the peak HRR, the two excelsior fuel packages and the fuel package with two bales of straw had parts of the fuel package fall off of the rack.

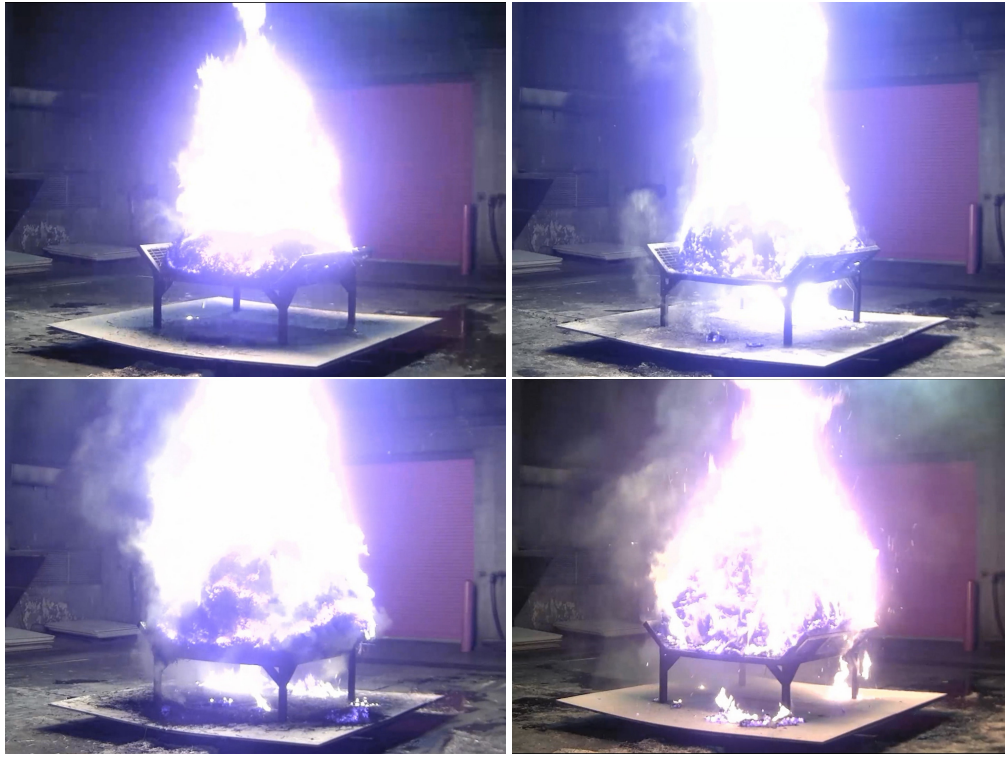


Figure 4.10: Visuals of fuel packages at the time of the peak free burn HRR. From top to bottom, left to right, the the fuel packages consist of one bale of straw (1.04 MW), one bale of excelsior (1.69 MW), two bales of straw (2.09 MW), and two bales of excelsior (1.52 MW).

The reason for the growth difference between the two fuels is related to their structures. Straw is composed of dried grass stalks and other tubular plants and is commonly used as bedding for livestock. The center of the straw chute is hollow, which has two important implications: a large percentage of the straw's surface is exposed to incident heat, and the mass of the straw is small compared to its volume. The high surface area results in rapid pyrolysis and growth, but it does not have a long burn duration because of the low fuel weight. Excelsior, on the other hand, is shredded lumber, typically aspen wood. Excelsior also has a high surface area to mass ratio, but is not hollow like the straw. Because excelsior is more dense than straw, a bale of excelsior weighs more than a similarly sized bale of straw, providing a fuel package with more mass and thus more energy. The difference in structure is responsible for the high peak HRRs and lower total energy contents of the straw fuel packages compared to the excelsior.

### **Training Fuel HRR Repeatability**

Three replicate experiments were conducting using a training fuel load of three pallets and a bale of straw in a triangle arrangement to characterize the repeatability of a common training fuel package.

Figure 4.11 shows the HRR of each of these experiments as a function of time and Table 4.6 lists the fuel weight, peak HRR, and total energy for each of these packages. The total fuel weight was similar among the three experiments, ranging from 69.8 kg to 70.1 kg. Following ignition, each pallet experienced growth to an HRR between 1.5 MW and 2 MW in the first 100 seconds. The peak HRRs varied from 1.60 to 1.91 MW. The difference between the lowest peak HRR and the highest peak HRR was 28%, which is a significant difference. Replicate 3 showed the most deviance from the other two experiments, exhibiting lower a HRR during the period from approximately 75 seconds to 200 seconds. After 200 s, the behavior of the three replicates was similar, as is reflected in the total energy release among the three experiments, which ranged from 880.86 MJ/kg to 820.47 MJ/kg, a 7% difference.

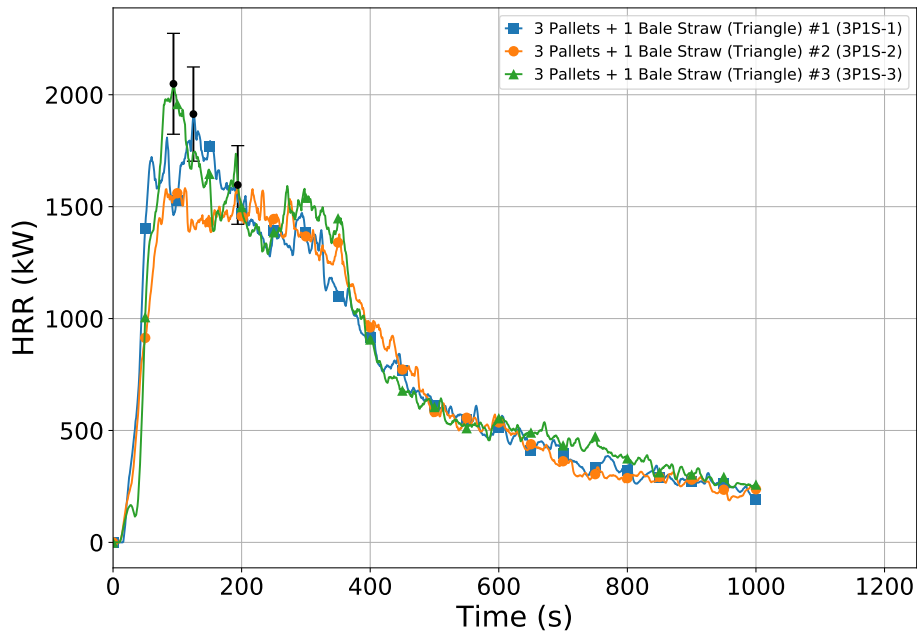


Figure 4.11: HRR (kW) vs. time for three pallets, arranged in a triangle, with one bale of straw replicate experiments.

Table 4.6: Three Pallet Triangle Replicate Experiments Results

Replicate Number	Total Weight (kg)	Peak HRR (kW)	Total Energy (MJ)
1	70.1	1.91	854.14
2	69.4	1.60	820.47
3	69.8	2.05	880.86

Thus, the HRR varied most among the three experiments in the 100 seconds following ignition, in the period leading up to the peak HRR. In this period, the straw is the primary fuel that is burning, and the difference in growth likely reflects the differences in moisture content and packing density between the three fuel packages. The HRRs were only significantly different among the three

experiments for a total of 135 seconds, which is denoted by the red shaded areas on Figure 4.11. Repeatable training fuel loads are an important part of conducting live fire training, because it ensures that the lesson taught during a particular evolution will be consistent among different groups of students. Additionally, it can provide the instructors a degree of confidence that the expected magnitude of thermal conditions will be consistent for a similar fuel package in a similar compartment. Since the three replicates were not substantially different, the remainder of this report will use Replicate 1 as a representative fuel package of three pallets and one bale of straw in a triangle.

### Increasing Fuel Mass By Adding Additional Pallets

The effect of adding additional pallets to a fuel load composed of pallets and straw was evaluated by comparing fuel loads with three, four, five, six, and seven pallets, stacked vertically, with a single bale of straw. These five fuel packages are shown in Figure 4.12. Figure 4.13 shows the HRR time histories for the five vertical pallets fuel packages.

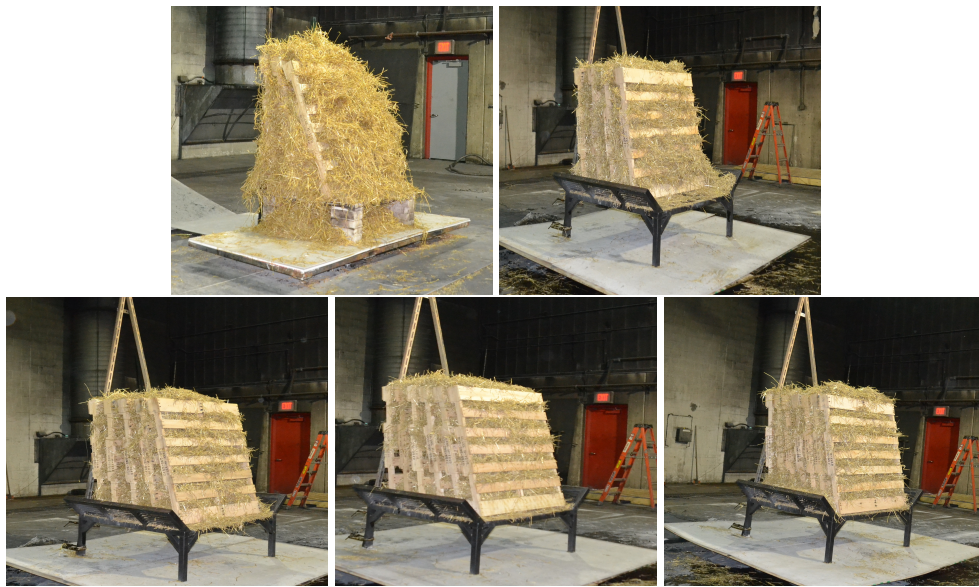


Figure 4.12: Lean-to fuel packages consisting of (left to right, top to bottom) three, four, five, six, and seven pallets.

The initial growth of the lean-to fuel packages was quite similar in the first 75 seconds, with each fuel package reaching an HRR of approximately 1.75 MW in this period. This behavior suggests that the straw is responsible for most of the initial growth of the fire. The three pallet configuration had a peak free burn HRR of 2.00 MW, and a peak burning duration of 169 seconds. The addition of one pallet resulted in a peak HRR of 2.29 MW (15% increase), and had a peak burning duration of 180 seconds. The addition of two pallets resulted in a peak HRR of 2.91 MW (46% increase) and a peak burn duration of 124 seconds. The addition of three pallets resulted in a peak HRR of 3.19 MW (60% increase from three pallet peak HRR) and a peak burning duration of 185 seconds.



The addition of four pallets resulted in a peak HRR of 3.42 MW (71% increase from three pallet peak HRR) and a peak burning period of 204 seconds.

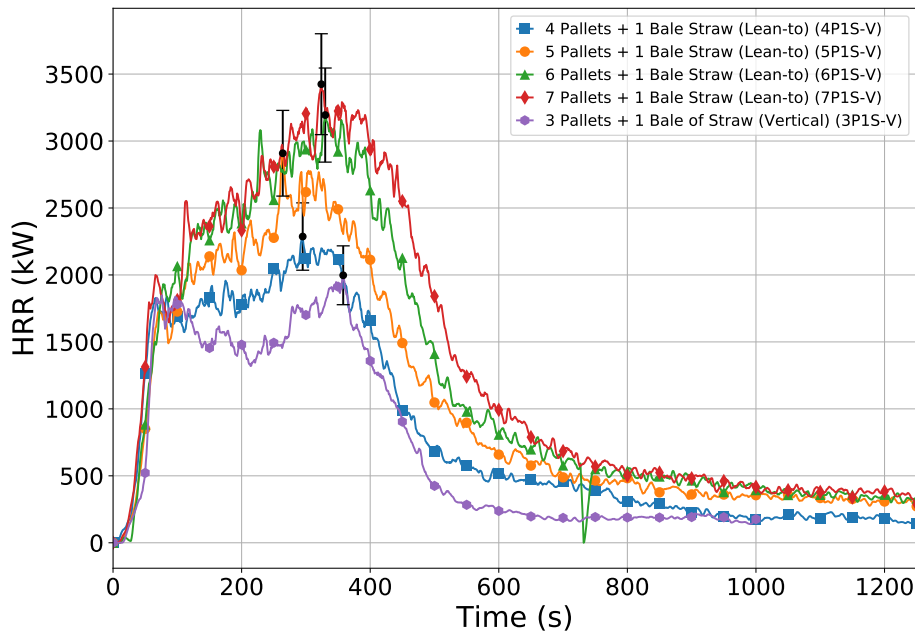


Figure 4.13: Effect of pallet count on HRR (kW)

Table 4.7: Lean-to Fuel Package Experiments Results

Number of Pallets	Total Weight (kg)	Peak HRR (kW)	Total Energy (MJ)
3	69.8	2.00	814.17
4	85.8	2.29	1025.26
5	103.4	2.91	1341.55
6	121.1	3.19	1575.49
7	138.7	3.42	1815.34

Table 4.7 lists the total weight, peak HRR, and total energy release for the lean-to pallet fuel packages. While measurement uncertainty makes it difficult to distinguish the difference in HRR and total energy release caused by a single pallet, the results indicated that as fuel weight increased in the form of additional pallets, the peak HRR and total energy increased. In particular, the difference between the HRR of the six and seven pallet lean-to fuel packages was minimal. The reason for this is likely because the seven pallet fuel package is almost bigger than the rack, as shown in Figure 4.12. This compresses the straw that is between the pallets, reducing the amount of air that can be entrained and restricting the peak HRR. Further, as more pallets are added in this orientation, the fuel package becomes larger in the horizontal direction than the vertical direction and the flame spread is not as efficient. Thus, as more pallets are added to a lean-to fuel package, the peak HRR can be expected to increase, although the magnitude of these HRR gains may change, depending on the number of pallets.

Although the magnitude of the peak HRR varied by 1.42 MW between the five lean-to fuel packages, there was not a significant visible difference among the five fuel packages in a free burn scenario. Figure 4.14 shows each of the lean-to fuel packages at the time of the peak HRR. This would indicate that, in a free burn scenario, it is difficult to assess the fire size by visual means alone. It is possible that the visible difference between fires of different sizes would be more pronounced had they been burned inside of a compartment, or in a configuration where compartment effects had been introduced, but additional testing is needed to further investigate this.

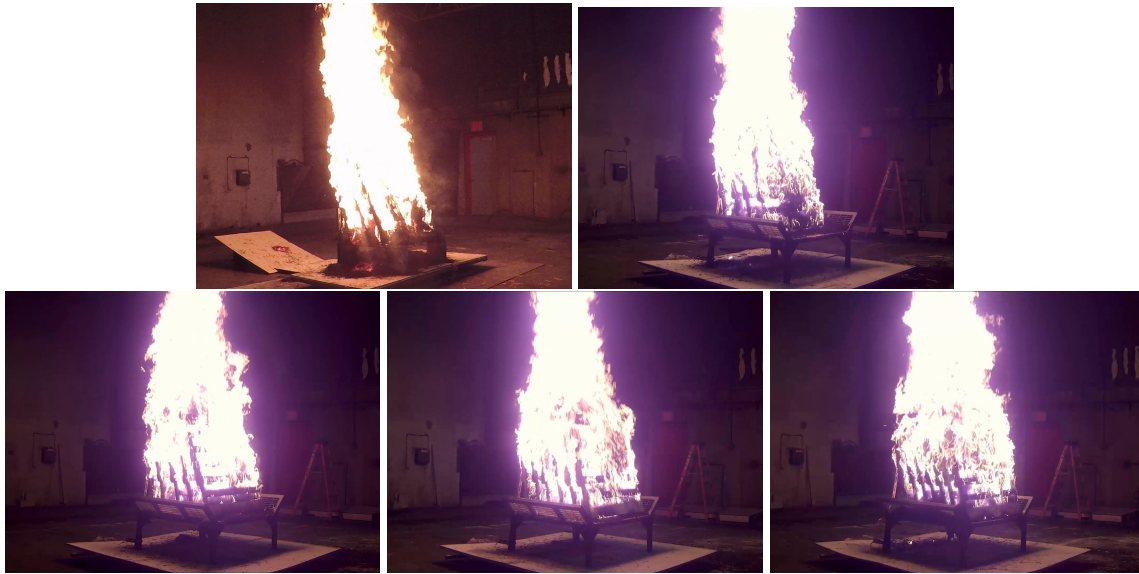


Figure 4.14: Visuals of lean-to fuel packages at the time of the peak free burn HRR. From top to bottom, left to right, the images show the 3P1S-V (2.00 MW), 4P1S-V (2.29 MW), 5P1S-V (2.91 MW), 6P1S-V (3.19 MW), and 7P1S-V (3.42 MW) fuel packages.

### Effect of Additional Straw or Excelsior in Pallet Fuel Package

Table 4.8: Fuel Loads Used with Pallets and Straw or Excelsior

Label	Fuel Package
3P1S-1	three pallets, arranged in a triangle, stuffed with 1 bales of straw (Replicate #1)
3P2S	three pallets, arranged in a triangle, stuffed with 2 bales of straw
3P1E	three pallets, arranged in a triangle, stuffed with 1 bale of excelsior

Table 4.8 lists three experiments that can be compared to examine the effect of adding weight to a base fuel package of three pallets and a bale of straw by either adding an additional bale of straw or replacing the bale of straw with a bale of excelsior. In each of these experiments, three pallets were arranged into a triangle formation with either excelsior or straw. The third replicate of the three pallet triangle with one bale of straw was used as a comparison, which had the highest peak HRR of the three replicate experiments.

Figure 4.15 compares the HRR time histories of these training fuels loads (3P1S3, 3P2S, and 3P1E). The fuel load consisting of three pallets and one bale of straw (3P1S) exhibited a peak free burn HRR of 2.05 MW. The fuel package with three pallets and two bales of straw had a 20% higher peak free burn HRR of 2.45 MW. Both of these peaks occur between 75 and 100 seconds. The growth of these two experiments is similar for the 150 seconds following ignition, leading up to the peak HRR for each of the fuel loads. After the peak however, the fuel package with two bales of straw is maintained at a higher HRR for a longer period of time. The HRR of each experiment begins to decay at approximately 400 seconds after ignition. The fuel package with three pallets and a bale of excelsior grows more slowly than the other two fuel packages, reaching a peak HRR after 150 seconds. The peak HRR of this fuel package is 3.04 MW, which is greater than the other two fuel packages. The decay phase of this fuel package also begins close to 400 seconds.

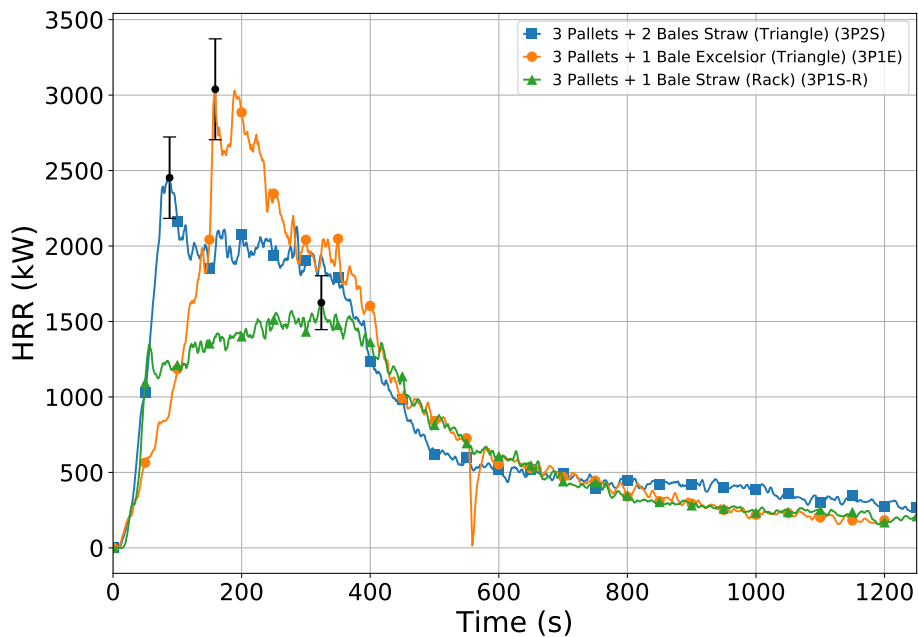


Figure 4.15: HRR (kW) vs. time for 3 pallet configurations



Figure 4.16: Visuals of three pallet fuel packages at the time of the peak free burn HRR. From top to bottom, left to right, the images show the 3P1S (2.05 MW), 3P1E (3.04 MW), and 3P2S (2.45 MW) fuel packages



Replacing the bale of straw with a bale of excelsior significantly increased the peak HRR, but decreased the growth rate of the HRR. The 3PIE training fuel package had a peak HRR of 3.04 MW, which was 24% higher than three pallets with two bales of straw and 48% higher than three pallets with one bale of straw. Adding an additional bale of straw to the base fuel package of three pallets and one bale of straw resulted in a similar growth rate, but resulted in a higher HRR following the peak. Thus, the addition of straw to the fuel package can extend the peak burning period.

### Effect of Pallet Orientation

Table 4.9 lists four experiments with a fuel load of three pallets and a bale of straw in different orientations, which were conducted to evaluate the effect of fuel package geometry on fire growth. Three of these fuel packages were conducted on a makeshift rack and were elevated 1 ft. (0.3 m) from the scale. The fourth experiment, 3PR, instead incorporated three pallets and a bale of straw into the hooded rack shown in Figure 4.17.

Table 4.9: Fuel Loads Used with three pallet Configuration

Label	Fuel Package
3P1S-1	3 pallets, arranged in a triangle, stuffed with 1 bales of straw (Replicate #1)
3P1S-V	3 pallets, arranged vertically, stuffed with 2 bales of straw
3P1S-H	3 pallets, arranged horizontally, stuffed with 1 bales of straw
3P1S-R	3 pallets, stuffed with 1 bale of straw, arranged in a metal rack with a hood



Figure 4.17: Innovative fuel rack

The growth of the triangle (3P1S-3), lean-to (3P1S-V), and rack (3PR) fuel packages was similar

for the first 50 seconds. It is likely that the majority of the fuel contributing to burning at this time is the straw. After the first 50 seconds, the lean-to and triangle fuel package continue to grow, while the rack fuel package transitions to a period of slower growth, leading to a peak HRR of 1.62 MW at 324 seconds. The three pallet triangle reaches a peak HRR of 2.05 MW at 94 seconds, after which the HRR decreases to below 0.5 MW over the next 500 seconds. The three pallet lean-to reaches a local peak at approximately the same time that the three pallet triangle reaches its peak HRR, followed by a brief decrease in HRR, followed by the peak HRR of 2.0 MW at 358 seconds after ignition. Following the peak HRR, the HRR of the three pallet lean-to decreases below 0.5 MW over the next 150 seconds. The longer duration of high HRR in the three pallet lean-to compared to the three pallet triangle is related to the orientation of the pallets. While the rapid initial growth of both fuel packages is likely due to straw, the vertical orientation of the pallets in the lean-to facilitates a higher rate of heat release during this period.

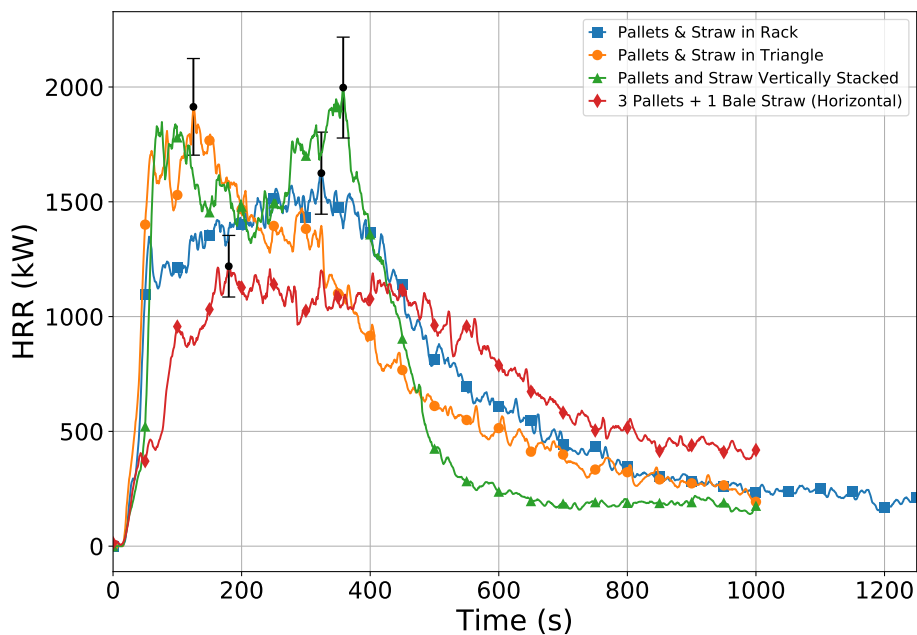


Figure 4.18: HRR (kW) vs. time for three pallet configurations

The growth of the three horizontally stacked pallets (3P1S-H) was markedly slower than the other three three pallet fuel packages. The three horizontally stacked pallets reached a peak HRR of 1.22 MW at 180 seconds after ignition, and maintained an HRR close to this value until approximately 500 seconds after ignition. The HRR for this fuel package remains above 0.5 MW until approximately 800 seconds after ignition.

Although the total energy release among the four experiments listed in Table 4.9 are similar, the timeframe in which the energy was released for these fuel packages varied. The three pallet triangle reached a peak HRR before 100 seconds, followed by a gradual decay over the next 500 seconds. The three pallet lean-to maintains a high HRR between 100 and 350 seconds, followed by a more rapid decline over the next 150 seconds. The horizontally stacked pallets had the lowest peak HRR of the four fuel packages, but maintained an HRR close to this peak for a longer period of time, and

declined slowly from this peak. Much like the difference between six and seven vertical pallet fuel loads discussed in Section 4.1.4, the rack fuel load increases the packing density of the pallets and straw, which dampened the initial growth of the fire, leading to a peak later in the experiment. After this peak, the HRR decreased gradually. These differences in behavior illustrate the importance of geometry in the growth of three pallet fuel packages.

In order to further examine the effect of geometry on fire growth, three of the training fuel loads were composed of six pallets and one bale of straw in different orientations. These fuel loads are shown in Figure 4.19. Figure 4.20 shows the HRR time histories for each of these three cases to examine the effects of geometry on fire growth.



Figure 4.19: 6 Pallet Fuel Package Comparison. Each fuel package has 6 pallets and one bale of straw. Fuel packages shown are labeled 6P1S (left), 6PGa (center), and 6PFi (right)

Label	Fuel Package
6P1S-V	6 pallets, arranged vertically, stuffed with 1 bale of straw
6P1S-Ga	6 pallets, stuffed with 1 bale of straw, with three pallets arranged into a triangle, one pallet placed on each end, and one over the top
6P1S-Fi	6 pallets, stuffed with 1 bale of straw, with three pallets used to create a platform for the other three pallets to sit atop.

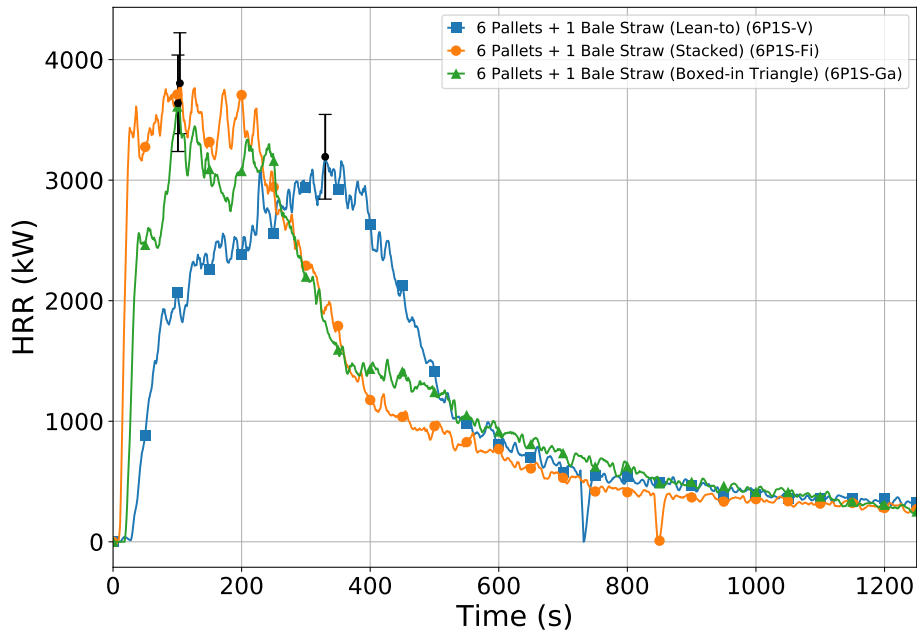


Figure 4.20: HRR (kW) vs. time for 6 pallet configurations

The six pallet fuel loads tested had similar peak HRRs ranging from 3.19 MW to 3.80 MW. The most distinct difference between the three training fuel loads was the slope of the HRR in the period leading up to the peak. This value indicates how quickly the HRR increases following ignition. The highest peak slope of the HRR was observed in the 6P1S-Fi configuration, with a slope of 68 kW/s. The 6P1s-Ga had the next highest peak HRR slope of 51 kW/s. The lowest peak HRR slope measured in the six pallet configurations was 37 kW/s, observed in the 6P1S-V configuration.

Since each of the fuel packages has a similar weight of fuel, and thus a similar total energy content, the difference in the growth rate can be attributed to the arrangement of the pallets and straw. Figure 4.19 shows the three six pallet configurations that were evaluated. In the 6P1S-Fi fuel package (shown on the right), the pallets are stacked approximately two pallet-heights high. This means that following ignition, this fuel is exposed to the high heat fluxes in the plume, facilitating the ignition of a large quantity of fuel at the same time, hence the rapid initial slope of the HRR graph. The two other fuel packages had the majority of the fuel located closer to the ground. The difference between these two fuel packages lies in the amount of surface area of the fuel that is exposed. The 6P1S orientation (shown on the left) has the slowest growth to the peak HRR, which is likely because the packing density of the pallets and straw is higher. In the 6P1S-Ga case (center), the pallets are arranged in so that more faces of the pallets are exposed and the packing density of the straw is not as high. The difference between these two cases would be similar to a fluffed bale of excelsior compared to a compacted bale. Since oxygen is not available to the burning surfaces between the stacked pallets in the 6P1S case, the growth is slower than in the 6PGa case, where the pallets are more spread out. Thus, while fuel package orientation influenced peak HRR and growth for the three pallet geometries, the six pallet geometries only varied in terms of the growth rate.



Figure 4.21: Visuals of fuel packages at the time of the peak free burn HRR. From left to right, the images show the 6P1S-V (3.19 MW), 6P1S-Fi (3.80 MW), and 6P1S-Ga (3.64 MW) fuel packages

### **Other Wood Products in Training Fuel Packages**

Among the materials considered permissible as fuels for live fire training according to *NFPA 1403* are engineered wood products, such as OSB and MDF. Engineered wood products are typically composed of small wood chips pressed together and bonded with some type of resin. Typical resins used in OSB include phenol formaldehyde (PF), melamine fortified urea formaldehyde (MUF), or isocyanate (PMDI). These materials may be selected in addition to or in place of pallets for any number of reasons. One of the discussions among training instructors who incorporate these materials into training fuel packages is whether the benefits of using engineered wood products is offset by potential health concerns based on the synthetic resins in these materials. In fact, some training facilities have opted for using dimensional lumber instead of engineered wood products, with the belief that it is cleaner than other products.





Figure 4.22: OSB (left), MDF (middle), and 1 in. x 6 in. dimensional lumber (right) fuel packages. Each fuel package has three pallets and one bale of straw in addition to the boards/lumber.

Label	Fuel Package
3P1SO	three pallets, arranged in a triangle, stuffed with 1 bale of straw, with two vertical 4 ft x 8 ft sheets of OSB
3P1SDL	three pallets, arranged in a triangle, stuffed with 1 bale of straw, with 12 vertical 1 in. x 6 in. boards of dimensional lumber
3P1SM	three pallets, arranged in a triangle, stuffed with 1 bale of straw, with two vertical 4 ft x 8 ft sheets of MDF

Figure 4.22 shows the training fuel packages which incorporated OSB, MDF, and 1 in. x 6 in. dimensional lumber were comparable in terms of peak free burn HRR, peak burning duration, and peak growth rate, which can be seen in Figure 4.23. They were characterized by rapid growth shortly following ignition to their peak HRR. The 3P1SO and 3P1SDL fuel packages each had a similar peak free burn HRR of 2.40 MW and 2.44 MW, respectively. Further, the peak slope of the HRR graph was 44 kW/s for both fuel packages. The peak burning period was 239 seconds for the dimensional lumber fuel package, compared to 151 seconds for the OSB fuel package. The fuel package consisting of pallets, straw, and MDF (3P1SM) weighed approximately 20 kg more than the 3P1SO and 3P1SDL fuel packages. The 3P1SM fuel package had a peak free burn HRR of 2.73 MW and a peak growth rate of 52 kW/s. The peak HRR and slope of the HRR graph observed for the 3P1SM configuration was slightly higher than the other two training fuel packages which included engineered wood products.

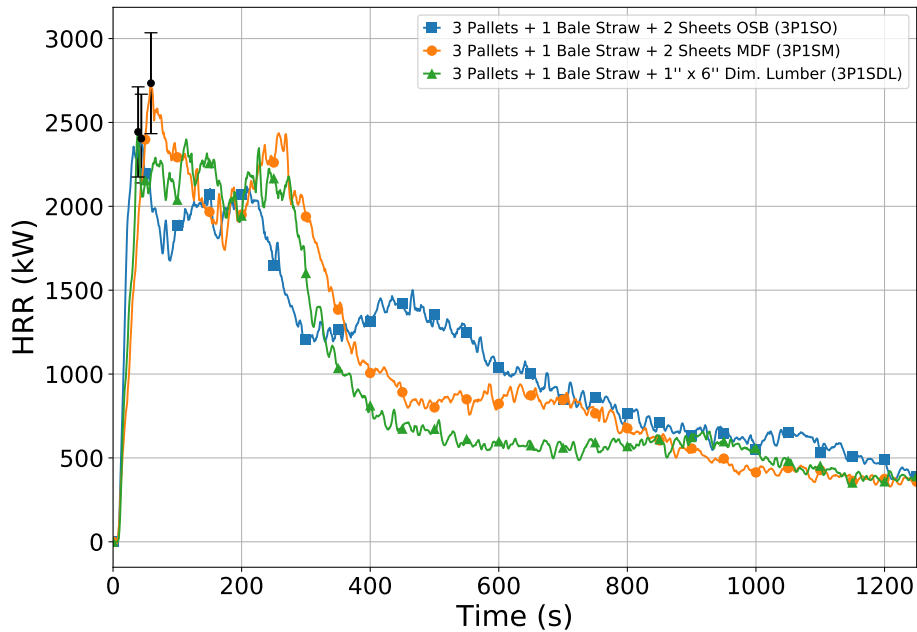


Figure 4.23: Comparison of HRR for OSB, MDF, and 1 in. x 6 in. dimensional lumber

The peak free burn HRR values for the OSB (3P1SO) and dimensional lumber (3P1SDL) fuel packages were comparable to the fuel package with three pallets and two bales of straw (3P2S), which had a peak HRR of 2.45 MW. The duration of the peak burning period for this experiment was 140 seconds, and the peak growth rate was 42 kW/s. Although the OSB and dimensional lumber fuel packages had a larger fuel weight than the fuel package with three pallets and two bales of straw, the peak free burn HRR, peak HRR growth rate, and peak burning duration were all comparable. The pallets and straw fuel package with a fuel weight closest to that of the OSB and dimensional lumber fuel packages is the fuel package with five vertically stacked pallets and a bale of straw (5P1S-V). The peak HRR for this fuel package (2.91 MW) was higher than that observed for the OSB and dimensional lumber fuel packages. The weight of the MDF fuel package (3P1SM) was comparable to the fuel packages consisting of six pallets and one bale of straw. The 3P1SM fuel package had a peak free burn HRR of 2.73, which was between 17% and 39% lower than the three six pallet configurations, which had peaks HRRs of 3.19 MW, 3.80 MW, and 3.64 MW for 6P1S-V, 6P1S-Fi, and 6P1S-Ga, respectively.

The magnitude of the peak HRR was less for the fuel packages which included engineered lumber than was observed in training fuel packages of a similar weight that incorporated more traditional training fuels such as pallets, straw, and excelsior. Thus, the inclusion of engineered lumber into the fuel package did not have a significant impact in terms of increasing the peak free-burn HRR nor the duration of peak burning, although the fuel packages incorporating engineered lumber did exhibit growth rates as high or higher than fuel packages of a similar weight that did not incorporate engineered lumber.

### 4.1.5 Training Fuel Packages vs. Furnishings

The effective heat of combustion analysis from Section 4.1.4 indicated that the  $\Delta h_c$  values for wood-based products were constant, with the geometry and amount of fuel in the fuel package being the most important parameters dictating fire dynamics. This is because these fuel packages are primarily composed of different types of wood and similar materials. The wood-based fuels permitted for use in live fire training by *NFPA 1403* are different from many of the materials that make up the furnishings in modern homes. These synthetic foams and plastics typically have higher effective heats of combustion than wood-based fuels. For example, the heat of combustion of polyurethane is 23.90 MJ/kg [34], compared to the effective heat of combustion computed for the training fuels packages (14.0-14.1 MJ/kg). In order to further characterize the difference in energy release between these two groups of fuels, consider the HRR experiments conducted on a sofa, a chair, and a bed in the context of the 17 training fuel packages.

The upholstered sofa that was tested weighed slightly more than the single bale of excelsior, but less than two bales of excelsior. The peak free burn HRR that was observed for the sofas varied between the three experiments. Figure 4.25 shows the peak free burn HRR plotted against the initial weight for each of the three sofa tests and comparable training fuel packages. When the sofa was ignited in the left arm, the peak HRR was 2.46 MW, which was comparable to the three pallet configurations with two bales of straw, one bale of excelsior, dimension lumber, or OSB (3P2S, 3P1E, 3P1SO, and 3P1SDL). When ignited on the cushion close to the right arm of the sofa or in the center, however, growth was more rapid and the peak HRR was between 3.70 and 3.72 MW, which was comparable to the six and seven pallet configurations. These high peak HRRs relative to the initial weight of the sofa are indicative of the high  $\Delta h_{c,eff}$  of the sofa components. The peak free burn HRRs observed for the kit sofas were lower than the highest peak HRRs observed for the upholstered sofas. Images of the two sofas are shown in Figure 4.24. The peak HRRs observed for the kit sofas was 1.82 MW. The kit sofa weighed about 20 kg less than the upholstered sofas, making it comparable by weight and peak HRR to the training fuel loads consisting of two bales of straw or one bale of excelsior. The peak burning duration for the kit sofa experiments was 108 s, which was longer than the 1E or 2S training fuel packages.



Figure 4.24: Images of the two sofas evaluated in HRR testing. The upholstered sofa (left) and the kit sofa (right). The kit sofa required assembly, whereas the upholstered sofa was delivered in one piece.



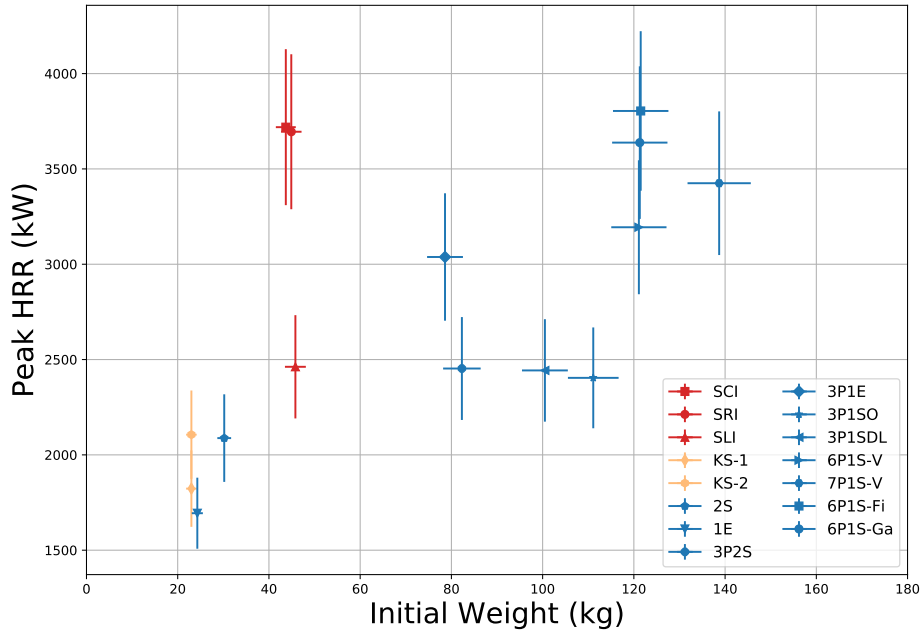


Figure 4.25: Weight vs. peak HRR comparison for sofa and comparable training fuel packages. Blue markers denote training fuel packages, red markers denote the upholstered sofa (SRI, SCI, SLI), and orange markers denote the kit sofa (KS-1, KS-2)

The difference in combustion between the upholstered sofa and the wood-based training fuels did not only affect the energy release characteristics. Figure 4.26 shows two of the sofa experiments at the time of the peak HRR compared to wood-based training fuels of a similar peak HRR. Visually, the sofas produced a greater quantity of soot, which had the effect of obscuring the lighting within the laboratory. The pallet fuel packages, on the other hand, did not produce a sufficient quantity of soot to obscure the lighting. This is indicative of the higher soot yield of synthetic materials, such as polyurethane, compared to wood-based fuels. Although the peak free burn HRRs vary by only 2%, it is important to note that the smoke released by the upholstered sofas contains fuel which would have the potential to ignite again if mixed with the appropriate amount of oxygen in a compartment setting. The visual differences in the free burn experiments help to illustrate the differences in combustion between the sofas, which have a primarily synthetic makeup, and the wood-based training fuels.



Figure 4.26: Images corresponding to the peak HRR for the upholstered sofa ignited in the center (top left) and right arm (bottom left) compared to wood-based training fuel packages of comparable peak HRRs. The center-ignition sofa had a peak free burn HRR of 3.47 MW which is comparable to the six pallet boxed-in triangle fuel load (top right) which had a peak HRR of 3.64 MW. The right-ignition sofa had a peak HRR of 3.72 MW, which is comparable to the six pallet lean-to (bottom right), which had a peak HRR of 3.21 MW. The error bars corresponding to each point indicate the uncertainty of the measurement.

The peak free burn HRRs of the upholstered chairs (SC-1 - SC-3, YC-1 and YC-2) that were tested fell between 1.61 and 2.14 MW and the weights ranged from 24.8 kg to 28.3 kg. Figure 4.27 shows that these chairs are comparable in terms of both peak HRR and initial weight to the training fuel packages consisting of two bales of straw or one bale of excelsior. Other training fuel packages which weighed more but had a comparable peak HRR were the four vertical pallets and straw, the two bales of excelsior, and the three pallets and straw in the innovative rack configuration. The barrel chair weighs substantially less than any of the other furniture items or training fuel packages. Despite this, the peak free burn HRR observed was 0.85 MW.

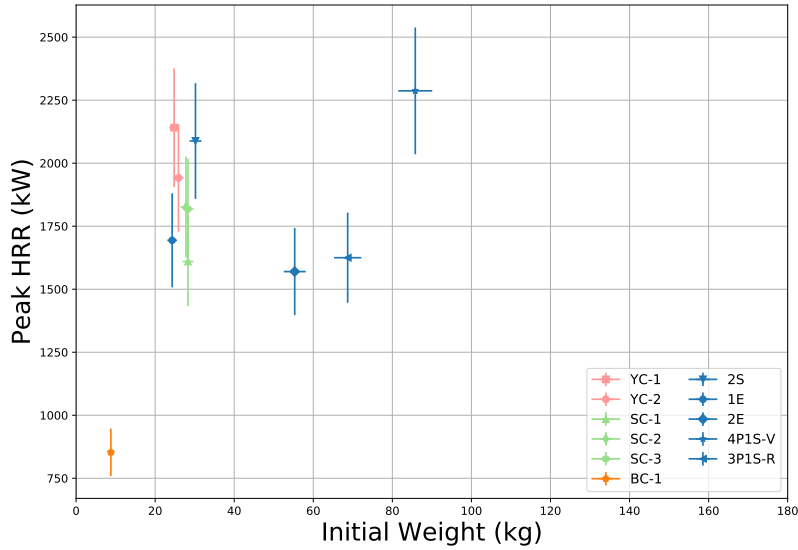


Figure 4.27: Weight vs. peak HRR comparison for chairs and comparable training fuel packages. Blue markers denote training fuel packages, pink markers denote replicates of the yellow upholstered chair, and green markers denote replicates of the striped upholstered chair. The error bars corresponding to each point indicate the uncertainty of the measurement.

The two bed sets had the highest fuel weight of the furniture items tested, weighing between 229 kg and 231 kg. Figure 4.28 compares the peak free burn HRR of the bed sets to training fuel packages of a similar weight. Although the bed sets weighed more than the armchairs, the peak HRRs were in a similar range, 1.85 MW and 2.23 MW. This places the peak HRR of the bed sets in a range that is comparable to the three pallet configurations with two bales of straw, one bale of excelsior, dimension lumber, or OSB (3P2S, 3P1E, 3P1SO, and 3P1SDL).

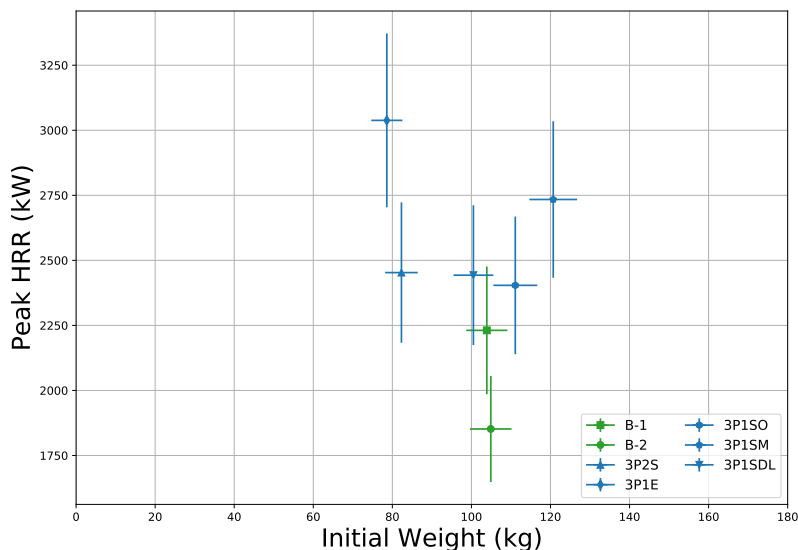


Figure 4.28: Weight vs. peak HRR comparison for bed sets and comparable training fuel packages. Blue markers denote training fuel packages and green markers denote replicates of the bedset fuel package. The error bars corresponding to each point indicate the uncertainty of the measurement.

The highest peak free burn HRR among the furniture items were the upholstered sofas. These two fuel packages had a fuel weight similar to the three-pallet training fuel packages, but a peak HRR similar to the six pallet configurations. The higher  $\Delta h_{c,eff}$  of the synthetic components of the sofa enables the high peak HRR that were observed. The chairs had a similar weight and peak HRR to the high-surface area wood fuels, such as straw and excelsior. The fire growth of the bed sets was hampered by the geometry of the beds, since the fire had to spread laterally across the bed, rather than being aided by concurrent-flow flame spread, as was the case in many of the training fuel packages.

The higher energy content of the furniture items can be seen by plotting the average HRR against the corresponding MLR during the peak burning period, as was done in Figure 4.5. Figure 4.29 shows the peak burning HRR and MLR for both the training fuel packages and furniture items. The chart shows that for a given MLR, the furniture items tend to have a higher HRR than training fuels of a similar weight. Thus, while high HRRs in the training fuels were primarily driven by the geometry of the fuel package and the weight of fuel in the packet, the peak HRR of the furniture items that were tested was driven by both the geometry of the items and the higher  $\Delta h_{c,eff}$  of the components.

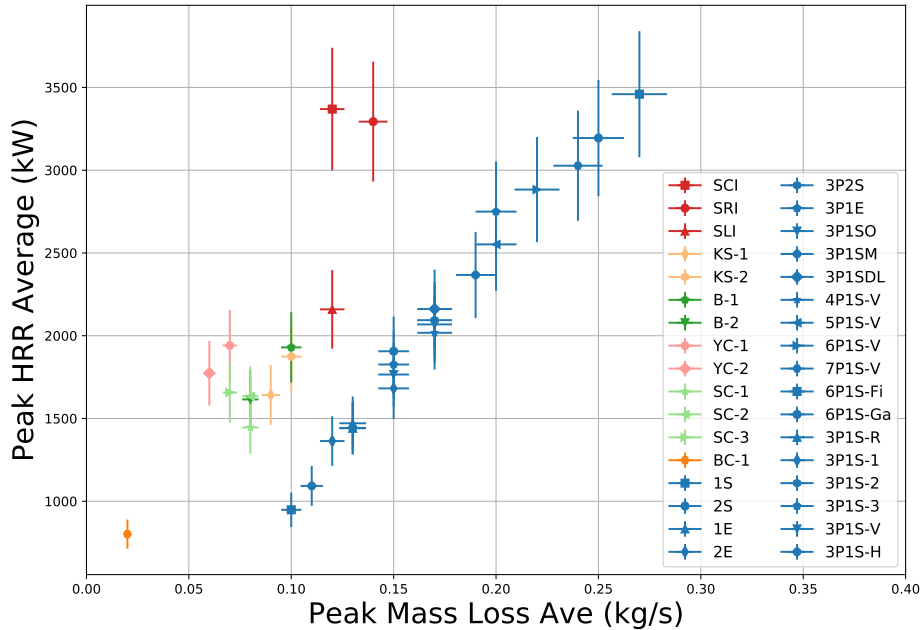


Figure 4.29: Average HRR (kW) vs. average MLR (kg/s) over peak burning period for wood-based and synthetic fuels. Blue markers denoted wood-based training fuel packages, red markers denote upholstered sofas, dark green markers denote bed sets, pink and light green markers denote upholstered chairs, orange markers denote barrel chairs, and yellow markers denote kit sofas. The error bars corresponding to each point indicate the uncertainty of the measurement.

#### 4.1.6 Free Burn HRR Limitations

While precautions were taken to minimize procedural error during the free burn HRR experiments, the limitations of these HRR experiments should be considered when reviewing the free burn HRR results. Because of budget and time constraints, no replicate experiments were conducted for the training fuel packages. Because of this, the repeatability of the peak HRR measurements for each fuel package is unknown. It is important to consider the uncertainty associated with the HRR measurements when comparing the reported free burn HRR values for these experiments. The free burn HRR experiments were also conducted without any compartment effects from walls or ceilings. It is possible that re-radiation from compartment surfaces may affect fire growth. Additionally, ignition of smoke within a compartment would impact the HRR and the fire growth within the compartment. Further, while fuel weights were recorded and reported, the moisture content and packing density of the fuel packages were not recorded. These two parameters have the propensity to vary significantly depending on the supply, storage conditions, and construction of a particular training fuel configuration. Further experiments should be conducted, with replicates, to examine the effect of these parameters on training fire growth.

## 4.2 Compartment HRR Experiments

The previous section details the results of the free burn HRR experiments that were conducted on various training fuel packages and furniture items. It is important to note that the peak HRR values reported for these experiments are free burn HRRs, and it is possible that the peak HRR would change if the training fuel load was burning in a compartment. In order to examine these compartmentation effects, four additional HRR experiments were conducted in a 12 ft. x 12 ft. (3.6 m x 3.6 m) room with 8 ft. (2.4 m) ceilings. The compartment was framed with dimensional lumber and had an interior finish of gypsum board. The room had a 8 ft. (2.4 m) wide x 6.67 ft. (2.0 m) tall doorway to provide ample ventilation to the compartment. While the fire dynamics produced by each of the training fuel packages would likely change depending on the dimensions, ventilation, and lining materials of the compartment, this HRR data can be used to compare the fuels in a compartment using a common ventilation configuration.

Two training fuel loads and two furnished rooms were evaluated. The training fuel loads consisted of three pallets and one bale of straw and three pallets, one bale of straw, and 2 0.44 in. x 4 ft. x 8 ft. sheets of OSB. The pallets were arranged in a triangle on top of a steel burn rack. The burn rack, which consisted of four steel legs supporting a frame, on top of which is laid an approximately 4 ft. x 4 ft. (1.22 m x 1.22 m) flattened, perforated steel sheet, allowing air entrainment into the bottom of the pallet assembly. The frame supports the pallets so that they sit 1 ft. (0.30 m) above the floor of the fire room. The burn rack was placed along the wall of the compartment opposite the opening, as shown in Figure 4.30.



Figure 4.30: Training fuel load position for pallets (left) and OSB (center) and furniture locations (right) for compartment HRR experiments.

The furniture fuel load consisted of the furniture items listed in Table 4.10 and arranged as shown in Figure 4.30. The kit sofas and barrel chairs used in the fuel package were purchased from the same manufacturer as those that were evaluated in Section 4.1. The furniture was selected to simulate the living room of a modern home. The combined weight of the furnished room fuel package was approximately 309.2 lbs. (140.5 kg).

Table 4.10: Furnished Room Contents

Furniture Item	Quantity	Weight per Item (lbs. (kg))	Total Weight (lbs. (kg))
Kit Sofa	2	50.7 (23.0)	101.4 (46.0)
Barrel Chair	2	8.4 (3.8)	16.8 (7.6)
End Table	2	17.0 (7.7)	34.0 (15.4)
Coffee Table	1	45.4 (20.6)	45.4 (20.6)
Tall Table	1	47.6 (21.6)	47.6 (21.6)
Carpet	1	34.8 (15.8)	34.8 (15.8)
Carpet Padding	1	24.0 (10.9)	24.0 (10.9)
Lamp	2	2.6 (1.2)	5.1 (2.3)
Total			309.2 (140.5)

### 4.2.1 Results

The results of the HRR characterization experiments are summarized in Figures 4.31 and 4.32 and Table 4.11.

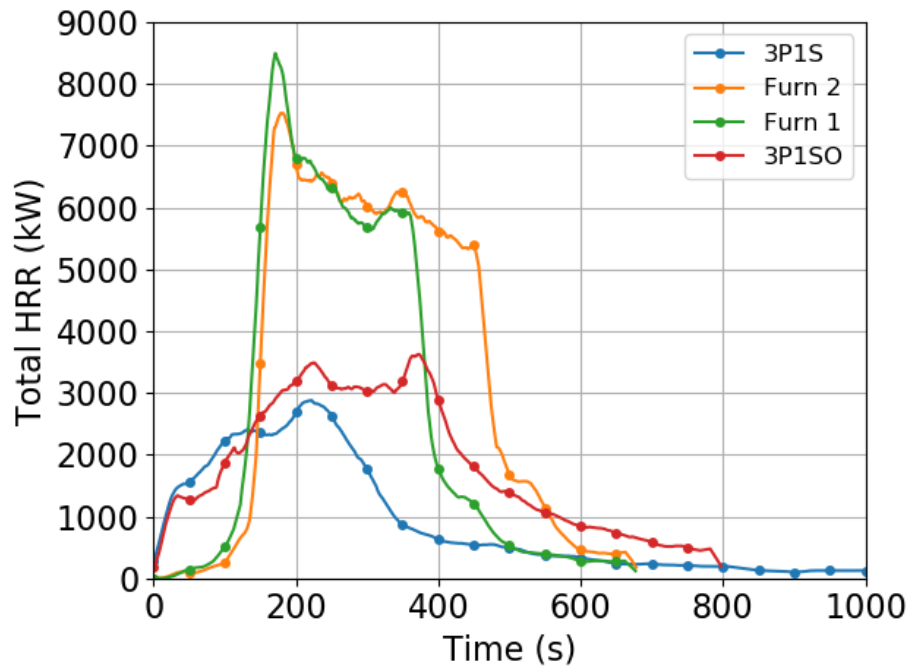


Figure 4.31: HRR vs. Time for Compartment HRR Characterization Experiments.

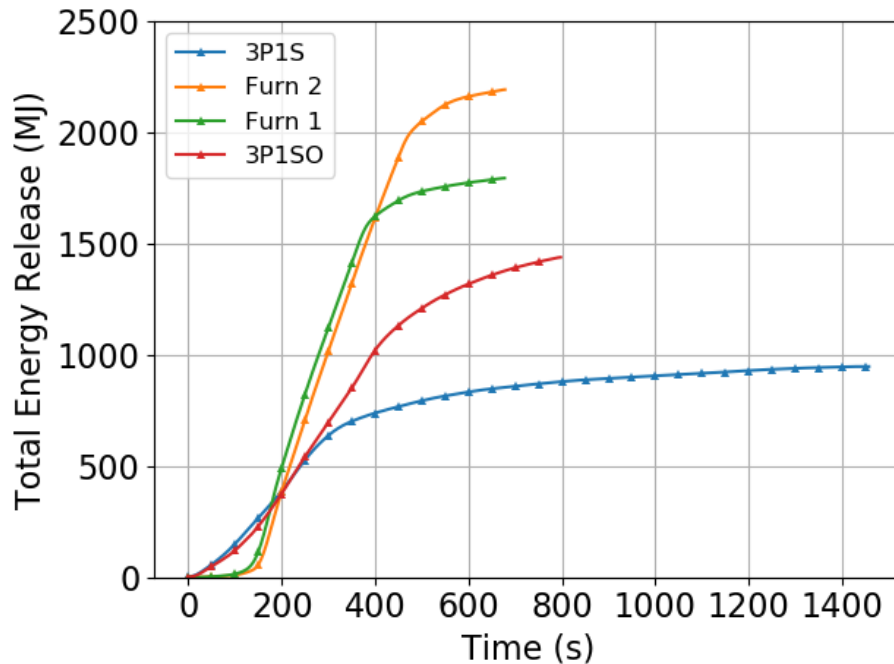


Figure 4.32: Total Energy Released vs. Time for Compartment HRR Characterization Experiments.

Table 4.11: Peak HRR and Total Energy Released for HRR Characterization Experiments

Fuel Package	Peak HRR (MW)	Total Energy Released (MJ)
3P1S	3.05	950
3P1SO	3.77	1440
Furnished Room 1	9.12	1790
Furnished Room 2	8.06	2190

The time history plots used to develop Table 4.11 are located in Appendix A.3.

The rate of change of the HRR in the pallets and straw experiment remained positive until approximately 250 seconds after ignition. The peak slope of the heat release curve was noted in the period following the start of fire growth, where the rate of change of HRR was 30 kW/s. The peak HRR was 59% greater than the free burn pallets HRR experiment. The total heat release in the pallets and straw compartment experiment was similar ( $\pm 11\%$ ) to the total heat release in the free burn pallets experiment. Similarly, the peak HRR observed for the OSB fuel package in the compartment was 3.77 MW, which was 57% higher than the peak free burn HRR, which was 2.40 MW. The rate at which the HRR increased in the period leading up to the peak HRR, however, was lower in the compartment than in the free burn scenario, which may be because the OSB was unable to



burn on the back side due to the rear wall of the compartment. The peak HRR growth rate during the OSB fuel package test was similar to the pallets and straw with a peak slope of approximately 30 kW/s. The total heat release in the OSB compartment experiment was similar ( $\pm 7\%$ ) to the total heat release in the free burn OSB experiment.

The peak HRR observed in the OSB fuel package was 24% higher than that noted in the pallets and straw experiment. Perhaps a more significant difference can be seen in Figure 4.32, which illustrates that the total energy released by the OSB fuel package was 52% greater than that released by the pallets and straw fuel package. This trend is also manifested in Figure 4.31, looking at the OSB fuel package, the HRR remained above 3 MW for another 200 seconds before beginning to decrease. Alternatively, looking at the pallets and straw plot, the HRR began to decrease almost immediately after reaching its maximum value. So, while the peak growth rates of the two training fuel packages were similar, the OSB exhibited a higher peak HRR. The additional fuel mass in the OSB fuel package enables a longer peak burning period than the pallets fuel package.

Two replicate HRR tests, Furnished Room 1 and Furnished Room 2, were performed using the same furnishings and layout. In both experiments, the HRR did not begin to increase significantly until more than 50 seconds from the beginning of the experiment. Once this point was reached, however, the rate of HRR increase was above 150 kW/s, approximately five times the rate of the training fuels. Both furnished rooms reached their peak HRR between 150 and 200 seconds. The peak HRR in Furnished Room 1 was 9.12 MW, which was 13% higher than the 8.06 MW peak observed in the Furnished Room 2. After reaching its peak, the HRR remained high, which resulted in total energy releases that were higher than both training fuels. The HRR rapidly declined after this period. In Furnished Room 1 HRRs greater than 5.5 MW were observed for approximately 200 seconds. In the Furnished Room 2, HRRs above 5.5 MW were observed for approximately 300 seconds. Thus, in addition to exhibiting higher peak HRRs than the training fuel packages, the furnished rooms maintained a fully developed period for longer than either the pallets or the OSB training fuel packages.

## 4.2.2 Discussion

A significant increase in peak HRR was observed for both the 3P1S and 3P1SO fuel packages in the compartment as compared to their peak free burn HRR. The effect of the compartment on the growth of the fire may be attributed to a number of factors, including re-radiation from ceiling, the contribution of the burning drywall, and ignition of unburned fuel in the smoke produced by the fuel packages. This increase in HRR may be significant if instructors are attempting to select a fuel package that will not result in flashover for a given compartment by using the free burn HRR. *NFPA 1403* Section A.4.13.7 provides a method published by Babrauskas for evaluating the minimum HRR required for flashover, which is shown in Equation 4.4. This equation is provided in *NFPA 1403* in an effort to help instructors design a fuel package large enough to bring a room to flashover in order to demonstrate ventilation-limited fire behavior. Since the free burn peak HRR provides a conservative estimate for fire size, this method is appropriate for predicting the minimum fire size required to cause flashover. However, if this method was instead used to predict

the maximum fuel package size while still preventing unwanted flashover, the use of free burn HRR results may be misleading. The minimum HRR required for flashover defined in Equation 4.4 is based on the characteristics of the compartment, where  $A_o$  is the area of the vent and  $H_o$  is the height of the vent. This correlation predicts that a HRR of 5.0 MW is required for flashover in the compartment used for these experiments.

$$\dot{Q} = 750A_o\sqrt{H_o} \quad (4.4)$$

Figure 4.33 shows the free burn and compartment HRR results for the 3P1S and 3P1SO fuel packages. The peak free burn HRR of the 3P1SO training fuel package was 2.40 MW, but the results of the compartment HRR experiment showed that the peak HRR for the same fuel package was 3.63 MW when placed in the compartment. The 3P1S fuel package increased in a similar way, from a 1.60 MW peak in the free burn experiment to 3.05 MW in the compartment experiment. Although the peak HRR increased for both the pallet fuel package and the OSB fuel package due to compartmentation, it remained below the minimum HRR required for flashover predicted by Babrauskas. For each of the training fuel packages, the compartment effects resulted in an increase in peak HRR of between 57% and 59%. It is likely that at least part of this increase is the contribution of the burning gypsum lining of the compartment. A series of cone calorimeter experiments conducted by Mowrer [35] indicates that the unit heat release rate of unpainted gypsum wallboard ranges from 50-100 kW/m<sup>2</sup>. Another possible reason for the increase in HRR in the compartment is that unburned fuels in the smoke produced by the training fuel packages was able to ignite as it traveled along the ceiling of the compartment and mixed with fresh air. This increase in burning would not be possible in the free burn scenario, and would result in a higher HRR.

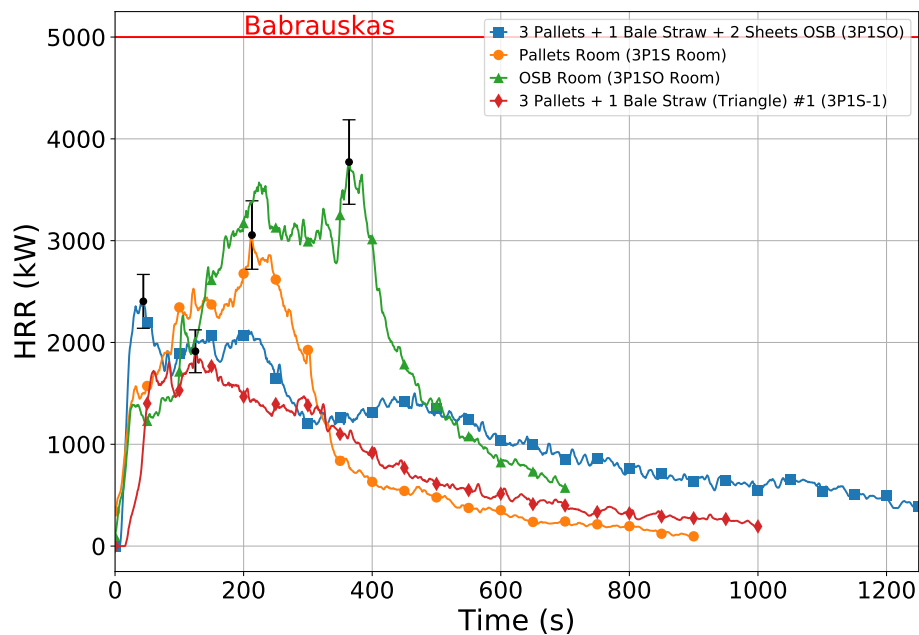


Figure 4.33: Comparison of free burn vs. compartment HRR for training fuel loads. The horizontal red line denote the predicted minimum HRR required for flashover from Equation 4.4.



Figure 4.34: Comparison of peak burning conditions for 3P1S (left), 3P1SO (center), and furnished room (right).

The peak HRR observed in the furnished rooms was more than twice as high as either of the training fuels. Further, the peak rate of HRR increase in both of the furnished rooms was nearly five times greater than the peak rate observed in the chair or the sofa, indicating that compartmentation, ignition of smoke, and the amount of fuel in the room play important roles in fire development. The reason for this rapid growth is related to both the quantity and location of the fuel within the compartment. In the training fuel packages, all of the fuel in the room is centralized in the area of the fuel package. The growth of the fire produced by these fuel packages is largely related to the arrangement of the fuel, which is conducive to rapid fire spread. The most rapid growth during the training fuel experiments was noted shortly after ignition, and the magnitude of the peak HRR is related to the amount of fuel surface available for burning. In the furnished rooms, the fuel is spread across the room, rather than being confined to a central location. Instead of rapid fire spread immediately following ignition, the most rapid period of fire growth comes approximately 100 seconds after ignition, as radiation from the upper gas layer heats fuels in remote parts of the rooms to their ignition temperature. This phenomenon is responsible for the 7-8 MW increase in HRR in 100 seconds that was observed in both of the furnished room experiments. Thus, although individual items of furniture exhibited peak free burn HRR values that were comparable to or less than wood-based training fuel packages, when multiple furniture items are placed in the same compartment and ignited, their combined heat release rate can quickly overwhelm the available ventilation, resulting in flashover. Furthermore, peak free burn HRR values for training fuel packages should be treated as conservative estimates, since it is possible for the peak HRR to increase depending on the compartment characteristics, which may lead to undesired flashover.

### 4.2.3 Compartment HRR Limitations

Just as with the free burn HRR experiments, it is important to understand the limitations of the compartment HRR experiments when considering the results. No replicate experiments were conducted, emphasizing the importance of the measurement uncertainty when comparing values between experiments. The three compartment HRR experiments that were conducted offer a limited insight into the behavior of the various fuel packages that were evaluated in the free burn HRR testing. Additionally, the compartment that was used had a ventilation opening that was unrealistically large. Most vents in training props would be smaller, and would introduce ventilation effects in addition to the compartment effects. Further compartment HRR experiments should be conducted

to better understand the relationship between free burn and compartment HRR, characterize the repeatability of training fuel packages, and examine the effects of different compartment sizes and linings.

# 5 Training Prop Experiments

The HRR characterization described in Chapter 4 provides a comparison of several training fuel packages in an environment independent of compartment and ventilation effects. While this comparison is useful, it is also important to compare these fuels in a setting where the fire dynamics may be affected by ventilation and training prop configuration. It is also important for instructors and students to recognize that the fire dynamics produced by a particular training fuel package may vary considerably depending on the ventilation, interior volume, and lining of the training prop used in the evolution.

## 5.1 Methodology

In an effort to evaluate training fuel packages in an environment similar to that in which they may be used, 25 experiments were conducted in a metal-lined container prop, shown in Figure 5.1. The fuel packages that were used in these experiments consisted of wood-based fuel packages and fuel packages with combinations of wood-based and synthetic materials, which would not be compliant with *NFPA 1403*. Different sizes of wood-based fuel packages were evaluated, as well as fuel-packages using engineered wood-products instead of pallets or dimensional lumber. The metal-lined container props, the instrumentation that was installed in these props, and the fuel packages used in the experiments are detailed in the following sections.

## 5.2 Structure

The metal container prop was in the shape of a “T” and contained a dividing wall down the middle, separating the prop into two “L”-shaped sides that were mirror images of one another. This prop was previously used in Part II of this project. The metal prop was chosen for this series of experiments for several reasons. Metal training props are growing in popularity among fire training facilities because of their modular nature and low cost compared to concrete live fire training buildings. *Evaluation of Ventilation-Controlled Fires in L-Shaped Training Props* [10] showed that metal container props are capable of being used to demonstrate ventilation-controlled fires, whereas concrete buildings were not as effective at doing so because of their high leakage area. Additionally, the configuration of these props allowed for a configuration of a fire room connected to a hallway, which can be used to estimate the thermal conditions to which a hose crew advancing down the hallway would be subjected.

The leakage of the structure was determined through the use of a blower door test in accordance with ANSI E1872. A Retrotec model 5101 blower door was used in accordance with the user manual [36].



Figure 5.1: Exterior views of the Metal Prop. Top image is of the front and the bottom images are of the left and right sides.

The standard for leakage of a structure is determined by the International Energy Conservation Code (IECC). In 2009 the leakage for all climate zones could not exceed seven air changes per hour. In the 2012 version, the requirement was increased to less than or equal to three or five air changes per hour, depending on the climate zone. The structure had a leakage rate of 25 air changes per hour making it significantly higher than the permissible leakage for residential structures.

Another measure of air leakage, Equivalent Leakage Area (ELA) was also calculated through the use of the blower door. This measurement takes into account all the leakage in a structure, as a flow, and calculates an opening size required to permit that flow. The structures used had an equivalent leakage area of  $1.2 \text{ ft}^2$  ( $0.11 \text{ m}^2$ ). This is equivalent to having a 15 in. diameter hole in the structure. In reality this area is distributed throughout all the smaller openings like those found around windows; however, this calculation allows for the visualization of the size of opening required to provide the leakage rate found in the test fixture utilized.





4 ft (1.2 m). and 7 ft (2.1 m). from the floor. The device used to measure opacity was a Green Instruments G26 Ambient Oil Mist Detector. The sensor operates by projecting a beam of green light to a reflector. The instrument measures the amount of light that is reflected, with an opacity higher than 0% indicating obscuration due to smoke.

## Measurement Uncertainty

There are different components of uncertainty in the length, mass, temperature, and heat flux reported here. Uncertainties are grouped into two categories according to the method used to estimate them. Type A uncertainties are those evaluated by statistical methods, and Type B are those evaluated by other means [37]. Type B analysis of systematic uncertainties involves estimating the upper (+ a) and lower (- a) limits for the quantity in question such that the probability that the value would be in the interval ( $\pm a$ ) is essentially 100 %. After estimating by either Type A or B analysis, the uncertainties are combined in quadrature to yield the combined standard uncertainty. Then, the combined standard uncertainty is multiplied by a coverage factor of two, which results in an expanded uncertainty with a 95 % confidence interval ( $2\sigma$ ). For some of these components, such as the zero and calibration elements, uncertainties are derived from referenced instrument specifications. For other components, referenced research results and past experience with the instruments provided input in the uncertainty determination.

Each length measurement was taken carefully. Length measurements, such as the room dimensions, instrumentation array locations, and fire apparatus (e.g., nozzle, sprinkler, or fan) placement, were made with a hand held laser measurement device that had an accuracy of  $\pm 6.0$  mm (0.25 in) over a range of 0.61 m (2.0 ft) to 15.3 m (50.0 ft) [38]. However, conditions affecting the measurement, such as levelness of the device, yields an estimated uncertainty of  $\pm 0.5$  % for measurements in the 2.0 m (6.6 ft) to 10.0 m (32.8 ft) range. Steel measuring tapes with a resolution of  $\pm 0.5$  mm (0.02 in) were used to locate individual sensors within an instrumentation array and to measure and position the furniture. The steel measuring tapes were manufactured in compliance with NIST Manual 44, which specifies a tolerance of  $\pm 1.6$  mm (0.06 in) for 9.1 m (30 ft) tapes and  $\pm 6.4$  mm (0.25 in) for 30.5 m (100 ft) tapes [39]. Some issues, such as “soft” edges on the upholstered furniture, result in an estimated total expanded uncertainty of  $\pm 1.0$  %.

The load cell used to weigh the fuels prior to the experiments had a range of 0 kg (0 lb) to 200 kg (440 lb) with a resolution of a 0.05 kg (0.11 lb) and a calibration uncertainty within 1 % [30]. The expanded uncertainty is estimated to be less than  $\pm 5$  %.

The standard uncertainty in temperature of the thermocouple wire itself is  $\pm 2.2$  °C at 277 °C and increases to  $\pm 9.5$  °C at 871 °C as determined by the wire manufacturer [40]. The variation of the temperature in the environment surrounding the thermocouple is known to be much greater than that of the wire uncertainty [41, 42]. Small diameter thermocouples were used to limit the impact of radiative heating and cooling. The estimated total expanded uncertainty for temperature in these experiments is  $\pm 15$  %.

In this study, total heat flux measurements were made with water-cooled Schmidt-Boelter gauges. The manufacturer reports a  $\pm 3$  % calibration expanded uncertainty for these devices [43]. Results from an international study on total heat flux gauge calibration and response demonstrated that the uncertainty of a Schmidt-Boelter gauge is typically  $\pm 8$  % [44].

## 5.4 Training Prop Experiment Description

Twenty two different fuel packages were evaluated in the metal training prop. These fuel packages can be considered in three groups, which correspond to the ventilation scenario used for the experiment. Three ventilation scenarios were used: door open and window closed at ignition, door and window closed with door opened six minutes after ignition, and door and window closed with window opened six minutes after ignition. Twenty-five experiments were conducted in total.

Table 5.1 lists the fourteen experiments that were conducted with the front door open at ignition. Most of these experiments were intended to be compared to a base fuel load of 3 wooden pallets and one bale of straw arranged in a triangle (Experiment 21). The triangle fuel package geometry is used by multiple fire training academies throughout the United States. Several of these fuel loads (Experiments 1, 2, 6, and 23) explored different methods to increase the optical density of the smoke in the prop, such as adding a small amount of synthetic material (tar paper or a sofa cushion) or smoke barrels. Experiments 10, 21, and 22 compare the effect of geometry on a fuel package of three pallets and one bale of straw. The remainder of the experiments explore the effect of additional fuel mass in different geometries, including adding additional pallets (Experiment 11), engineered wood products (Experiments 19 and 20), and other wood products, such as dimensional lumber or excelsior (12, 13, and 14). It should be noted that any fuel loads which include non-wood-based fuels would not be compliant with the guidelines in *NFPA 1403*.

Table 5.1: Fuel Package Descriptions with Door Open at Ignition

Experiment	Fuel Package	Total Weights lbs (kg)
1	3 pallets, 1 bale of straw, and 2.15 kg of tar paper	Pallets: 117.5 (53.4) Straw: 20.5 (9.3) Tar Paper: 4.8 (2.2)
2	3 pallets, 1 bale of straw, and 1 sofa cushion	Pallets: 118.6 (53.9) Straw: 30.1 (13.7) Cushion: 4.6 (2.1)
4	Fire Room: 3 pallets, 1 bale of straw, (3) 4 ft x 8 ft sheets of OSB (with two along the back wall of compartment and 1 across the ceiling) Hallway: (8) 4 ft x 8 ft sheets of OSB on walls and along floor	Pallets: 116.6 (53.0) OSB (fire room): 134.4 (61.1) Straw: 47.7 (21.7) OSB (hall) 273.5 (124.3)
6	3 pallets, 1 bale of straw, and 1 smoke barrel with leaf blower directed into bottom	Pallets: 106.7 (48.5) Straw: 27.5 (12.5)
10	3 pallets and 1 bale of straw oriented in a lean-to	Pallets: 107.6 (48.9) Straw: 26.8 (12.2)
11	6 pallets and 1 bale of straw oriented in a lean-to	Pallets: 209.9 (95.4) Straw: 29.7 (13.5)
12	3 pallets, 1 bale of straw, (24) 8' 1" x 6" pieces of dimensional lumber in place of OSB	Pallets: 106.7 (48.5) Straw: 24.6 (11.2) 1 x 6: 137.1 (62.3)
13	1 bale of excelsior	Excelsior: 71.7 (32.6)
14	3 pallets and 1/2 a bale of excelsior	Pallets: 106.7 (48.5) Excelsior: 35.4 (16.1)
19	3 pallets, 1 bale of straw, and (3) 4 ft x 8 ft pieces of MDF in place of OSB	Pallets: 113.5 (51.6) Straw: 27.3 (12.4) MDF: 178.0 (80.9)
20	3 pallets, 1 bale of straw, (3) 4 ft x 8 ft sheets of OSB (with two along the back wall of compartment and 1 across the ceiling)	Pallets: 125.4 (57.0) Straw: 56.1 (25.5) OSB: 134.6 (61.2)
21	3 pallets and 1 bale of straw, oriented in a triangle	Pallets: 104.3 (47.4) Straw: 28.4 (12.9)
22	3 pallets, stacked horizontally, and 1 bale of straw	Pallets: 136.8 (62.2) Straw: 27.5 (12.5)
23	3 pallets, 1 bale of straw, and 1 smoke barrel	Pallets: 101.0 (45.9) Straw: 22.7 (10.3)

Table 5.2 lists the nine experiments where the window and door to the metal prop were closed at the time of ignition, with the door being opened 6 minutes following ignition. Experiment 24 uses the same fuel load as Experiment 21, with three pallets and one bale of straw arranged in a “triangle.” These experiments explore the effect of different fuel loads and arrangements on fire dynamics. Experiment 5 examines whether covering the floor of the fire compartment with pallets can cause the room to transition to flashover. Experiments 7 and 8 examine the effect of increasing the fuel load from three to six pallets and one bale of straw. Experiment 9 compares the use of additional pallets on the rear wall and ceiling of the fire compartment, in an arrangement similar to the pallets, straw, and OSB fuel package (Experiment 25). Experiment 3 examines the effect of lining the hallway ceiling with OSB. The fuel load in Experiments 15 and 16 are comprised of furnishings such as those that may be found in a residential home. These fuel loads are intended only to serve as a comparison between synthetic fuels and wood-based training fuels, and are not training fuel loads.

Table 5.2: Fuel Package Descriptions with Door Open at 6 Minutes

Experiment	Fuel Package	Total Weights lbs (kg)
3	Fire Room: 3 pallets, 1 bale of straw, (3) 4 ft x 8 ft sheets of OSB (with two along the back wall of compartment and 1 across the ceiling) Hallway: (2) 4 ft x 8 ft sheets of OSB along hallway ceiling	Pallets: 118.6 (53.9) Straw: 20.0 (9.1) OSB (fire room): 141.0 (64.1) OSB (hall): n.a.
5	3 pallets and 1 bale of straw, oriented in a “triangle,” with 8 additional pallets laid along the floor	Pallets (triangle): 107.4 (48.8) Straw: 23.8 (10.8) Pallets (floor): 261.4 (118.8)
7	6 pallets, stuffed with 1 bale of straw, with 3 pallets arranged into a triangle, one pallet placed on each end, and one over the top	Pallets: 233.9 (106.3) Straw: 38.9 (17.7)
8	6 pallets, stuffed with 1 bale of straw, with pallets stacked to the ceiling.	Pallets: 244.4 (111.1) Straw: 28.8 (13.1)
9	3 pallets and 1 bale of straw, oriented in a “triangle,” with 4 additional pallets on the wall and 2 on the ceiling, in place of OSB	Pallets (triangle): 113.5 (51.6) Straw: 18.7 (8.5) Pallets (wall): 236.9 (107.7)
15	Furnished room consisting of upholstered sofa, coffee table, end table, carpet, and carpet padding	Sofa: 109.1 (49.6) Carpet: 27.7 (12.6) Padding: 16.1 (7.3) Tables: 78.1 (35.5)
16	Furnished room consisting of upholstered sofa, coffee table, end table, carpet, and carpet padding	Sofa: 109.1 (49.6) Carpet: 27.7 (12.6) Padding: 16.0 (7.3) Tables: 78.1 (35.5)
24	3 pallets and 1 bale of straw, oriented in a triangle	Pallets: 130.0 (59.1) Straw: 31.5 (14.3)
25	3 pallets, 1 bale of straw, (3) 4 ft x 8 ft sheets of OSB (with two along the back wall of compartment and 1 across the ceiling)	Pallets: 108.5 (49.3) Straw: 41.6 (18.9)

Table 5.3 lists the two experiments where the door and window to the training prop were closed at the time of ignition, with the fire room window being opened six minutes following ignition. These two experiments compare hay and dry straw in a fuel package consisting of three pallets arranged in a triangle.

Table 5.3: Fuel Package Descriptions with Door Closed, Window Open at 6 Minutes

Experiment	Fuel Package	Total Weights lbs (kg)
17	3 pallets and 1 bale of hay, oriented in a triangle	Pallets: 126.7 (57.6) Hay: 30.8 (14.0)
18	3 pallets and 1 bale of straw, oriented in a triangle	Pallets: 123.2 (56.0) Straw: 25.0 (11.35)



## 5.5 Results

Table 5.4 summarizes the results of the container prop experiments. The table shows the peak heat flux in the fire room and at the end of the hallway closest to the fire room, as well as the hot gas layer (HGL) temperatures at the end and start of the hallway. While these quantities certainly do not comprehensively describe the conditions produced by the various training fuels within the training prop, they can help describe the growth and characterize the magnitude of thermal conditions produced by these fuels. The fire room heat flux gauge provides an approximation of the heat flux to the floor in the fire room, and can be used as an indicator of the growth of the fire and the severity of conditions within the fire room.

Table 5.4: Container Experiments Results Summary

Exp.	Fuel Load	Peak Heat Flux		Peak HGL Temperature	
		Fire Room (kW/m <sup>2</sup> )	End Hall (kW/m <sup>2</sup> )	End Hall °F (°C)	Start Hall °F (°C)
1	3 pallet triangle, tar paper	24	13	764 (407)	466 (241)
2	3 pallet triangle, sofa cushion	19	12	736 (391)	441 (227)
3	3 pallets + OSB with OSB on hallway ceiling	52	25	1188 (642)	930 (499)
4	3 pallets + OSB with OSB on hallway walls	43	52	1194 (645)	1595 (869)
5	3 pallets with pallets on floor of fire room	91	26	1072 (578)	679 (359)
6	3 pallets with smoke barrel (leaf blower)	3	14	837 (447)	503 (262)
7	6 pallets, boxed-in triangle	51	15	1042 (561)	787 (420)
8	6 pallets, stacked to ceiling	50	15	883 (473)	598 (314)
9	3 pallets + pallets on wall and ceiling	45	26	1182 (639)	763 (406)
10	3 pallets (lean-to)	15	9	704 (373)	407 (208)
11	6 pallets (lean-to)	21	14	839 (449)	504 (262)
12	3 pallets + 1" x 6" dimensional lumber	21	20	969 (521)	582 (305)
13	1 bale excelsior, fluffed	20	9	873 (467)	503 (261)
14	3 pallets with 1/2 bale excelsior	20	12	793 (423)	456 (236)
15	Furniture	168	27	1104 (596)	683 (361)
16	Furniture	164	28	927 (497)	550 (288)
17	3 pallets + hay	18	8	669 (354)	463 (239)
18	3 pallets + straw	20	8	697 (369)	484 (251)
19	3 pallets + MDF	34	45	1140 (616)	943 (506)
20	3 pallets + OSB	38	31	1096 (591)	727 (386)
21	3 pallet triangle	18	12	748 (398)	475 (246)
22	3 pallets, horizontally stacked	17	10	733 (390)	438 (226)
23	3 pallets with smoke barrel	9	13	791 (421)	496 (258)
24	3 pallet triangle	30	11	777 (414)	496 (258)
25	3 pallets + OSB	41	20	1063 (573)	766 (408)

The end hall heat flux is an indication of the energy transfer from the products of combustion escaping the fire room to a target at the end of the hallway. This value can be used to characterize the conditions to which students advancing towards the end of the hallway may be exposed. Additionally, the HGL temperatures at the end and start of the hall can be used to approximate the conditions in the hallway and particularly the duration of the peak, or fully developed, phase.

The hot gas layer temperature comes from a simple, two-zone compartment fire model. This model assumes that there are two thermal zones, a hot upper layer and a cooler, lower layer. Each zone is a single, homogeneous temperature, and the two zones are separated by an interface, whose height is labeled  $z_{int}$ . While it is important to recognize that the two zone model is merely an approximation and that the actual temperature profile within a room is continuous, knowledge of the height of the interface and the approximated gas layer temperature,  $T_u$ , can give a simple, useful insight into the temperature profile within the hallway. Several methods exist for predicting the interface height of the hot gas layer, and the resulting temperature of said layer. One method used is outlined in the FDS Validation guide [45]. In this method, the floor-to-ceiling temperature profile is considered to be a continuous function,  $T(z)$ . Integration of  $T(z)$  from the floor ( $z = 0$ ) to the height of the room,  $H$ , yields a quantity,  $I_1$ . Using the assumption that the upper and lower gas layers are each a uniform temperature throughout, it can then be said that the  $I_1$  is then equal to the sum of two terms: the product of the hot gas layer temperature and the distance between the interface height and the height of the room, and the lower gas layer temperature and the interface height.  $I_1$  is defined in Equation 5.1.

$$I_1 = \int_0^H T(z) dz = (H - z_{int})T_u + z_{int}T_l \quad (5.1)$$

A similar method can be used to calculate a second term,  $I_2$ . In this instance, rather than integrating the temperature profile, the integral of the inverse of the temperature profile is taken. Using the same assumption as stated above,  $I_2$  is defined as shown in Equation 5.2. By solving for  $z_{int}$ , the interface height, and combining the two equations, an expression for the interface height is then obtained, as shown in Equation 5.3. In this equation,  $I_1$  and  $I_2$  are defined above,  $H$  is the height of the room, and  $T_l$  is the temperature of the lower gas layer. It assumed that  $T_l$  is equal to the temperature recorded in the lowest grid cell [45]

$$I_2 = \int_0^H \frac{1}{T(z)} dz = (H - z_{int})\frac{1}{T_u} + z_{int}\frac{1}{T_l} \quad (5.2)$$

$$z_{int} = \frac{T_l(I_1 I_2 - H^2)}{I_1 + I_2 T_l^2 - 2T_l H} \quad (5.3)$$

Once the interface height has been calculated, the hot gas layer temperature can then be computed by integrating the temperature profile,  $T(z)$ , from the interface height,  $z_{int}$ , to the ceiling height,  $H$ , and dividing by the total height of the hot gas layer,  $H - z_{int}$ , as shown in Equation 5.4.

$$T_u = \frac{\int_{z_{int}}^H T(z) dz}{H - z_{int}} \quad (5.4)$$

For these experiments, integration for the  $I_1$  and  $I_2$  terms, and for  $T_u$ , was performed numerically using a right hand scheme. The thermocouple trees had thermocouples every 1 ft from 1 ft off the

ground to 7 ft from the ground (1 ft from the ceiling). Each thermocouple was assumed to define the temperature for 6 in. in either vertical direction from the thermocouple. Additionally, the 1 ft and 7 ft thermocouples were assumed to cover the 1 ft space between the sensor and the floor or ceiling. The resulting hot gas layer temperature profiles can be used to explain the flashover phenomenon of the three fuels.

For each of the experiments, the hot gas layer descended as the fire grew, reaching a steady height between 2 ft. and 3 ft (0.9 m). from the floor for each of the experiments. The figures for the height of  $z_{int}$ , along with the remainder of the experimental charts, can be found in Appendix A.3

## 5.6 Discussion

### 5.6.1 Effect of Geometry & Quantity

The free burn HRR characterization from Section 4.1 indicated that the arrangement of fuel within the fuel package had an effect on the timing and magnitude of fire growth. In order to further examine this effect, three experiments (Experiments 10, 21, and 22) were conducted with three pallets and one bale of straw in three different orientations shown in Figure 5.3: a triangle, a lean-to, and horizontally stacked pallets.



Figure 5.3: Three pallets and one bale of straw oriented in a triangle (left), a lean-to (middle), and horizontally stacked (right)

Figure 5.4 shows the heat flux to the floor in the fire room (left) and the heat flux at the end of the hallway (right) for the three experiments. For each of the heat flux locations, the lean-to and hor-

horizontal fuel packages had similarly-shaped growth curves, while the triangle orientation followed a slightly different growth curve. In the lean-to and horizontal pallet fuel package experiments, the first peak in the heat flux charts occurs approximately 75 seconds after ignition. This peak is approximately  $10 \text{ kW/m}^2$  in the fire room and  $9 \text{ kW/m}^2$  in the hallway, and roughly corresponds with the period during which most of the straw is involved. As the straw burns away, there is a decrease in heat flux, followed by a period of steady growth to a peak heat flux. During this period, the pallets are the primary fuel that is contributing to heat release. The timing and magnitude of this second peak varied between the two fuel orientations. The lean-to fuel package reaches its peak fire room and hallway heat flux during this second growth period at approximately 400 seconds, with values of  $15 \text{ kW/m}^2$  and  $7 \text{ kW/m}^2$ , respectively. The horizontally stacked fuel package reaches its second peak later in the experiment, between 550 and 600 seconds, with peak values in the fire room and hallway of  $17 \text{ kW/m}^2$  and  $10 \text{ kW/m}^2$ , respectively. The peak heat fluxes that were observed for the lean-to fuel package were slightly lower, particularly in the hallway, than the horizontally stacked pallet fuel load. The reason for this may be the difference in fuel weight between the two experiments. The lean-to package weighed 134.4 lbs (61.2 kg), which is 29 lbs (13.2 kg) less than the horizontally stacked fuel load, which weighed 164.3 lbs (74.7 kg). The difference in weight is nearly equivalent to the weight of an additional pallet, which may be responsible for the higher peak heat fluxes.

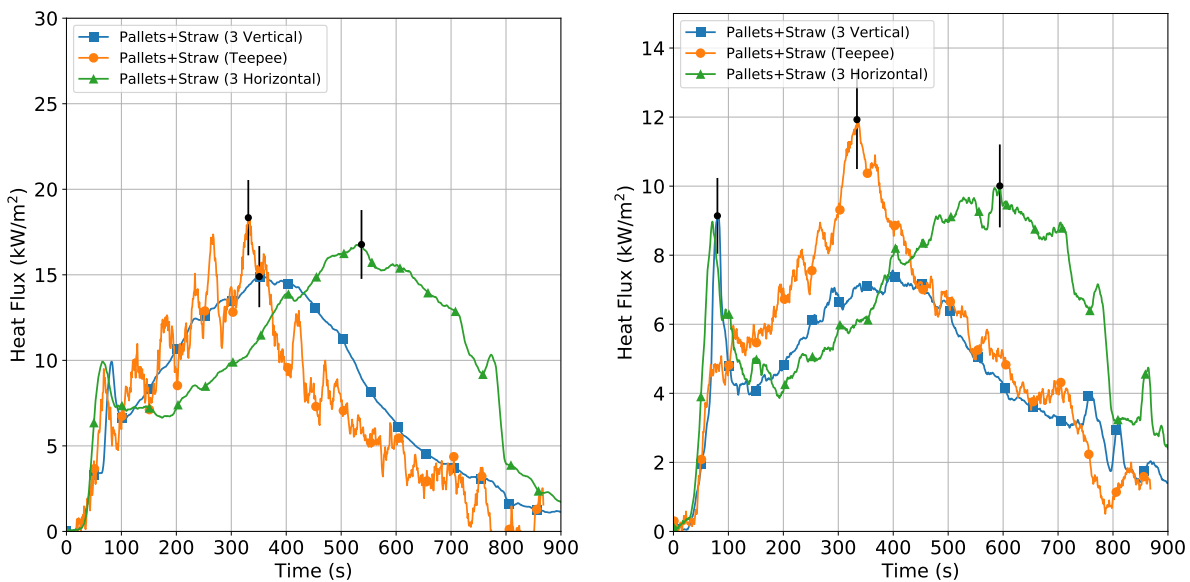


Figure 5.4: Fire room 6 in. heat flux (left) and hallway 3 ft (0.9 m) heat flux (right) for 3 pallet experiments

The heat flux data indicated that the growth of the triangle fuel package was similar to the other two orientations for the first 75 seconds. Similar to the other two three pallet fuel packages, the early growth of the pallets fuel package is characterized by burning of the straw in the center of the triangle. However, unlike these other two fuel packages, there are not two distinct peaks in the heat flux data. Rather, there is a steady growth to a peak, which occurs approximately 325 seconds after ignition. The peak heat flux values in the fire room and hallway were  $18 \text{ kW/m}^2$  and  $12 \text{ kW/m}^2$ ,

respectively. The magnitude of the peak heat flux is comparable to the horizontal fuel package, although the weight is comparable to the lean-to fuel package (137.2 lbs (60.3 kg)). The lack of the initial peak heat flux indicates that the transition between straw burning and pallets burning is more efficient in the triangle than in the other two fuel packages. In the triangle, most of the bale of straw is concentrated in the center void of the fuel package, where it can be loosely packed. The low packing density and high quantity of straw in this location exposes both sides of the pallets to high-temperature gases, increasing the surface area available for pyrolysis and facilitates burning. In the lean-to and horizontal fuel packages, the pallets are stacked or leaned against each other, which minimizes the exposed surfaces of the fuel. For these two experiments, the growth rate is largely related to the orientation of the pallets. The lean-to fuel package experiences a peak earlier in the experiment because the fuel orientation takes advantage of vertical flame spread. The horizontally stacked pallets, on the other hand, do not take advantage of vertical flame spread, and thus do not reach their peak as quickly as the more efficiently oriented fuel packages.

In addition to having effects on the timing of growth, the orientation of the pallets also affected the visibility conditions in the doorway. Figure 5.5 shows the doorway obscuration for the lean-to and horizontally stacked fuel packages, along with an image corresponding to the peak 4 ft (1.2 m) obscuration in each case, with the time indicated by a red vertical line on the chart. The chart shows that the peak obscuration for the lean-to configuration is higher than that observed for the horizontal stack, with a peak obscuration at both the 4 ft (1.2 m) and 7 ft (2.1 m) measurement locations of approximately 60%. This peak roughly corresponds with the peak burning period of the straw which caused a peak in the hallway heat flux data. The obscuration data for this fuel package followed a similar trend to the heat flux data, periods of greatest obscuration corresponding to the peak heat flux. This minimum value, shown in Figure 5.6, is still greater than the peak obscuration observed for the horizontal stacked pallet configuration.



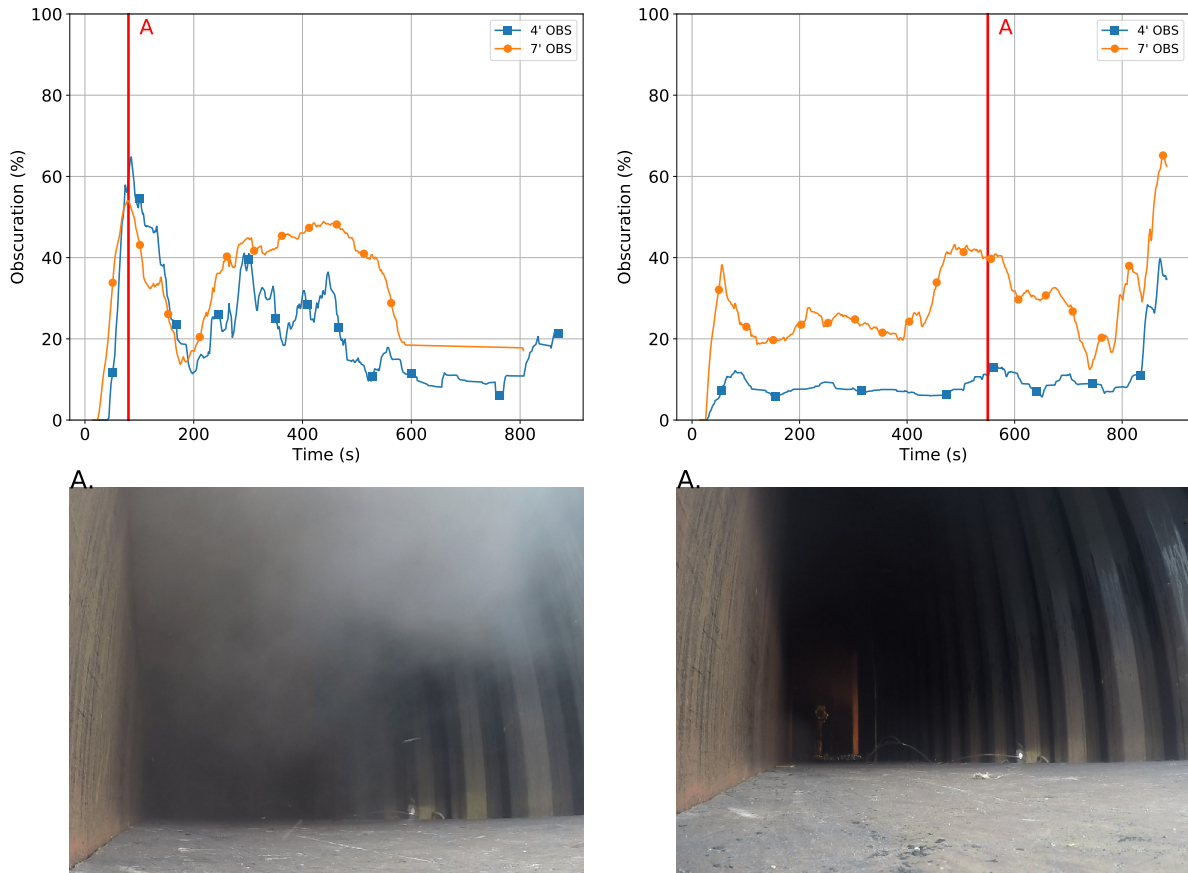


Figure 5.5: Smoke opacity in hallway for vertical (left) and horizontal (right) pallet fuel packages. Red lines denote the points in time to which the images correspond.



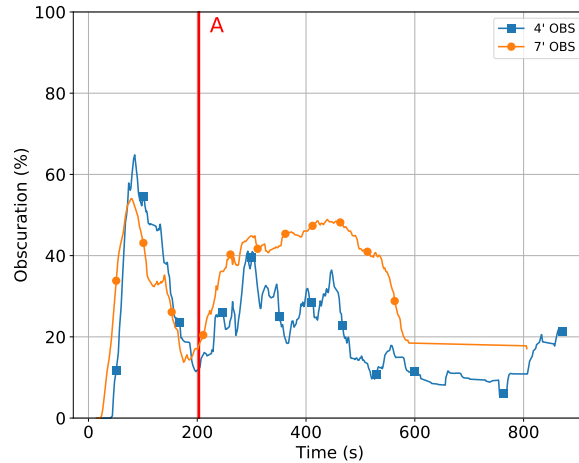


Figure 5.6: Minimum Obscuration for Experiment 10

Thus, while the magnitude of the peak thermal conditions in the training prop was comparable between the three pallet experiments, the time at which the peak value occurred was dependent on orientation, with the horizontal stacked pallets reaching a peak several minutes after the other two configurations. It is possible that the more rapid growth of the three pallet lean-to fuel package in Experiment 10 resulted in less efficient combustion, which produced more soot and resulted in the higher obscuration when compared to the horizontal pallet stack in Experiment 22.

## 5.6.2 Effect of Additional Pallets

Section 4.1.4 indicated that adding additional pallets resulted in an increase in the peak heat release rate. Experiments 7, 8, 10, 11, and 24 were conducted to examine the fire dynamics produced by varying the fuel package size and orientation using only pallets and straw. Table 5.5 lists the number of pallets, the orientation of the pallets, and the ventilation sequence for these five experiments.

Table 5.5: Extra Pallet Comparison Tests

Experiment	Fuel Package	Orientation	ventilation
7	6 pallets, 1 bale of straw	Boxed-in triangle	Front door opened, six minutes
8	6 pallets, 1 bale of straw	Stacked on platform	Front door opened, six minutes
10	3 pallets, 1 bale of straw	Lean-to	Front door open at ignition
11	6 pallets, 1 bale of straw	Lean-to	Front door open at ignition
24	3 pallets, 1 bale of straw	triangle	Front door opened, six minutes



Figure 5.7: Images of 3 and 6 pallet configurations. From left to right: three pallet triangle, six pallet boxed-in triangle, six pallets stacked to form a platform, three pallet lean-to, and six pallet lean-to.

Figure 5.8 shows the HGL temperatures and heat flux in the hallway door for Experiments 7, 8, and 24. Experiments 7 and 8 represent pallets and straw fuel packages described in fire service trade journals [46, 47] for use in live fire training. The measurements taken in these areas can be used to approximate the thermal conditions in areas of the prop in which firefighters could operate. Within the fire room itself, conditions would be dangerous even for a firefighter in full PPE. Table 5.6 summarizes the peak HGL temperatures at the start and end hall locations and the peak end hall heat flux. The peak HGL temperature for the six pallet boxed-in triangle fuel load was significantly higher than the three pallet triangle for both the start and end hall locations. The difference between the six pallet platform fuel load and the three pallet triangle, on the other hand, was less than the uncertainty of the thermocouple measurement for both the start and end hall locations.

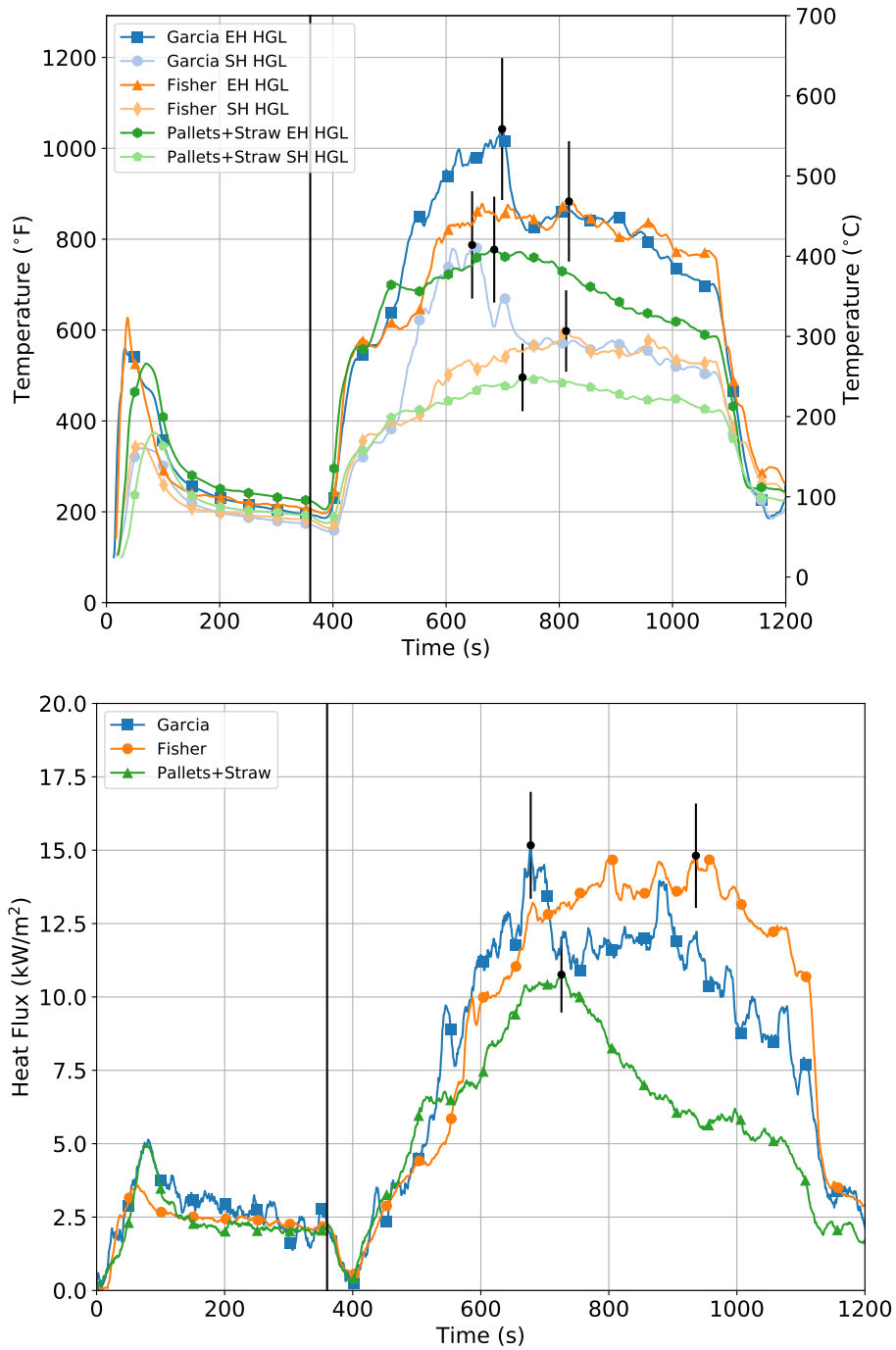


Figure 5.8: Comparison of HGL temperature (left) and hall heat flux (right) for two 6 pallet configurations from literature [46,47] and 3 pallet triangle

Table 5.6: Peak Thermal Conditions for Experiments 7, 8, and 24

	Exp. 7	Exp. 8	Exp. 24
Fuel	6 pallets, boxed-in triangle	6 pallets, stacked	3 pallets, triangle
Peak End Hall HGL (°C)	561	473	414
Peak Start Hall HGL (°C)	420	314	258
Peak End Hall Heat Flux (kW/m <sup>2</sup> )	15	15	11

Perhaps more significant than the differences in peak HGL temperatures were the duration of the peak period for hallway temperatures. For example, at the end hall location, the three pallet triangle exceeded 750°F (400°C) for approximately 100 seconds. Both of the six pallet configurations exceeded this temperature for close to 475 seconds. Thus, while the additional fuel weight did not necessarily increase the magnitude of the peak duration, they resulted in a longer period of temperatures close to this peak.

Both of the six pallet fuel packages exhibited peak end hall heat fluxes of 15 kW/m<sup>2</sup>, compared to the peak end hall heat flux of 11 kW/m<sup>2</sup> observed in the three pallet triangle. As was the trend with the HGL temperatures, the six pallet fuel packages produced high heat fluxes for longer periods of time than the three pallet triangle. The three pallet fuel package produced heat fluxes in the hallway that exceeded 10 kW/m<sup>2</sup> for less than 100 seconds, a significantly shorter time than the boxed-in triangle and stacked six pallet configurations, which exceeded 10 kW/m<sup>2</sup> for approximately 425 and 500 seconds, respectively.

Experiments 10 and 11 provide a comparison of two lean-to pallet configurations with three and six pallets, respectively. Figure 5.9 shows the hallway thermal conditions for these two experiments, which were conducted in the metal prop with the door open from the time of ignition. The chart shows that for each of the fuel loads, there was a local peak in the HGL temperatures and end hall heat flux close to 100 seconds. The magnitude of this peak was comparable for both fuel packages. In the three pallet fuel load, this peak corresponds to the beginning of a steady period where the HGL temperatures in the hallway are maintained at 705°F (375°C) and 390°F (200°C) for the end and start hall locations, respectively. During this period, which lasts from 100 seconds to approximately 600 seconds after ignition, the heat flux at the end hall position reached a peak of 9 kW/m<sup>2</sup> before dropping below 5 kW/m<sup>2</sup> and gradually increasing back to a value of 7 kW/m<sup>2</sup> towards the end of this steady period.

The thermal conditions observed in the six pallet test were considerably higher than in the three pallet test. Additionally, the peak HGL temperatures and heat flux in the hallway occur later in the test than in the three pallet fuel package. The peak HGL temperatures were 895°F (479°C) and 510°F (266°C) for the end and start hall locations, respectively. These higher peak temperatures are maintained for approximately 400 seconds. The hallway heat flux climbs steadily to a peak of 16 kW/m<sup>2</sup> occurring around 400 seconds and maintaining a peak heat flux for approximately

200 seconds. The peak HGL temperatures and heat flux produced by this fuel package were of a similar magnitude to the six pallet fuel packages described in Figure 5.8 and Table 5.6.

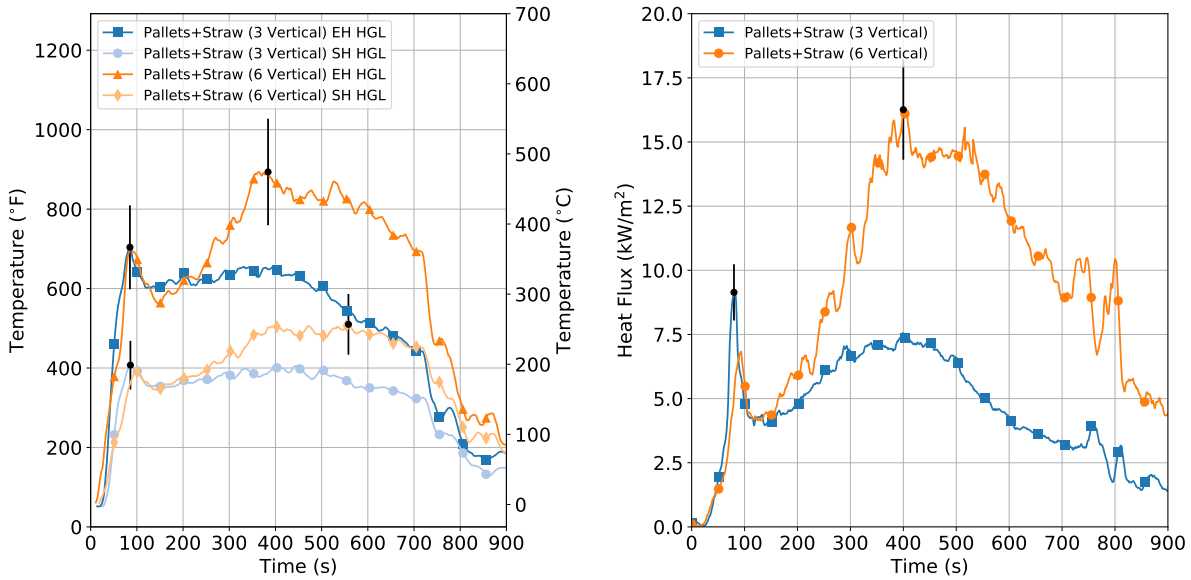


Figure 5.9: Comparison of hallway HGL temperature (left) and heat flux (right) for 3 and 6 pallet vertically stacked fuel loads.

Thus, the additional three pallets increased the fuel load in Experiment 11 to result in significantly higher HGL temperatures and heat flux values in the hallway leading up to the fire room. In a similar way, the additional fuel mass resulted in significantly higher smoke obscuration, as shown in Figure 5.10. This chart shows the opacity measurements in the doorway for the two different sizes of pallet fuel packages. For each of the two experiments, the peak doorway obscuration that was measured approximately corresponded with the periods in which thermal conditions in the hallway were at their peak.

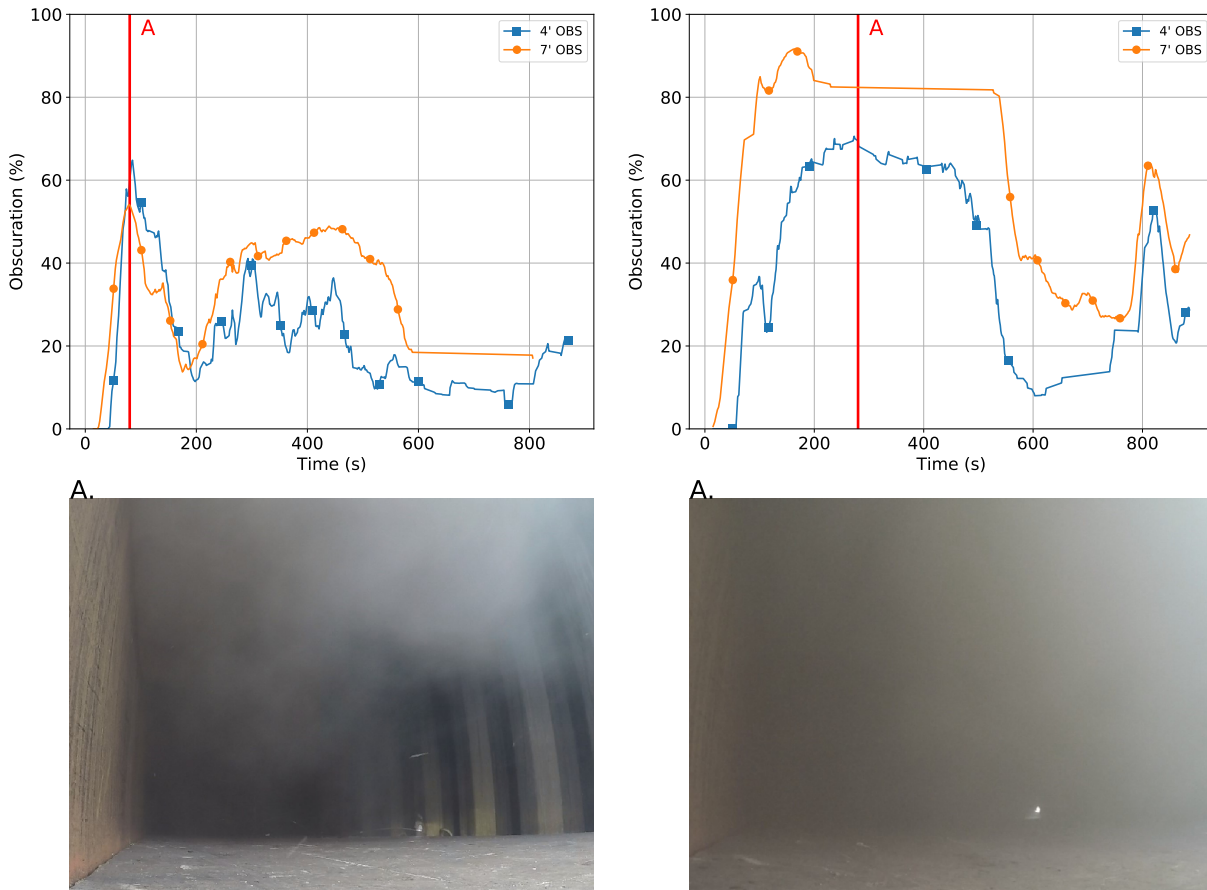


Figure 5.10: Peak smoke opacity in hallway for 3 pallet (left) and 6 pallet (right) vertically stacked fuel packages. Red lines denote the points in time to which the images correspond.

The higher obscuration observed in a six pallet lean-to is likely related to the higher HRR of this configuration, as indicated in Section 4.1.4. The higher obscuration corresponded with higher temperatures and heat flux values in the hallway. The magnitude of these thermal conditions was comparable to the other two six pallet configurations tested. The total weight of the six pallet lean-to was 239.6 lbs (108.9 kg), which is 105.3 lbs (47.8 kg) heavier than the three pallet lean-to, which weighed 134.4 lbs (61.1 kg). The additional fuel mass produces more energy, resulting in an increase in the magnitude and duration of the peak thermal conditions. The positive correlation between fuel load size and severity of thermal conditions is consistent with the HRR data from Section 4.1.4, and the increase in obscuration observed for the larger fuel package may be related to a decrease in combustion efficiency due to having a larger fuel package in the same compartment with the same ventilation.

### 5.6.3 Comparison of Engineered Lumber to Dimensional Lumber

Recognizing the gap between the fire dynamics produced by conventional training fuel packages and the more severe conditions that are often encountered in residential structures filled with synthetic furnishings, some instructors and training academies have begun to explore wood-based fuel packages other than pallets. Examples of these fuel packages include MDF, OSB, and dimensional lumber. Experiments 12, 19, and 20 examined these three large wood-based fuel packages.

Figure 5.11 shows the fire room and end hall heat flux for Experiments 12, 19, and 20. For each of the experiments, the peak heat flux values that were recorded were significantly higher than those observed in the three pallet training fuel loads described in Section 5.6.1. Out of the three experiments, the lowest peak heat fluxes of 28 kW/m<sup>2</sup> and 21 kW/m<sup>2</sup> were observed in the dimensional lumber fuel load in the fire room and hallway, respectively. The peak fire room and hallway heat flux for the MDF were 35 kW/m<sup>2</sup> and 47 kW/m<sup>2</sup>, respectively. In the OSB experiment, one of the pieces of OSB from the ceiling fell on top of the heat flux gauge, leading to a misleadingly high peak heat flux. Without this outlier, the peak fire room heat flux was approximately 38 kW/m<sup>2</sup> and the peak hallway heat flux was 37 kW/m<sup>2</sup>.

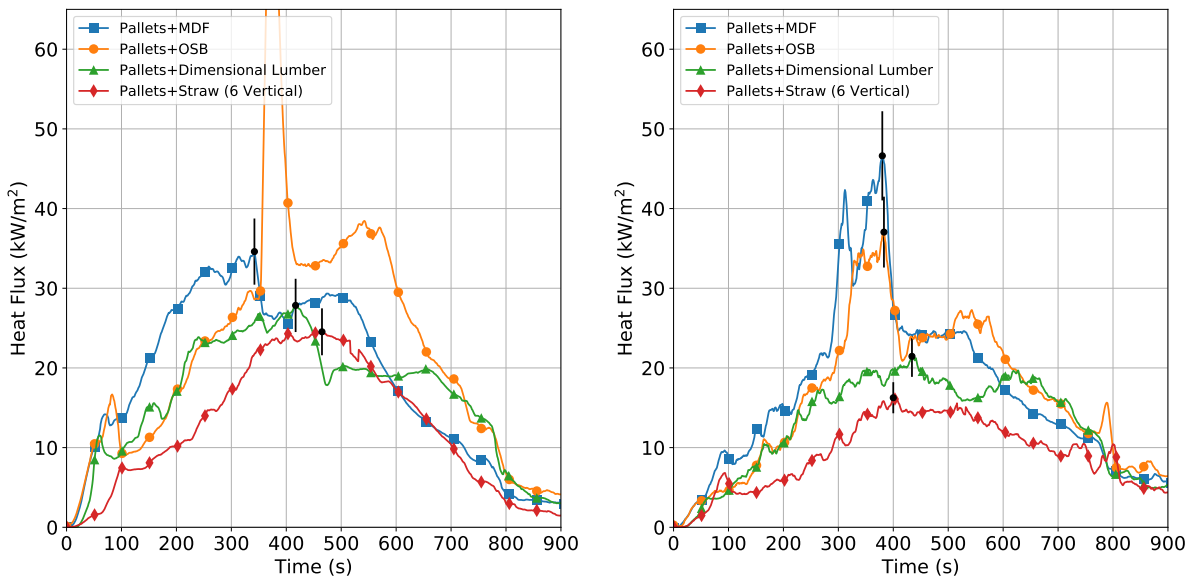


Figure 5.11: Fire room (left) and hallway (right) heat flux for OSB, MDF, 1 in. x 6 in. dimensional lumber, and 6 pallet lean-to fuel packages

These hallway heat flux values were the highest of any of the training fuels evaluated other than those where fuel was located in the hallway. The severe thermal conditions in the hallway itself are further evidenced by the hallway HGL temperatures shown in figure 5.12. For the MDF fuel package in particular, the peak end hall HGL temperature was in excess of 1110°F (600°C), and flames were sustained down the hallway, as shown in Figure 5.13. For the dimensional lumber and OSB fuel packages, the peak end hall HGL temperatures were in excess of 932°F (500°C),



approximately 210°F (100°C) higher than the peak end hall HGL temperatures described in section 5.6.1.

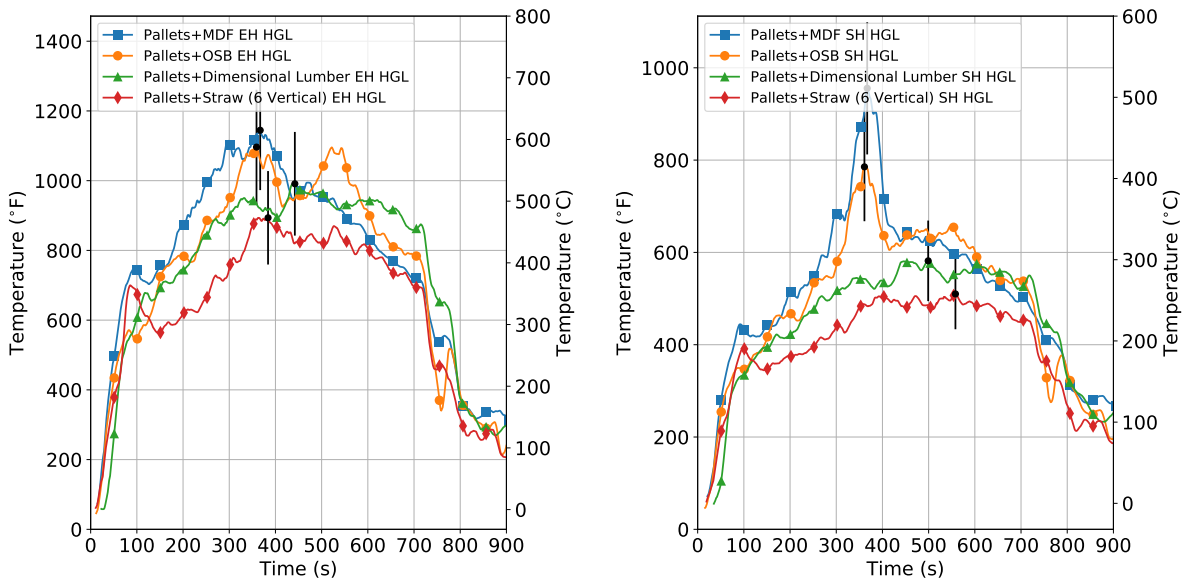


Figure 5.12: End hall HGL temperatures (left), and start hall HGL temperatures (right) for OSB, MDF, 1 in. x 6 in. dimensional lumber fuel packages



Figure 5.13: Burning in hallway for Experiment 19 (MDF)

Figure 5.14 shows the doorway obscuration for the OSB, MDF, and dimensional lumber fuel packages. These experiments exhibited some of the highest doorway obscuration at the 4 ft (1.2 m). level. In a similar manner to the six pallet lean-to (Experiment 11) described in Section 5.6.2, the 7 ft (2.1 m). obscuration rose to approximately 90 % obscuration within the first 100 seconds, and the 4 ft (1.2 m). obscuration was maintained close to 60% for the duration of the peak burning period of the fuel package.

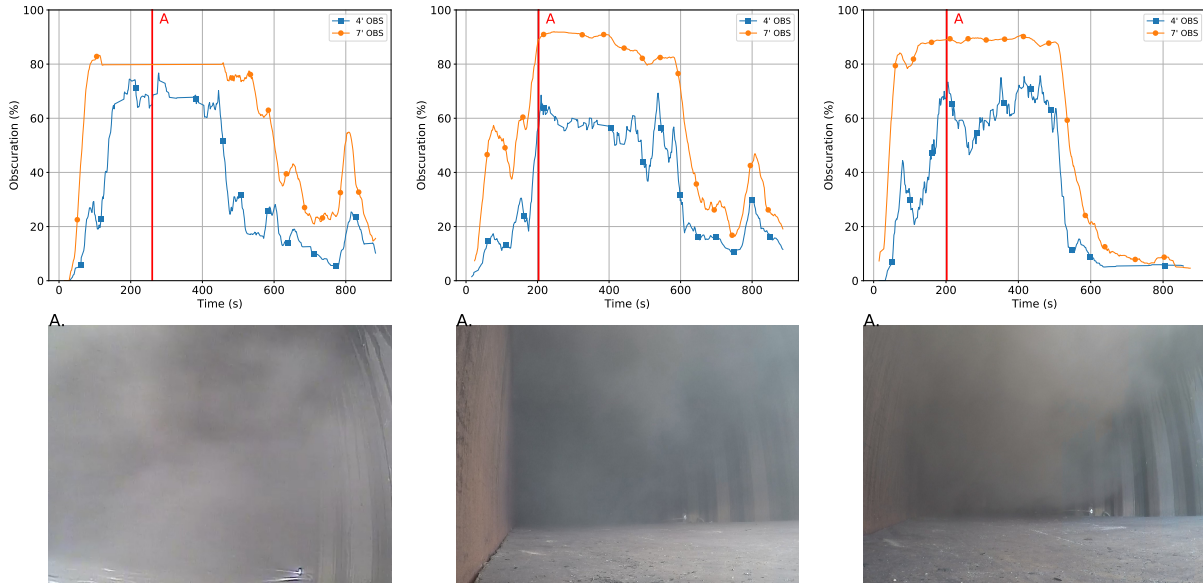


Figure 5.14: Peak smoke opacity in doorway for OSB, MDF, and dimensional lumber fuel packages. Red lines denote the points in time to which the images correspond.

### 5.6.4 Use of Smoke Barrels

Smoke barrels are a device used by some instructors in an effort to increase the optical density of smoke. Several of these devices may be used in conjunction with each other, with the intention of supplementing the smoke produced by the fuel package without increasing the severity of thermal conditions. Additionally, some instructors supplement the airflow provided to these smoke barrels using an appliance such as a leaf blower in order to produce more turbulent smoke. Two experiments with smoke barrels were conducted, one with and one without a leaf blower. To examine the effects of these devices, these experiments can be compared to Experiments 21 (three pallets and one bale of straw in a triangle formation) and 10 (three vertical pallets and one bale of straw).

The smoke barrels used in these experiments consisted of a 55-gallon drum with a fuel load composed of broken pallets, dry straw, and OSB. These dry fuels were placed in the barrel as indicated in Figure 5.15, ignited, and allowed to burn for approximately seven minutes (420 seconds) to develop a bed of hot coals. At this point, wet straw was added to the barrel and in Experiment 6, the leaf blower was turned on. After two additional minutes of smoke production from the barrels, the pallets and straw fuel package was ignited.



Figure 5.15: Smoke Barrel Contents

Figure 5.16 shows the thermal conditions in the hallway for the two smoke barrel experiments compared to the same fuel package without smoke barrels. The fire growth and peak behavior was not remarkably different between the three experiments. The peak hallway temperatures were reached between 100 and 200 seconds following the ignition of the fuel package, and the peak hallway heat flux was reached approximately 350 seconds following ignition. Thus firefighters participating in the three training evolutions would likely experience thermal conditions with comparable magnitudes and timing.

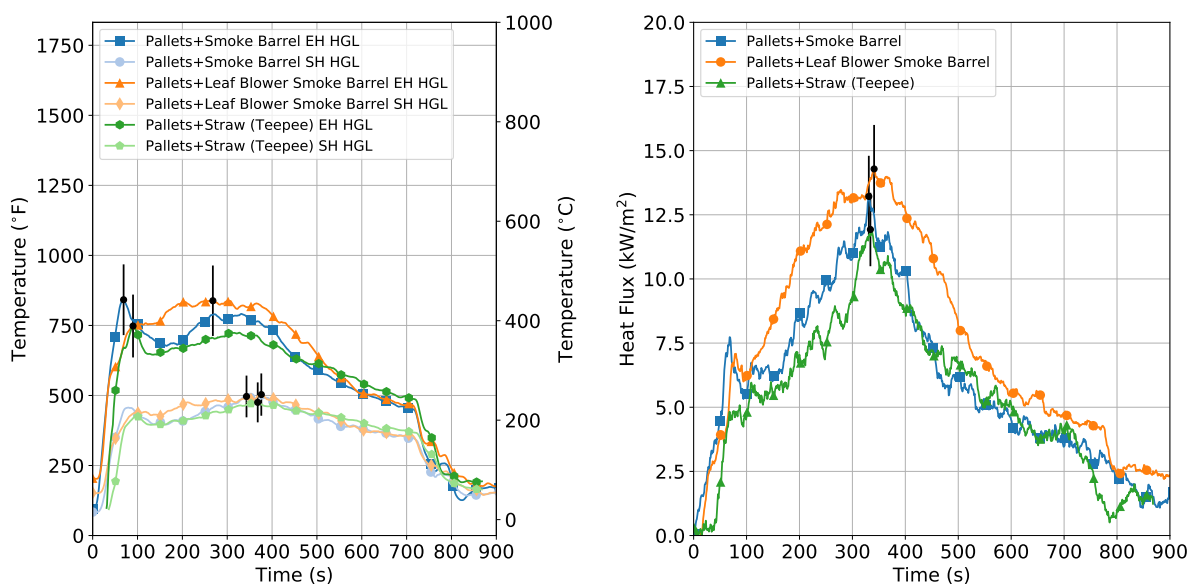


Figure 5.16: HGL Temperature (left) and end hall heat flux (right) for 3 pallet triangle with and without smoke barrels

While the impact of the smoke barrels on fire dynamics was minimal, the use of these devices did increase the opacity of the smoke. No tests with opacity measurements were conducted on the triangle fuel package which was used for the smoke barrel experiments, so the three pallet vertical configuration was used to compare the optical density of the smoke. Figure 5.17 shows the opacity measurements for Experiment 23, which used smoke barrels without the use of supplemental airflow. The results show that the use of smoke barrels in the fire room prior to ignition of the fuel package results in the development of a smoke layer prior to ignition, resulting in obscuration of approximately 90% at the 7 ft level and 25% at the 4 ft level in the doorway prior to ignition. After

ignition, the obscuration in the doorway decreases at approximately the same time in which the obscuration in the three pallet configuration without smoke barrels begins to increase. Following this decrease, doorway obscuration at the 7 ft (2.1 m). level is maintained at approximately 90% for the remainder of the peak burning period, while the 4 ft (1.2 m). obscuration varies between 20% and 45%. Thus, the inclusion of burn barrels in the fuel package resulted in an increase in doorway obscuration at the beginning of the experiment and at the 7 ft (2.1 m). level during the peak burning period, although there was a decrease in obscuration during the initial growth of the fire.

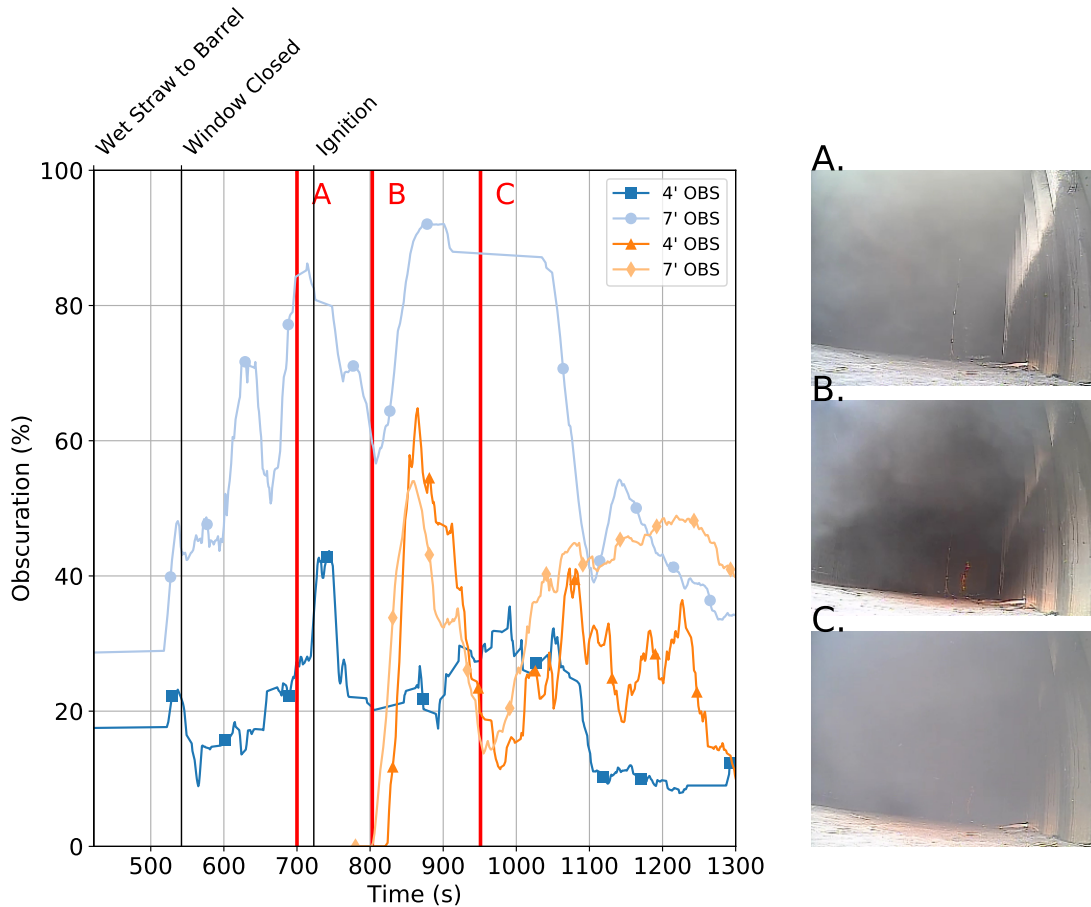


Figure 5.17: Smoke opacity for smoke barrel experiment without increased airflow. Images correspond to A. the peak obscuration prior to ignition of the pallets and straw, B. the dip in obscuration following growth of the fire, and C. peak obscuration following ignition of the pallets and straw (denoted by red vertical lines)

Visually, the use of a leaf blower to increase airflow through the smoke barrel increased the velocity of smoke venting from the metal training prop. The increased airflow resulted in a higher peak doorway obscuration at both the 4 ft (1.2 m). and 7 ft (2.1 m). levels in the period prior to ignition of the pallets and straw fuel package. Similarly to the other experiment using smoke barrels, a significant decrease in obscuration was observed in the period following ignition, as temperatures

in the fire room increased. After this decrease, the smoke density once again increases, maintaining peak doorway obscuration values of approximately 90% at the 7 ft (2.1 m). level and 50% at the 4 ft (1.2 m). level. While the peak 4 ft (1.2 m). value is comparable to the peak 4 ft (1.2 m). value observed in the three vertical pallets and straw experiment, the peak 7 ft (2.1 m). doorway obscuration value was significantly higher. It should be noted that at an unknown point following ignition of the fuel package in Experiment 6, the leaf blower sustained thermal damage and was no longer supplying supplemental airflow to the smoke barrel. If the leaf blower had continued to operate, the opacity behavior of the smoke exiting the doorway of the prop may have been different.

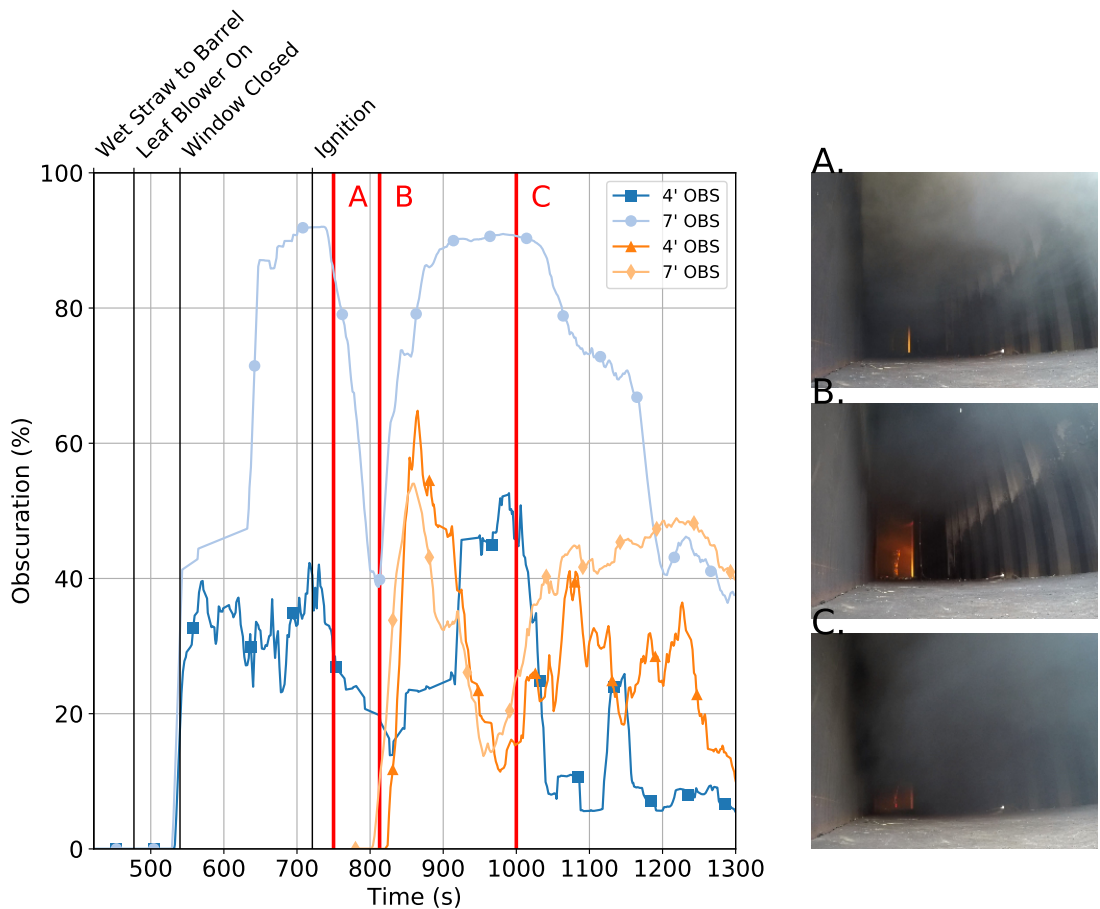


Figure 5.18: Smoke opacity measurements for smoke barrel experiment with increased airflow. Images correspond to A. the peak obscuration prior to ignition of the pallets and straw, B. the dip in obscuration following growth of the fire, and C. peak obscuration following ignition of the pallets and straw (denoted by red vertical lines).

The use of smoke barrels within the fire room of the training prop did not result in a change in fire dynamics, regardless of whether or not supplemental airflow was provided to the smoke barrel. Following ignition of the pallets and straw triangle, temperatures in the fire room and hallway and heat flux in the hallway were comparable between the smoke barrel, smoke barrel with leaf blower,

and no smoke barrel cases. Rather, the growth of the fire had a negative impact on opacity, resulting in a temporary decay period where the obscuration in the doorway and hallway decreased. It is possible that the higher temperatures produced by the fire's growth "cooked off" the moist, dense smoke produced by the wet straw in the smoke barrels. After this initial decrease in obscuration, the peak doorway obscuration measured at the 7 ft (2.1 m). level was greater for both smoke barrel experiments than in the experiment with pallets and straw by themselves. Further, the doorway obscuration prior to ignition at the 4 ft (1.2 m). level was greater in the experiment with the leaf blower than in the case without the leaf blower, as can be seen in Figure 5.19.

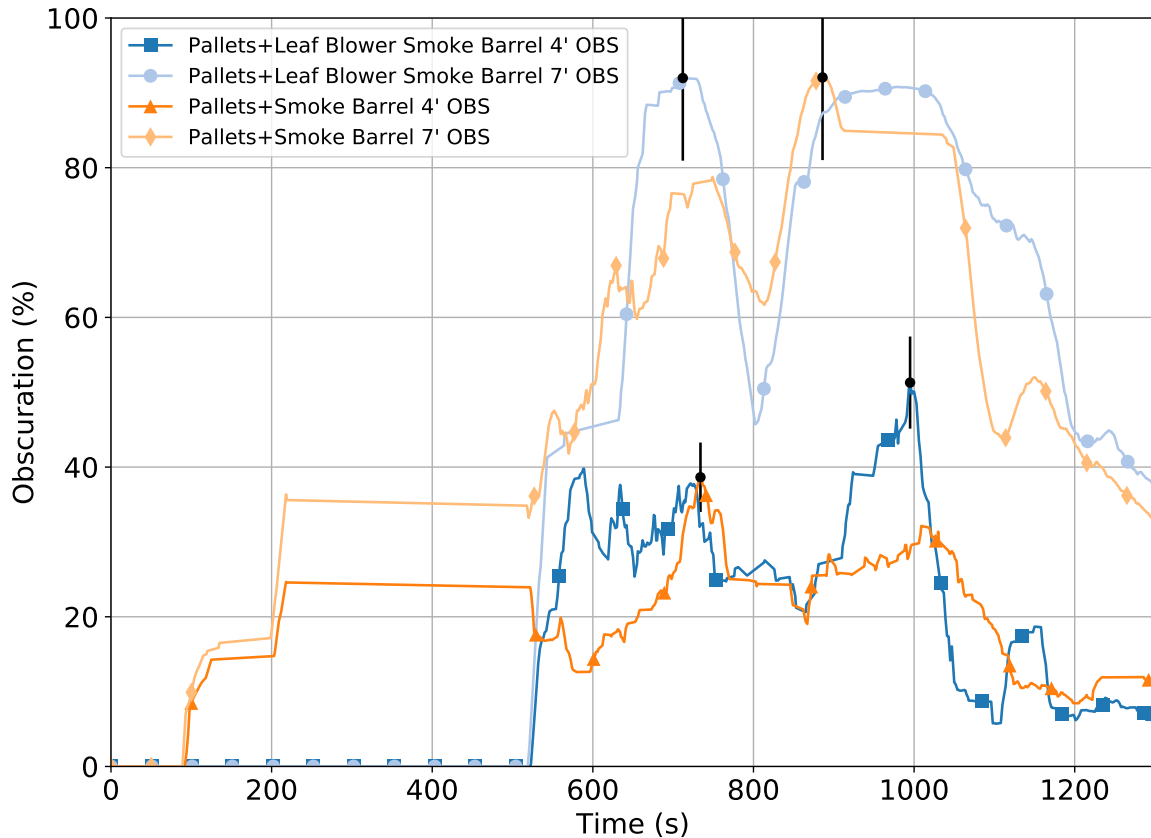


Figure 5.19: Smoke barrel comparison for the smoke barrel experiments with and without airflow.

### 5.6.5 Use of Synthetic Materials in Training Fuel Packages

In an effort to create more optically dense smoke, consistent with the thick, dark smoke produced by fires involving synthetic furnishings, some instructors elect to add a small amount of synthetic material, such as tar paper or polyurethane foam, to a training fuel package. The motivation behind these actions is to create realistic smoke without drastically affecting the fire dynamics that are produced. Images of these fuel packages are shown in Figure 5.20. In the sofa cushion fuel package, the cushion was secured to the top of the triangle with baling wire. In the tar paper fuel package, strips of tar paper were placed in the slats of the top two pallets.





Figure 5.20: Three pallets and one bale of straw oriented in a triangle with no synthetic material (left), with tar paper (center), and with a polyurethane sofa cushion (right). 4.8 lbs (2.2 kg) of tar paper and 4.6 lbs (2.1 kg) of polyurethane foam were used in the fuel packages.

Figure 5.21 shows the heat flux in the fire room and at the end of the hallway for Experiments 1, 2, and 21. These experiments had fuel loads of pallets, straw, and tar paper; pallets, straw, and a polyurethane sofa cushion; and pallets and straw, respectively. The pallets, straw, and tar paper had a significantly higher peak fire room heat flux of  $28 \text{ kW/m}^2$ , compared to  $19$  and  $18 \text{ kW/m}^2$  for the three pallet fuel packages with and without a sofa cushion, respectively. The hallway heat flux and HGL temperatures (Figure 5.22) were comparable among the three experiments.



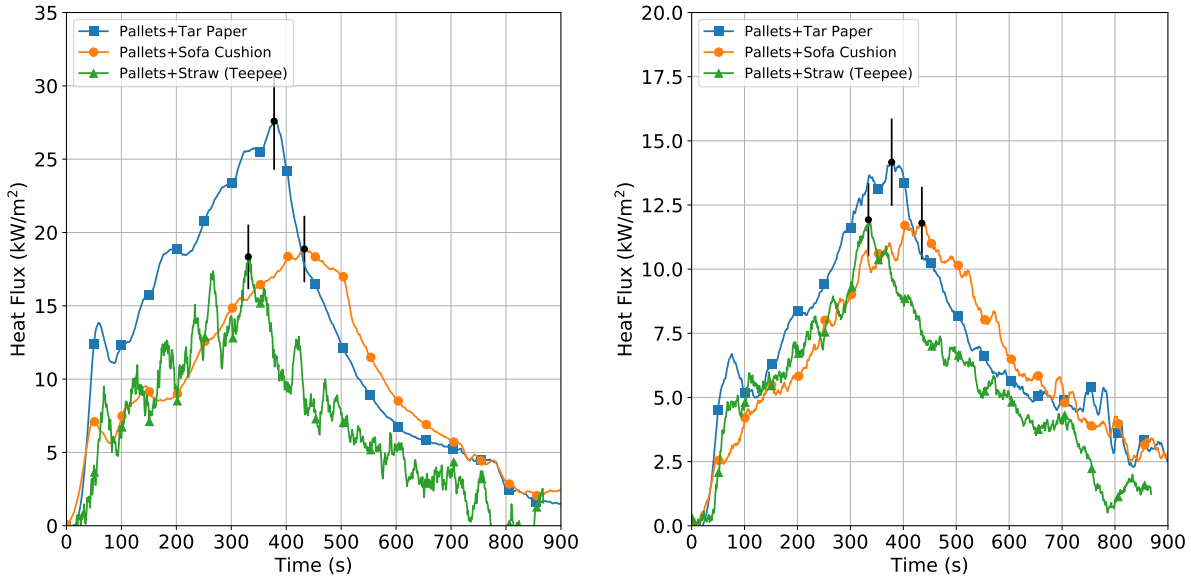


Figure 5.21: Comparison of fire room (left) and hallway (right) heat flux for experiments with a small amount of additional synthetic fuel.

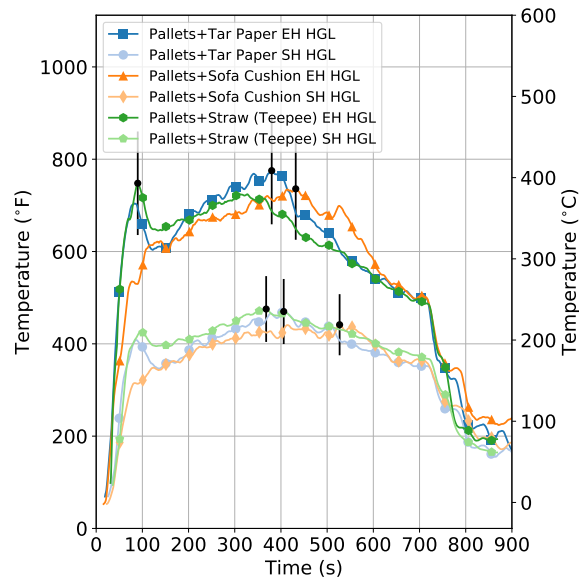


Figure 5.22: Hallway HGL temperature for experiments with a small amount of additional synthetic fuel.

Table 5.7: Peak Thermal Conditions for Experiments 1, 2, and 21

		Exp. 1	Exp. 2	Exp. 21
Fuel		3 pallets, Tar Paper	3 pallets, Sofa Cushion	3 pallets
End Hall HGL	Peak (°C)	413	391	414
	Duration (s)	397	482	497
Start Hall HGL	Peak (°C)	243	227	258
	Duration (s)	430	542	591
End Hall Heat Flux	Peak (kW/m <sup>2</sup> )	14	12	12
	Duration (s)	134	213	76

While small amounts of tar paper or polyurethane foam did not result in a significant increase in the temperatures or heat fluxes to which firefighters would be exposed outside of the fire room, the doorway obscuration that was measured in these experiments was higher than three pallets and one bale of straw without synthetic materials added to the fuel load. Consider Figure 5.23, which shows the doorway opacity measurements for Experiments 1, 2, and 10. The charts show that for both Experiments 1 and 2, the doorway obscuration is maintained at 90% for approximately 300 seconds. During this period, the 4 ft (1.2 m). obscuration values vary between 40% and 60%. These values are higher than those observed in the three pallet lean-to fuel package in Experiment 1, where the peak obscuration at the 7 ft (2.1 m). level was close to 60% and the 4 ft (1.2 m). obscuration during the peak burning period was between 20% and 40%.

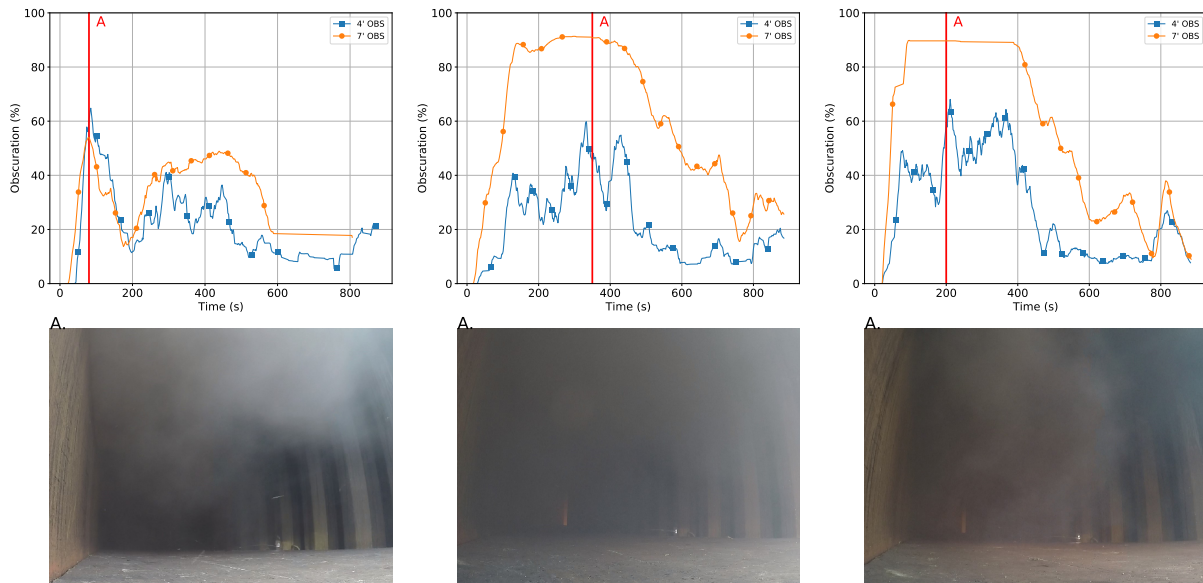


Figure 5.23: Peak smoke opacity in doorway for three pallets (lean-to) without synthetic fuel (left), sofa cushion (center) and tar paper (right) with pallets and straw fuel packages. Red lines denote the points in time to which the images correspond.

Although the addition of a relatively small amount of synthetic material increased the obscuration that was measured in the doorway, it did not produce the same level of obscuration as a furnished room. Figure 5.24 shows the visibility conditions at the start of the hallway for Experiment 15, which had a fuel load consisting of furniture. Comparison of this image to the images of the peak obscuration for Experiments 1 and 2 indicates that the smoke density increase that results from the addition of a small amount of synthetic fuel is still not enough to replicate the smoke density produced by a furnished room. If the learning objectives of a training evolution require optically dense smoke to increase visual obscuration, the addition of a small amount of polyurethane foam or tar paper does increase obscuration, but it is important to note that these materials are explicitly prohibited by *NFPA 1403*. While the addition of these materials in the amount used in these experiments did not have a significant impact on the severity of thermal conditions, several line-of-duty deaths and injuries have resulted from the inclusion of non-NFPA 1403 compliant synthetic materials in training fuel packages which resulted in a fire size that was larger than was appropriate for the training evolution. Additionally, the combustion products of synthetic materials such as tar paper or polyurethane foam has the potential to cause health concerns, particularly after repeated exposures.

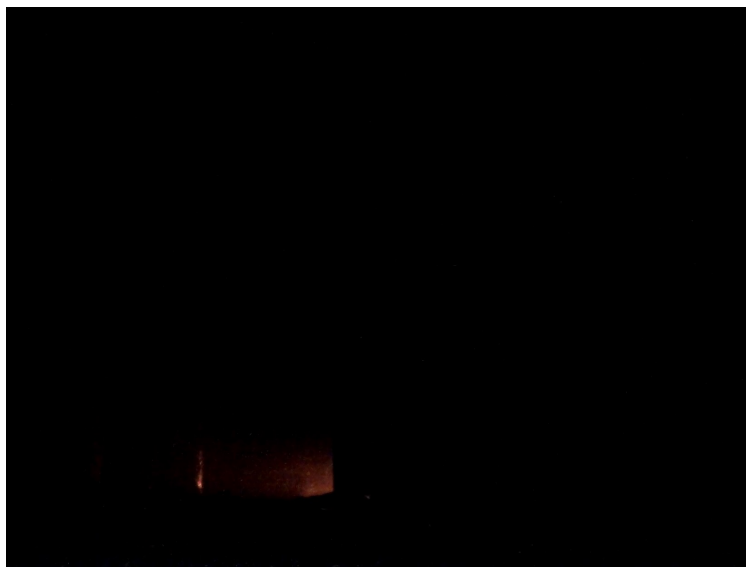


Figure 5.24: Smoke conditions at start of hallway for furnished room experiment (Experiment 15)

### 5.6.6 Hay vs. Straw

Experiments 17 and 18 examined the difference in fire dynamics produced by pallets and straw compared to pallets and hay. While straw is an agricultural waste product consisting of the dried stalks of cereal plants, hay is dried grass or similar plant products and is typically used as animal feed. The moisture content of straw and hay can vary depending on the conditions under which they are baled, although typical moisture contents are less than 20%. Figure 5.25 shows the hallway HGL temperatures and end hall heat flux for the straw and hay experiments.

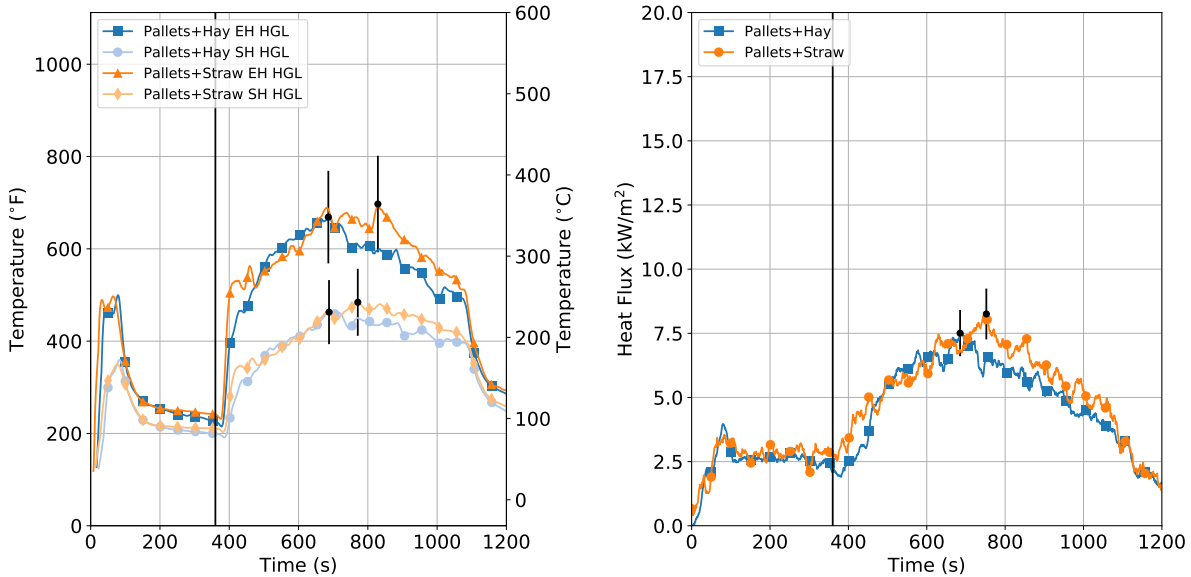


Figure 5.25: Hallway HGL temperatures (left) and heat flux (right) for pallets with straw and pallets with hay.

The thermal conditions in the hallway were comparable between the two experiments. The peak heat flux at the end of the hallway was  $8 \text{ kW/m}^2$  in each experiment, occurring at approximately 700 and 750 seconds after ignition for hay and straw, respectively. The peak HGL temperatures observed at the end of the hallway were  $670^\circ\text{F}$  ( $354^\circ\text{C}$ ) and  $695^\circ\text{F}$  ( $369^\circ\text{C}$ ) for hay and straw, respectively, and the peak HGL temperature at the start of the hall were  $465^\circ\text{F}$  ( $239^\circ\text{C}$ ) and  $485^\circ\text{F}$  ( $251^\circ\text{C}$ ) for hay and straw, respectively. The similar peaks and timing indicate that the difference in composition between hay and straw does not have a profound effect on the fire dynamics produced. It should be noted that the moisture content of the straw and hay bales was not known or measured, and it is possible that straw or hay with a higher moisture content may retard the growth of the fuel package in which they are used. Nevertheless, the difference in herbaceous products that are baled into straw or hay did not produce a distinguishable difference in fire growth, peak behavior, or burn duration.

### 5.6.7 Fuel Outside the Fire Room

While high HGL temperatures and heat flux values were observed for many of the fuel packages described in the previous sections, few of these fuel packages sustained any visible fire in the hallway other than for a brief period, such as the MDF fuel package (Experiment 19). Experiments 3 and 4 were conducted to determine if placing fuel in the hallway leading up to the fire room could produce sustained rollover down the hallway to simulate the conditions that a hose team may face on the approach to the fire room. Such a training scenario could be useful as either a demonstration or to satisfy learning objectives which involve “softening the target” by applying water from a distance.

Experiments 3 and 25 utilized the same fire room fuel load of pallets, straw, and OSB. In Experiment 3, however, OSB was secured to the ceiling in half of the hallway closest to the fire room, as shown in Figure 5.26. The ventilation sequence for Experiments 3 and 25 began with the door and fire room window closed, with the door being opened six minutes following ignition.



Figure 5.26: OSB on hallway ceiling for Experiment 3

Figure 5.27 shows the fire room (left) and end hall (right) heat flux for Experiments 3 and 25. The addition of the OSB along the ceiling of the fire room resulted in an increase in the peak fire room heat flux from  $41 \text{ kW/m}^2$  to  $52 \text{ kW/m}^2$ . The increase was not as high in the hallway, where the peak heat flux increased from  $20 \text{ kW/m}^2$  to  $25 \text{ kW/m}^2$ . While the peak heat flux was not significantly different between the two cases, the addition of OSB in the hallway resulted in a longer peak period, with sustained heat fluxes above  $15 \text{ kW/m}^2$  for approximately 600 seconds, compared to approximately 350 seconds for the fuel package without OSB on the hallway ceiling. This longer period of sustained heat fluxes was accompanied by high HGL temperatures at both the start and end of the hallway, as shown in Figure 5.27. These HGL temperatures followed a similar trend to the heat flux, with a longer period of elevated temperatures, which were between  $930^\circ\text{F}$  ( $500^\circ\text{C}$ ) and  $1110^\circ\text{F}$  ( $600^\circ\text{C}$ ) at the end of the hall and between  $750^\circ\text{F}$  ( $400^\circ\text{C}$ ) and  $930^\circ\text{F}$  ( $500^\circ\text{C}$ ) at the start of the hall. Further, fire was sustained down the hallway for approximately 180 seconds from approximately 520 seconds to 700 seconds after ignition, as shown in Figure 5.27.

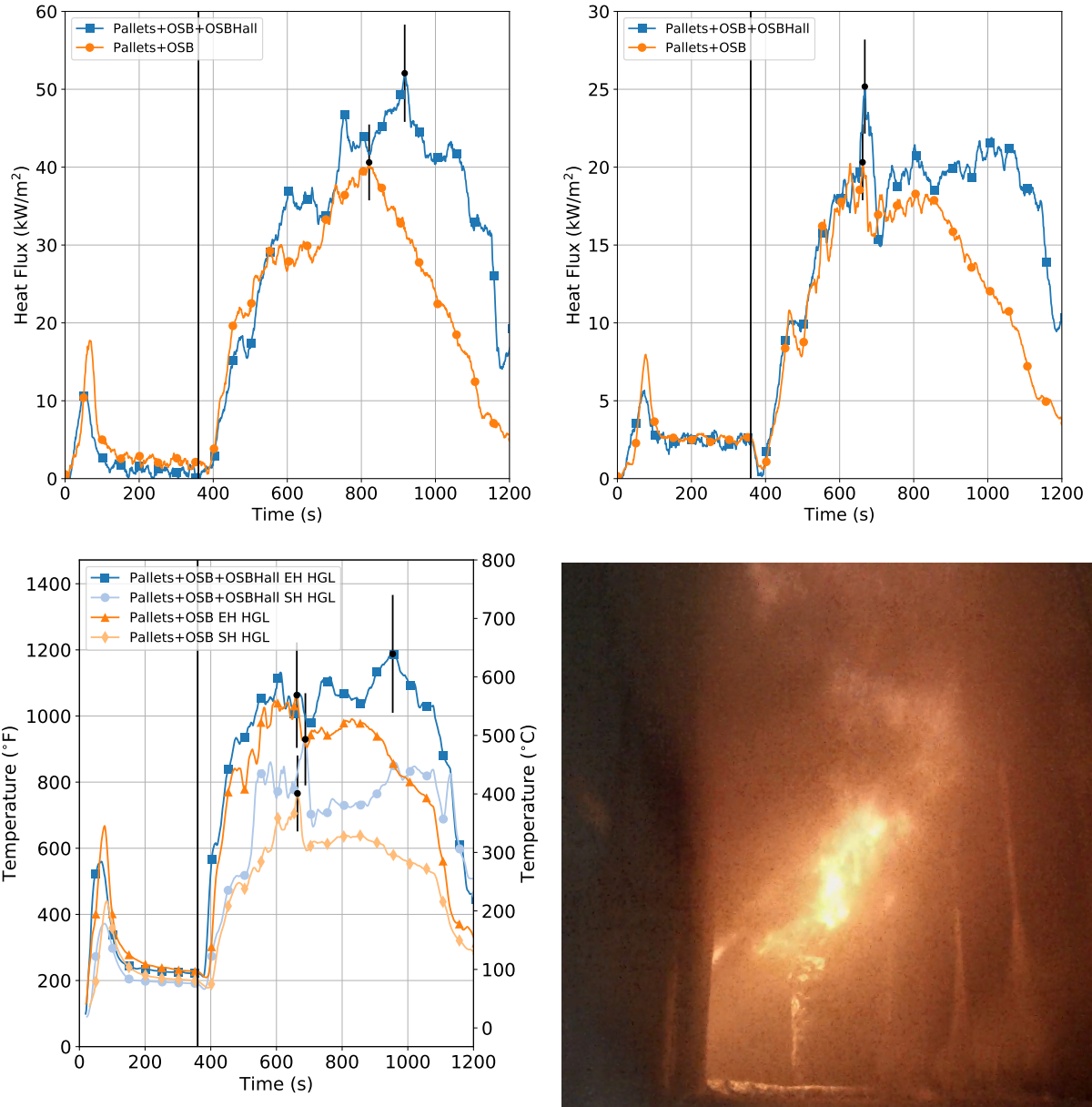


Figure 5.27: Hallway (top left) and fire room (top right) heat flux and hallway HGL temperatures (bottom left) for OSB fuel package with and without OSB on the hallway ceiling. Temperatures were sufficient to maintain fire in hallway for extended period of time (bottom right).

In addition to potential thermal hazards posed to students and instructors by rollover down the hallway, pieces of OSB falling from the ceiling may present an additional hazard to participants of a training evolution using a setup such as that used in Experiment 3. It is possible that this hazard may be mitigated by prop design, but it could also be avoided by affixing OSB to the walls of the hallway. Thus, rather than affixing OSB to the ceiling, OSB was placed along the floor and walls of the half of the hallway closest to the fire room for Experiment 4, as shown in Figure 5.28.





Figure 5.28: OSB on hallway walls for Experiment 4

Figure 5.29 shows the fire room and end hall heat flux and HGL temperatures in the hallway for Experiment 4, with OSB on the walls and floor halfway down the hallway, and Experiment 20, with the same fire room fuel package but no fuel in the hall. The growth of the two fuel packages is similar up until approximately 350 seconds after ignition, when the fire room heat flux decreases from above  $50 \text{ kW/m}^2$  to less than  $10 \text{ kW/m}^2$ , whereas the fuel package without hallway OSB continues to grow at its previous trajectory. The hallway heat flux does not decrease like the fire room, but instead reaches a peak above  $50 \text{ kW/m}^2$  before decreasing to a steady heat flux close to  $30 \text{ kW/m}^2$ . This peak, which was higher than the peak without hallway OSB, is due to the fire that is rolling out of the fire room door and down the hallway. The OSB on the hallway allows for sustained flames in the hallway, as shown in the bottom right of Figure 5.29 and in the elevated HGL temperatures in the bottom right of the same figure. The hallway HGL temperatures were among the highest observed out of any of the fuel packages, particularly at the start hall location. The end hall HGL temperature was maintained close to  $1110^\circ\text{F}$  ( $600^\circ\text{C}$ ) from 300 seconds after ignition until the end of the experiment. The start hall HGL temperature reached a peak of  $1600^\circ\text{F}$  ( $875^\circ\text{C}$ ) at approximately 385 seconds after ignition. This peak corresponds with the time that fire begins to vent out of the hallway door, as can be seen in Figure 5.30.



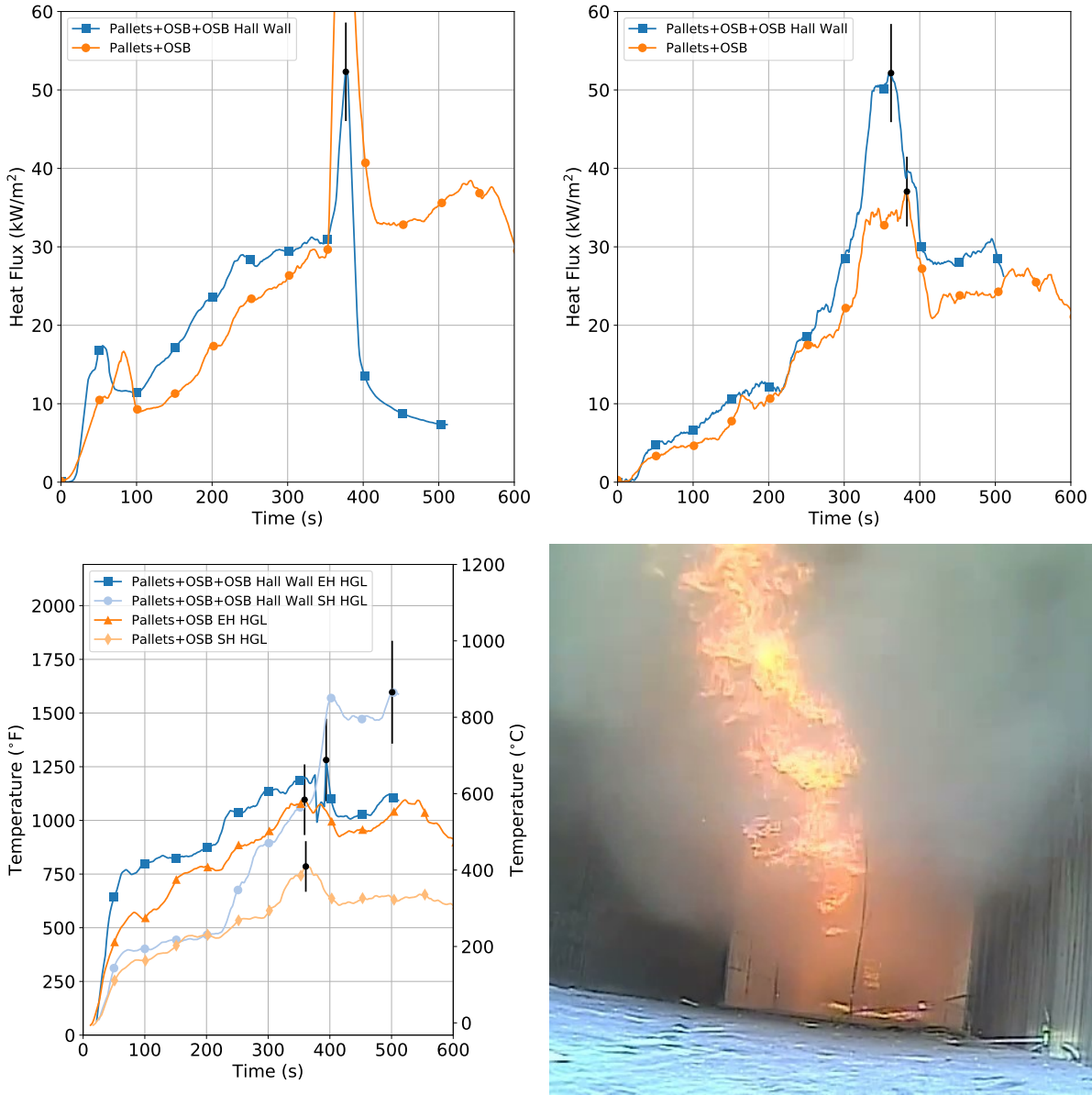


Figure 5.29: Fire room (top left) and hallway (top right) heat flux and hallway HGL temperatures (bottom left) for OSB fuel package with and without OSB on the hallway floor and walls. Bottom right image shows burning in the hallway.



Figure 5.30: Fire venting from prop doorway in Experiment 4

Lining the walls of the hallway with fuel resulted in a decrease in heat flux and temperature in the fire room. As the fuels located within the hallway began to burn, air was not able to reach the fire room, and the thermal conditions began to decrease due to a lack of oxygen. The thermal conditions that were observed in the hallway were the most severe of any of the training fuel loads evaluated, with sustained fire throughout the hallway for most of the experiment and fire out the doorway of the prop later in the experiment. The thermal conditions were significantly more severe than the fuel load with OSB on the ceiling of the prop. This is because with the OSB on the walls, there is a sufficient quantity of fuel in a location where oxygen can reach it to precipitate burning. Later in the experiment, the OSB continued burning in the hallway, while the fuel in the fire room entered a state of oxygen-depleted decay. When the OSB was placed on the ceiling instead, it was exposed to the high temperature flows exiting the fire room down the hallway, but was not located in an area with sufficient oxygen to burn. Thus, the OSB on the ceiling allowed for sustained fire in the hallway, but not the burning fuel in the hallway that was observed with the OSB on the walls and floor.

### 5.6.8 Pallets in Place of Other Wood Fuels

In Experiment 9, pallets were placed against the back wall and across the ceiling of the fire room, over the three pallet and straw triangle, in a configuration intended to mimic that of the OSB, MDF, and dimensional lumber, as shown in Figure 5.31. Figure 5.32 shows the fire room and hallway heat fluxes and the hallway HGL temperatures for the fuel packages with pallets on the wall compared to OSB on the wall. The figure shows that the magnitude of the peak thermal conditions is similar between the two experiments. The timing at which these peaks occurred differed, as the pallets lining the wall reached peak burning approximately 50-100 seconds later in the experiment than the OSB fuel package in Experiment 20. While the OSB fuel package in Experiment 20 took longer for the pallets to reach their peak burning period, the duration of this period was slightly longer in the pallet fuel package. The reason for the later peak in the pallets may be because the OSB has a surface area that is more conducive to rapid growth of the fire. The OSB sheets consist

of a continuous surface which facilitates rapid flame spread along the boards. The surface of the pallets is broken up by the space between the slats, preventing the continuous flame spread along the surface of the board. Similarly, the larger fuel weight of the pallets contributes to the longer peak burning duration. The total fuel weight of the pallets fuel package is 369.1 lbs (167.8 kg), compared to 316.1 lbs (143.7 kg) for the OSB. This difference would approximately be equal to two additional sheets of OSB. The relative similarity between the pallets mounted on the wall and across the ceiling and the OSB reinforces the HRR characterization data from Section 4.1, which indicated that the heats of combustion of various wood products were comparable.



Figure 5.31: Fuel package with pallets on wall and ceiling (left) vs. OSB on wall and ceiling (right).

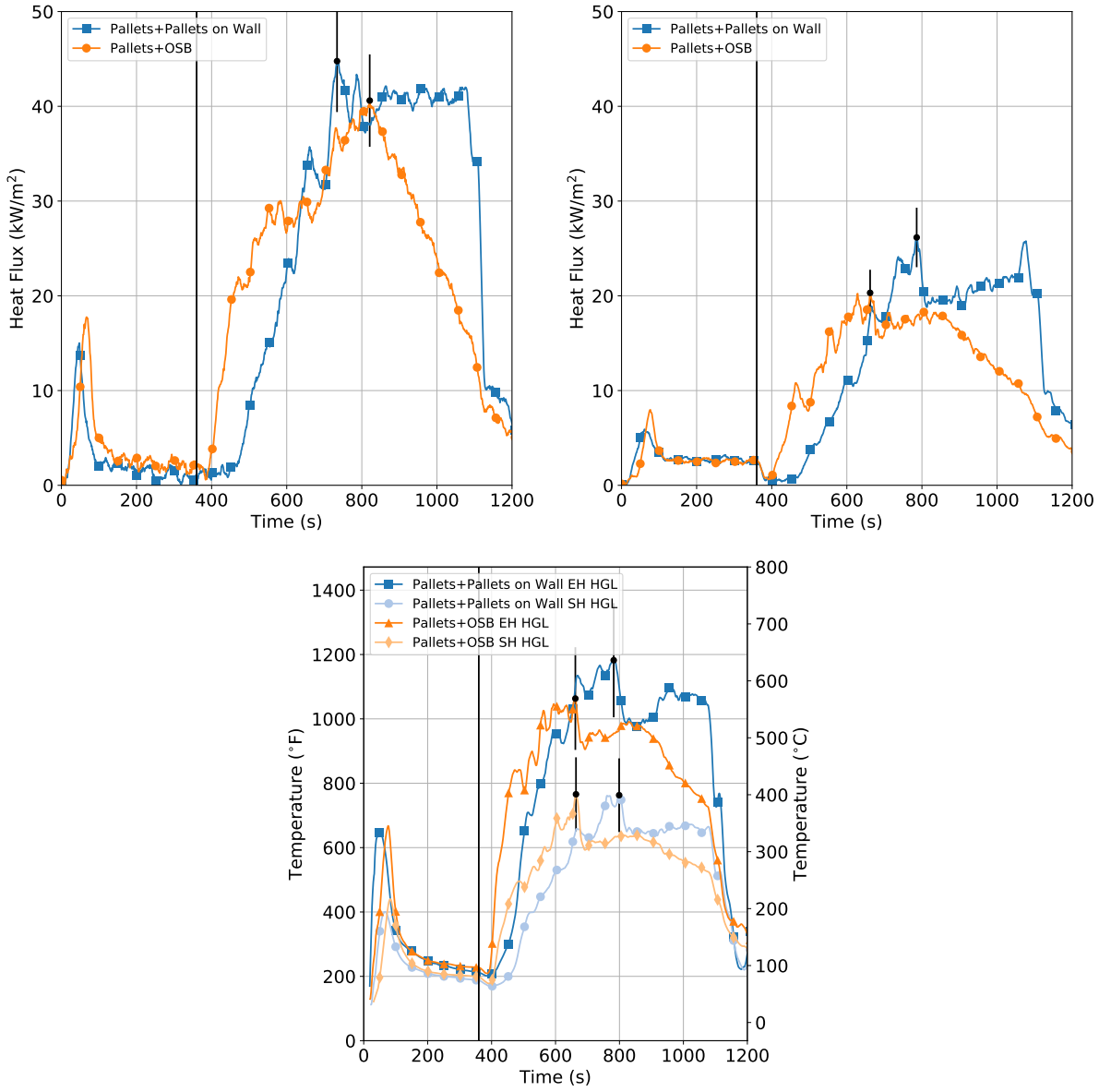


Figure 5.32: Fire room (top left) and hallway (top right) heat flux and hallway HGL temperatures (bottom) for OSB fuel package compared to pallets on wall.

A number of differences between furnished rooms and common training fuel packages affect the fire dynamics produced by training fuel packages. One example of this is the location of the fuel within the room. In the furnished room, most of the fuel is located in the lower half of the room and covers the floor in the form of carpet and carpet padding. Experiment 5 was conducted to evaluate if flashover could be achieved by placing pallets along the floor of the fire room, with a fuel load consisting of three pallets with one bale of straw in a triangle, as shown in Figure 5.33.





Figure 5.33: Fuel package with pallets on floor

Figure 5.34 shows the fire room and hallway heat fluxes and the hallway HGL temperatures for the pallets triangle with pallets on the floor compared to the pallets triangle alone. The chart shows that the growth of the pallets is quite similar until approximately 700 seconds after ignition. At this point, the fire room heat flux in each case is approximately  $30 \text{ kW/m}^2$ , but the fire room heat flux for the experiment with pallets on the floor continues to increase, reaching a peak of approximately  $90 \text{ kW/m}^2$ . The key difference between the two fuel loads is the presence of fuel on the floor that can be heated by the developing thermal layer. In both experiments, the peak fire room heat flux of  $30 \text{ kW/m}^2$  exceeds the commonly referenced threshold of  $20 \text{ kW/m}^2$  for flashover, but in the case of the pallets triangle alone, there is no fuel for this radiant flux to pyrolyze. When the floor pallets are provided, the surface of these pallets heats and pyrolyzes, resulting in conditions consistent with flashover in the fire room. This phenomenon is significant, since only wood-based fuels were used in both experiments.

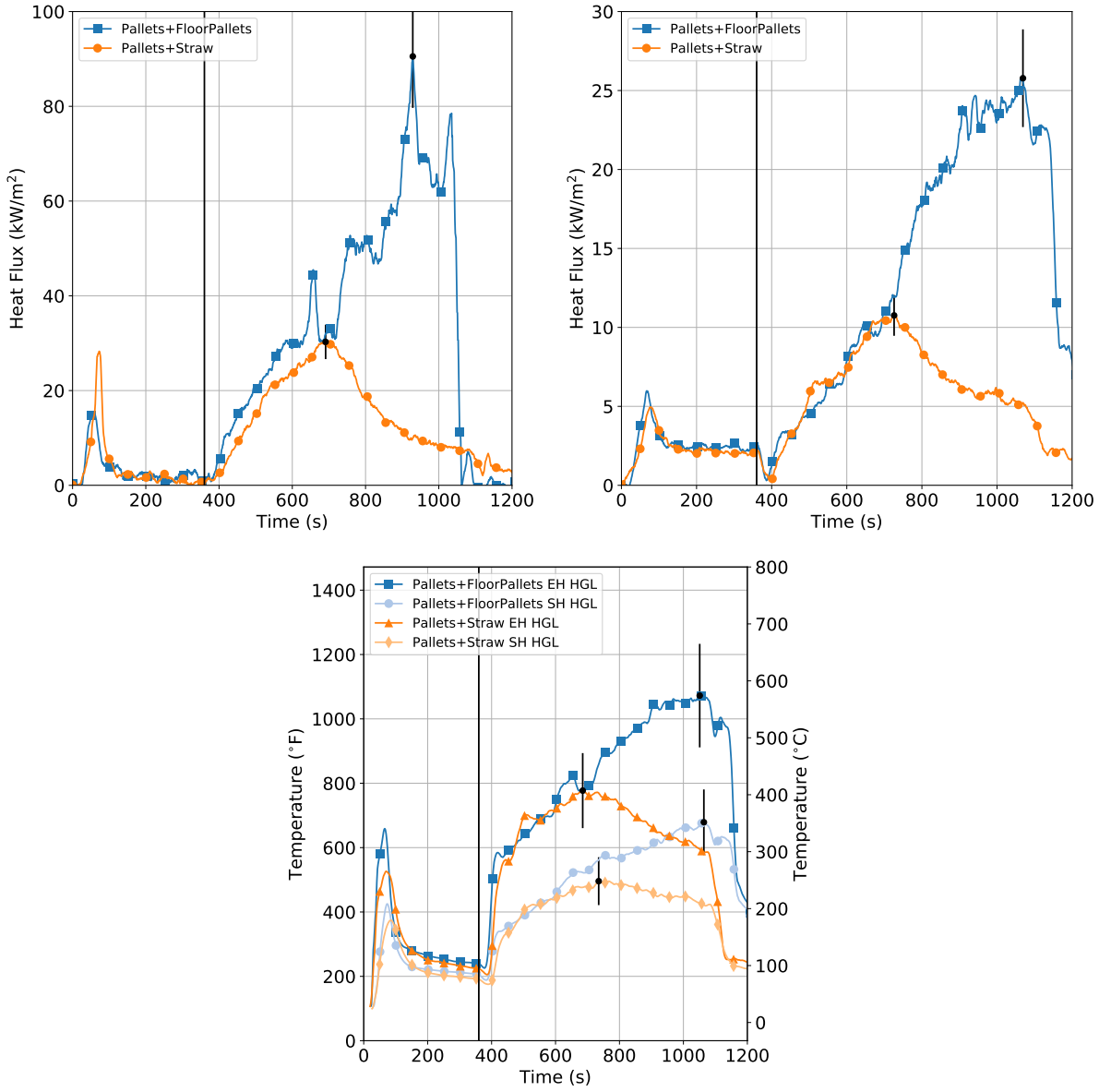


Figure 5.34: Hallway HGL temperatures and heat flux for OSB fuel package with and without OSB on the hallway floor and walls.

### 5.6.9 Flashover in Training Fuel Loads

Among the stipulations in *NFPA 1403* is that the fuel load used in a training evolution should be limited to avoid unwanted flashover. Appendix A.4.13.7 offers a method to estimate the HRR required for flashover of a compartment, including Equation 4.4, previously listed in Section 4.2. This equation predicts that for the metal container prop, with the door as the only ventilation opening, a HRR of 1.7 MW is required for flashover. With only the window open, a HRR of 1.96 MW is required for flashover, and with both the door and window open, a HRR of 3.66 MW is

required for flashover. The ventilation configuration in this series of experiments matched the first case, with the front door as the primary sources of ventilation. Thus, this minimum HRR required for flashover of 1.78 MW can be compared to the peak free burn HRR, fire room floor heat flux, and end hallway heat flux for the 8 experiments listed in Table 5.8 where both free burn HRR and compartment heat flux data was available.

Table 5.8: Free Burn HRR and Compartment Thermal Conditions

Fuel Package	Peak Free Burn HRR (MW)	Peak Fire Room Heat Flux (kW/m <sup>2</sup> )	Peak End Hall Heat Flux (kW/m <sup>2</sup> )
1 Bale Excelsior	1.69±0.19	21	10
3 Pallet Triangle	1.91±0.21	18	12
3 Pallet Horizontal Stack	1.22±0.13	17	10
3 Pallet Lean-to	2.00±0.22	15	9
3 Pallets, OSB*	2.40±0.26	88	37
3 Pallets, MDF*	2.73±0.30	35	47
3 Pallets, 1x6*	2.44±0.27	28	21
6 Pallet Lean-to	3.19±0.35	25	16
6 Pallet Box	3.64±0.40	51	15
6 Pallets, Stacked	3.80±0.42	50	15

\*Fuel packages used in free burn HRR experiments did not have fuel suspended above the pallets triangle, as was the case in the compartments. If this extra fuel were included, the results of the compartment experiments suggest that the peak free burn HRR would have been comparable to or greater than the 6 pallet fuel loads

Of the training fuels in the table, the one bale of excelsior, the three pallet triangle, the three pallet lean-to, and the three pallet horizontal stack had peak HRRs that were similar to the 1.7 MW threshold for flashover. Additionally, the peak heat flux in the fire room for these fuel packages was less than or similar to 20 kW/m<sup>2</sup>, which is the value typically considered to correspond to the onset of flashover [48]. Predictably, the peak end hall heat fluxes for these two fuel packages were lower than those observed in the larger wood-based fuel packages. The larger wood-based fuel loads (with OSB, MDF, dimensional lumber, more pallets) had peak free burn HRRs higher than 1.7 MW, with correspondingly higher heat fluxes in the fire room and at the end of the hallway. While the severity of these thermal conditions is significantly greater than the smaller wood fuel packages, the fire room never reaches the point of having a single zone of mixed burning. This phenomenon can be seen in Figure 5.35, which shows the fire room temperatures for the OSB experiment. While the temperatures from the 3 ft (0.9 m). level to the ceiling are uniformly in excess of 1110°F (600°C), the 1 ft. and 2 ft. temperatures remain well below this benchmark. Compare this to the fire room temperatures from Experiment 5, which had a pallets triangle as the fuel load with pallets on the floor. At approximately 900 seconds after ignition, the temperatures throughout the fire room are uniformly in excess of 1470°F (800°C), in a behavior similar to that which would be observed in a furnished room. In many conventional training fuel packages, the fuel is centralized in one location, so while free burn HRR and fire room heat flux are consistent



with thresholds for flashover, the fire dynamics produced by these fuel packages, such as those listed in Table 5.8, are different than flashover as it would be observed in a furnished room.

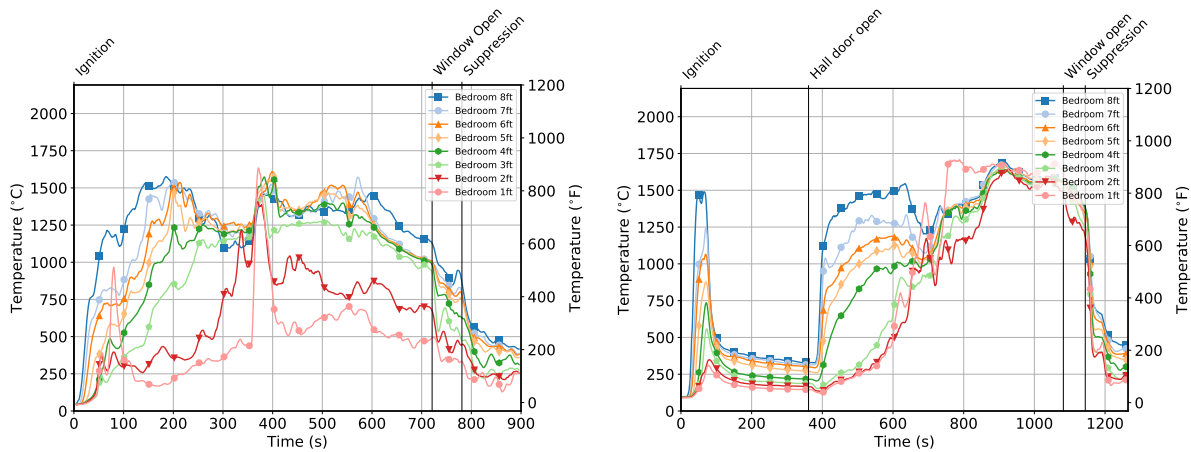


Figure 5.35: Fire room temperatures for OSB fuel package (left) compared to fuel package with pallets on floor (right)

This difference is important for several reasons. First, it illustrates the effect that fuel close to the floor of the compartment, such as carpet or pallets, can have on the conditions within the compartment. As described in Section 5.6.8, the presence of fuel on the ground can result in flashover, even with a comparatively small training fuel load such as three pallets and one bale of straw. Perhaps even more important from a training perspective, instructors and students should recognize that merely preventing flashover does not prevent the potential for thermal injury. All of the end hall heat flux values have the potential to cause damage to firefighter PPE, particularly SCBA face pieces [27], for extended durations, and the heat flux values for all of the experiments but the one bale of excelsior and three pallet triangle exceed the heat flux to which some components of the PPE ensemble are tested [25, 26]. These thermal conditions have the potential not only to damage PPE, but result in thermal injuries after short exposures, particularly if cooling is not done prior to firefighters advancing into the area. Thus, when selecting a fuel load, it is important that instructors consider the size of the fire compartment, the amount of ventilation available to that compartment, and the potential exposures to students and instructors.

## **5.7 Training Prop Experiment Limitations**

The intent of the series of training prop experiments described in Section 5 was to evaluate training fuel packages in a training prop with different ventilation configurations. It is important to note that the fire dynamics documented in this section would be subject to change if the same fuel package or fuel configuration were used in a different training building or prop with different ventilation tactics. For this reason, instructors should always evaluate the fire dynamics produced by a fuel package from a safe observation area before including students in the evolution.

# 6 Training Considerations

## 6.1 Fuel Package Design Can Take Advantage of *NFPA 1403* Compliant Fuels

NFPA 921 defines fire dynamics as “detailed study of how chemistry, fire science, and the engineering disciplines of fluid mechanics and heat transfer interact to influence fire behavior”. [49] A student of fire dynamics understands how fires grow and spread in all types of materials. The fire dynamics of a particular fuel depends not only on the quantity and material properties of the fuel but its geometry as well as where it is located. The available ventilation and geometry of the compartment its located both play a role in the ultimate size of the fire. When conducting live fire training it is often desired to conduct multiple evolutions during the same day in the same structure to allow all trainees the opportunity to gain a similar experience for the intended lesson. With inherent complexities of fire dynamics, this can be difficult if not impossible to teach the same lesson if the fuel load, compartment and available ventilation are not repeatable. This is especially important for suppression based evolutions.



Figure 6.1: Characteristics of some common fuel packages. Less dense easily ignitable material surrounded by more dense longer burning duration fuels. 1 bale of excelsior with a 3 pallet triangle (top left), 1 bale of straw with a 3 pallet triangle (top middle), 1 bale of straw with a 3 pallet triangle and 3 pallet box (top right), 4 Pallets vertical with 1 bale of straw (bottom left), 5 pallets vertical with 1 bale of straw (bottom middle), 6 pallets vertical with 1 bale of straw (bottom right).

The burning characteristics of materials vary due to their chemical make up as well their density, specific heat and heat of combustion. Understanding these concepts allows instructors to develop a compliment of materials to meet the needs of the specific training scenario. If a rapid growth

rate is desired, using materials such as straw, hay and excelsior as the item first ignited provides the easily ignitable, rapidly developing fire desired due to their low density high surface area. The same material properties that permit them to be easily ignited, limit the duration of burning. If the lesson requires a longer burning period, more dense materials such as pallets, OSB or MDF, which all have a higher density and thus more mass, but are harder to ignite are required for the desired burning duration.

The training fuel packages evaluated, surround the easily ignitable material with a more dense material such as the fuel packages in Figure 6.1. This compliment of fuels and geometry provide the easily ignitable, predictable growth desired coupled with the steady state energy release needed for evolutions where timing is flexible.

In addition to adding different fuels, orientation also plays a significant role in the fire heat release rate. When the same amount (mass) of fuel is stacked differently as shown in Figure 6.2 the resulting fire will have different peak heat release rates, and will produce different periods of steady burning.

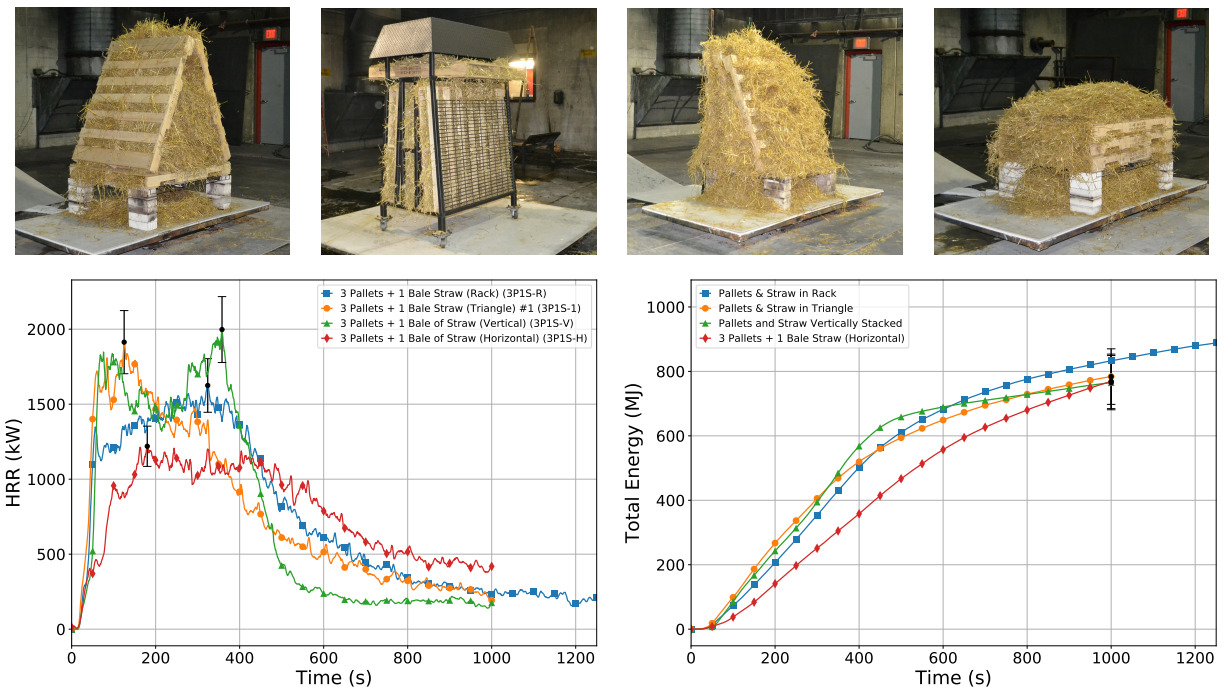


Figure 6.2: Example of how the same quantity (mass) of fuel can produce very different heat release rates. One Bale of Straw surrounded by three pallets in a triangle (top left), One bale of straw packed in three pallets using a rack and hood (top middle left), One Bale of Straw with Three Pallets Stacked Vertically (top middle right), One Bale of Straw with Three Pallets Stacked Horizontally (top left). HRR vs. Time in a free burn configuration comparing a the four different orientations (bottom left), and Total Energy Released (bottom right).

When the pallets are stacked vertically the peak is approximately 2.0 MW, however when the pallets are stacked horizontally the peak is just over 1.0 MW. Using a Triangle method or a rack

provide results in between the 1.0 MW and 2.0 MW range. When the same amount of initial fuel is used, those with a lower the peak release the energy over a longer duration. The vertically stacked pallets had a HRR in excess of 500kW for 7.3 minutes while the horizontally stacked pallets stayed above 500 kW for 12.1 minutes. Although the peak heat release rate and time in excess of 500 kW was quantifiable different, because the each fuel package had relatively the same mass of fuel, the total energy release was indistinguishable when utilizing this measurement technique.

Matching the duration of the evolution to the steady burning duration and the peak heat release rate to the intended fire “experience” utilizing different geometry is one way instructors can use their understanding of fire dynamics as they relate to training fuels to develop a fuel package that will meet the intent of the lesson.

## **6.2 Training Fuel Packages Do Not Need To Be Tended During Evolutions**

The practice of “tending” or “stoking” the fuel package during evolutions is practiced by some training academies, and is typically done in an effort to minimize the amount of time between evolutions. This process can place instructors close to the fire room, and expose them to more sever thermal conditions for extended periods of time.

The results of these experiments indicate that several of the fuel packages could produce steady peak thermal conditions for durations on the order of minutes in the metal training prop. For example, the MDF, OSB, and 1 in x 6 in dimensional lumber fuel loads all had sustained end hall heat flux values in excess of 15 kW/m<sup>2</sup> for nine minutes and end hall HGL temperatures in excess of 750°F (400°C) for 10.5 minutes.

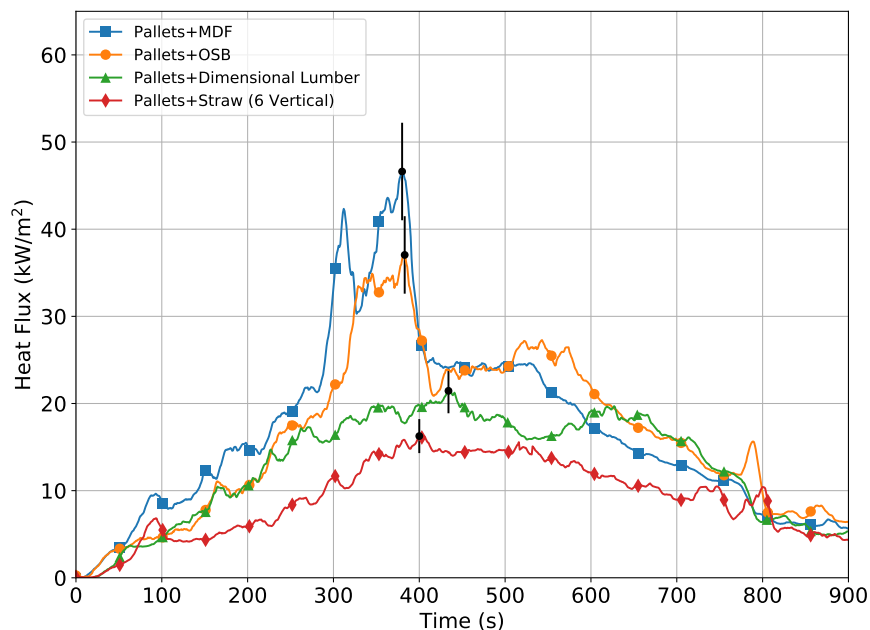


Figure 6.3: Peak hallway heat flux for large wood training fuels (OSB, MDF, Dimensional Lumber, 6 Pallets).

The duration of this peak period was related to the quantity of fuel in the fuel package. Because of this, instructors should consider the learning objectives of the evolution when selecting a fuel package. For example, if the intended scenario requires a longer period of peak temperatures and heat fluxes, a larger fuel package could be used to prolong the peak burning period. Another option that instructors could consider is delaying the ignition of a smaller fuel package until a time when students are closer to the fire room. This could be useful for evolutions conducted in a larger burn building or evolutions requiring a longer hose advancement. It is important for instructors to recognize that the peak durations observed in this series of experiments may increase or decrease depending on the available ventilation and type of training prop in which the scenario is being conducted. By tailoring the evolution to fit a specific objective, instructors can reduce or eliminate the need for tending fuel packages, reducing the need for unnecessary thermal exposures.

### 6.3 Obscuration Can Be Increased Without Using Synthetic Fuels

Recognizing that the smoke produced by some training fuel packages is not as optically dense as the smoke produced by the plastics and foam products that make up the furnishings in residential homes, some instructors have begun to explore methods to increase the density of smoke. The results of these experiments indicated that the addition of a small amount of tar paper or polyurethane foam in the form of a sofa cushion impacted the fire dynamics of a training fuel package with three

pallets and one bale of straw in a triangle configuration, as indicated by the fire room heat flux values at the end of the hallway, shown in the left chart of Figure 6.4. Despite the higher peak heat flux in the fire room for the tar paper fuel package, the end hall heat flux measurements show that the peak heat flux and temperatures to which students and instructors outside of the fire room would be exposed were comparable among the three experiments.

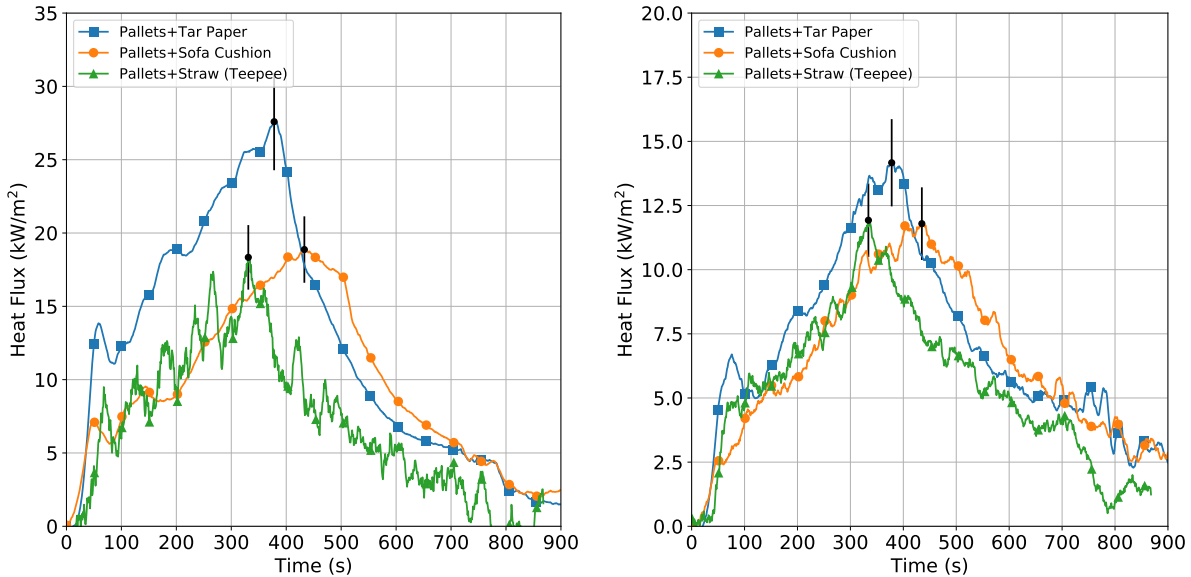


Figure 6.4: Difference in fire growth in fire room (left) and heat flux in hallway (right) for experiments with a small amount of additional synthetic fuel.



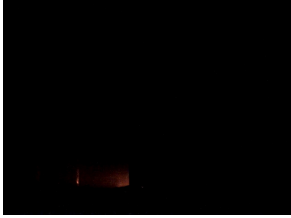




While the addition of these materials did not drastically affect the fire dynamics, it did result in an increase in smoke obscuration at the doorway of the metal prop. Table 6.1 compares the peak obscuration values, measured at 4 ft (1.2 m) and 7 ft (2.1 m) from the bottom of the doorway, for the training fuel packages evaluated in the metal prop and a furniture fuel load, for comparison. The two three pallet configurations exhibited different obscuration behavior. The three pallets in a lean-to configuration grew more quickly, resulting in a short-lived peak obscuration which was comparable to the two cases with synthetic addition, before decreasing. The three pallets in a horizontal configuration did not grow as rapidly, and thus the peak obscuration was significantly less than both the lean-to and both pallet fuel loads with synthetic additions.





In both of the training fuel packages with synthetic fuel, the 7 ft obscuration was significantly higher than the three pallet training fuel packages with no synthetic materials. The peak 4 ft obscuration for the synthetic training fuel packages was higher than the peak 4 ft obscuration of the horizontally stacked pallets, but was comparable to the lean-to fuel package. The increase in obscuration that was observed in the sofa cushion and tar paper fuel packages is likely due to a combination of the additional fuel mass in the fuel package and the higher soot yield of the synthetic components. Soot yields cited for flexible polyurethane foam range from 0.131-0.227 g/g, compared to 0.015 g/g for different species of wood. The soot yield of synthetic materials can be as much as an order of magnitude higher than the soot yield of wood products. Because of this,



it would be expected that training fuel packages with synthetic contents, such as a sofa cushion or tar paper, would produce sootier, more optically dense smoke. While the tar paper and sofa cushion fuel loads did result in a sustained increase in obscuration compared to both pallet-only fuel loads, the visibility conditions were still far different than those observed with a furnished room as a fuel package. While obscuration measurements were not taken for the furniture fuel load, the qualitative difference between the visibility in the hallway for this fuel package and the visibility conditions in the hallway for the training fuel packages can be seen in Table 6.1.

Table 6.1: Peak Obscuration for Non-NFPA 1403 Compliant Fuel Packages

Fuel Package	Peak Obscuration (%)	
Pallets w/ Tar Paper	7 ft (2.1 m): 90% 4 ft (1.2 m): 68%	
Pallets w/ Sofa Cushion	7 ft (2.1 m): 91% 4 ft (1.2 m): 60%	
Furniture	7 ft (2.1 m): n.a. 4 ft (1.2 m): n.a.	
3 Pallets (Lean-to) and Straw	7 ft (2.1 m): 54% 4 ft (1.2 m): 65%	
3 Pallets (Horizontal) and Straw	7 ft (2.1 m): 65% 4 ft (1.2 m): 40%	
Smoke Barrel	7 ft (2.1 m): 92% 4 ft (1.2 m): 44%	
Smoke Barrel w/ Leaf Blower	7 ft (2.1 m): 92% 4 ft (1.2 m): 53%	

Fuel Package	Peak Obscuration (%)	
6 Pallets (Lean-to) and Straw	7 ft (2.1 m): 91% 4 ft (1.2 m): 71%	
3 Pallets, Straw, and OSB	7 ft (2.1 m): 92% 4 ft (1.2 m): 69%	
3 Pallets, Straw, and MDF	7 ft (2.1 m): 92% 4 ft (1.2 m): 53%	
3 Pallets, Straw, and 1 x 6 Dim. Lumber	7 ft (2.1 m): 83% 4 ft (1.2 m): 76%	

Adding a small amount of synthetic fuel to a wood-based fuel load was one method that resulted in an increase in obscuration, but was not the only method that was successful in increasing smoke opacity. The addition of smoke barrels in the fire room of the metal prop resulted in a similar sustained increase in doorway obscuration, as Table 6.1 shows. Two smoke barrel experiments were conducted, each with a fuel load of three pallets and straw in a triangle. One of these experiments incorporated a leaf blower to entrain additional air into the smoke barrel. The obscuration measurements and corresponding images show that the smoke barrels resulted in similar obscuration at the 7 ft (2.1 m). level in the doorway to the sofa cushion and tar paper fuel packages, while the 4 ft (1.2 m). obscuration was slightly lower. The use of a leaf blower to supplement airflow into the smoke barrel resulted in an increase in 4 ft (1.2 m). obscuration compared to the experiment with no leaf blower. The smoke barrels are designed to produce smoke, but not flaming combustion, by increasing the moisture content and packing density of the straw within the barrel. By doing this, the barrels produces supplemental smoke to complement the smoke produced by the primary fuel package, which in this case was a three pallet triangle. The addition of the leaf blower increases the airflow through the smoke barrel, and thus the production rate of smoke.

Another method of increasing the smoke density while using *NFPA 1403*-compliant fuels was using a larger wood-based fuel load, as was done in the experiments where OSB, MDF, 1 in. x 6 in. dimensional lumber, or 3 additional pallets were added to the base fuel load of three pallets and one bale of straw. The peak obscuration values and images from Table 6.1 show that all of these fuel loads exhibited doorway obscuration values that were comparable to or greater than the wood-based fuel loads with a small addition of synthetic material. The higher peak obscuration of these heavier fuel packages may be related to the combustion efficiency of the fuel packages. Section 4 indicated that the OSB, MDF, dimensional lumber, and six pallet fuel packages had higher peak HRRs than smaller fuel packages. Further, the peak free burn HRR of these fuel packages exceeded the minimum HRR required for flashover calculated using Equation 4.4 of the metal container prop (1.78 MW). Thus, the higher obscuration observed for these experiments may be because of inefficient combustion, which resulted in a greater quantity of unburned fuel in the gases escaping from the fire room.

While adding a small amount of synthetic material to a training fuel load can increase the optical density of the smoke without drastically affecting the fire dynamics, there are other ways to achieve reduced visibility while still using fuel materials compliant with *NFPA 1403*. Furthermore, while a small amount of synthetic material did not result in an increase in peak fire conditions, a larger addition of such fuels, such as a sofa, almost certainly would result in significantly more severe thermal conditions within the training prop. Indeed the addition of an inappropriate amount of synthetic materials to the fuel load has resulted in several LODDs related to live fire training [18, 19].

## **6.4 When using NFPA 1403 compliant wood-based fuels, orientation and quantity are important for predicting fire size**

When designing a fuel package for a training evolution, it is important for instructors to recognize that the orientation and quantity of fuel are predictors for the fire dynamics that will be produced by the evolution. These effects can be visualized in Figure 6.5, which shows the hallway heat flux for the three pallet lean-to and horizontally stacked configurations and the six pallet lean-to. The figure shows that changing the orientation of three pallets and one bale of straw from horizontal to vertical shifts the timing of the peak earlier in the experiment. The peak burning period, indicated by the heat flux at the end of the hallway, occurs approximately 600 seconds after ignition for the horizontally stacked pallets and approximately 400 seconds after ignition for the lean-to fuel package. The chart also shows that the peak heat flux during this peak burning period is slightly lower in the lean-to fuel package than the horizontal fuel package, which is likely tied to the difference in weight between them. The horizontally stacked package weighs 30 lbs. (13.6 kg) more than the lean-to fuel package. This effect of fuel weight on the magnitude of peak thermal conditions is better demonstrated by the difference between the three pallet and six pallet lean-to fuel packages. The additional three pallets resulted in an increase in weight from 61.1 kg to 108.9 kg. This increase in fuel weight was reflected by an increase in the peak burning heat flux from approximately 8 kW/m<sup>2</sup> to approximately 16 kW/m<sup>2</sup>. While the magnitude of the heat flux during

this peak period increased, the timing of the peak was similar, occurring close to 400 seconds.

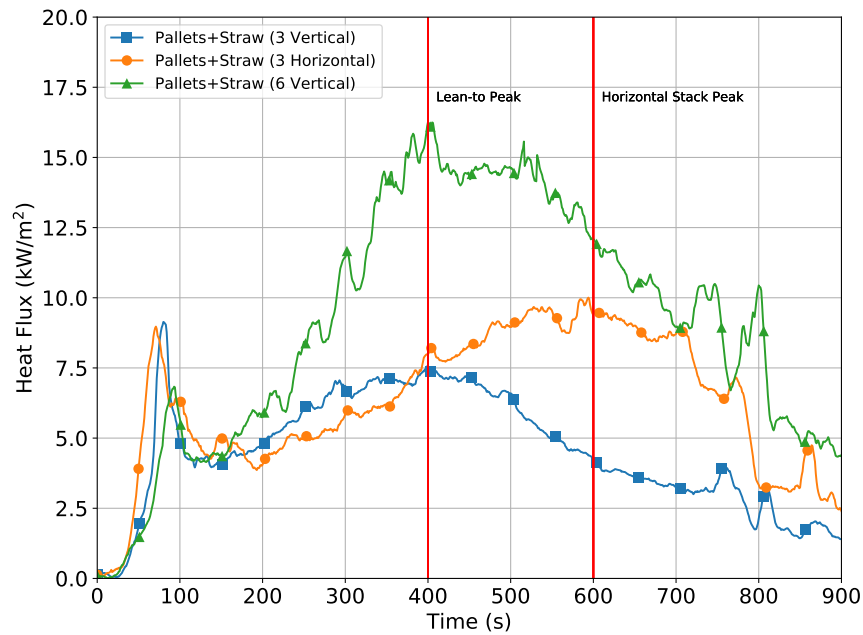


Figure 6.5: Timing of peak thermal conditions for vertically- and horizontally-oriented pallet fuel packages

In general, the magnitude and duration of the peak thermal conditions within the prop were related to the quantity of fuel in the fuel package. To illustrate this, Figure 6.6 shows the relationship between the end hall heat flux numerically integrated over the duration of the experiment and fuel package weight. This “cumulative energy exposure” provides an estimate of the total amount of heat energy that the end hall heat flux gauge is exposed to during each experiment. The chart shows that as the fuel weight increases, the hallway exposure also tends to increase. The higher hallway exposures indicate that higher heat flux values are maintained for longer durations. The chart also shows that for fuel packages of a similar initial weight, the exposure was comparable. This would seem to indicate that changing the fuel weight had a greater effect on the magnitude and duration of heat flux at the end hall location than changing the orientation of the fuel package. This is consistent with the results of the HRR characterization experiments from Section 4.1.

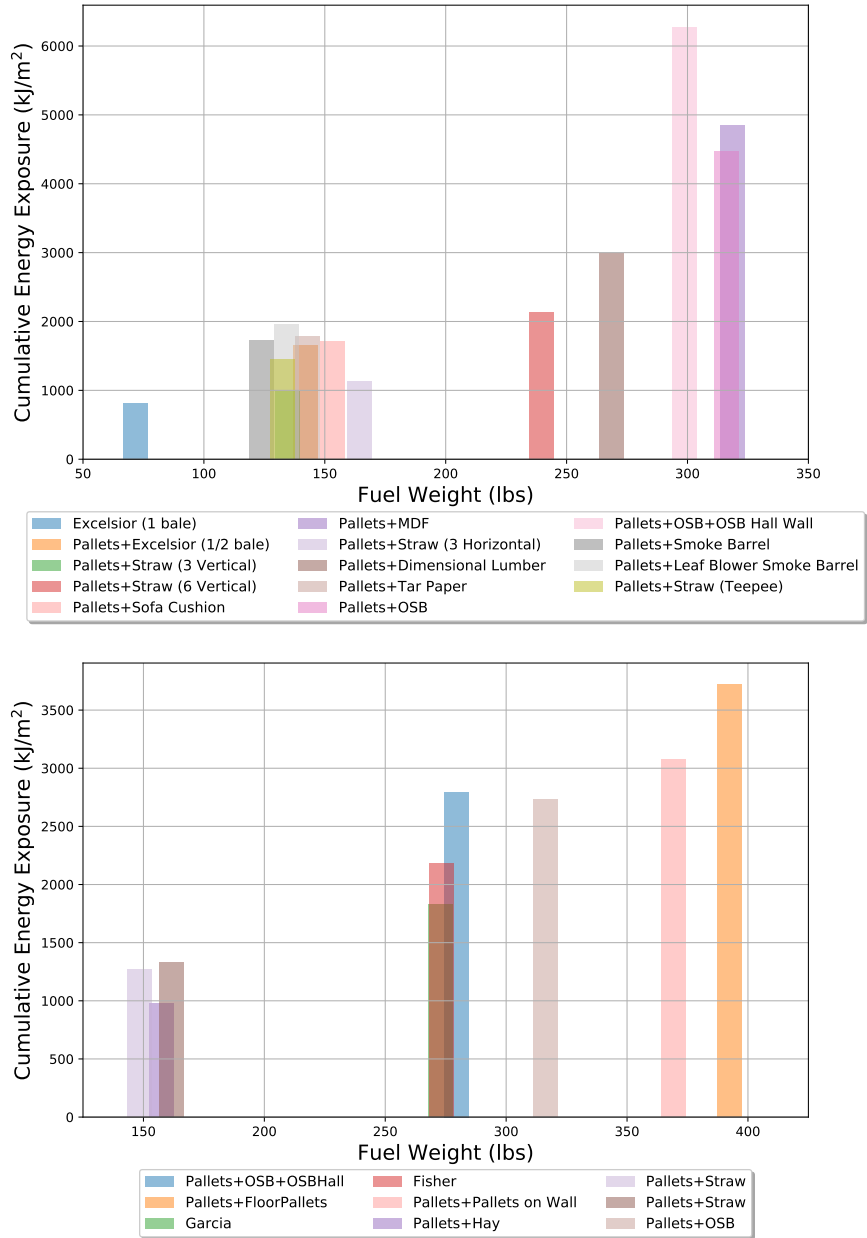


Figure 6.6: Total energy exposure vs. fuel weight at end hall heat flux location for experiments with door open at ignition (top) and door open at 6 minutes (bottom).

Figures 6.5 and 6.6 illustrate that arrangement of wood-based fuels within the fuel package can have significant impacts on the timing of the fire growth. Instructors should keep these effects in mind when attempting to match the configuration of the fuel with the intended lesson. The results of these experiments also showed that larger training fuel packages tended to result in longer fully-developed” stages, often with higher peak heat flux values, than smaller fuel packages. In effect, the timing and magnitude of the “fully-developed” portion of a training fire’s growth curve can be

manipulated by changing the orientation and fuel weight to fit the intended learning objectives.

## 6.5 Select the Fuel Package for the Intended Lesson

While selecting a fuel load for a training evolution, instructors should consider the learning objectives of the evolution, and how the fuel package can be selected to satisfy the learning objectives while balancing the safety of participants. *NFPA 1403* recommends that “Fuel materials shall be used only in the amounts necessary to create the desired fire size” [8]. In many instances, the fuel load necessary to create the appropriate fire size or visual cues may not create the largest fire or the most severe thermal conditions. Further, a fuel load that may be appropriate for a particular training evolution in one type of prop may not be appropriate for the same training evolution in a different prop, since different fuel packages in different buildings will produce different fire dynamics.

### Fire Dynamics Lesson

Section 4.3 of *NFPA 1403* lists several training subjects as prerequisites for participating in live fire training. Among these topics are fire dynamics, fundamentals of fire behavior, and fire development within a compartment. Rather than immediately trying to teach these topics using a full scale demonstration, instructors may want to explore using small-scale models and demonstrations to complement the classroom training on these topics.



Figure 6.7: Candle demonstrations of fire dynamics principals. Wood fuels (left) and synthetic fuels (right).

One method of accomplishing this would be a lesson on fire dynamics utilizing a candle flame and small samples of fuel. Instructors can introduce students to the fire triangle, expanding to



concepts such as pyrolysis, and unburned fuel. Figure 6.7 shows examples of these concepts being demonstrated with candle flames. The next step could be placing a small fire in a scaled model of a compartment, or compartments, that can be used to demonstrations on the effects of ventilation, neutral plane or flow path. Figure 6.8 shows the use of small scale compartment fires for instruction before moving to full scale rooms. The use of simple or scaled models and small amounts of fuel may be the most effective method of teaching fire dynamics concepts without the added complexities of wearing full protective equipment in a limited visibility hot environment.



Figure 6.8: Scaled house burns demonstrating ventilation limited fire, from NFFF Fire Dynamics Boot Camp Howard County Maryland (left); neutral plane, from FireHouse Expo Aggressive Fire Control, Flow Path and VEIS Tactics class 2018 by All Hands Fire Photos (center); and flow path from FireHouse Expo Aggressive Fire Control, Flow Path and VEIS Tactics class 2018 by All Hands Fire Photos (right).

If demonstrating ventilation limited fires and the response to ventilation is the intent, the fuel package and structure must be complimentary to create the intended fire dynamics. In order to create a ventilation limited fire the lesson should occur in a structure where there is minimal leakage around closed windows and doors, thus limiting the oxygen available for combustion to the oxygen present in the structure. The fuel package should release enough energy such that, it will become ventilation limited, while keeping its peak HRR below the level required for flashover.

The growth of fires in materials made of wood, paper or natural fibers with little to no flammable plastics (Class III Commodities as defined by NFPA 13 [50]) can be impacted when the oxygen in the area of the fire is reduced. The fire may self extinguish when the oxygen in the area of the fire reaches a range between 13.6%-15.0%. [51] After selecting a structure with little to no natural leakage with openings which can be well sealed, the instructor may want to conduct an evaluation of the volume of the structure compared to the total energy available in the fuel package to approximate if enough oxygen will be consumed to cause the fire to self extinguish.

Figure 6.9 shows the potential energy available for combustion when assuming the growth rate of the fire will be impacted when oxygen in the area of the fire reaches 15% (yellow zone) or 13.6% orange zone. Locations in the gray zone would be less likely to have the growth of a wood-based fuel be impacted by the available oxygen. The vertical lines on the Figure represent the total energy released from common fire service training fuel packages. To determine if a particular fuel package has the potential to have its growth affected by ventilation in a tightly sealed, given volume structure, compartment or compartments; find the volume of the compartment, compartments or entire structure if all doors are open and locate the point at which it intersects with the proposed fuel package. If the intersection is in the gray zone, the growth of a wood-based fuel will most likely respond as if the fire had unlimited oxygen available. If the intersection is in the yellow zone, the growth of the fire has the potential to become affected by the available oxygen. If the intersection is in the orange zone it has the potential to self extinguish due to the lack of oxygen. The further towards the right and bottom of the chart the scenario is the greater potential there would be for a back draft.

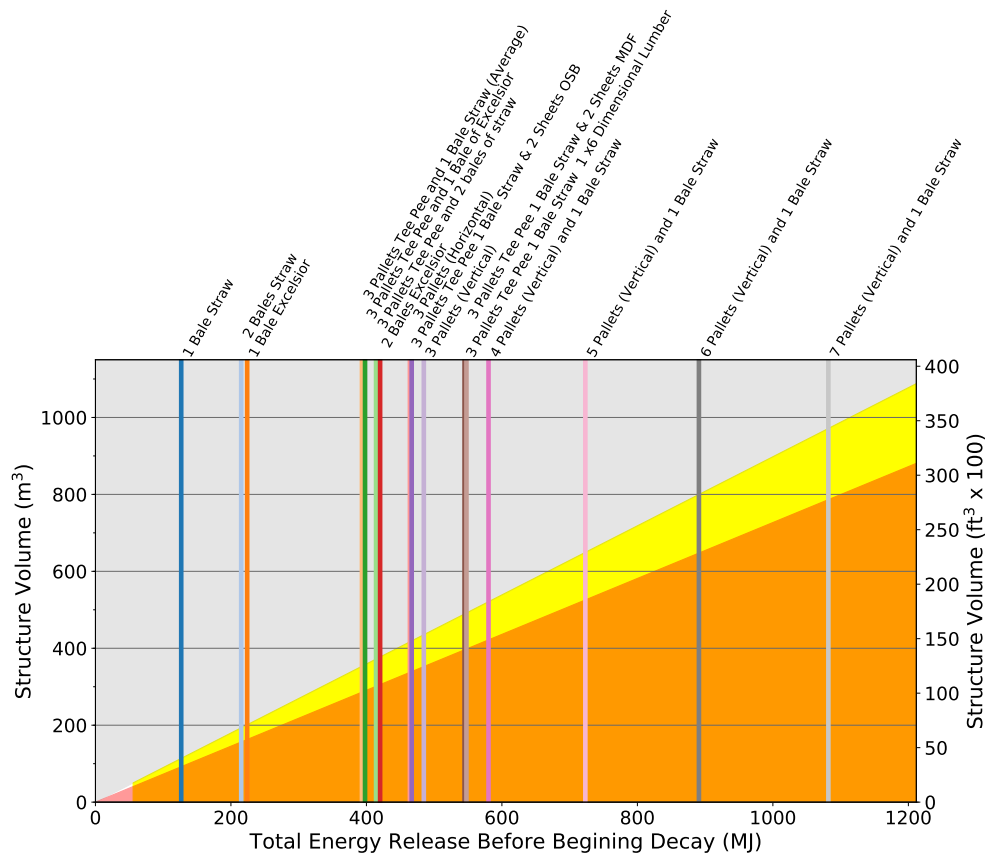


Figure 6.9: Comparisons of Structure Volume vs the Approximate Energy Needed to Consume Oxygen in a compartment, or structure where little to no natural ventilation exists and all openings can be tightly sealed. In structures where an appreciable amount of leakage exists this concept would not apply. Vertical lines represent the total energy release of a given fuel package prior to it starting to decay.



that students participate in the evolution from a safe observation area, a large fuel load capable of flashover would be appropriate for such an evolution.

$$\dot{Q} = 750A_o\sqrt{H_o}$$

## Search and Rescue

When students are actively participating and operating within the training prop while conducting live fire training, using the fuel package necessary for the lesson becomes even more critical, as the potential for injury of students and instructors increases. In some cases, it may be advantageous to use alternative methods of creating the necessary conditions, such as when conducting search and rescue training in a low visibility environment. Section 6.3 described how low visibility conditions could be achieved by using large wood-based training fuel packages. These fuel packages, however, may produce thermal conditions with the possibility to cause injury or damage to equipment when operating close to the fire room. Instead, instructors might opt to use smoke barrels or a similar method to create optically dense smoke to simulate searching in a low visibility situation. Figure 6.11 shows the obscuration during the burn barrel experiments where the barrel was located in the fire room. The barrel was ignited prior to the ignition of the main fuel package in the room (three pallets and one bale of straw). While in these experiments, the smoke production from the burn barrel was less effective for the 100 seconds immediately after the ignition of the primary fuel package, it is possible that locating the burn barrel remote from the primary fuel package may provide more constant smoke production, producing the desired limited visibility environment.

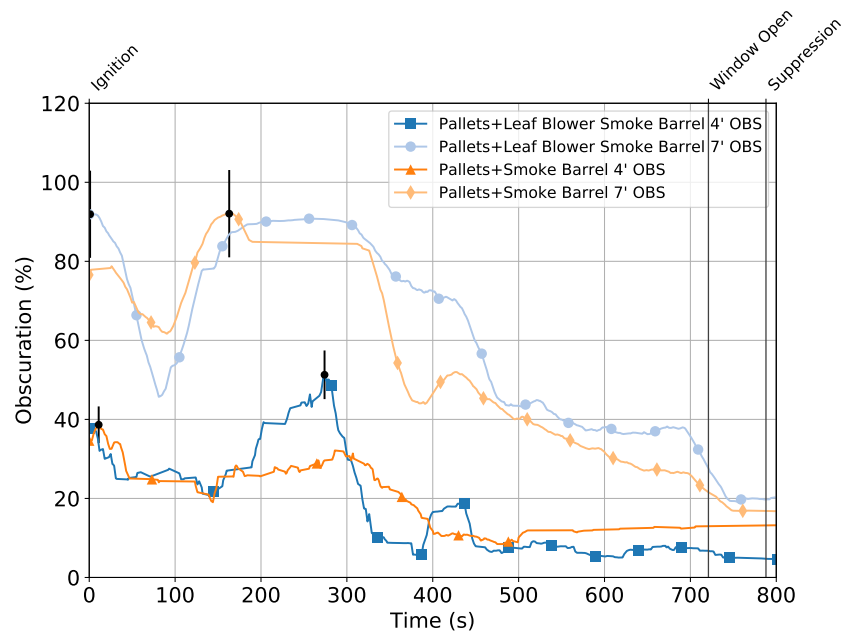


Figure 6.11: Effect of igniting primary fuel package on obscuration from smoke barrels.

When developing limited visibility conditions for search and rescue, it is important to remember locating the smoke generation point on a floor below the fire can provide students with the impression smoke conditions will exist on the floor below the fire as well as the fire floor. As shown in the *Impact of Ventilation on Fire Behavior in Legacy and Contemporary Residential Construction* [11], when the fire is located on the second floor, it is difficult to develop any appreciable smoke conditions on the first floor of the structure. Once the smoke layer descends below the level of the fuel on the second floor, combustion becomes limited due to the limited oxygen, greatly reducing the generation of products of combustion. For a fire on an upper level, the smoke layer will likely stratify at that level, rather than below it, due to buoyancy. It is important that the conditions during the training evolution be placed into the appropriate context, to avoid potential misunderstandings.

Although not specifically evaluated in this project, consideration should be given to placing the smoke barrel(s) in a location which limit the thermal insult to the instructor tasked with maintaining it. This may involve placing the barrel in a location remote from the fuel package or outside the structure with a mechanism to pipe the smoke into the areas needed.

## **Hoseline Advancement & Suppression**

A live fire training evolution which looks and feels similar to an attack team advancing on a fire may aim to replicate the high heat and low visibility that a firefighter on the nozzle would experience. Reproducing the severe thermal conditions to which an advancing attack team would be exposed while maintaining a degree of safety for instructors and students can be challenging, however. By conducting a designated hose advancement evolution, with a specifically selected fuel package and training prop, instructors can exert a greater amount of control on the training evolution. This may help to maintain a balance of fidelity and safety in a training evolution designed to produce more severe thermal conditions.

Figure 6.12 shows the heat flux in the end of the hallway outside of the fire room for several of the training fuel packages evaluated in the metal container prop. The fuel packages with higher fuel weights, such as the MDF, OSB, and dimensional lumber fuel packages produced peak heat fluxes which were similar to or greater than the peak heat flux measured in the furniture fuel package. For these fuel packages, without cooling prior to advancing to the end of the hallway, an attack team would be subjected to peak heat flux values which exceed the design criteria of PPE.



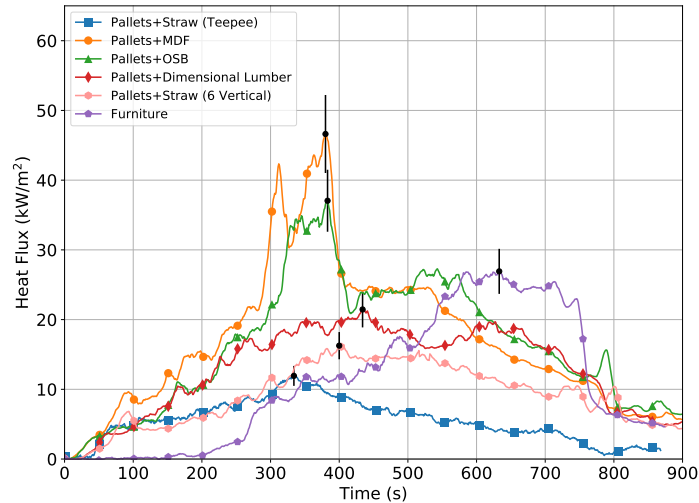


Figure 6.12: Effect of adding additional fuel on heat flux in hallway outside of the fire room during a hallway and room burn in a container prop.

While the peak thermal conditions produced by the training fuels shown in Figure 6.12 were severe, none of the fuels, including furniture, had extended periods of rollover in the metal container prop. If visible rollover or fire venting from the prop is required to satisfy learning objectives for either a demonstration or a tightly monitored hose advancement drill, placing fuel outside of the fire room may help to satisfy these conditions.

Affixing OSB to the ceiling of the hallway exposed this fuel to the high-temperature flows exiting the fire room, causing the OSB on the ceiling to pyrolyze. This resulted in a longer period of severe thermal conditions in the hallway compared to the fuel package with OSB only in the fire room. The heat flux exceeded  $15 \text{ kW/m}^2$  for 600 seconds during the experiments with pallets, straw, and OSB with OSB on the hallway ceiling compared to 350 seconds for the experiments with pallets, straw, and OSB in the fire room. The addition of OSB to the ceiling resulted in a sustained period of rollover for 180 seconds, which was not observed in the experiment without OSB lining the hallway ceiling, as shown in the hallway camera view, in Figure 6.13. Because of the extended period of severe thermal conditions in the hallway and presence of fuel on the ceiling, the ability to visually demonstrate rollover down the hallway by lining the ceiling of the hall with OSB comes at the expense of safety of potential participants.



Figure 6.13: Difference in visible rollover with three pallets, one bale of straw, and three sheets of OSB in fire room with OSB on hallway ceiling (left) and without OSB on hallway ceiling (right)

The most severe thermal conditions in the hallway for the training fuel packages evaluated in these experiments were observed when OSB was placed outside the fire room on the hallway walls and ceiling. Placing the OSB low in the hallway rather than along the ceiling still exposes the fuel to the high temperature flows exiting the fire room, but also places it where there is sufficient oxygen to precipitate combustion. This led to flashover in the hallway and fire venting from the front door of the prop. While this training fuel load was able to successfully replicate the visual cue of fire venting from the front door of the prop, the peak heat flux at the end of the hallway was nearly twice as high as the furniture fuel package, as shown in figure 6.14. The peak heat flux observed in the hallway for the furniture experiment was  $15 \text{ kW/m}^2$ , compared to  $27 \text{ kW/m}^2$  for the pallets straw and OSB and  $52 \text{ kW/m}^2$  for pallets, straw, and OSB, with OSB on the hallway walls and floor.

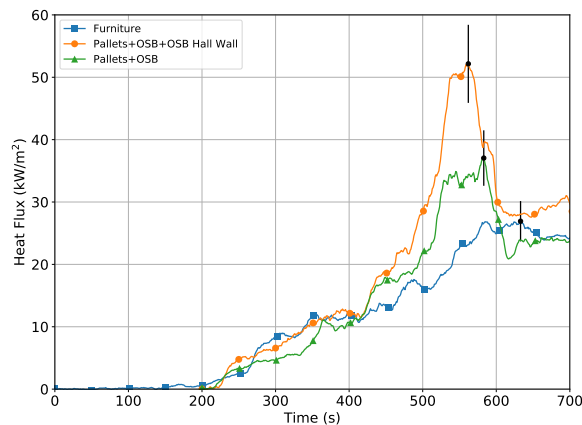


Figure 6.14: Heat flux at the level of a kneeling firefighter just outside the fire compartment (left) and still image from camera outside the hallway door at 410 s (right), demonstrating the effect of adding additional fuel to the hallway during a hallway and room burn in a container prop. The growth of the training fuel props was offset by 200 seconds to match the growth of the furnished room.



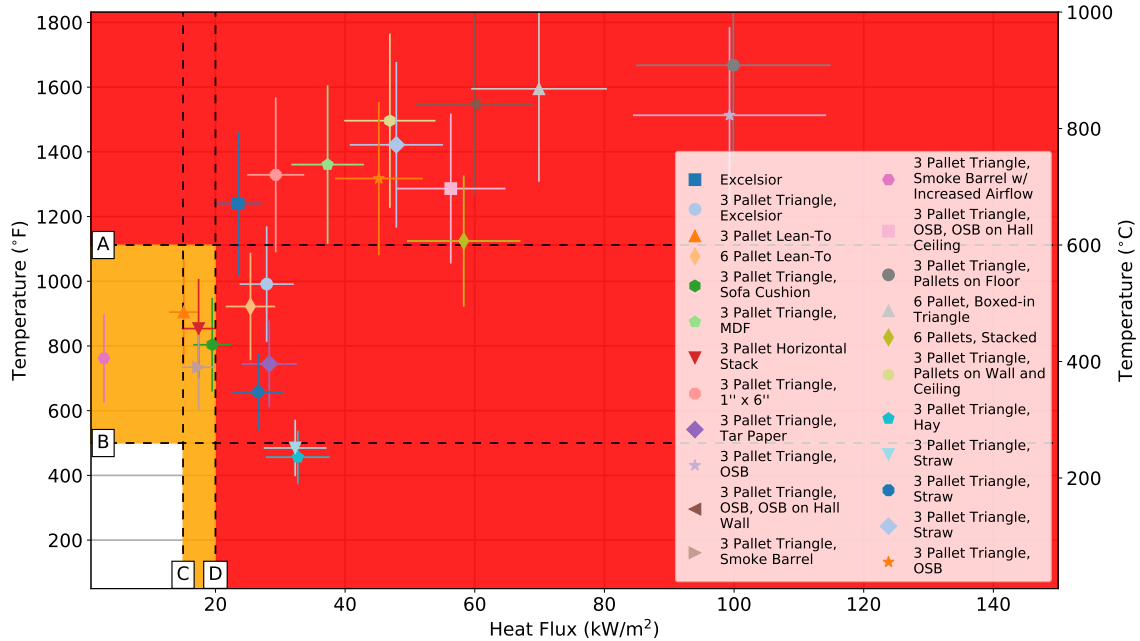
Conducting training which satisfies learning objectives and provides students with lessons in the correct context while balancing their safety while participating in these evolutions can be challenging. Recognizing the difference in heat content, soot yield, and other material properties between *NFPA 1403* compliant wood-based fuels and synthetics and foam plastics, instructors may be tempted to select a fuel package which will produce the largest fire possible, in an effort to recreate the high heat and low visibility conditions identified in many residential structure. By using only the amount of fuel necessary to create the desired conditions, however, instructors may be able to create a training evolution which will be safer and more beneficial to their students than by using the same fuel package for every live fire training scenario, or the largest fuel package possible. Further, it is critical for instructors to recognize that the construction and geometry of the training prop and the available ventilation will both affect the fire dynamics produced by any fuel package. The fire dynamics detailed in this section may be drastically different than those if the same fuel package were used in a concrete building, acquired structure, or other training prop. Because of this, instructors should always evaluate a new fuel package and do so with the anticipated ventilation intended for the scenario, without students, and from a safe distance before employing it in live fire training.

## **6.6 Wood-based training fuels can create hazardous conditions without transitioning to flashover**

A controlled flashover conducted as part of a fire behavior demonstration can be a useful tool for teaching fire dynamics to students. *NFPA 1403* Section A.4.13.7 provides a methodology for conducting such an evolution, with safety precautions that include a charged hoseline and a safe viewing area for students and instructors. While a controlled flashover executed with appropriate precautions can successfully satisfy learning objectives, a flashover that was not planned as part of a demonstration and without the appropriate safeguards in place can be hazardous to students and instructors alike. *NFPA 1403* recommends that “The fuel load shall be limited to avoid conditions that could cause an uncontrolled flashover or backdraft” [8]. Although limiting the fuel has the potential to prevent flashover, it is important to recognize that conditions can be created, particularly close to the fire room, where firefighters in full protective gear have the potential for injury.

Common criteria for the onset of flashover can be based on temperature or heat flux. *ASTM E603-17: Standard Guide for Room Fire Experiments* states that the onset of flashover typically corresponds with a ceiling temperature between 500 and 600°C and a heat flux to the floor of 20 kW/m<sup>2</sup> [52]. Further, *NFPA 921: Guide to Fire and Explosion Investigations* describes flashover as a transition to a “single zone of well-mixed burning” [49]. In addition to being criteria for flashover, temperature and heat flux can be used to approximate the potential heat transfer to a firefighter operating in a given area. This method of using temperature and heat flux to approximate the hazards to a firefighter was proposed by Utech at the 1972 Fire Department Instructors Conference. His evaluation used the heat flux as an approximation of the energy a firefighter would be receiving via radiation and the gas temperature as an approximation of the energy a firefighter would be receiving via convection [24]. Figure 6.15 shows the maximum 3 ft (0.9 m) tempera-

ture, representative of the lowest temperature in the upper layer, plotted against the heat flux to the floor in the fire compartment. The red area represents values exceeding criteria consistent with the onset of flashover. The orange area represents criteria exceeding the test limits of the firefighters protective gear if too much time is spent at that exposure.



- 
- A 1112°F (600 °C) - Upper layer gas temperature indicative of the onset of flashover. [52]
  - B 500°F (260 °C) - NFPA 1971 - ASTM F2894/FM2894M Test for Heat Resistance. [25]
  - C 15 kW/m<sup>2</sup> - Design exposure for SCBA facepiece lens for Radiant Heat Test. [26]
  - D 20 kW/m<sup>2</sup> - Heat flux at floor level indicative of the onset of flashover. [53]
- 

Figure 6.15: Fire Room Flashover Criteria - Training Fuels

The peak thermal conditions in the fire room exceeded the design criteria for firefighter PPE for each of the twenty-three container prop experiments. Five of these experiments, (three pallet lean-to, three pallet horizontal stack, three pallets with a sofa cushion, and the two experiments with three pallets and a smoke barrel) exceeded the design criteria of turnout gear but did not meet the threshold for the onset of flashover. The remainder of the fuel packages exceeded either the heat flux or the temperature criteria for the onset of flashover. The fuel packages with the largest amount of fuel exceeded both the temperature and heat flux criteria for flashover. The reason for the severe thermal conditions that were observed in the fire room is related, in part, to the size of the fire room. Figure 6.16 shows the floor plan of the L-Shape training prop used. The size of the compartment used for the fire room was 7 ft 9 in by 14 ft 11 in (1.4 m x 4.5 m), or just over 115 ft<sup>2</sup> (10.7 m<sup>2</sup>), the equivalent size of a small residential bedroom. With a small compartment such as this one, even fuel loads as small as one bale of excelsior or three pallets and straw were capable of producing conditions that would result in thermal conditions with the potential to result in damage

to firefighters protective equipment and cause firefighter injury.

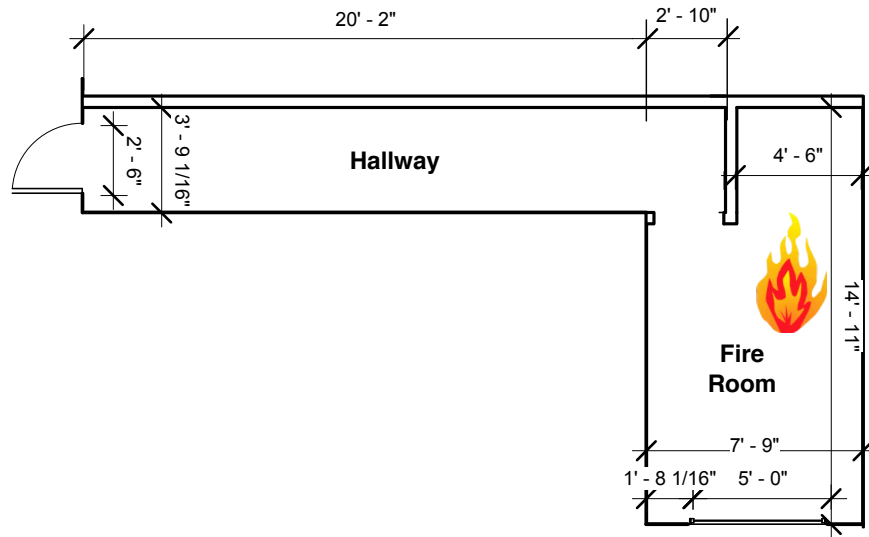
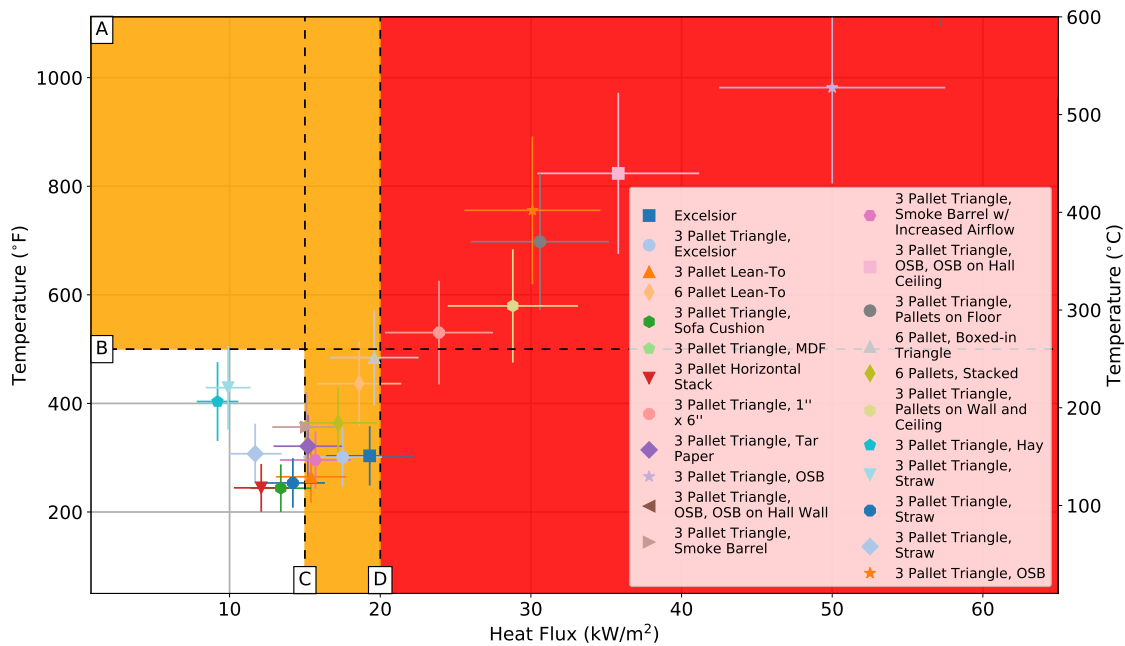


Figure 6.16: Floor Plan of L Shape Training Prop Used

Thus, for each of the fuel packages evaluated, the thermal conditions within the fire room would become hazardous in the short term for firefighters in full PPE. In addition to these hazards in the fire compartment, the location just outside of the fire compartment had the potential to damage a firefighters protective equipment. To understand this potential, consider Figure 6.17, which shows temperature and heat flux for each experiment along with the design criteria for firefighter PPE (orange shaded) and the threshold for the onset of flashover (red shaded). Even outside the compartment, 16 of the fuel loads exceeded the design criteria of firefighter PPE, and several of the experiments exceeded the criteria for the onset of flashover, although this exposure is more likely indicative of fire exiting the door of the fire room to the heat flux gauge at the end of the hallway.



- 
- A 1112°F (600 °C) - Upper layer gas temperature indicative of the onset of flashover. [52]
  - B 500°F (260 °C) - NFPA 1971 - ASTM F2894/FM2894M Test for Heat Resistance. [25]
  - C 15kW/m<sup>2</sup> - Design exposure for SCBA facepiece lens for Radiant Heat Test. [26]
  - D 20kW/m<sup>2</sup> - Heat flux at floor level indicative of the onset of flashover. [53]
- 

Figure 6.17: Modern PPE design criteria versus and thermal exposures in hallway of training prop. Note that the experiment with pallets, straw, and MDF and the experiment with pallets, straw, OSB, and OSB on the hallway walls both exceeded the axes of this figure.

Limiting the size of the training fuel package, and particularly keeping fuel off of the floor of the compartment, can help to avoid the single zone of well-mixed burning that is associated with flashover. It is important for instructors to realize, however, that fuel packages can produce conditions with the potential to damage firefighter PPE and cause thermal injury without reaching flashover. Therefore, it is important that instructors select fuel packages that are appropriate for the training prop being used, the learning objectives, and the participants.

## 7 Future Research Needs

As the fire service continues to utilize live fire training evolutions to educate members, constant questions arise as to the most effective and safest fuels. This report was able to provide some basic data needed to estimate the energy release from common fire service fuel packages along with provide some guidance to instructors for conducting live fire training evolutions. The scope of the experiments limited the conclusions which could be drawn, with further research needed. Additional heat release rate characterization experiments are needed to look at the repeatability of the fuel packages, as well as further quantifying the impact to geometry and the differences in pallet sizes/weights. Additionally, further characterization of how fully furnished rooms compare to multiple training fuel packages inside a compartment and the comparison of equations for flashover combine is needed to more accurately understand the implications for different fuel choices.

Further investigation should include expansion of the use of the fuel packages tested into different types of fire service training props. The fuel is only one component of the ability to replicate the fire dynamics on an actual emergency incident. The building and available ventilation play a crucial role in the peak energy release and potential thermal exposure. Conducting similar fuel characterizations experiments in concrete buildings, metal container buildings and even flashover simulators is needed to further quantify the effects of the fuels used to replicate the fire environment.

Although this project addressed the thermal exposure to firefighters, recent research into firefighters and cancer rates has caused some scrutiny on live fire training fuels as they relate the the carcinogenic exposure. The products of combustion of the various fuels should be investigated to determine potential exposure risks of the fuels. Ideally bench scale materials testing could be used to quantify the composition of the fuel pre-burn with effluent testing used to evaluate the chemical produced during combustion along with environmental monitoring of the training ground post evolution to quantify the effect on the training building an surrounding facilities.

## 8 Summary

As material science evolves, the fuels which the fire service will be exposed to on emergency incidents change. Replicating the fire dynamics of these fuels safely and effectively with substitute materials will lead to more accurate lessons during live fire training. This project was able to provide initial data on the peak heat release rates from some common training fuel packages which was in the range of 1.0 MW to 4.0 MW and total energy release in the range of 200.0 MJ to 2000.0 MJ. The calculated effective heat of combustions combustion ( $\Delta H_{c,eff}$ ) was in the range of 9 MJ/kg to 17 MJ/kg, with a reliable approximation for wood-based fuels being 14.9MJ/kg. The energy release related directly to the mass loss rate with a very strong correlation between the mass of fuel consumed and the total energy released regardless of the use of dimensional lumber, pallets or engineered wood products. As the fire service continues to use wood-based fuels required by *NFPA 1403* the focus should be more on the quantity (mass) and geometry of the fuels and not on the type of wood-based fuel, such as the difference between OSB and dimensional lumber.

The use of non-wood-based fuels for fire training, did provide some increase in smoke density or obscuration. However, the same results can be achieved using additional wood-based fuels. Fidelity can be increased in many instances simply by using the fuel package for the intended lesson. Acknowledging that limiting the fuel package to avoid flashover is a significant step to increasing safety however does not remove fully the potential for thermal injury.

# References

- [1] F. Reeder. The NFPA 1403 Debate. *Fire Rescue*, July 2013.
- [2] S. Kerber. Analysis of Changing Residential Fire Dynamics and Its Implications on Fire-fighter Operational Timeframes. *Fire Technology*, 48:865–891, October 2012.
- [3] M. Loflin. Lieutenant and fire fighter die and 13 fire fighters injured in a wind-driven fire in a brownstone - Massachusetts. NIOSH F2014-09, National Institute for Occupational Safety and Health, March 2014.
- [4] S. Wertman. One career fire fighter/paramedic dies and a part-time fire fighter/paramedic is injured when caught in a residential structure flashover - Illinois. NIOSH F2010-10, National Institute for Occupational Safety and Health, March 2010.
- [5] M.E. Bowyer, S.C. Wertman, and M. Loflin. Career Captain Sustains Injuries at a 2-1/2 Story Apartment Fire then Dies at Hospital – Illinois. NIOSH F2012-28, NIOSH Fire Fighter Fatality Investigation and Prevention Program, 2013.
- [6] F. Washenitz, R. Braddee, T.A. Pettit, and E. Schmidt. Two Fire Fighters Die and Two Are Injured in Townhouse Fire – District of Columbia. NIOSH 99-F21, NIOSH Fire Fighter Fatality Investigation and Prevention Program, 1999.
- [7] S.K. Hoglander and S. Conver-White. House Fire with Significant Firefighter Injuries – Riverdale Heights, MD. Safety Investigation Team Report, Prince George’s County Fire/Emergency Medical Services Department, Lanham, Maryland, 2013.
- [8] National Fire Protection Association, Quincy, Massachusetts. *NFPA 1403: Standard on Live Fire Training Evolutions*, 2018.
- [9] J. Regan and R. Zevotek. Study of the Fire Service Training Environment: Safety and Fidelity in Concrete Live Fire Training Buildings. Underwriters Laboratories, Columbia, Maryland, July 2018.
- [10] J. Willi, K. Stakes, J. Regan, and R. Zevotek. Evaluation of Ventilation-Controlled Fires in L-Shaped Training Props. Underwriters Laboratories, Columbia, Maryland, October 2018.
- [11] S. Kerber. Impact of Ventilation on Fire Behavior in Legacy and Contemporary Residential Construction. Underwriters Laboratories, Northbrook, Illinois, December 2012.
- [12] S. Kerber. Study of the Effectiveness of Fire Service Vertical Ventilation and Suppression Tactics in Single Family Homes. Underwriters Laboratories, Northbrook, Illinois, June 2013.
- [13] R Zevotek and S. Kerber. Study of the Effectiveness of Fire Service Positive Pressure Ventilation During Fire Attack in Single Family Homes Incorporating Modern Construction Practices. Underwriters Laboratories, Columbia, MD, 2016.



- [14] National Fire Protection Association, Quincy, Massachusetts. *NFPA 1001, Standard for Fire Fighter Professional Qualifications*, 2013.
- [15] Demers Associates Inc. Two die in smoke training drill. *Fire Service Today*, pages 17–20, 1982.
- [16] S. Berardinelli. Career officer injured during a live fire evolution at a training academy dies two days later - Pennsylvania. NIOSH F2005-31, National Institute for Occupational Safety and Health, October 2005.
- [17] J. Tarley. Career Probationary Fire Fighter Dies While Participating in a Live-Fire Training Evolution at an Acquired Structure - Maryland. NIOSH F2007-09, National Institute for Occupational Safety and Health, February 2007.
- [18] National Institute for Occupational Safety and Health. Career lieutenant and fire fighter die in a flashover during a live-fire training evolution - Florida. NIOSH F2002-34, National Institute for Occupational Safety and Health, July 2002.
- [19] J. Tarley and T. Mezzanotte. Volunteer fire fighter dies and two others are injured during live-burn training - New York. NIOSH F2001-38, National Institute for Occupational Safety and Health, September 2001.
- [20] D. Madrzykowski. *Fatal Training Fires: Fire Analysis for the Fire Service*. National institute of standards and technology, Gaithersburg, MD, 2007.
- [21] G. Horn J. Willi and D. Madrzykowski. Characterizing a Firefighter's Immediate Thermal Environment in Live-Fire Training Scenarios. *Fire Technology*, 2016.
- [22] R. Rossi. *Fire Fighting and its Influence on the Body*. National institute for occupational safety and health, August 2003.
- [23] J.R. Lawson M.J. Selepak M. K. Donnelly, W. D. Davis. Thermal Environment for Electronic Equipment Used by First Responders . NIST technical note, National Institute of Standards and Technology, 2006.
- [24] H. Utech. Status report on research programs for firefighters protective clothing. In *Proceedings of the Fire Department Instructor's Conference*, Indianapolis, Indiana, 1973.
- [25] National Fire Protection Association. *NFPA 1971: Standard on Protective Ensembles for Structural Fire Fighting and Proximity Fire Fighting*, 2013.
- [26] National Fire Protection Association, Quincy, Massachusetts. *NFPA 1981: Standard on Open-Circuit Self-Contained Breathing Apparatus (SCBA) for Emergency Services*, 2013.
- [27] Mensch A Bryner N. Braga G. Putorti, A. Thermal Performance of Self-Contained Breathing Apparatus Facepiece Lenses Exposed to Radiant Heat Flux. National Institute of Standards and Technology NIST TN 1785, Gaithersburg, MD, 2013.
- [28] D. Madrzykowski. *Fire Fighter Equipment Operational Environment: Evaluation of Thermal Conditions*. Fire protection research foundation, Quincy, MA, August 2017.

- [29] R.A. Bryant and G. Mullholland. A guide to characterizing heat release rate measurement uncertainty for full-scale fire tests. *Fire and Materials*, 32:121–139, 2008.
- [30] Ohaus Corporation, Pine Brook, New Jersey. *Manual for SD Series Bench Scale*, 2000.
- [31] M. Janssens. *SFPE Handbook of Fire Protection Engineering*, chapter Calorimetry. National Fire Protection Association, Quincy, Massachusetts, 4th edition, 2008.
- [32] V. Babrauskas. *Ignition Handbook*. Fire Science Publishers, Issaquah, Washington USA, 1st edition, 2003. Co-published by the Society of Fire Protection Engineers.
- [33] V. Babrauskas and S. Grayson. *Heat release in fires*. Taylor & Francis, 1990.
- [34] *Fire Protection Handbook*. National Fire Protection Association, Quincy, Massachusetts, 18th edition, 1997.
- [35] F.W. Mowrer and J.R. McGraw Jr. Flammability of Painted Gypsum Wallboard Subjected to Fire Heat Fluxes. 1999.
- [36] Retrotec, Everson, WA. *Retrotec 5101 Classic Blower Door Specifications*, 2017.
- [37] B.N. Taylor and C.E. Kuyatt. Guidelines for Evaluating and Expressing the Uncertainty of NIST Measurement Results. NIST Technical Note 1297, National Institute of Standards and Technology, Gaithersburg, Maryland, 1994.
- [38] Stanley Hand Tools, New Britain, Connecticut. *User Manual TLM 100*, 2013.
- [39] T. Butcher, S. Cook, L. Crown, and R. Harshman. NIST Handbook 44: Specifications, Tolerances, and Other Technical Requirements for Weighing and Measuring Devices. *National Institute of Standards, Gaithersburg, MD*, 2012.
- [40] Omega Engineering Inc., Stamford, Connecticut. *The Temperature Handbook*, 2004.
- [41] L.G. Blevins. Behavior of bare and aspirated thermocouples in compartment fires. In *National Heat Transfer Conference, 33rd Proceedings*, pages 15–17, 1999.
- [42] W.M. Pitts, E. Braun, R. Peacock, H. Mitler, E. Johnson, P. Reneke, and L.G. Blevins. Temperature uncertainties for bare-bead and aspirated thermocouple measurements in fire environments. *ASTM Special Technical Publication*, 1427:3–15, 2003.
- [43] Medtherm Corporation, Huntsville, Alabama. *64 Series Heat Flux Transducers*, 2003.
- [44] W.M. Pitts, A.V. Murthy, J.L. de Ris, J. Filtz, K. Nygård, D. Smith, and I. Wetterlund. Round robin study of total heat flux gauge calibration at fire laboratories. *Fire Safety Journal*, 41(6):459–475, 2006.
- [45] S. Hostikka J. Floyd C. Weinshenck K. Overholt K. McGrattan, R. McDermott. Fire Dynamics Simulator Technical Reference Guide Volume 3: Validation. National Institute of Standards and Technology, 2017.

- [46] G. Fisher. Conducting NFPA 1403-Compliant Live Burn Training in Acquired Structures. *Fire Engineering*, March 2015.
- [47] K. Garcia and R. Kauffman. Realistic Live Burn Training You Can Afford. *Fire Engineering*, May 2009.
- [48] R.D. Peacock, P.A. Reneke, W.D. Davis, and W.W. Jones. Quantifying fire model evaluation using functional analysis. *Fire Safety Journal*, 33:167–184, 1999.
- [49] National Fire Protection Association, Quincy, Massachusetts. *NFPA 921, Guide for Fire and Explosion Investigations*, 2017.
- [50] National Fire Protection Association, Quincy, Massachusetts. *NFPA 13, Standard for the Installation of Sprinkler Systems*, 2019.
- [51] X. Zhou and Y. Xin. Evaluation of Oxygen Reduction System (ORS) in Large-Scale Fire Tests. FM Global, Norwood, MA, January 2018.
- [52] American Society for Testing and Materials, Philadelphia, Pennsylvania. *ASTM E 603-77, Standard Guide for Room Fire Experiments*, 1977.
- [53] P.A.; Bukowski R.W. Peacock, R.D.;Reneke and V. Babrauskas. Defining Flashover for Fire Hazard Calculations. *Fire Safety Journal*, 32(4):331–345, 1999.

# Appendices

# Appendix A Free Burn Heat Release Rate Results

## A.1 Training Fuel Packages

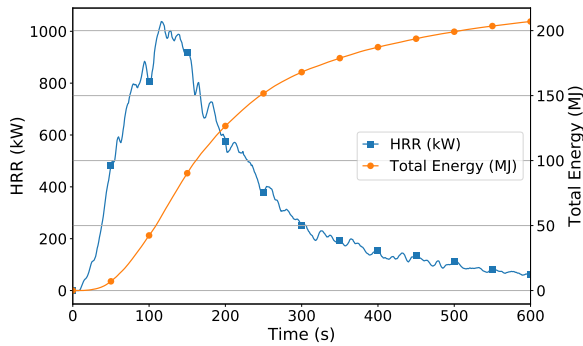


Figure A.1: 1 Bale Straw Energy Release

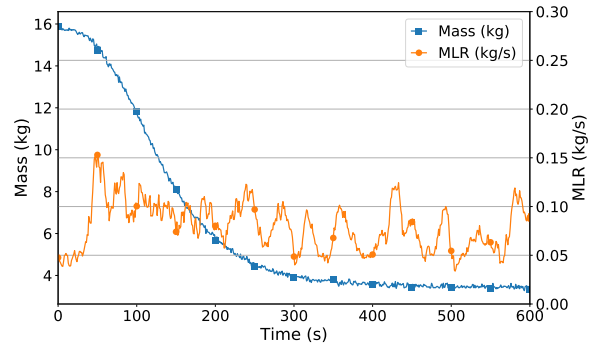


Figure A.2: 1 Bale Straw Mass

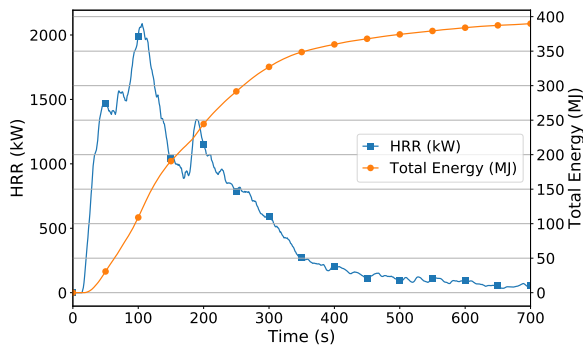


Figure A.3: 2 Bales Straw Energy Release

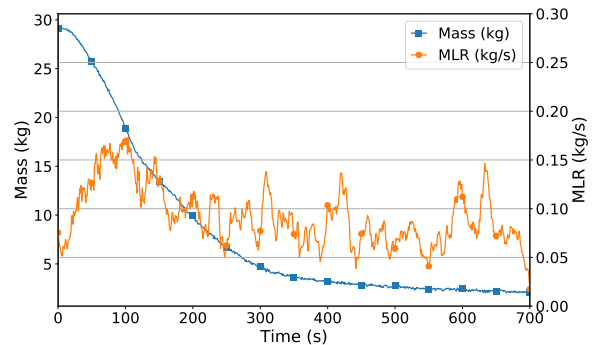


Figure A.4: 2 Bales Straw Mass

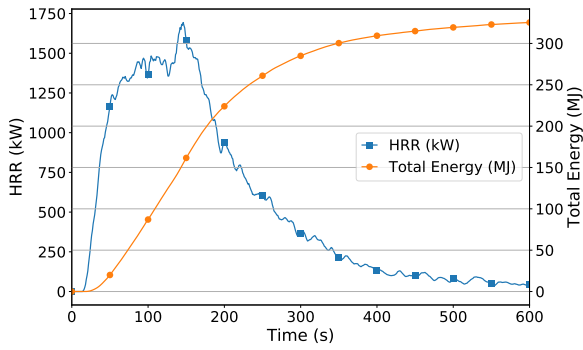


Figure A.5: 1 Bale Excelsior Energy Release

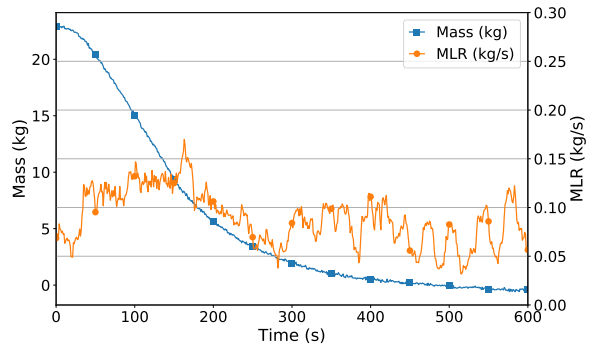


Figure A.6: 1 Bale Excelsior Mass

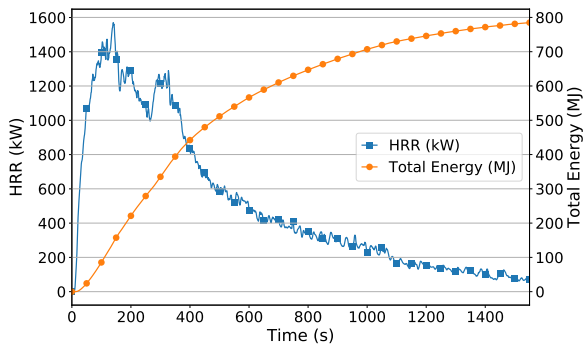


Figure A.7: 2 Bales Excelsior Energy Release

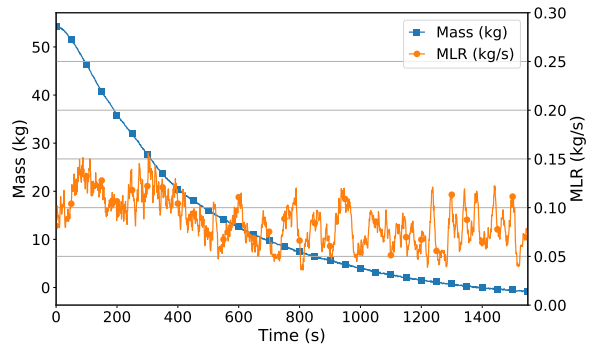


Figure A.8: 2 Bales Excelsior Mass

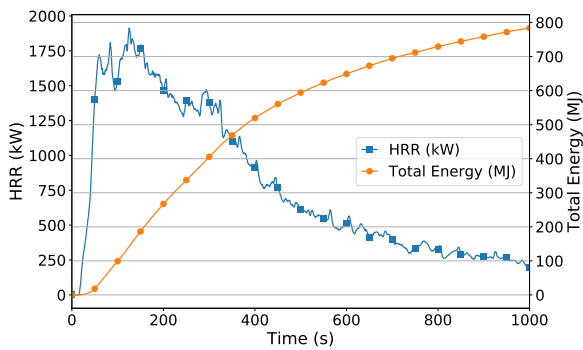


Figure A.9: 3P1S1 Energy Release

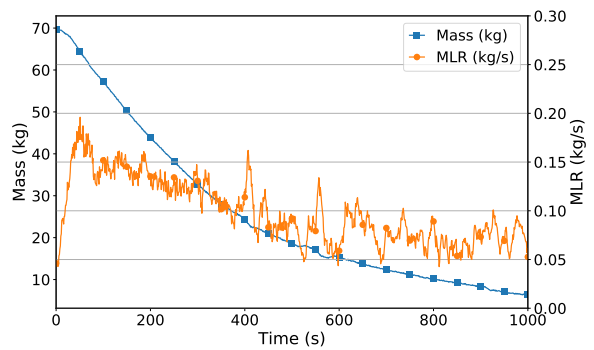


Figure A.10: 3P1S1 Mass

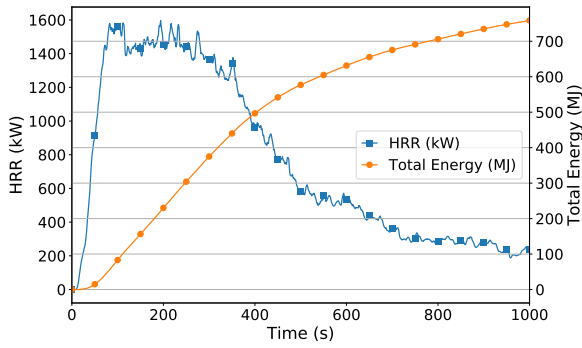


Figure A.11: 3P1S2 Energy Release

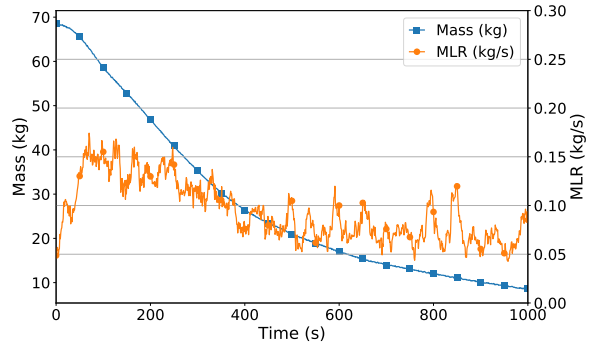


Figure A.12: 3P1S2 Mass

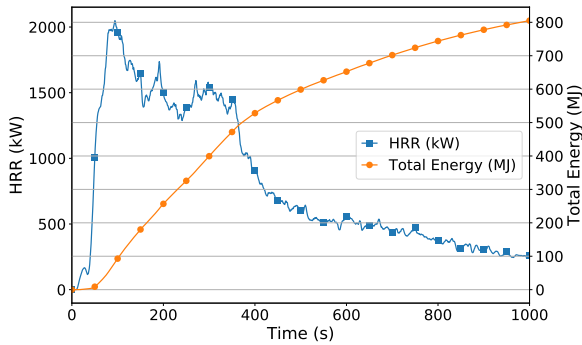


Figure A.13: 3P1S3 Energy Release

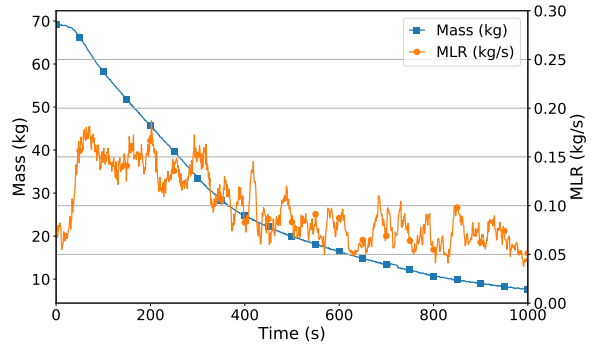


Figure A.14: 3P1S3 Mass

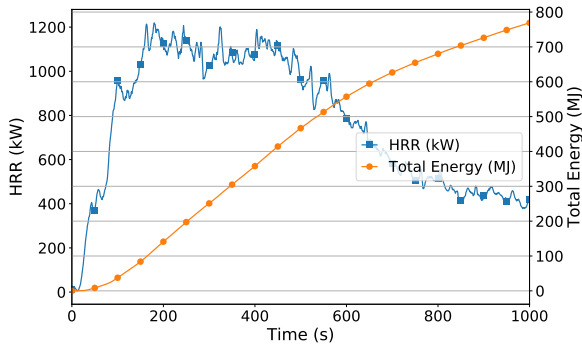


Figure A.15: 3 Pallets (Horizontal) Energy Release

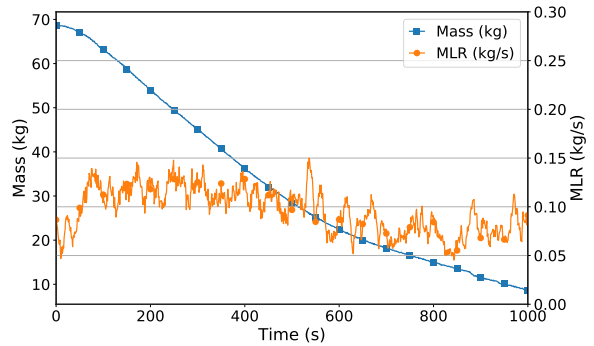


Figure A.16: 3 Pallets (Horizontal) Mass



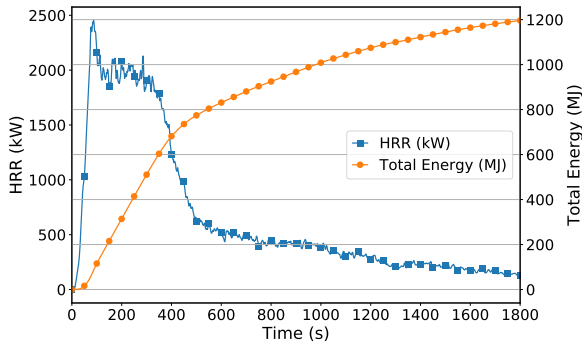


Figure A.17: Tee Pee and 2 bales of straw Energy Release

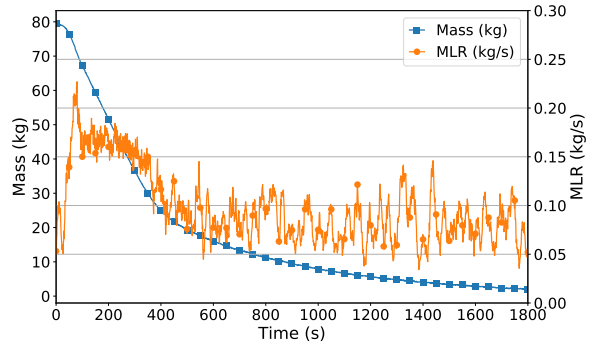


Figure A.18: Tee Pee and 2 bales of straw Mass

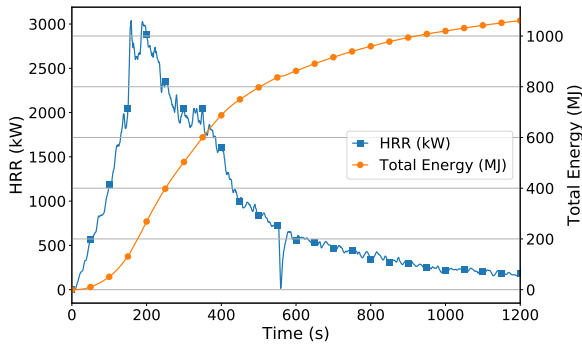


Figure A.19: Tee Pee and 1 Bale of Excelsior Energy Release

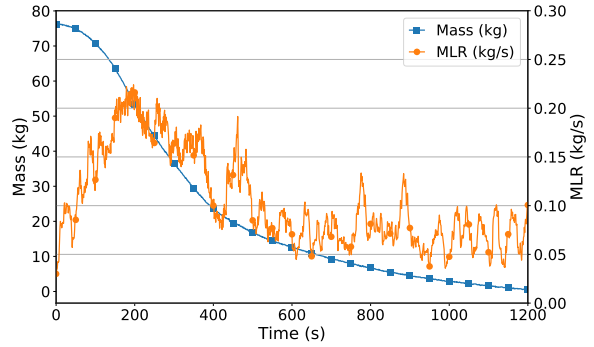


Figure A.20: Tee Pee and 1 Bale of Excelsior Mass

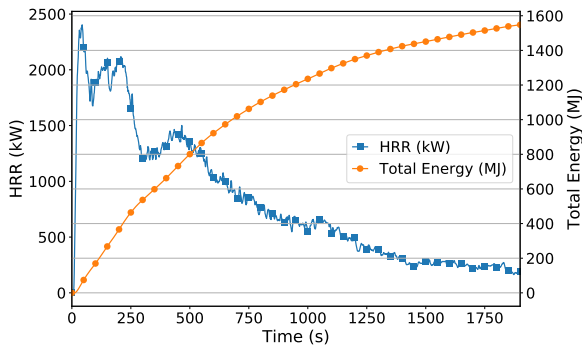


Figure A.21: Tee Pee 1 Bale Straw & 2 Sheets OSB Energy Release

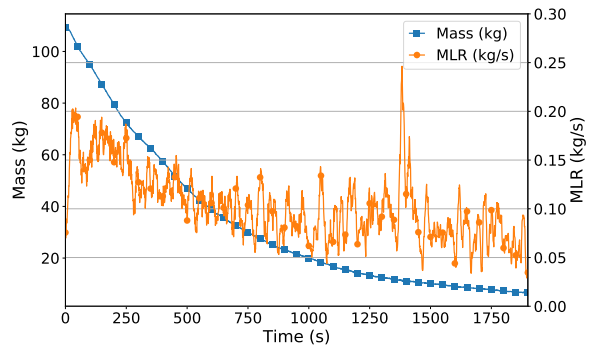


Figure A.22: Tee Pee 1 Bale Straw & 2 Sheets OSB Mass

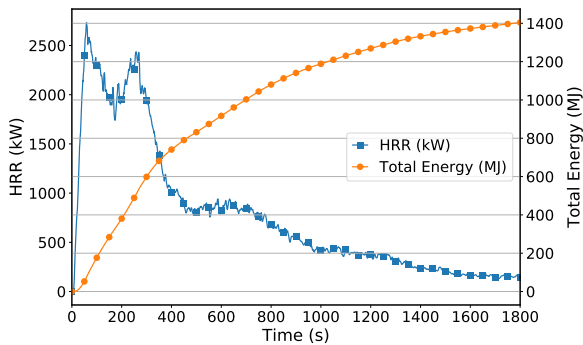


Figure A.23: Tee Pee 1 Bale Straw & 2 Sheets MDF Energy Release

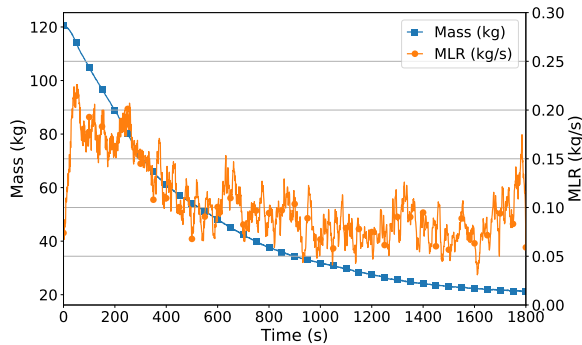


Figure A.24: Tee Pee 1 Bale Straw & 2 Sheets MDF Mass

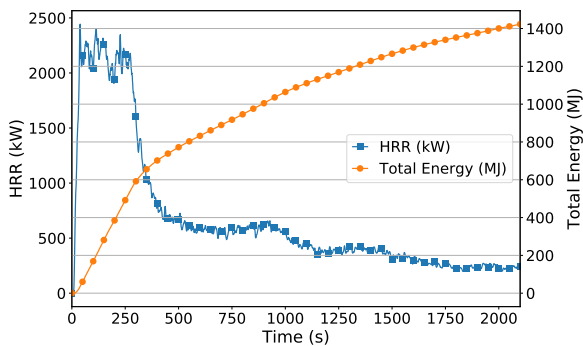


Figure A.25: Tee Pee 1 Bale Straw 1 x6 Dimensional Lumber Energy Release

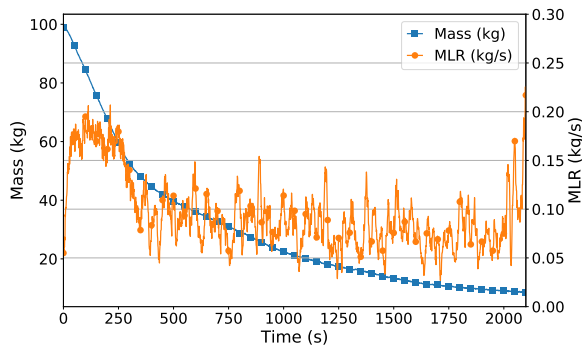


Figure A.26: Tee Pee 1 Bale Straw 1 x6 Dimensional Lumber Mass

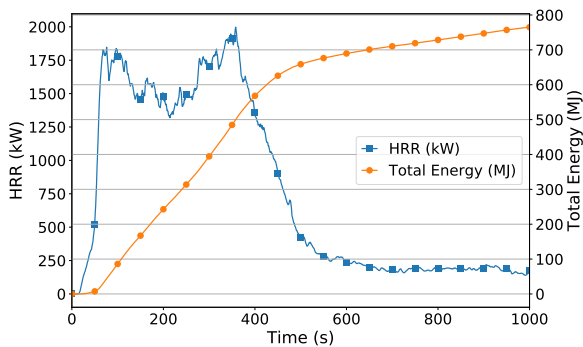


Figure A.27: 3 Pallets (Vertical) Energy Release

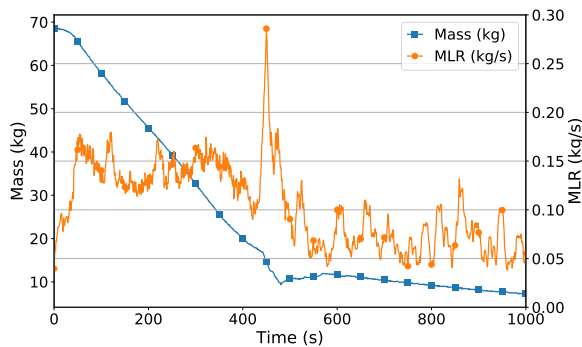


Figure A.28: 3 Pallets (Vertical) Mass

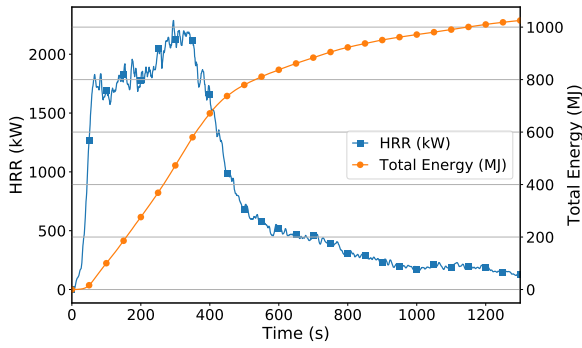


Figure A.29: 4 Pallets (Vertical) and 1 Bale Straw Energy Release

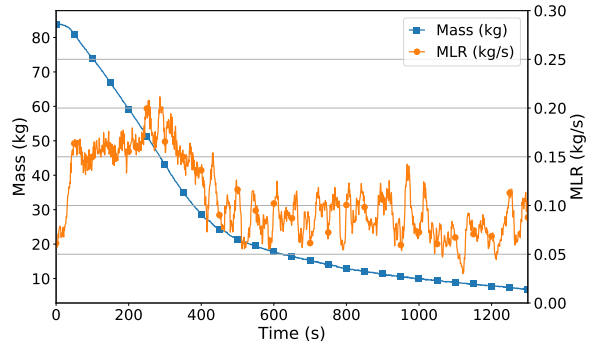


Figure A.30: 4 Pallets (Vertical) and 1 Bale Straw Mass

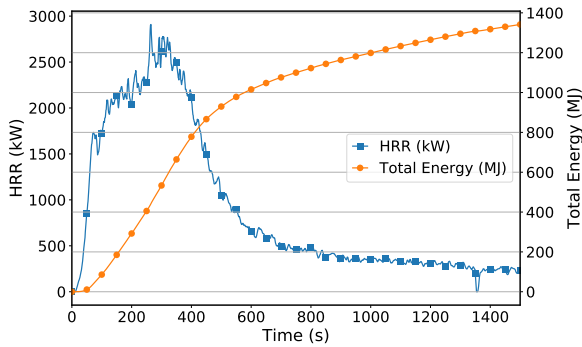


Figure A.31: 5 Pallets (Vertical) and 1 Bale Straw Energy Release

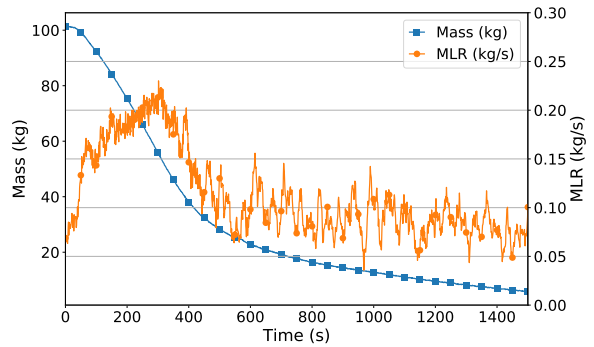


Figure A.32: 5 Pallets (Vertical) and 1 Bale Straw Mass

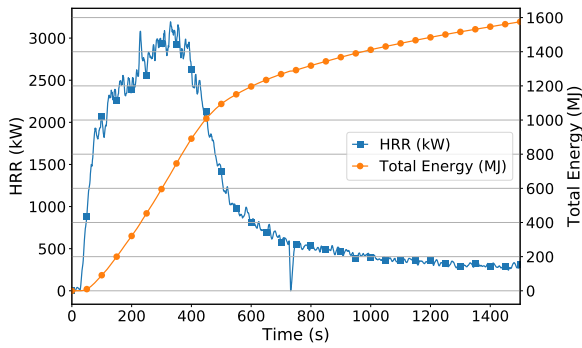


Figure A.33: 6 Pallets (Vertical) and 1 Bale Straw Energy Release

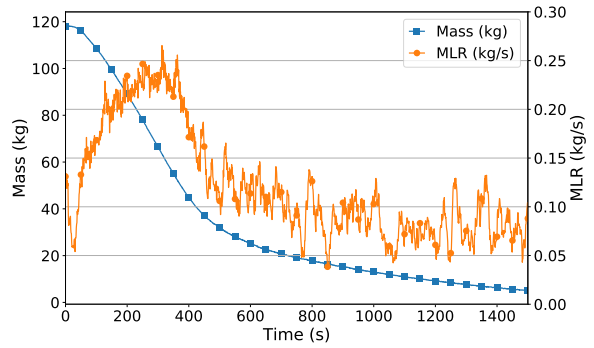


Figure A.34: 6 Pallets (Vertical) and 1 Bale Straw Mass

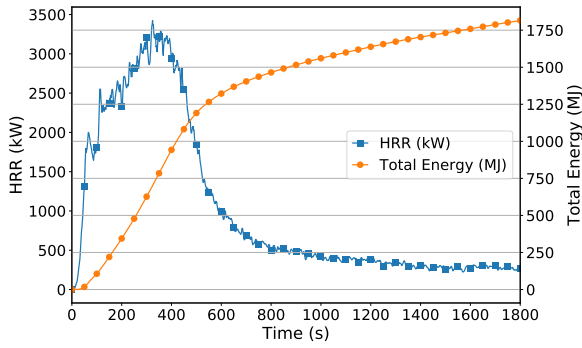


Figure A.35: 7 Pallets (Vertical) and 1 Bale Straw Energy Release

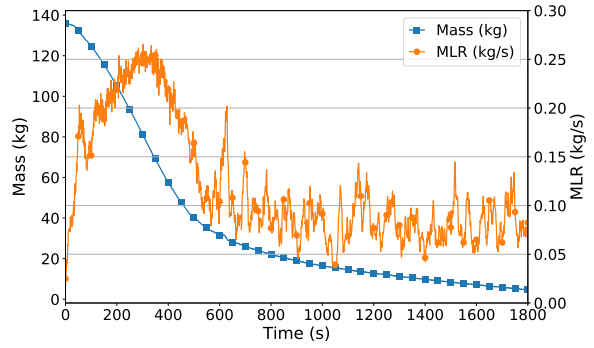


Figure A.36: 7 Pallets (Vertical) and 1 Bale Straw Mass

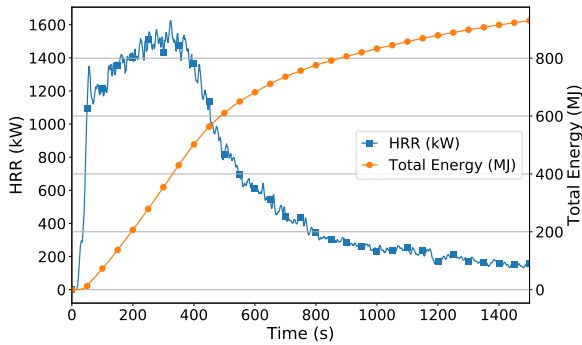


Figure A.37: Arnold Energy Release

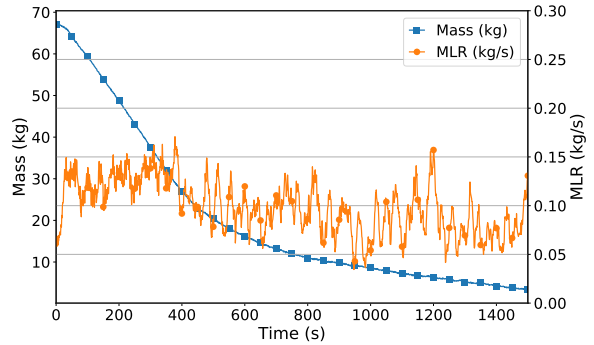


Figure A.38: Arnold Mass

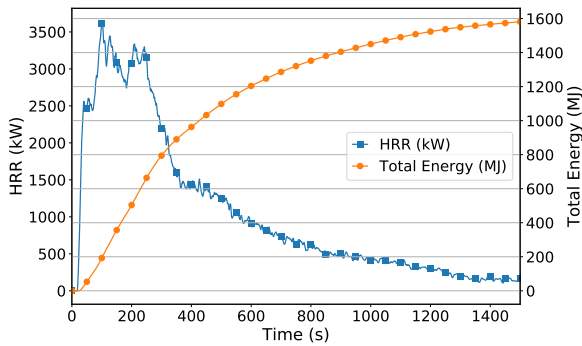


Figure A.39: Fisher Energy Release

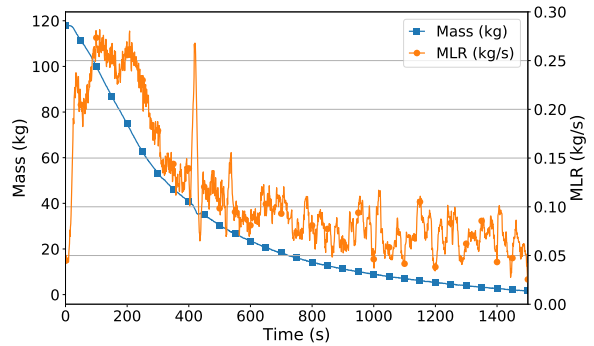


Figure A.40: Fisher Mass

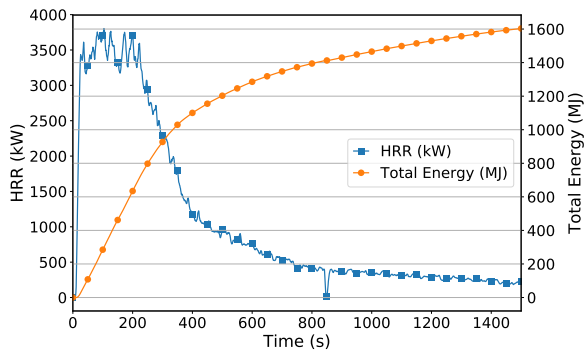


Figure A.41: Garcia Energy Release

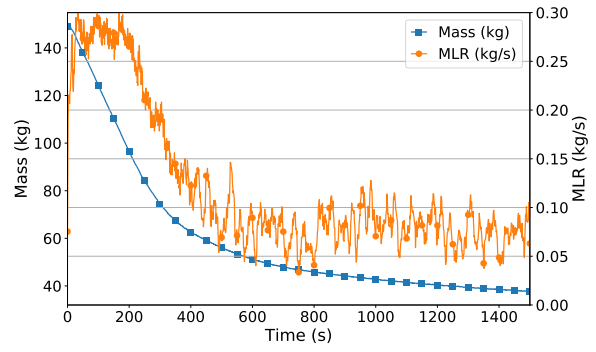


Figure A.42: Garcia Mass

## A.2 Comparison Fuel Packages

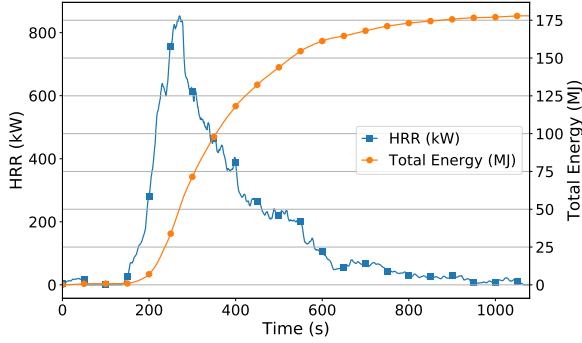


Figure A.43: Barrel Chair 1 Energy Release

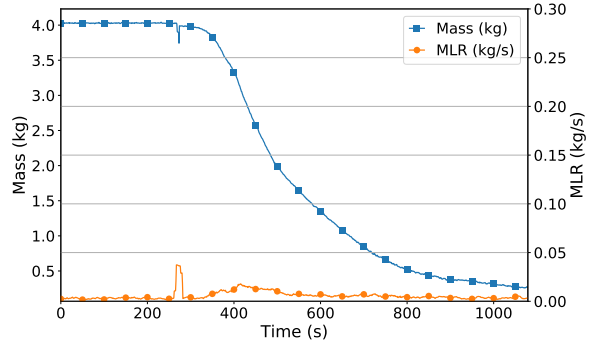


Figure A.44: Barrel Chair 1 Mass

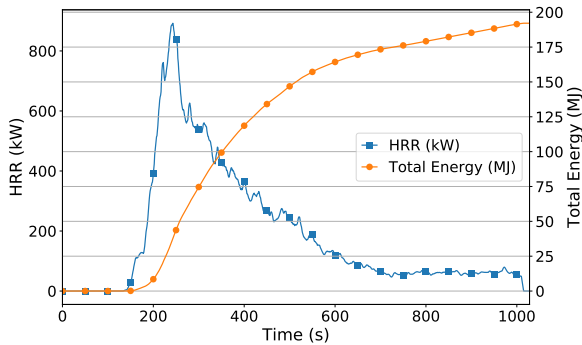


Figure A.45: Barrel Chair 2 Energy Release

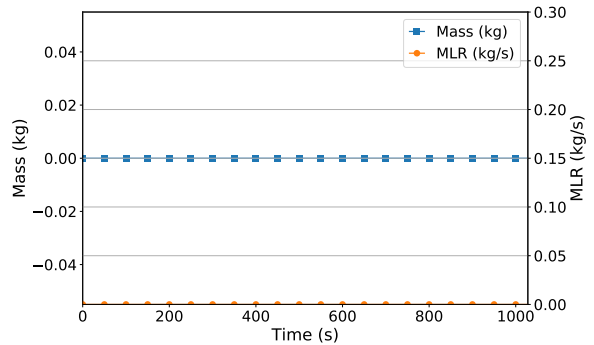


Figure A.46: Barrel Chair 2 Mass

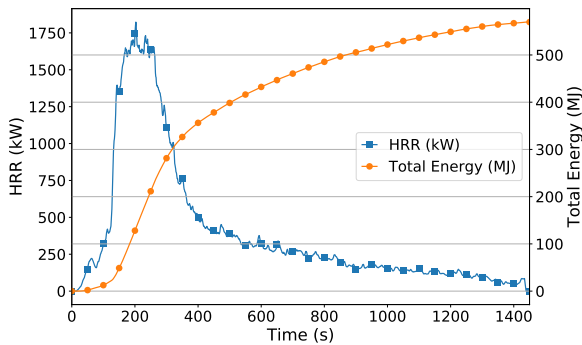


Figure A.47: Kit Sofa 1 Energy Release

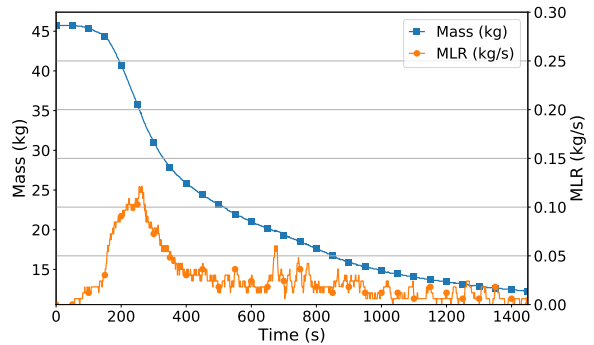


Figure A.48: Kit Sofa 1 Mass

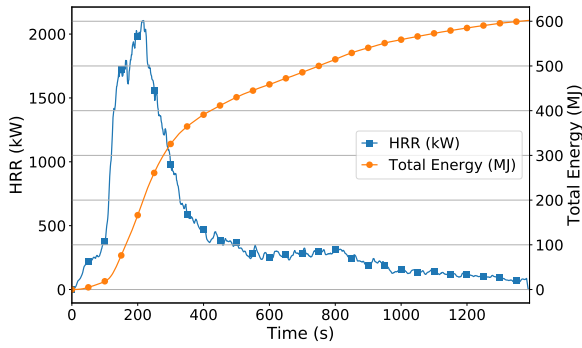


Figure A.49: Kit Sofa 2 Energy Release

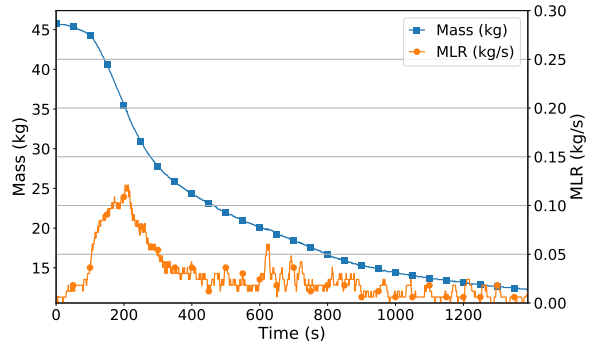


Figure A.50: Kit Sofa 2 Mass

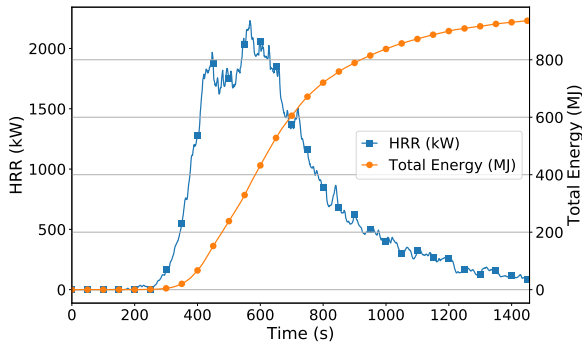


Figure A.51: Fire Attack Bed 1 Energy Release

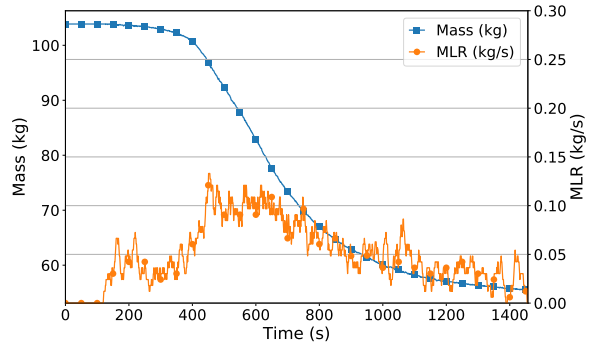


Figure A.52: Fire Attack Bed 1 Mass

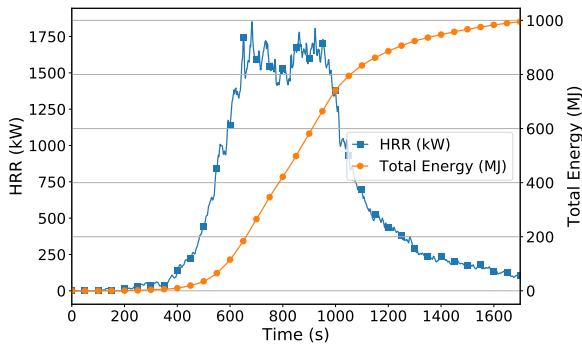


Figure A.53: Fire Attack Bed 2 Energy Release

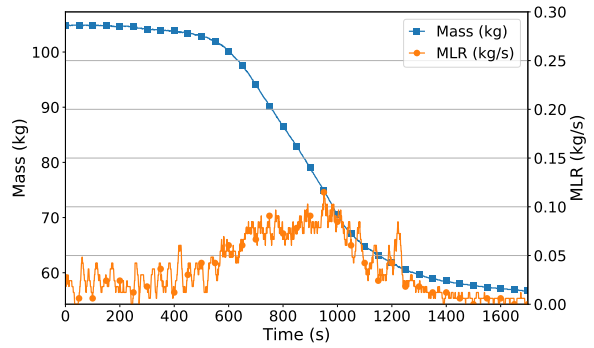


Figure A.54: Fire Attack Bed 2 Mass



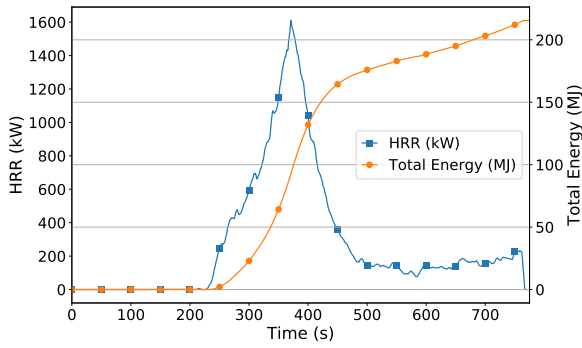


Figure A.55: Striped Chair 1  
Energy Release

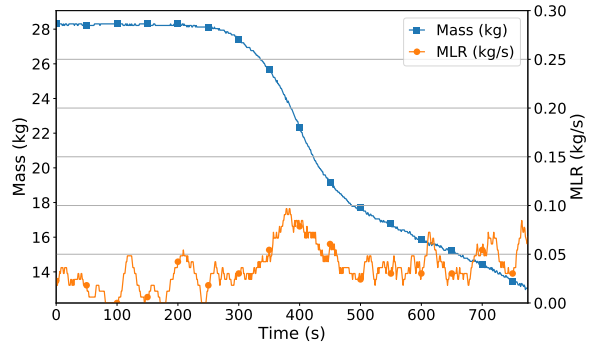


Figure A.56: Striped Chair 1  
Mass

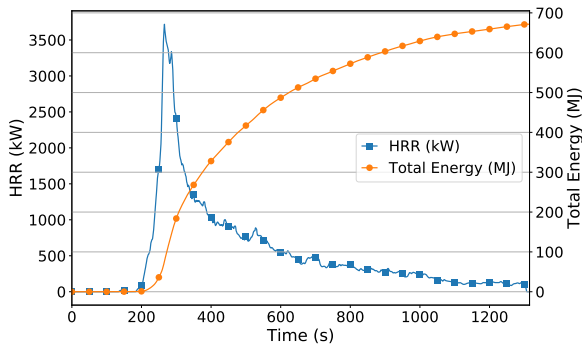


Figure A.57: Sofa Center Ignition  
Energy Release

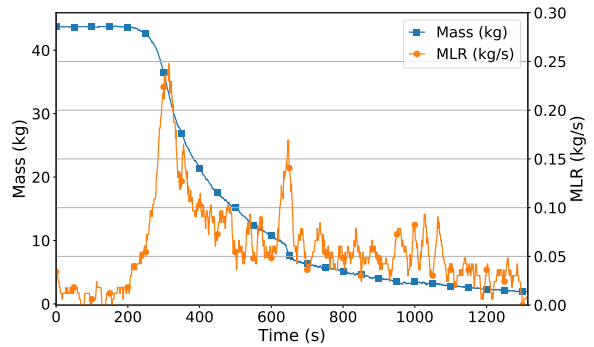


Figure A.58: Sofa Center Ignition  
Mass

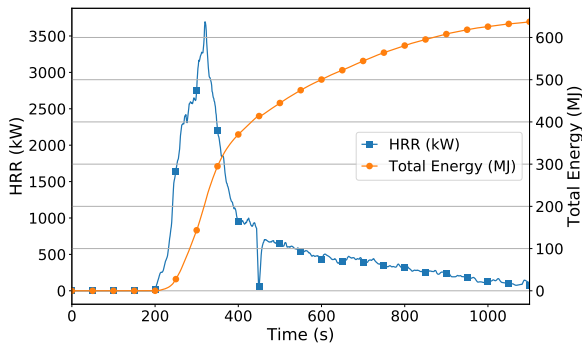


Figure A.59: Sofa Right Ignition  
Energy Release

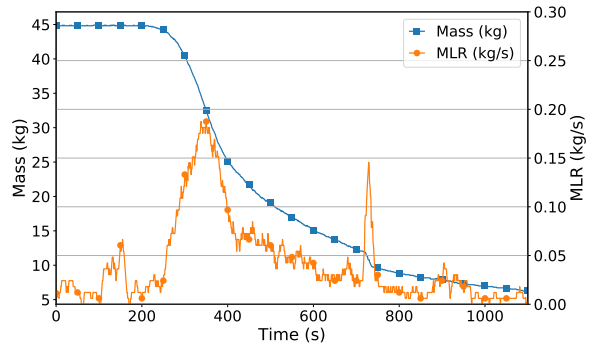


Figure A.60: Sofa Right Ignition  
Mass

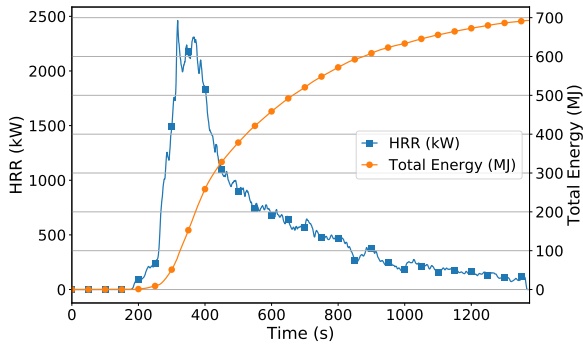


Figure A.61: Sofa Left Ignition Energy Release

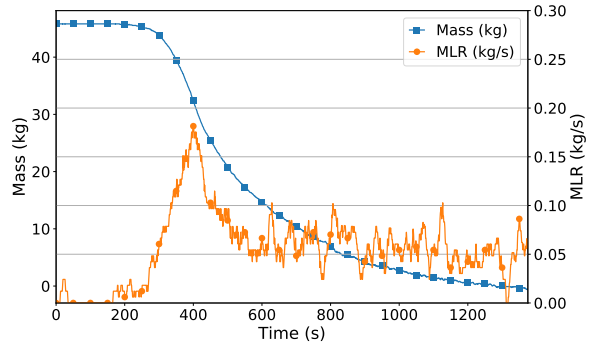


Figure A.62: Sofa Left Ignition Mass

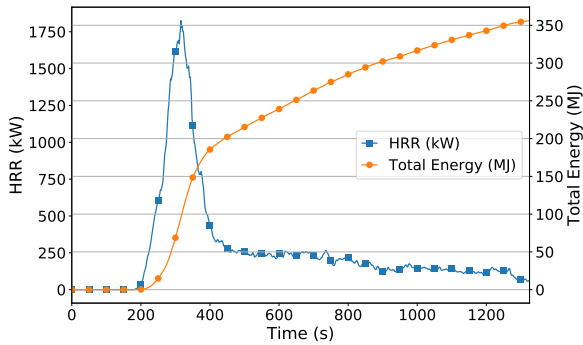


Figure A.63: Striped Chair 2 Energy Release

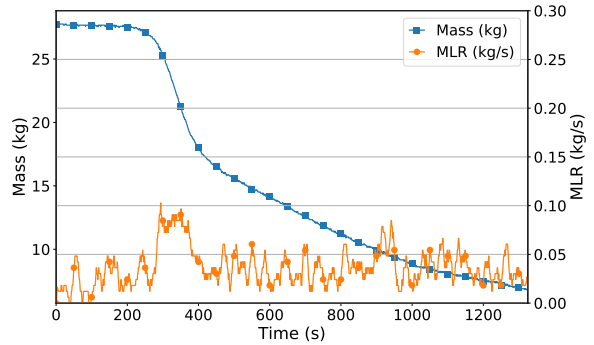


Figure A.64: Striped Chair 2 Mass

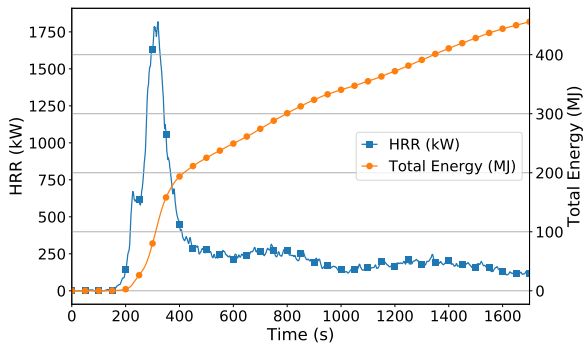


Figure A.65: Striped Chair 3 Energy Release

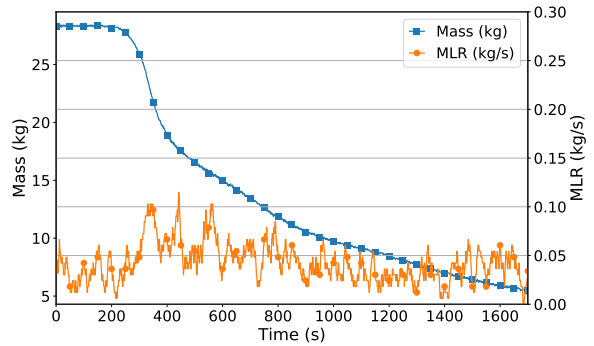


Figure A.66: Striped Chair 3 Mass

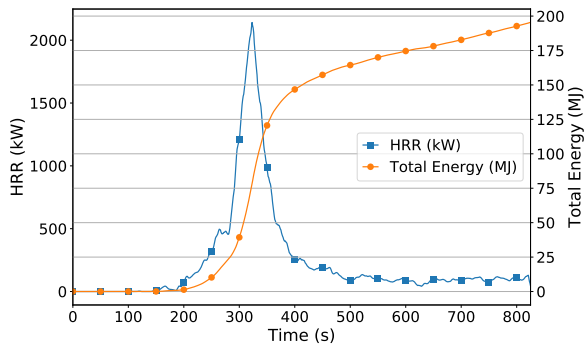


Figure A.67: Yellow Chair 1  
Energy Release

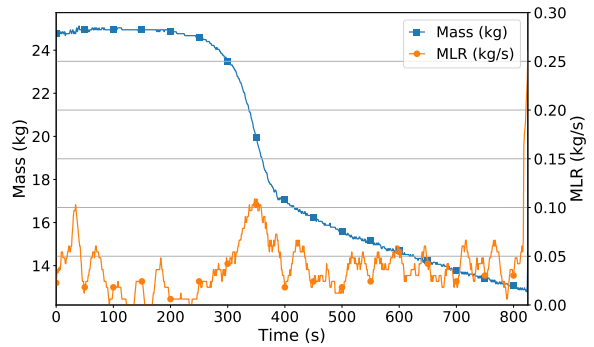


Figure A.68: Yellow Chair 1  
Mass

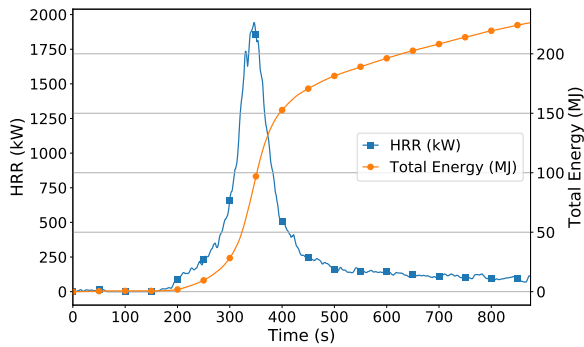


Figure A.69: Yellow Chair 2  
Energy Release

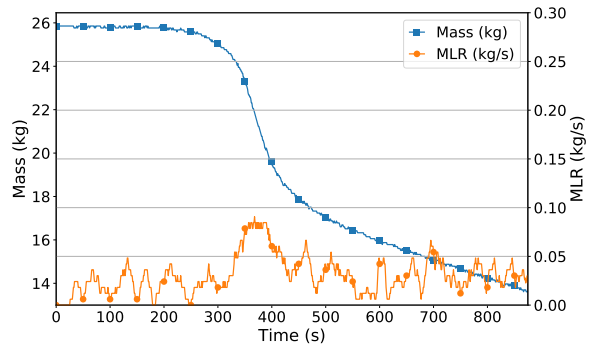


Figure A.70: Yellow Chair 2  
Mass

### A.3 Comparison Room Burns

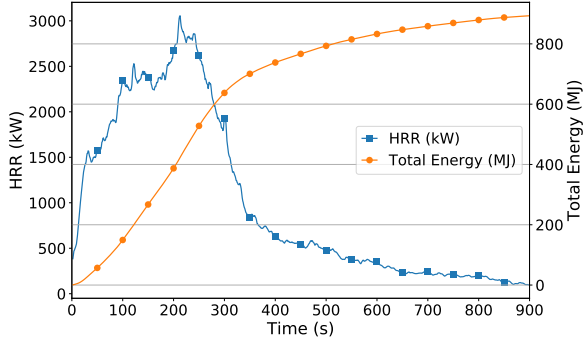


Figure A.71: Pallets Room Energy Release

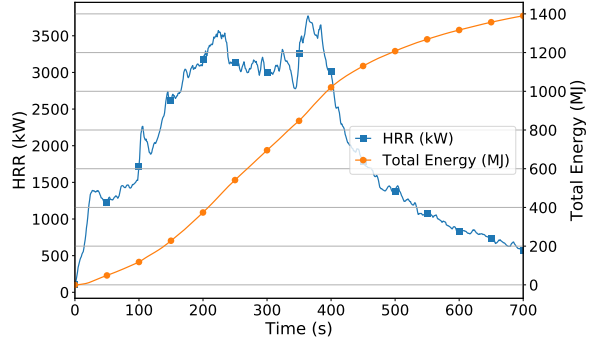


Figure A.72: OSB Room Energy Release

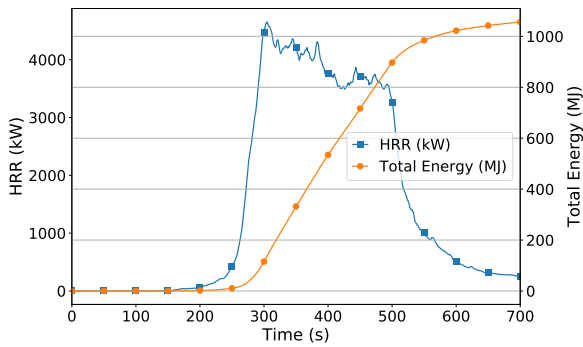


Figure A.73: Furnished Room 1 Energy Release

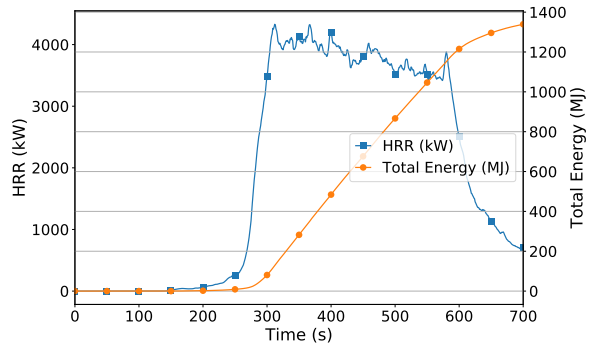


Figure A.74: Furnished Room 2 Energy Release

# Appendix B Container Burn Results

## B.1 Experiment 1 Results

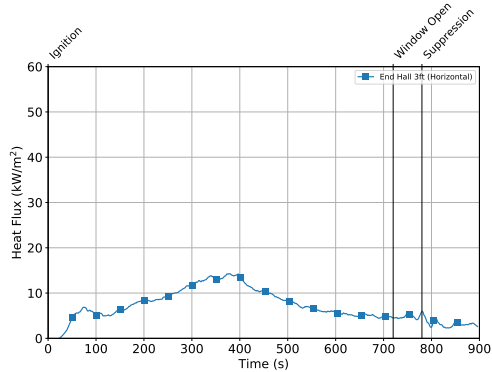


Figure B.1: Experiment 1 Hall Heat Flux

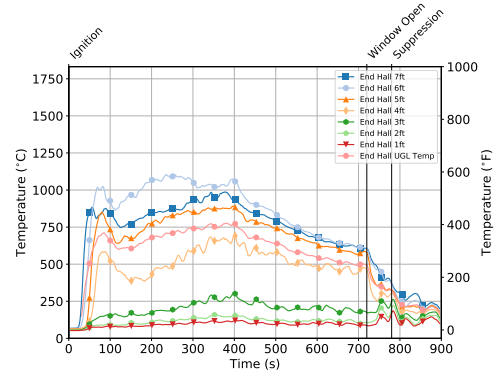


Figure B.2: Experiment 1 End Hall Temperature

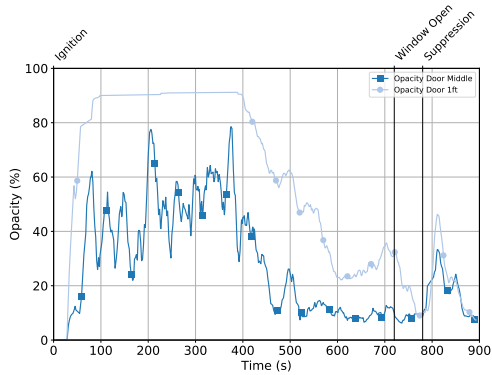


Figure B.3: Experiment 1 Door Obscuration

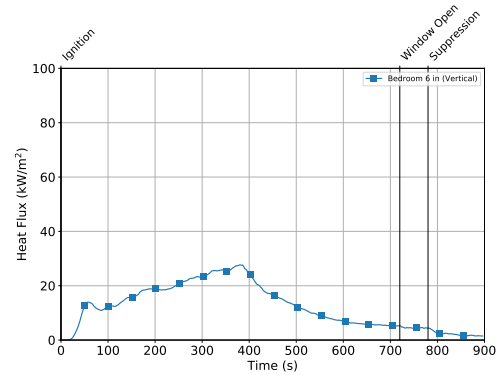


Figure B.4: Experiment 1 Bedroom Heat Flux

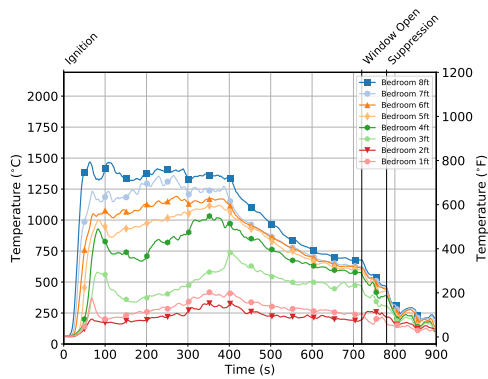


Figure B.5: Experiment 1  
Bedroom Temperature

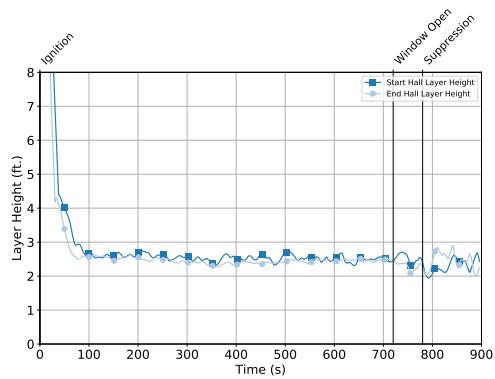


Figure B.6: Experiment 1 Layer  
Height

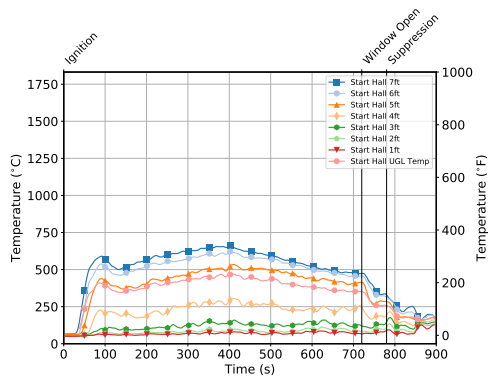


Figure B.7: Experiment 1 Start  
Hall Temperature

## B.2 Experiment 2 Results

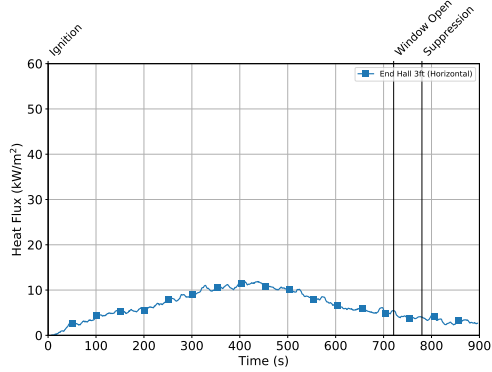


Figure B.8: Experiment 2 Hall Heat Flux

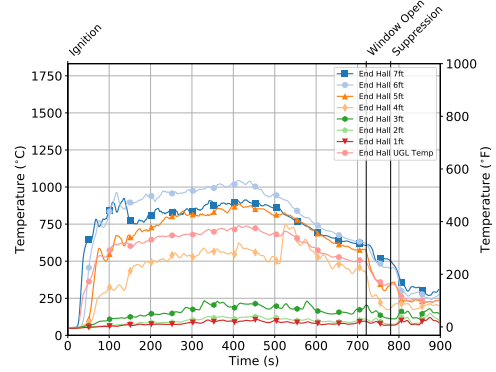


Figure B.9: Experiment 2 End Hall Temperature

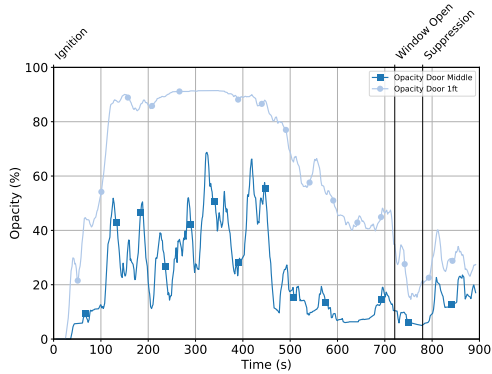


Figure B.10: Experiment 2 Door Obscuration

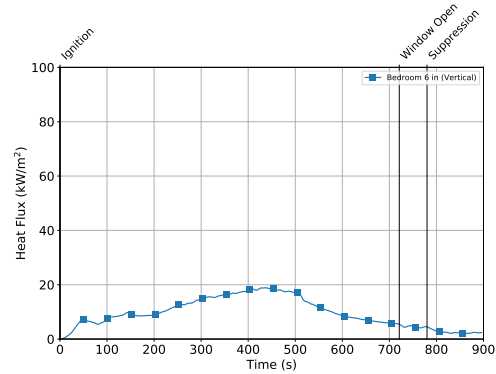


Figure B.11: Experiment 2 Bedroom Heat Flux

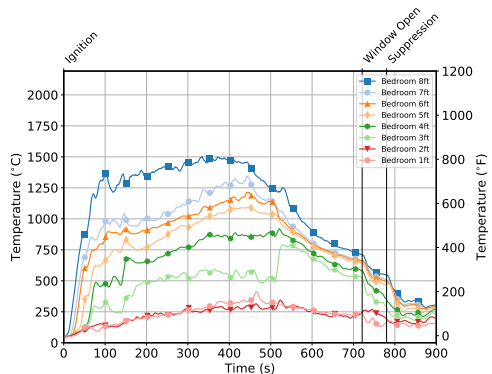


Figure B.12: Experiment 2 Bedroom Temperature

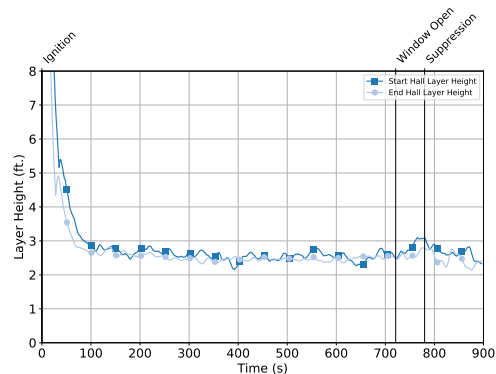


Figure B.13: Experiment 2 Layer Height



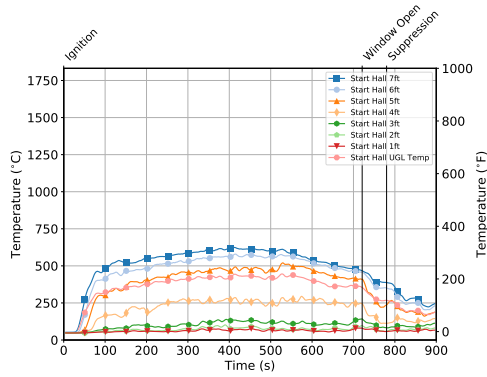


Figure B.14: Experiment 2 Start Hall Temperature

### B.3 Experiment 3 Results

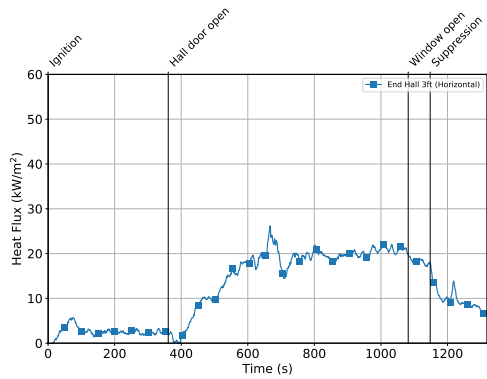


Figure B.15: Experiment 3 Hall Heat Flux

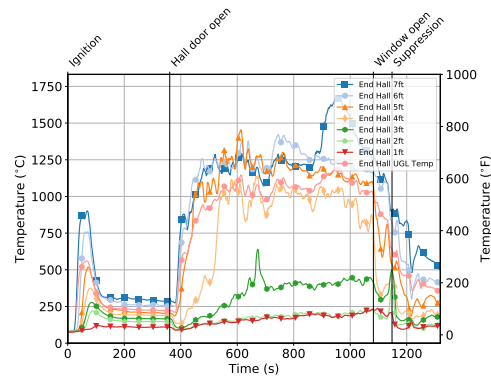


Figure B.16: Experiment 3 End Hall Temperature

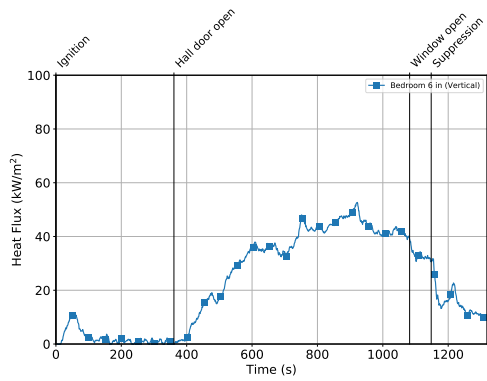


Figure B.17: Experiment 3  
Bedroom Heat Flux

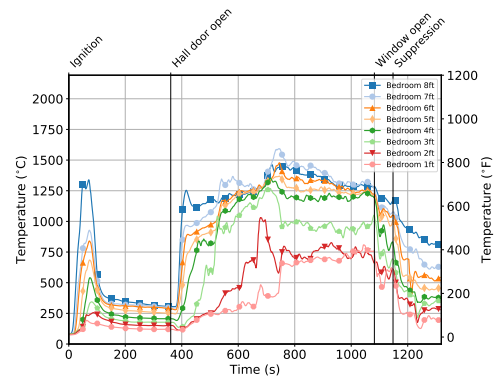


Figure B.18: Experiment 3  
Bedroom Temperature

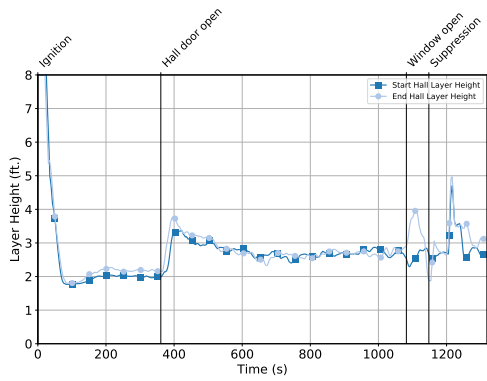


Figure B.19: Experiment 3 Layer  
Height

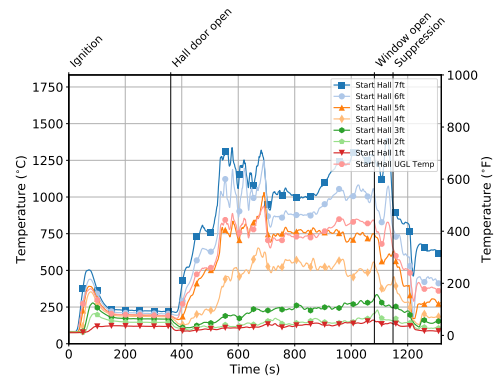


Figure B.20: Experiment 3 Start  
Hall Temperature

## B.4 Experiment 4 Results

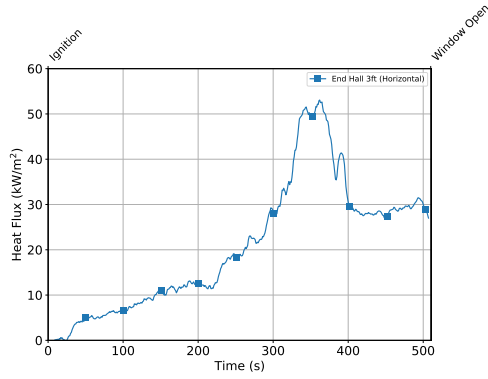


Figure B.21: Experiment 4 Hall Heat Flux

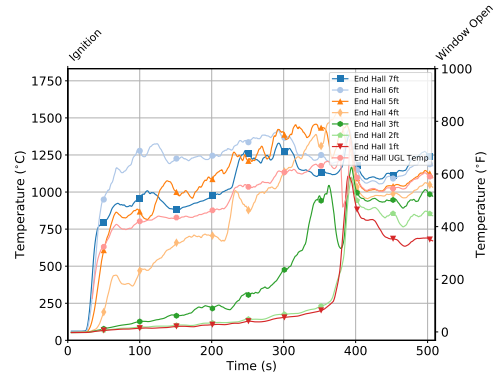


Figure B.22: Experiment 4 End Hall Temperature

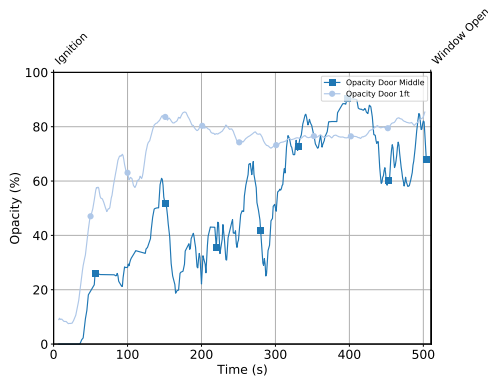


Figure B.23: Experiment 4 Door Obscuration

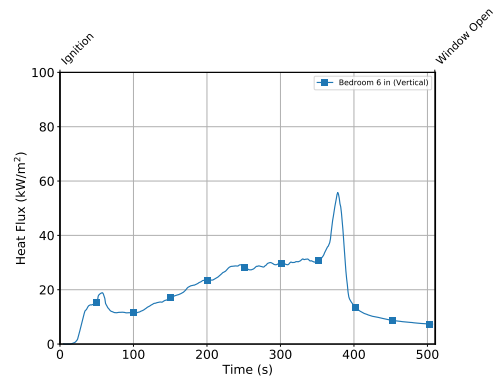


Figure B.24: Experiment 4 Bedroom Heat Flux

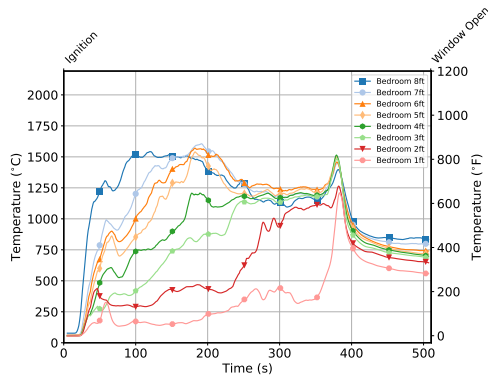


Figure B.25: Experiment 4 Bedroom Temperature

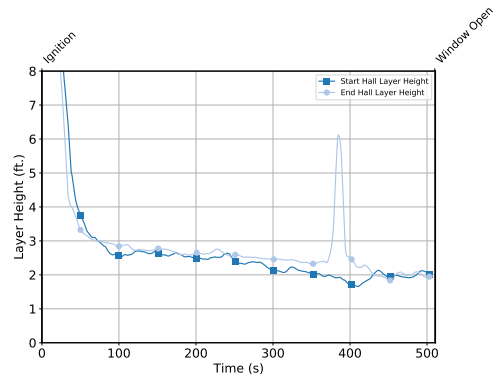


Figure B.26: Experiment 4 Layer Height

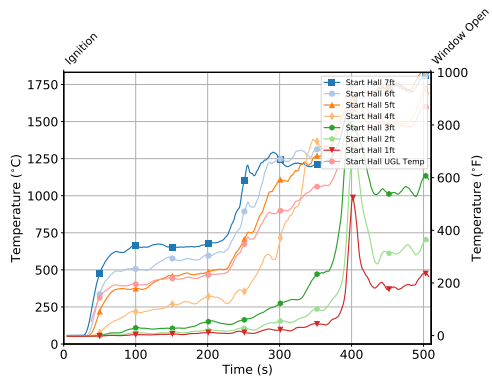


Figure B.27: Experiment 4 Start Hall Temperature

## B.5 Experiment 5 Results

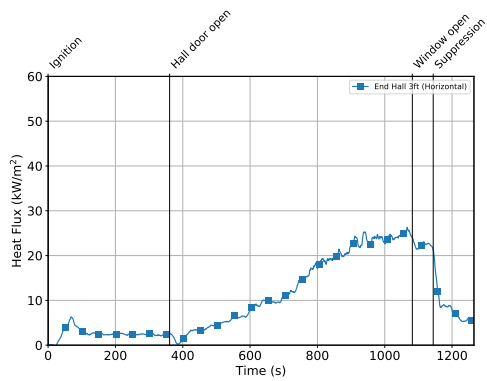


Figure B.28: Experiment 5 Hall Heat Flux

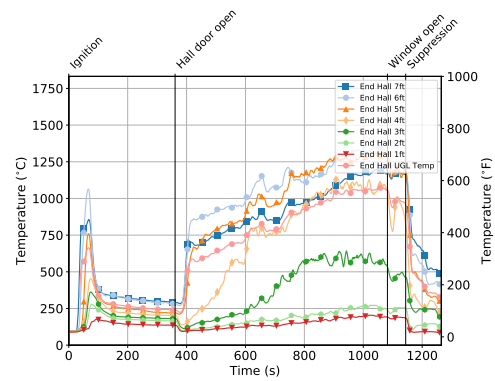


Figure B.29: Experiment 5 End Hall Temperature

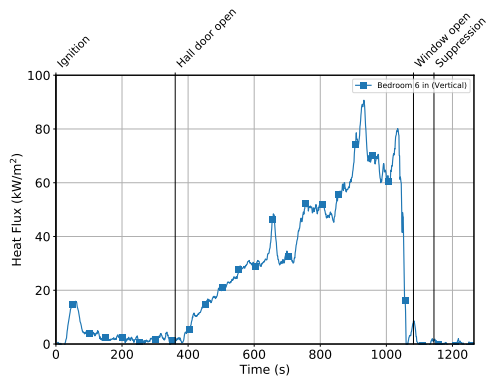


Figure B.30: Experiment 5  
Bedroom Heat Flux

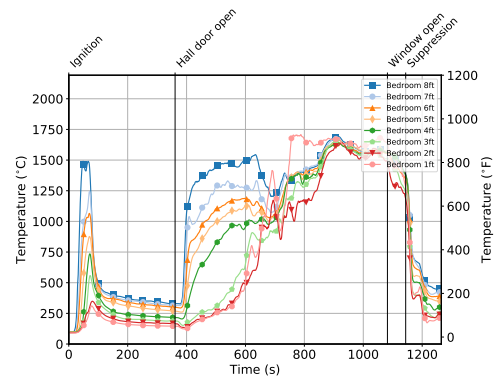


Figure B.31: Experiment 5  
Bedroom Temperature

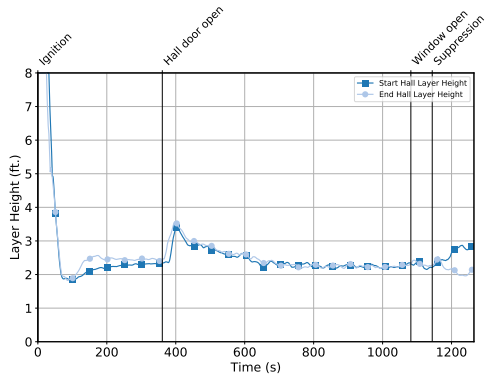


Figure B.32: Experiment 5 Layer  
Height

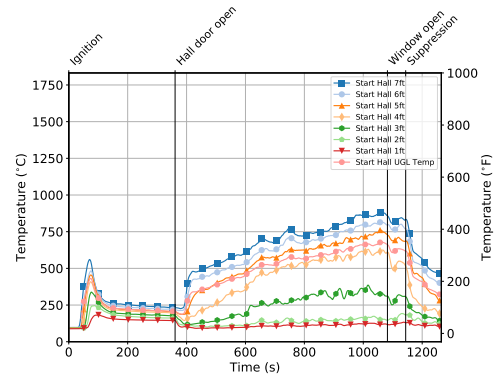


Figure B.33: Experiment 5 Start  
Hall Temperature

## B.6 Experiment 6 Results

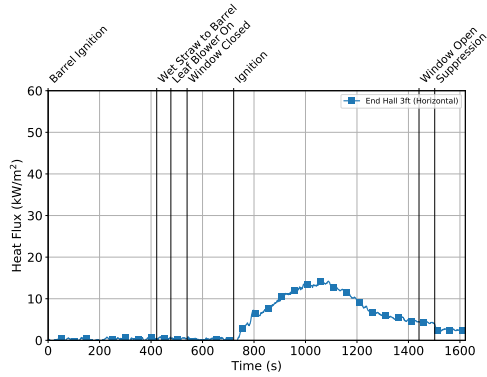


Figure B.34: Experiment 6 Hall Heat Flux

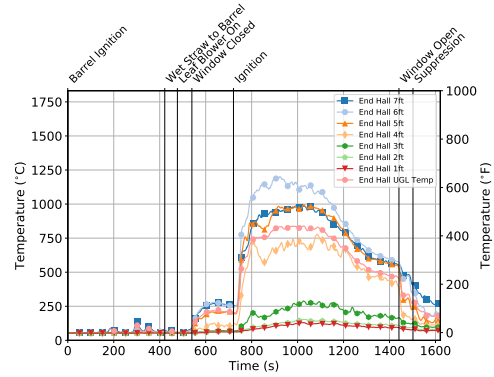


Figure B.35: Experiment 6 End Hall Temperature

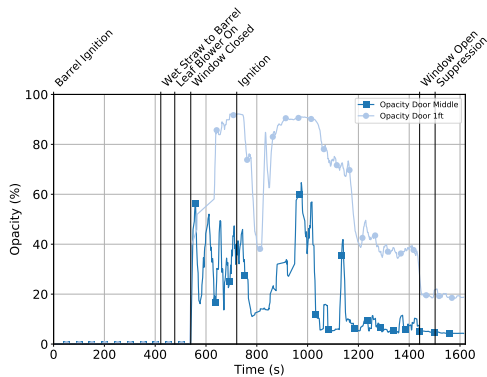


Figure B.36: Experiment 6 Door Obscuration

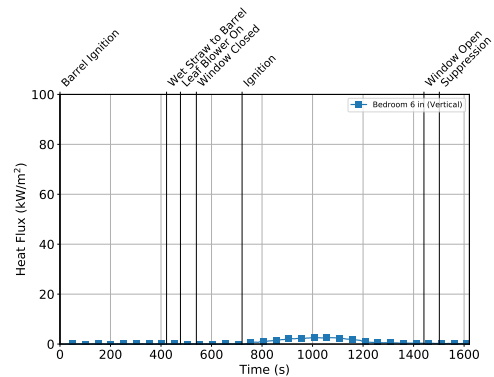


Figure B.37: Experiment 6 Bedroom Heat Flux

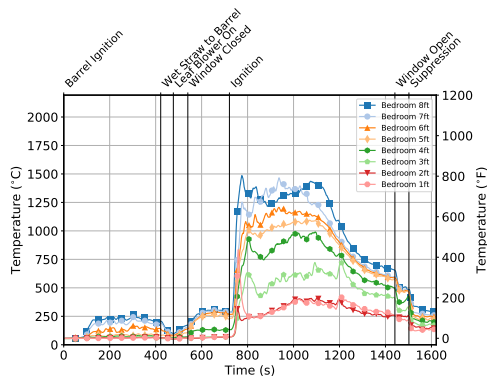


Figure B.38: Experiment 6 Bedroom Temperature

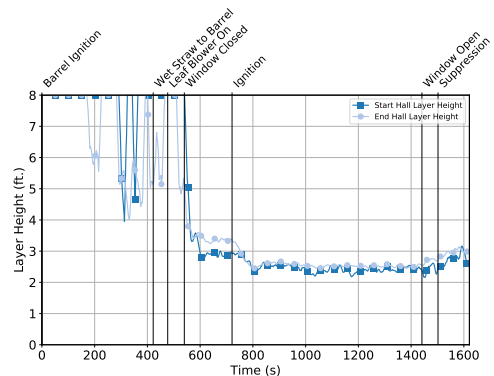


Figure B.39: Experiment 6 Layer Height

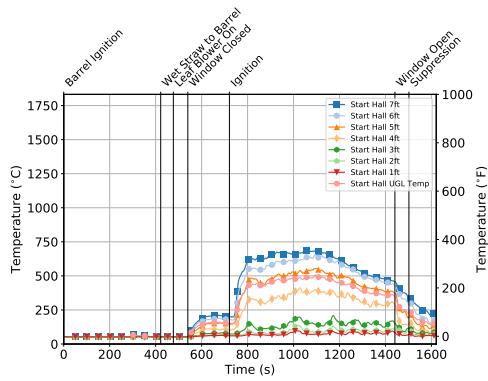


Figure B.40: Experiment 6 Start Hall Temperature

## B.7 Experiment 7 Results

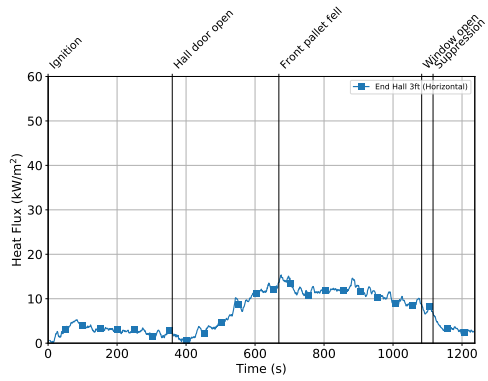


Figure B.41: Experiment 7 Hall Heat Flux

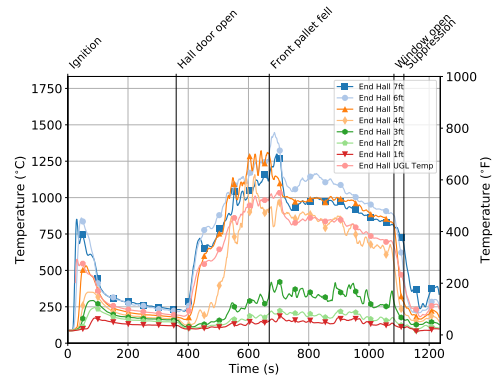


Figure B.42: Experiment 7 End Hall Temperature



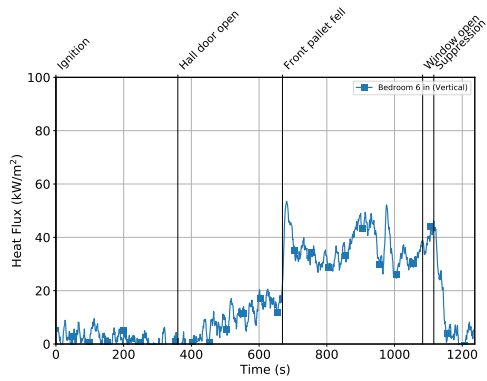


Figure B.43: Experiment 7  
Bedroom Heat Flux

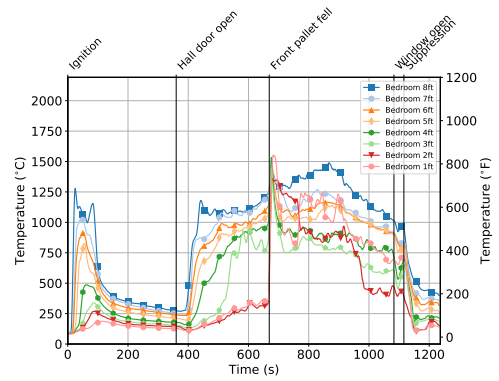


Figure B.44: Experiment 7  
Bedroom Temperature

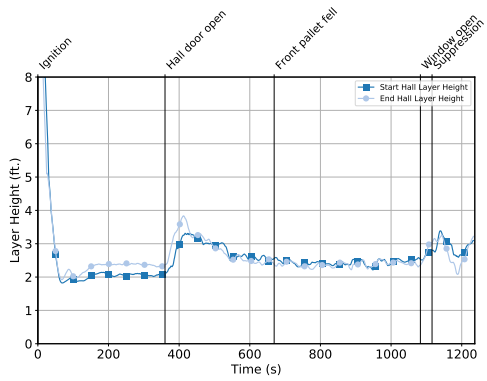


Figure B.45: Experiment 7 Layer  
Height

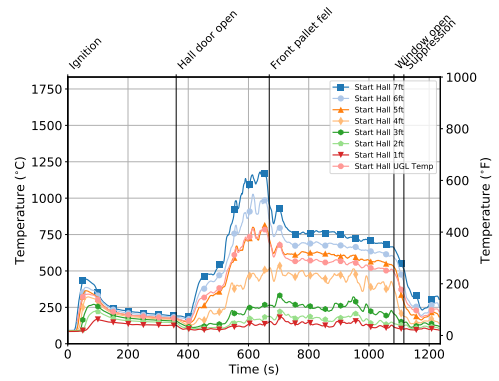


Figure B.46: Experiment 7 Start  
Hall Temperature

## B.8 Experiment 8 Results

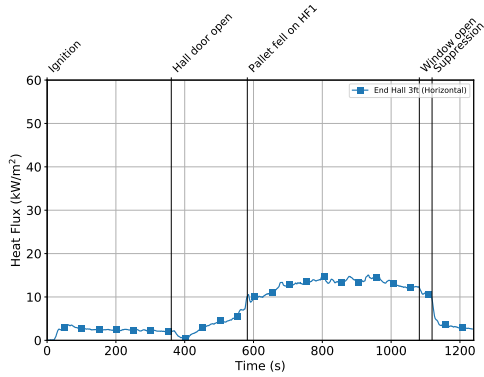


Figure B.47: Experiment 8 Hall Heat Flux

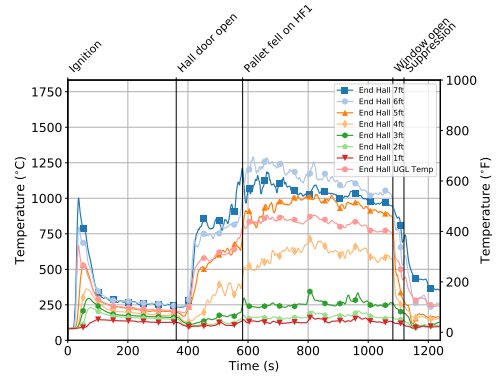


Figure B.48: Experiment 8 End Hall Temperature

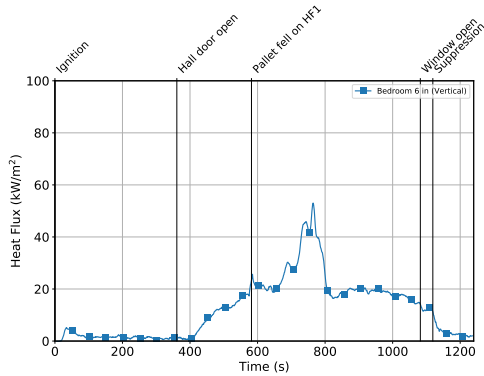


Figure B.49: Experiment 8 Bedroom Heat Flux

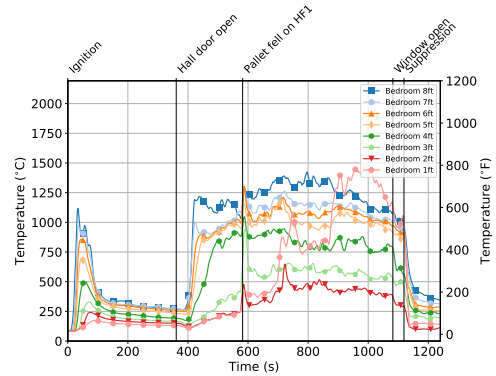


Figure B.50: Experiment 8 Bedroom Temperature

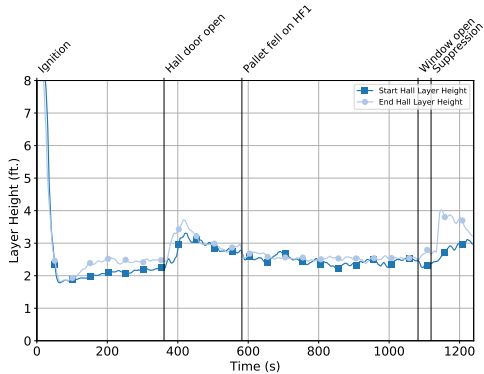


Figure B.51: Experiment 8 Layer Height

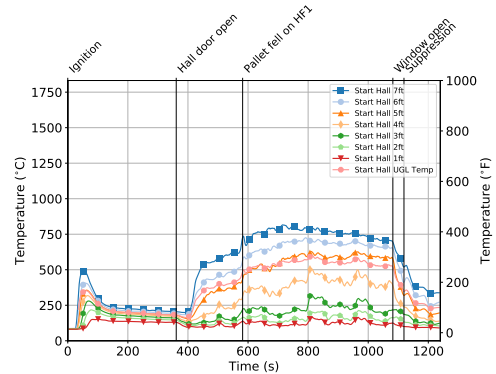


Figure B.52: Experiment 8 Start Hall Temperature

## B.9 Experiment 9 Results

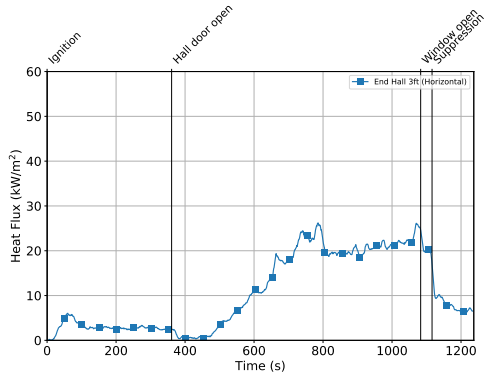


Figure B.53: Experiment 9 Hall Heat Flux

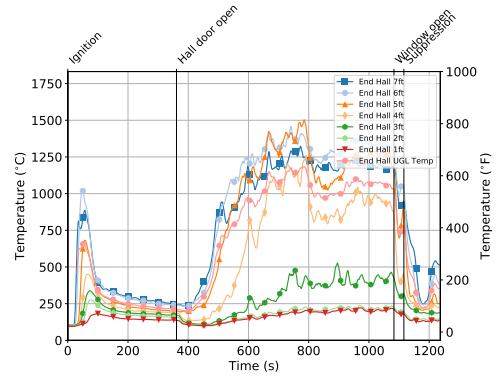


Figure B.54: Experiment 9 End Hall Temperature

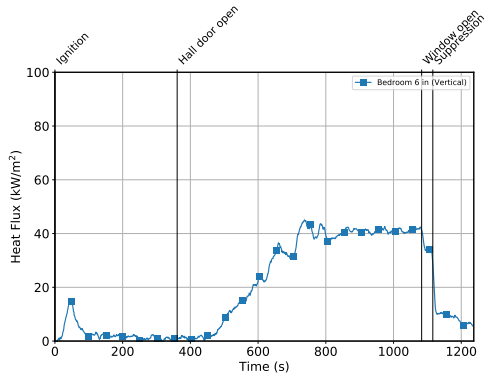


Figure B.55: Experiment 9 Bedroom Heat Flux

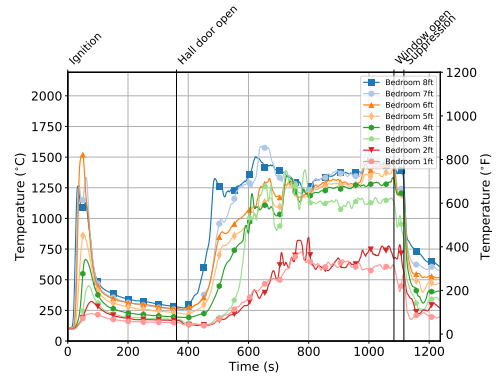


Figure B.56: Experiment 9 Bedroom Temperature

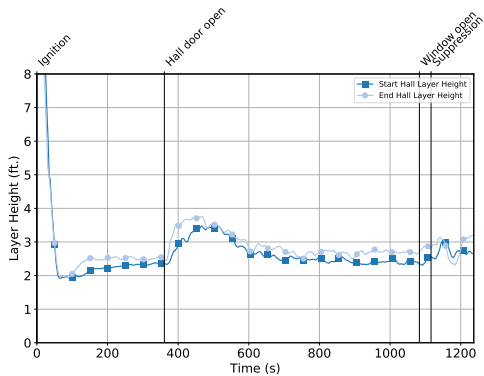


Figure B.57: Experiment 9 Layer Height

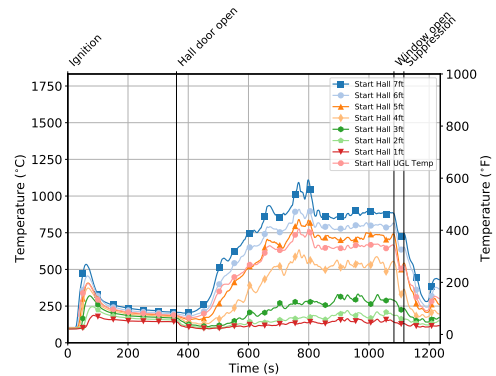


Figure B.58: Experiment 9 Start Hall Temperature

## B.10 Experiment 10 Results

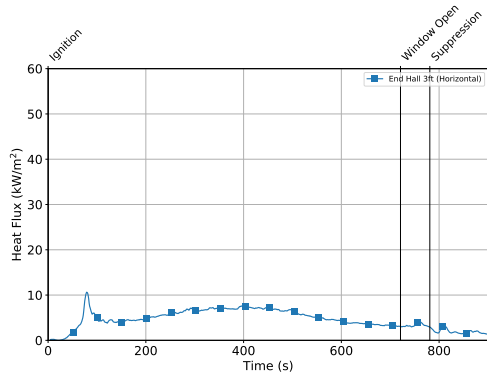


Figure B.59: Experiment 10 Hall Heat Flux

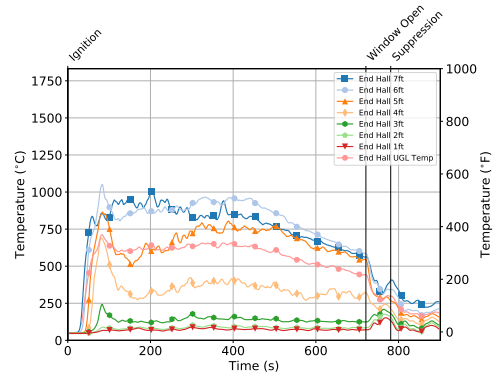


Figure B.60: Experiment 10 End Hall Temperature

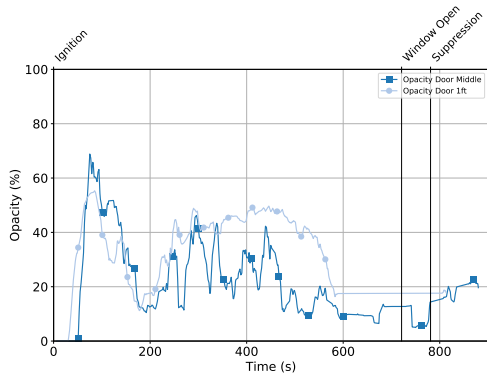


Figure B.61: Experiment 10 Door Obscuration

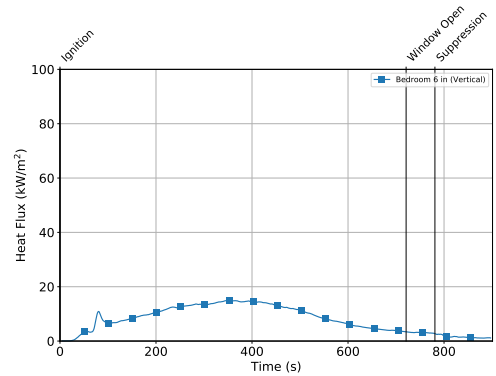


Figure B.62: Experiment 10 Bedroom Heat Flux

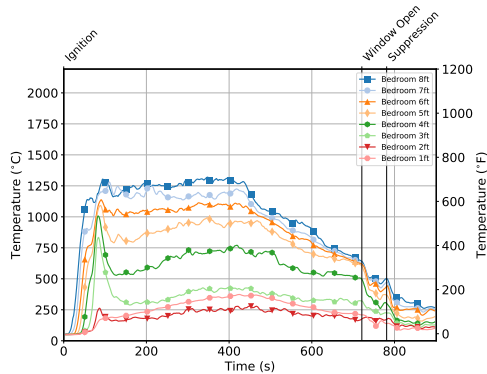


Figure B.63: Experiment 10 Bedroom Temperature

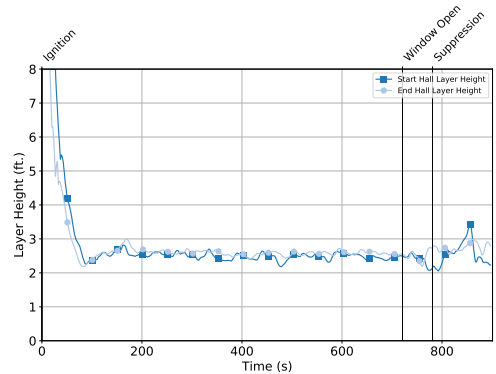


Figure B.64: Experiment 10 Layer Height

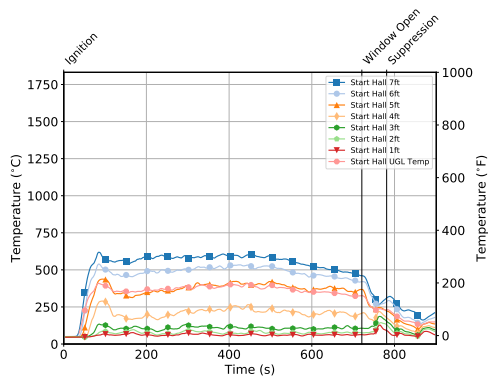


Figure B.65: Experiment 10 Start Hall Temperature

## B.11 Experiment 11 Results

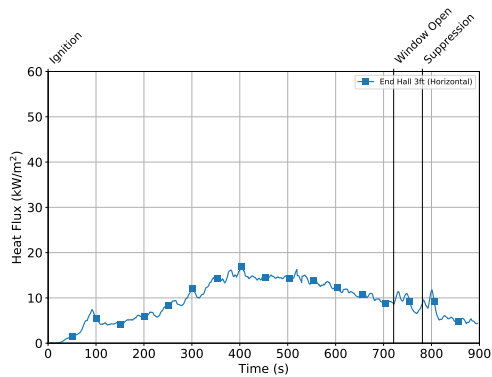


Figure B.66: Experiment 11 Hall Heat Flux

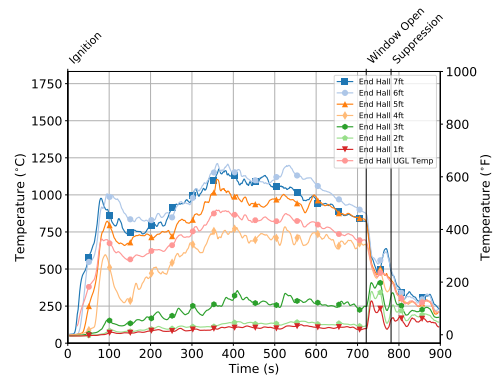


Figure B.67: Experiment 11 End Hall Temperature

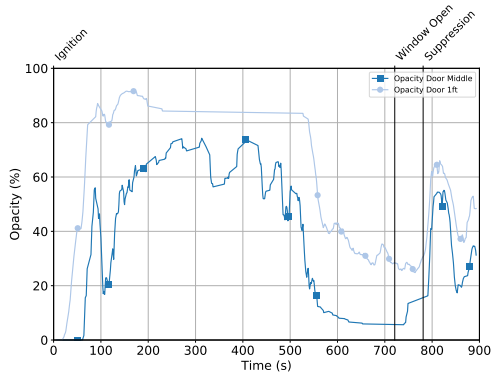


Figure B.68: Experiment 11  
Door Obscuration

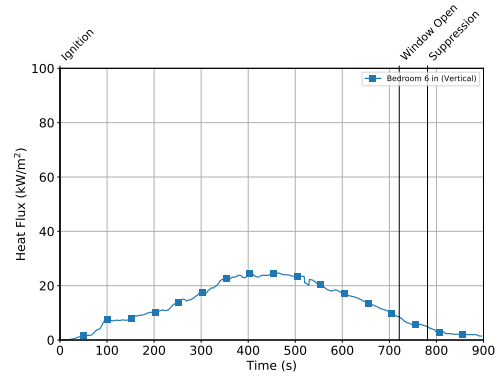


Figure B.69: Experiment 11  
Bedroom Heat Flux

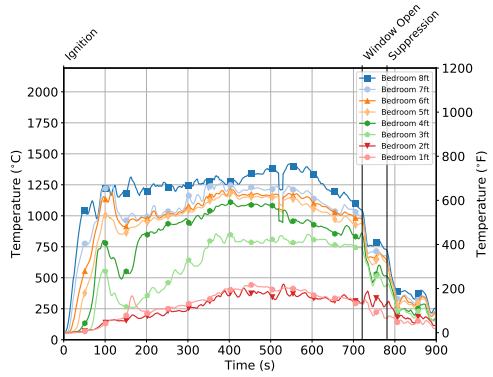


Figure B.70: Experiment 11  
Bedroom Temperature

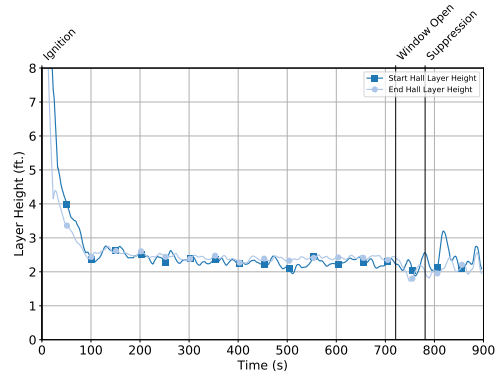


Figure B.71: Experiment 11  
Layer Height

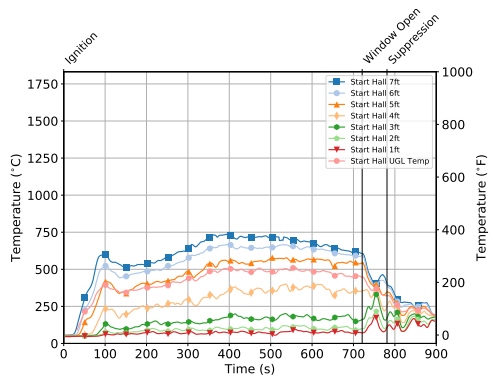


Figure B.72: Experiment 11 Start  
Hall Temperature

## B.12 Experiment 12 Results

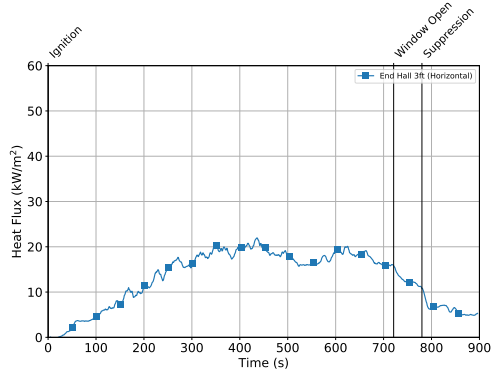


Figure B.73: Experiment 12 Hall Heat Flux

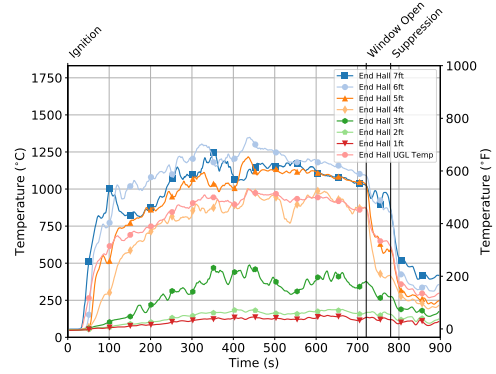


Figure B.74: Experiment 12 End Hall Temperature

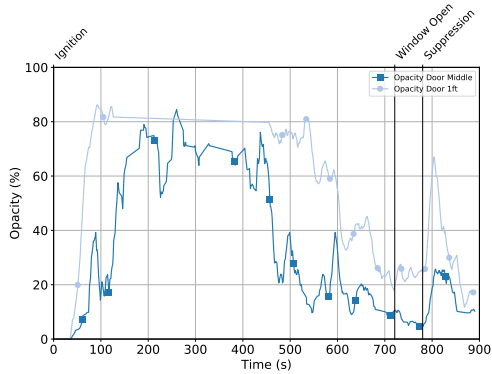


Figure B.75: Experiment 12 Door Obscuration

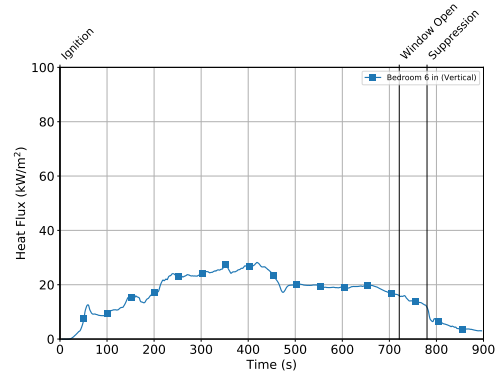


Figure B.76: Experiment 12 Bedroom Heat Flux

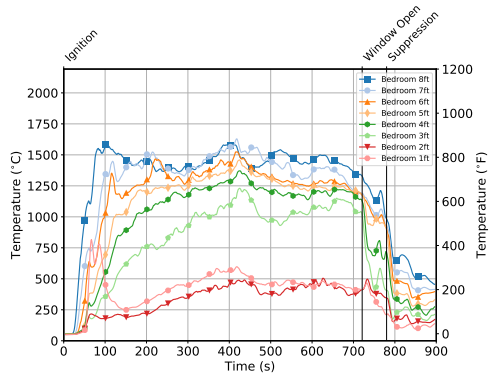


Figure B.77: Experiment 12 Bedroom Temperature

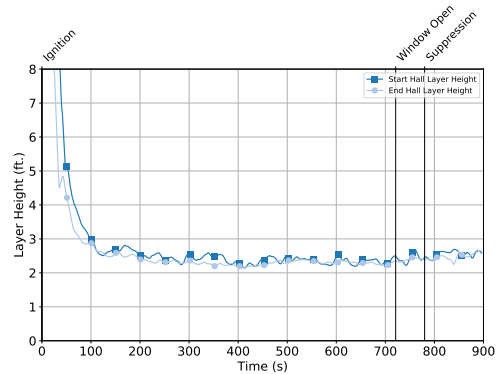


Figure B.78: Experiment 12 Layer Height

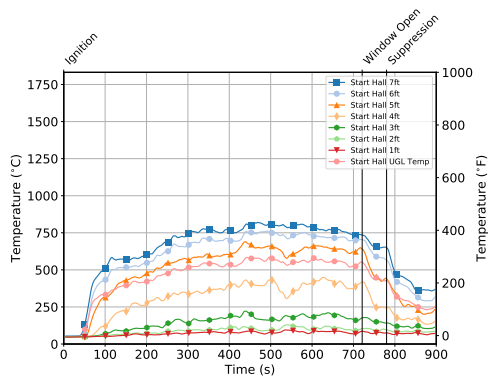


Figure B.79: Experiment 12 Start Hall Temperature

### B.13 Experiment 13 Results

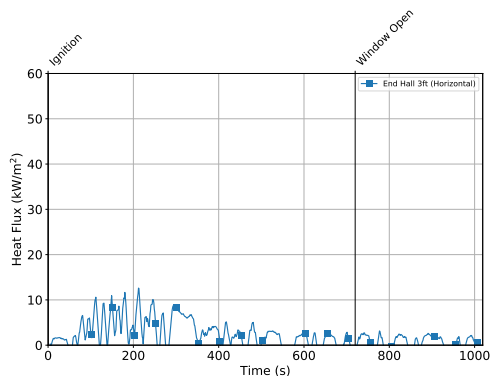


Figure B.80: Experiment 13 Hall Heat Flux

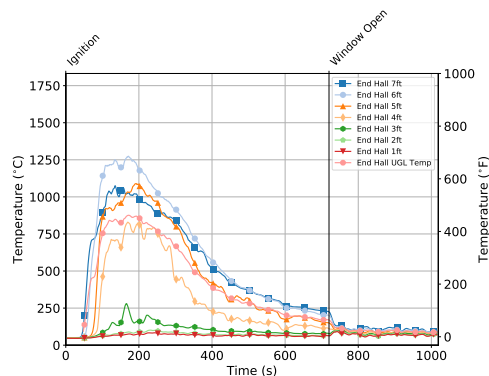


Figure B.81: Experiment 13 End Hall Temperature



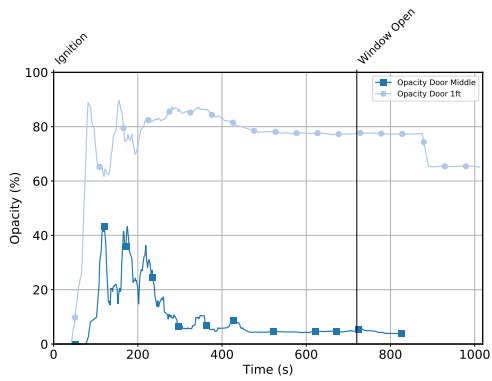


Figure B.82: Experiment 13  
Door Obscuration

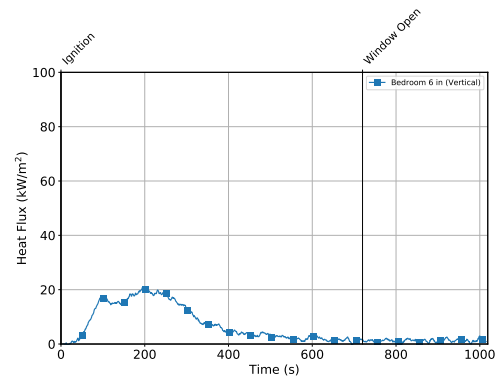


Figure B.83: Experiment 13  
Bedroom Heat Flux

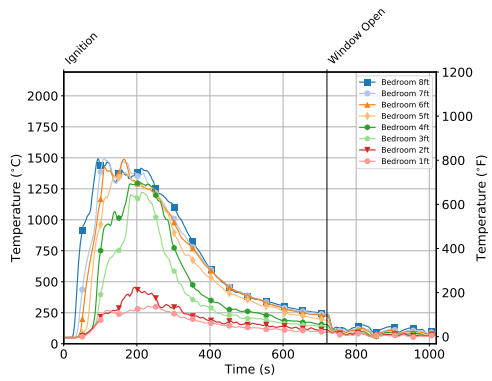


Figure B.84: Experiment 13  
Bedroom Temperature

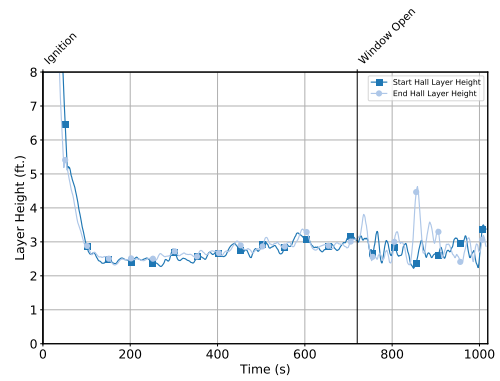


Figure B.85: Experiment 13  
Layer Height

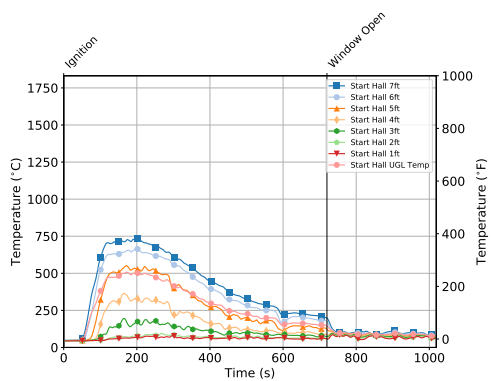


Figure B.86: Experiment 13 Start  
Hall Temperature

## B.14 Experiment 14 Results

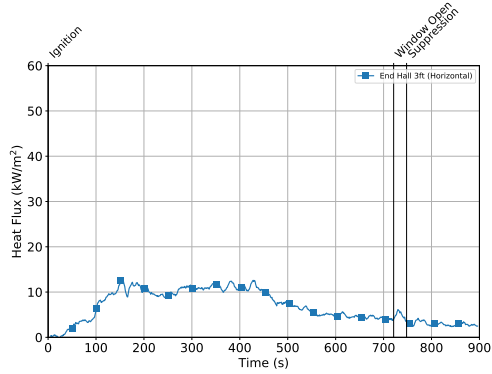


Figure B.87: Experiment 14 Hall Heat Flux

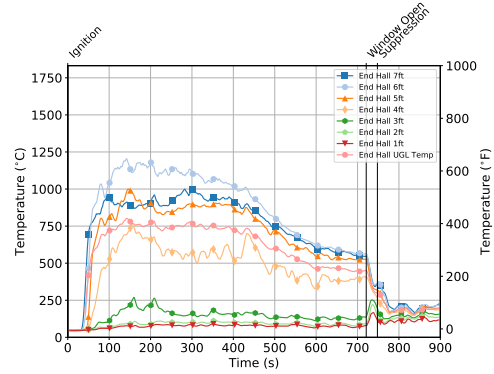


Figure B.88: Experiment 14 End Hall Temperature

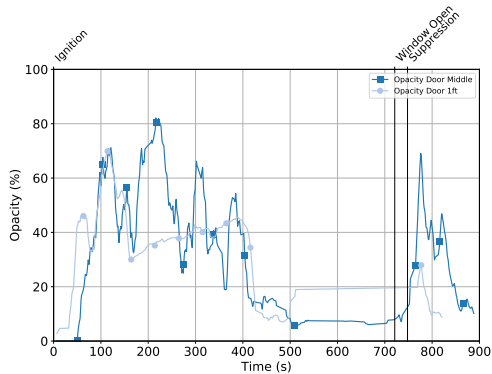


Figure B.89: Experiment 14 Door Obscuration

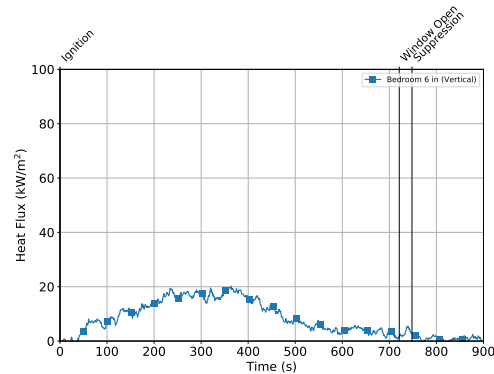


Figure B.90: Experiment 14 Bedroom Heat Flux

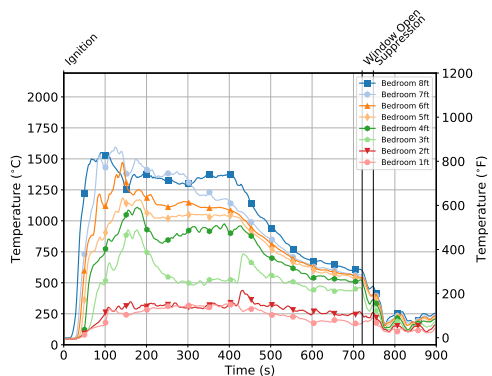


Figure B.91: Experiment 14 Bedroom Temperature

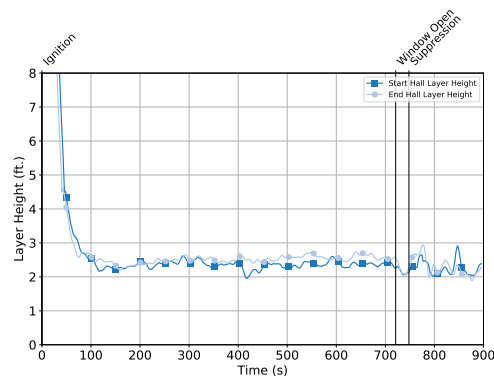


Figure B.92: Experiment 14 Layer Height

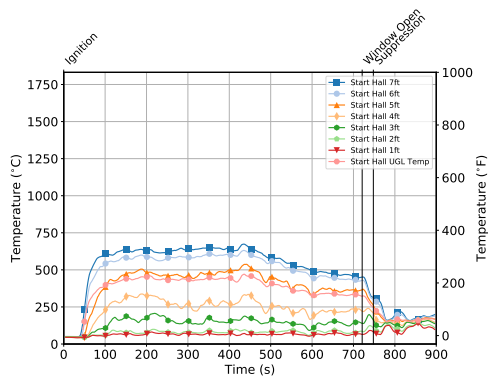


Figure B.93: Experiment 14 Start Hall Temperature

## B.15 Experiment 15 Results

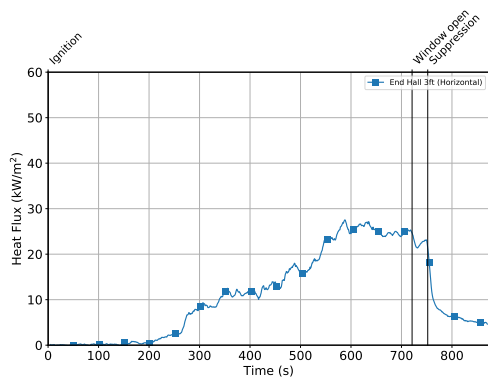


Figure B.94: Experiment 15 Hall Heat Flux

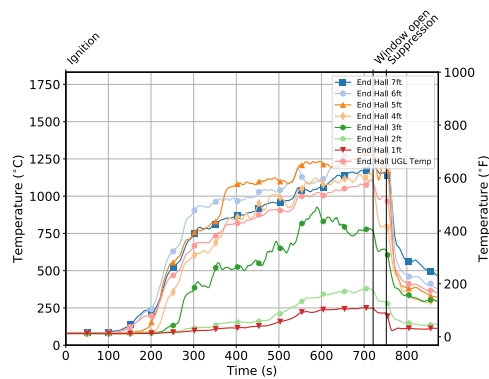


Figure B.95: Experiment 15 End Hall Temperature

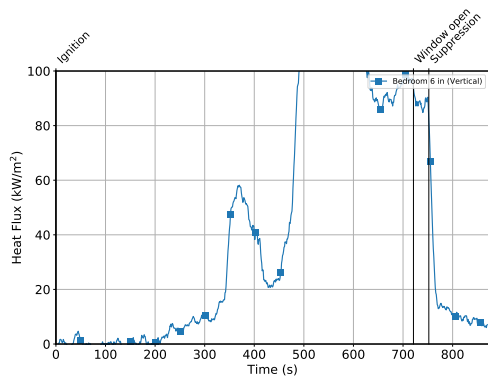


Figure B.96: Experiment 15  
Bedroom Heat Flux

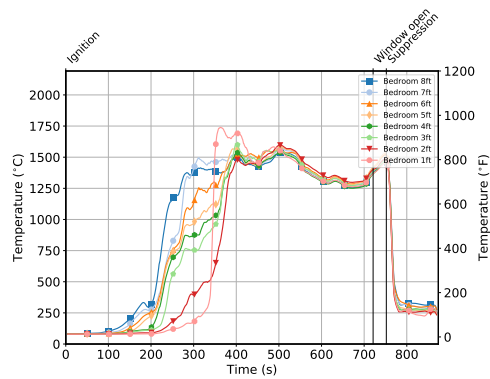


Figure B.97: Experiment 15  
Bedroom Temperature

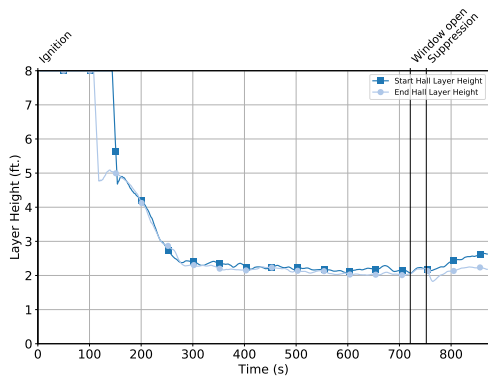


Figure B.98: Experiment 15  
Layer Height

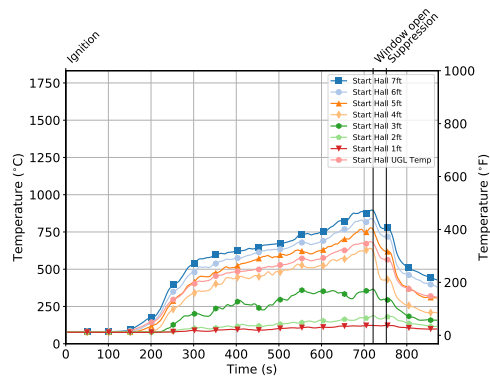


Figure B.99: Experiment 15 Start  
Hall Temperature

# B.16 Experiment 16 Results

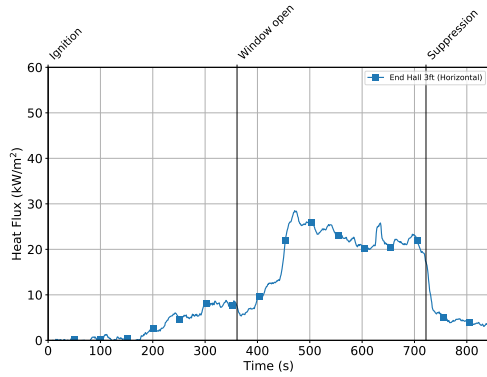


Figure B.100: Experiment 16 Hall Heat Flux

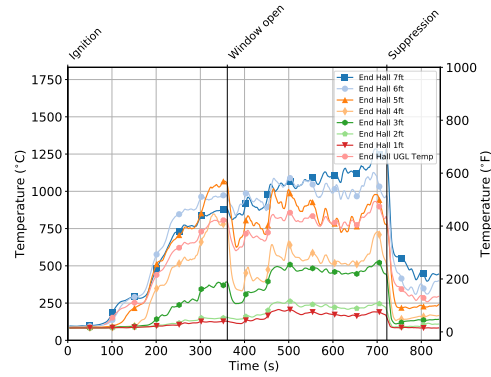


Figure B.101: Experiment 16 End Hall Temperature

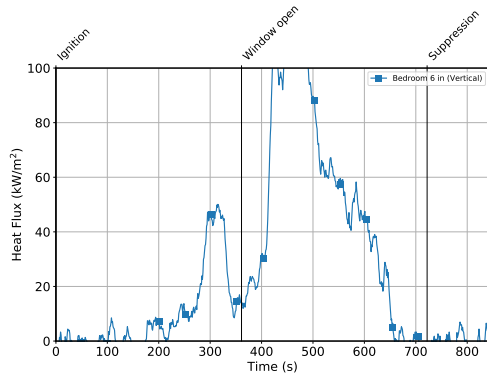


Figure B.102: Experiment 16 Bedroom Heat Flux

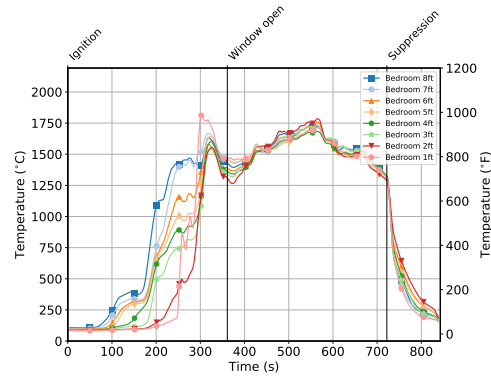


Figure B.103: Experiment 16 Bedroom Temperature

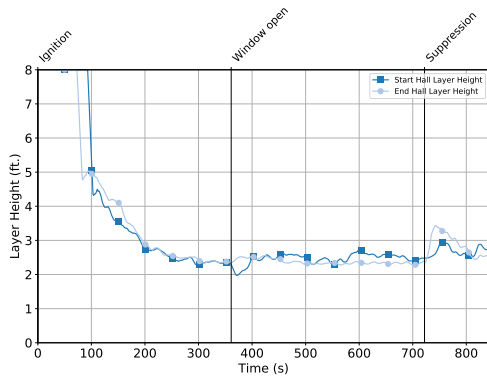


Figure B.104: Experiment 16 Layer Height

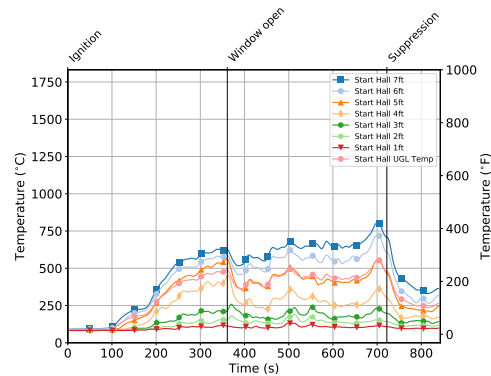


Figure B.105: Experiment 16 Start Hall Temperature

# B.17 Experiment 17 Results

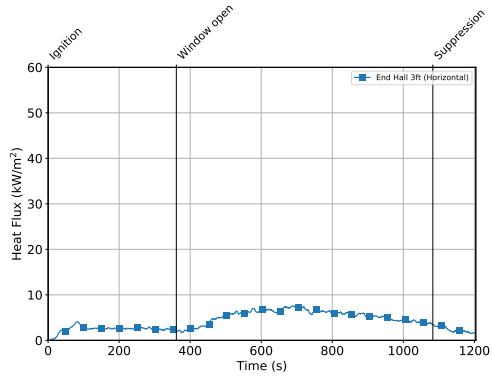


Figure B.106: Experiment 17 Hall Heat Flux

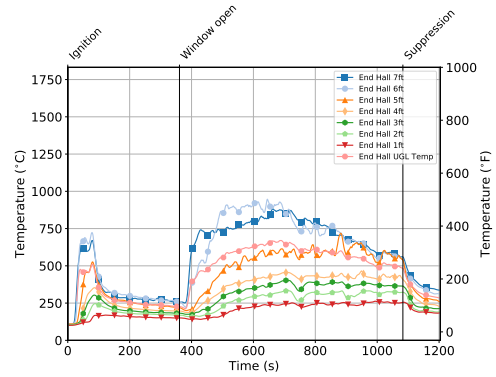


Figure B.107: Experiment 17 End Hall Temperature

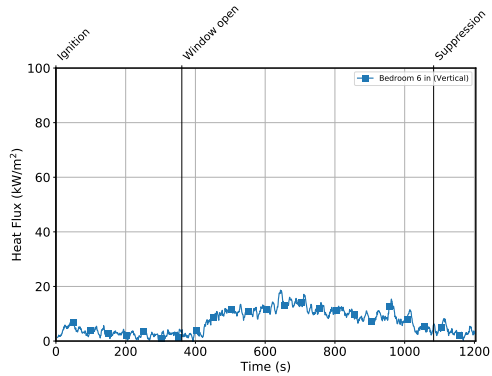


Figure B.108: Experiment 17 Bedroom Heat Flux

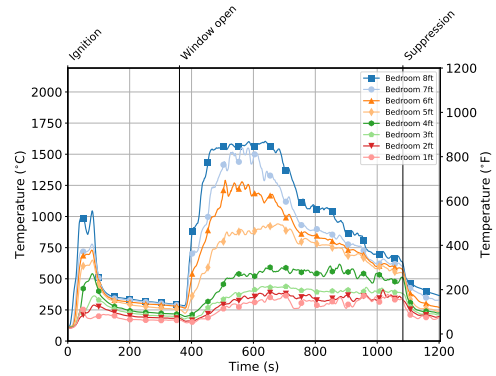


Figure B.109: Experiment 17 Bedroom Temperature

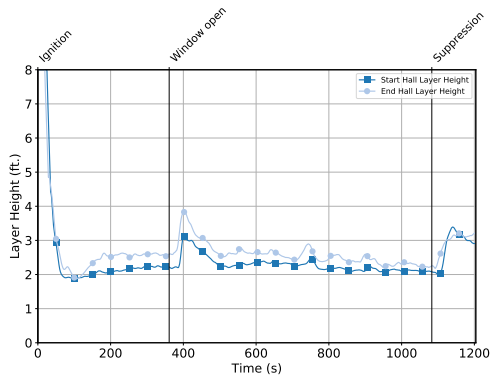


Figure B.110: Experiment 17 Layer Height

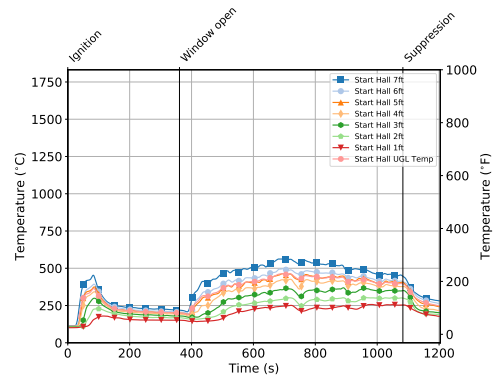


Figure B.111: Experiment 17 Start Hall Temperature

## B.18 Experiment 18 Results

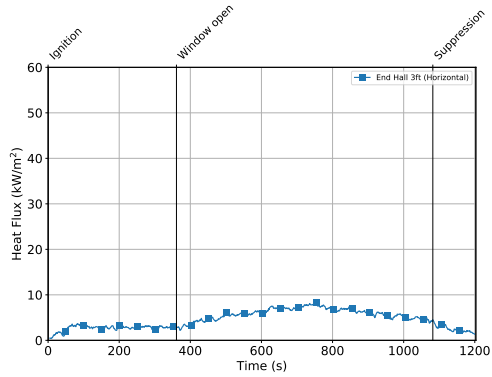


Figure B.112: Experiment 18  
Hall Heat Flux

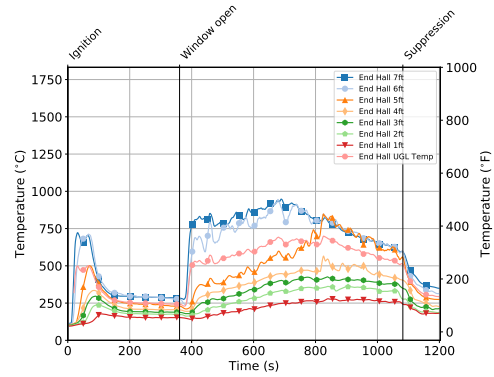


Figure B.113: Experiment 18  
End Hall Temperature

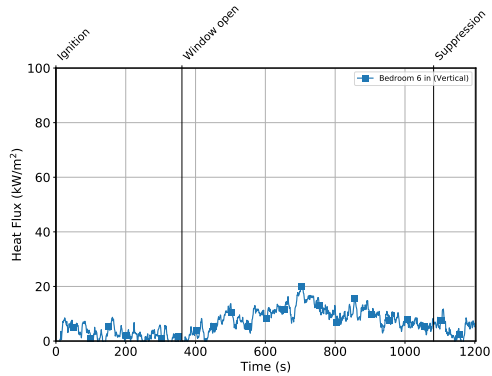


Figure B.114: Experiment 18  
Bedroom Heat Flux

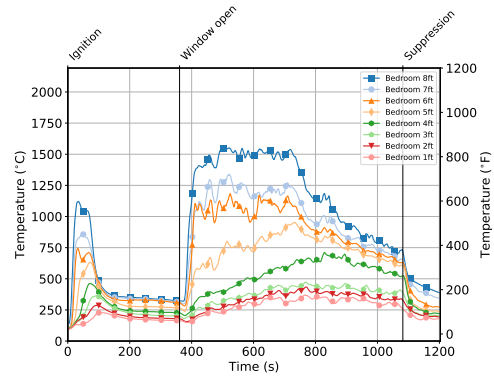


Figure B.115: Experiment 18  
Bedroom Temperature

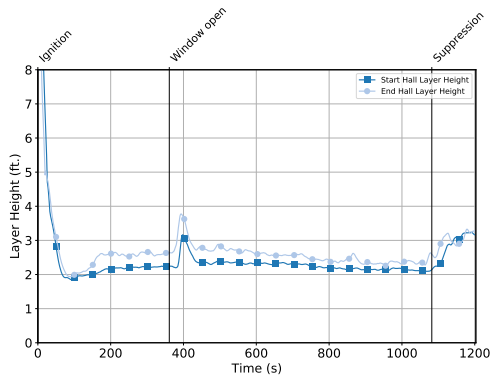


Figure B.116: Experiment 18  
Layer Height

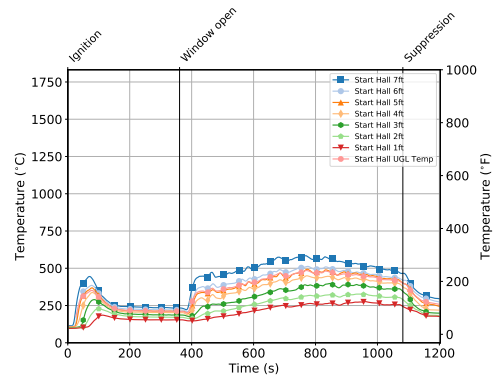


Figure B.117: Experiment 18  
Start Hall Temperature

## B.19 Experiment 19 Results

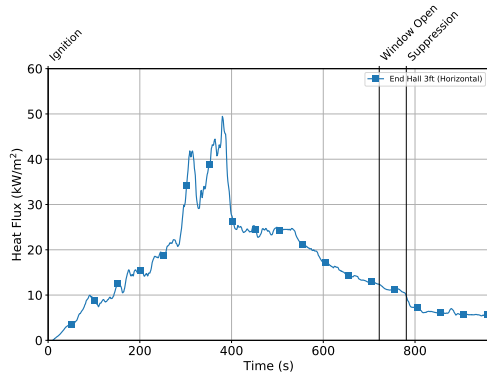


Figure B.118: Experiment 19  
Hall Heat Flux

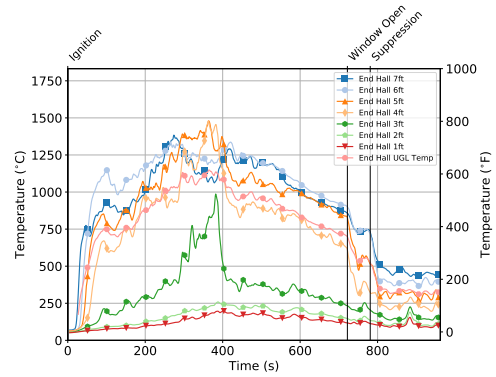


Figure B.119: Experiment 19  
End Hall Temperature

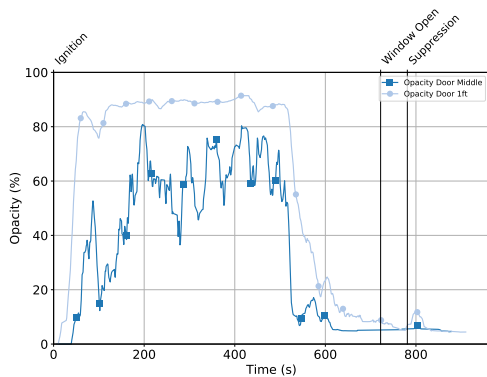


Figure B.120: Experiment 19  
Door Obscuration

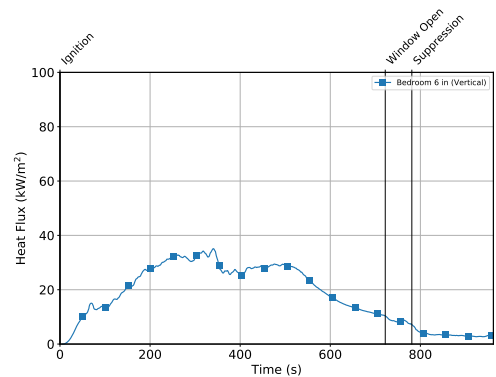


Figure B.121: Experiment 19  
Bedroom Heat Flux

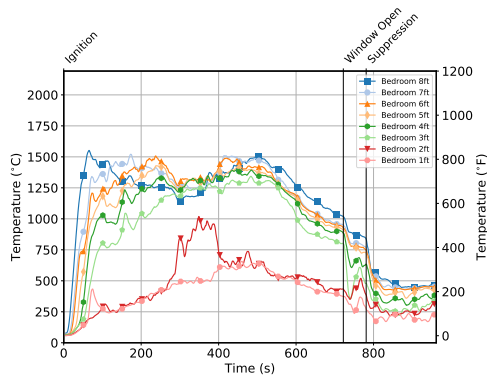


Figure B.122: Experiment 19  
Bedroom Temperature

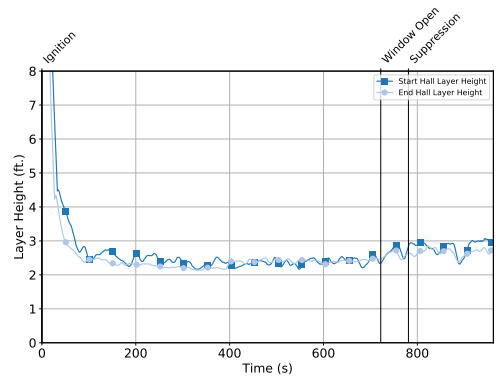


Figure B.123: Experiment 19  
Layer Height



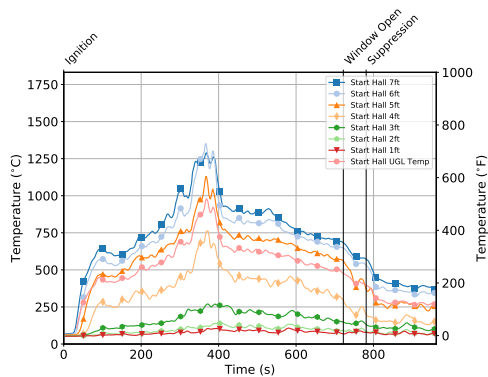


Figure B.124: Experiment 19  
Start Hall Temperature

## B.20 Experiment 20 Results

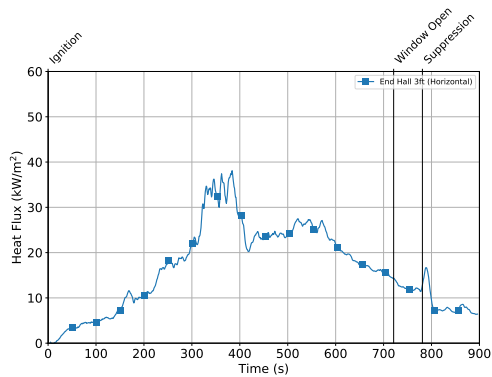


Figure B.125: Experiment 20  
Hall Heat Flux

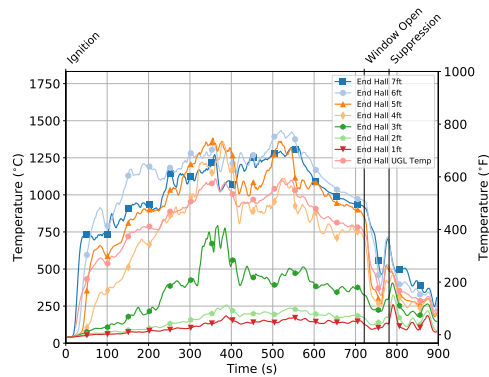


Figure B.126: Experiment 20  
End Hall Temperature

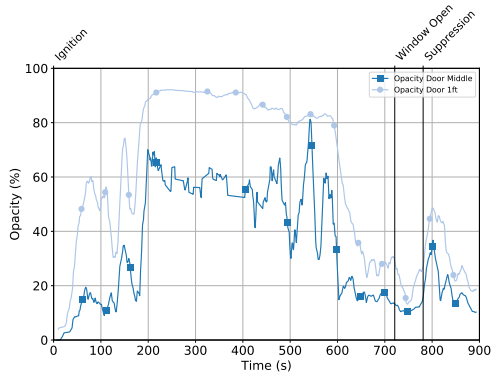


Figure B.127: Experiment 20  
Door Obscuration

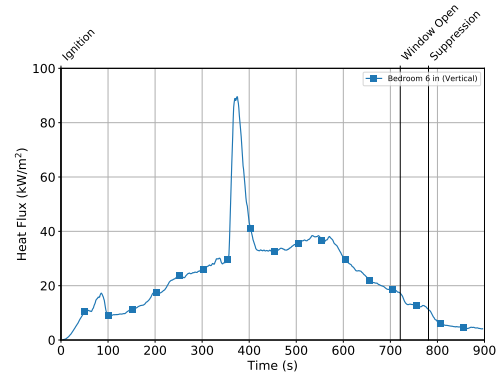


Figure B.128: Experiment 20  
Bedroom Heat Flux

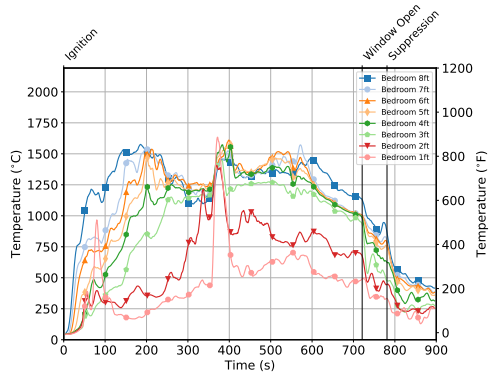


Figure B.129: Experiment 20  
Bedroom Temperature

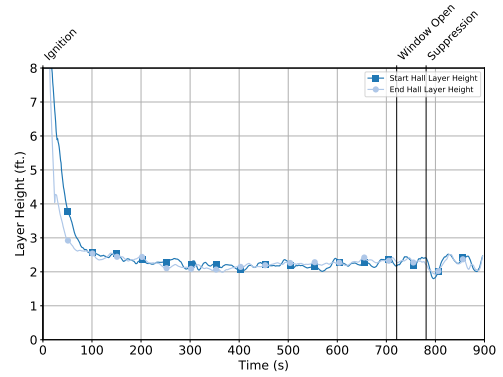


Figure B.130: Experiment 20  
Layer Height

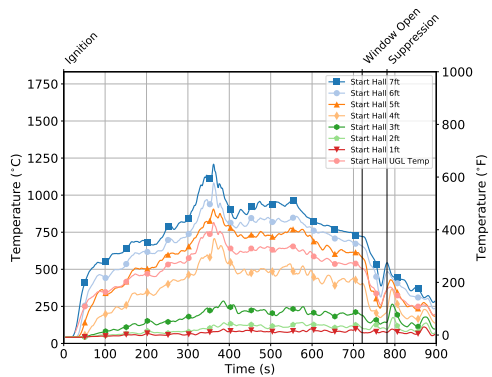


Figure B.131: Experiment 20  
Start Hall Temperature

## B.21 Experiment 21 Results

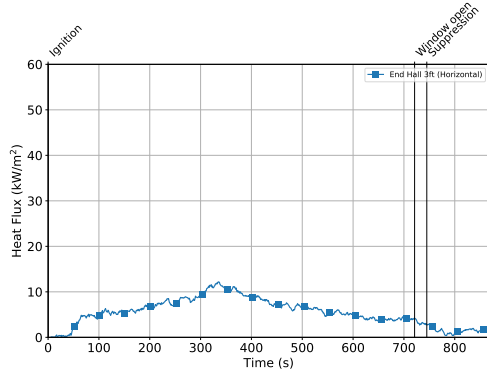


Figure B.132: Experiment 21  
Hall Heat Flux

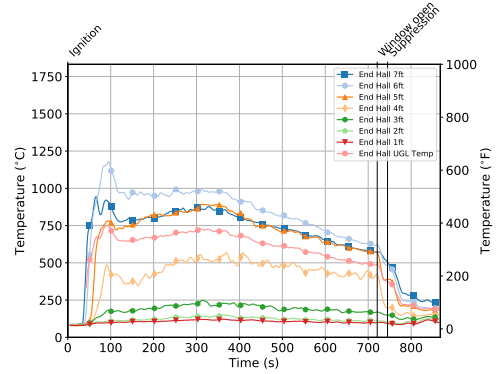


Figure B.133: Experiment 21  
End Hall Temperature

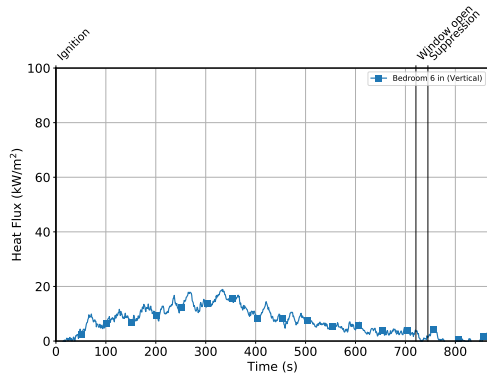


Figure B.134: Experiment 21  
Bedroom Heat Flux

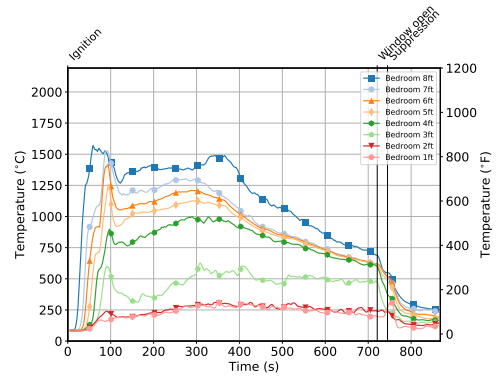


Figure B.135: Experiment 21  
Bedroom Temperature

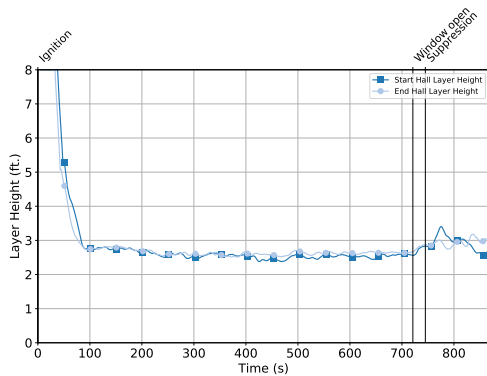


Figure B.136: Experiment 21  
Layer Height

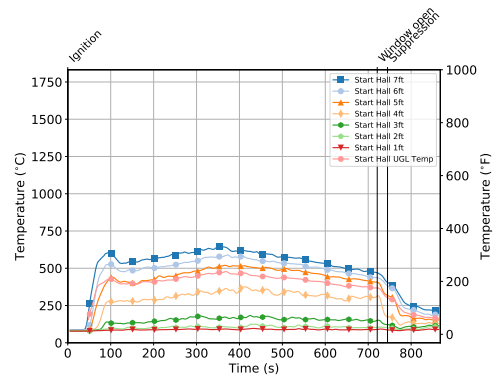


Figure B.137: Experiment 21  
Start Hall Temperature

## B.22 Experiment 22 Results

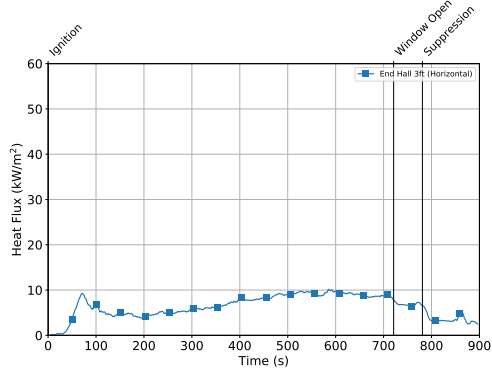


Figure B.138: Experiment 22  
Hall Heat Flux

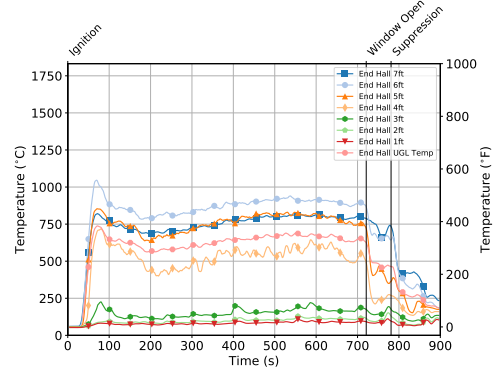


Figure B.139: Experiment 22  
End Hall Temperature

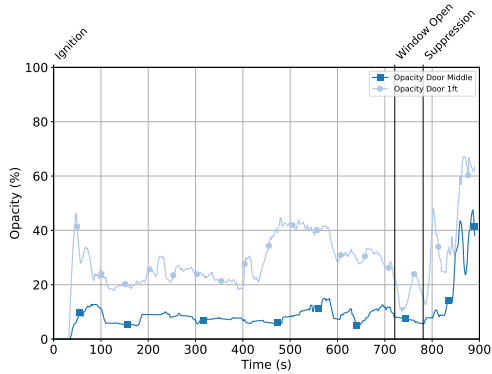


Figure B.140: Experiment 22  
Door Obscuration

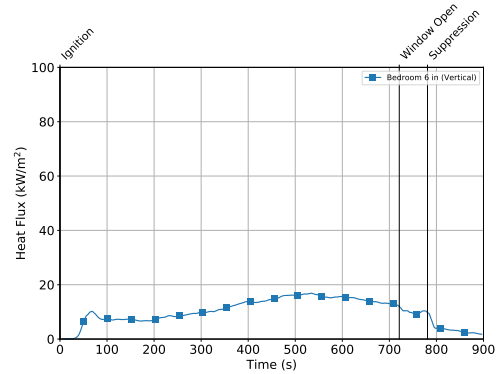


Figure B.141: Experiment 22  
Bedroom Heat Flux

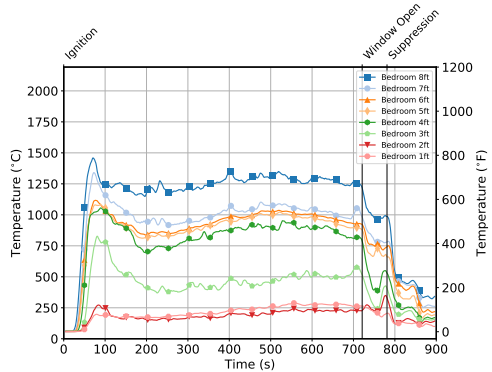


Figure B.142: Experiment 22  
Bedroom Temperature

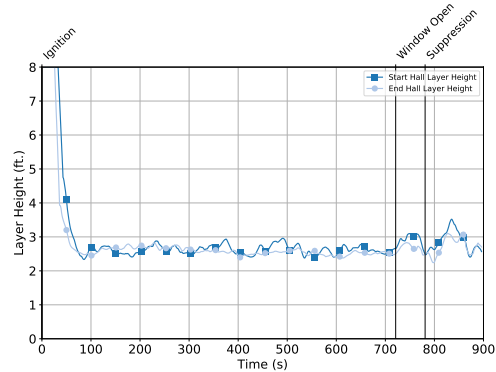


Figure B.143: Experiment 22  
Layer Height

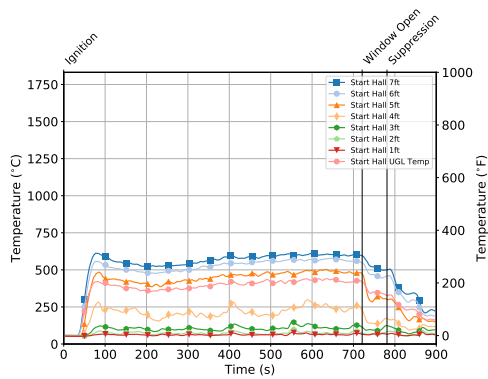


Figure B.144: Experiment 22  
Start Hall Temperature

## B.23 Experiment 23 Results

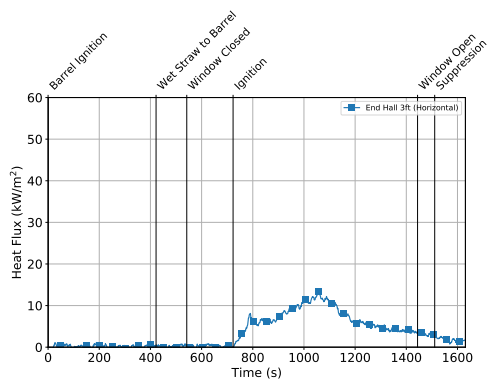


Figure B.145: Experiment 23  
Hall Heat Flux

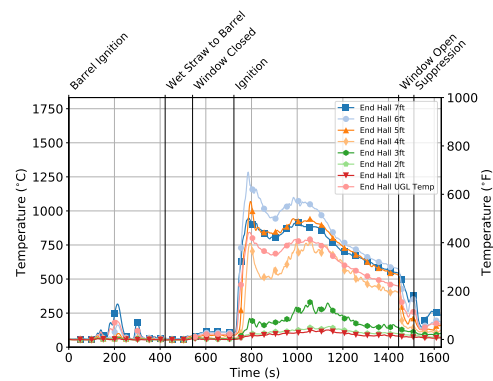


Figure B.146: Experiment 23  
End Hall Temperature

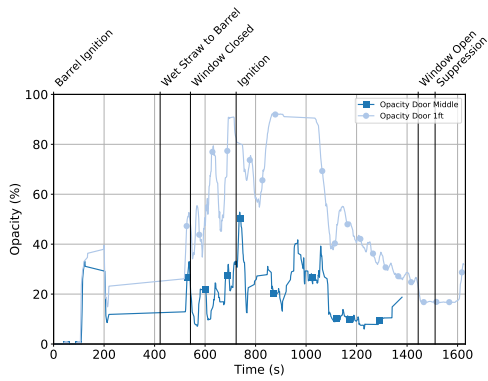


Figure B.147: Experiment 23  
Door Obscuration

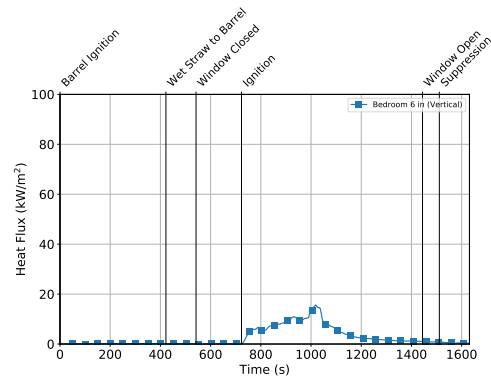


Figure B.148: Experiment 23  
Bedroom Heat Flux

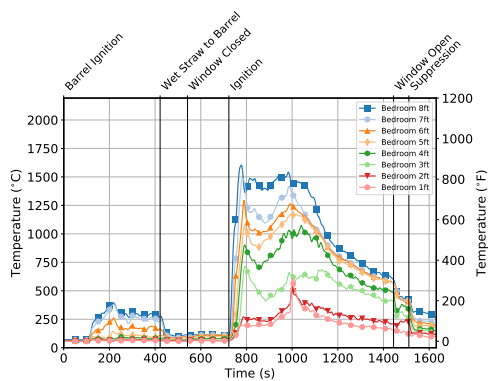


Figure B.149: Experiment 23  
Bedroom Temperature

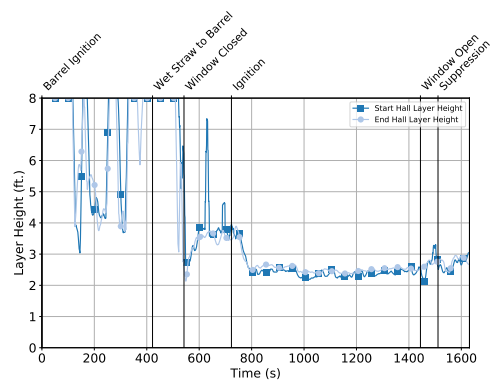


Figure B.150: Experiment 23  
Layer Height

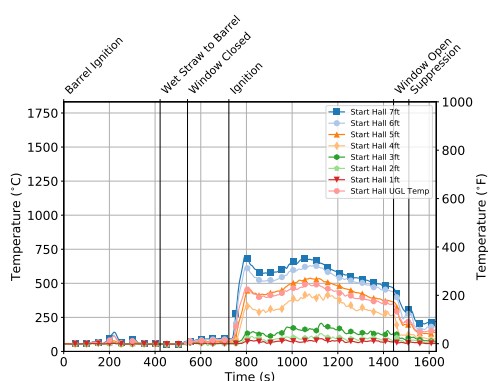


Figure B.151: Experiment 23  
Start Hall Temperature

## B.24 Experiment 24 Results

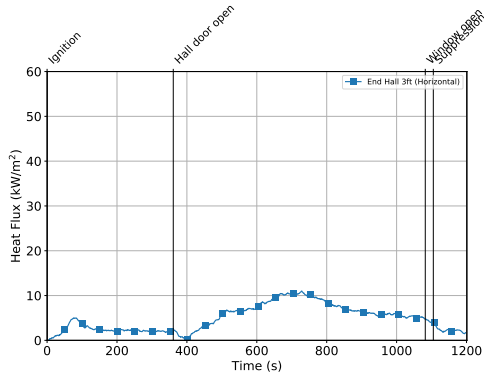


Figure B.152: Experiment 24 Hall Heat Flux

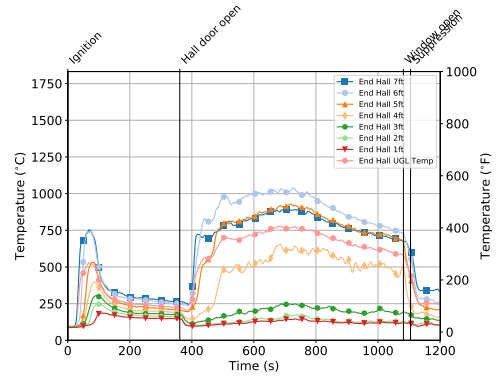


Figure B.153: Experiment 24 End Hall Temperature

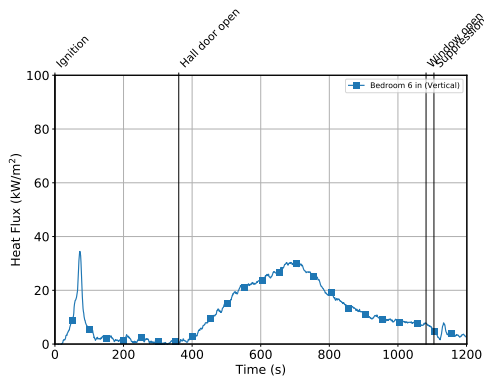


Figure B.154: Experiment 24 Bedroom Heat Flux

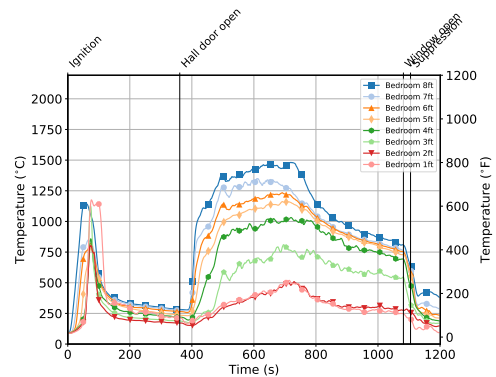


Figure B.155: Experiment 24 Bedroom Temperature

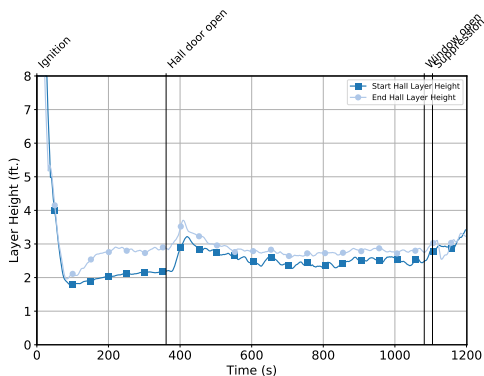


Figure B.156: Experiment 24 Layer Height

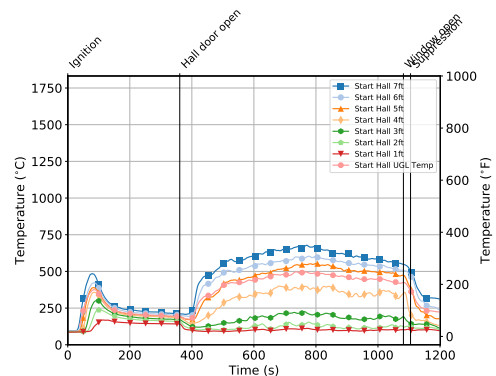


Figure B.157: Experiment 24 Start Hall Temperature

## B.25 Experiment 25 Results

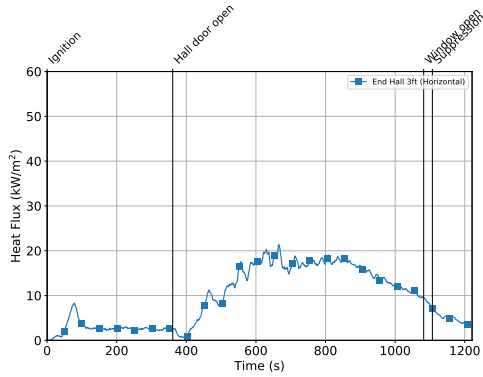


Figure B.158: Experiment 25  
Hall Heat Flux

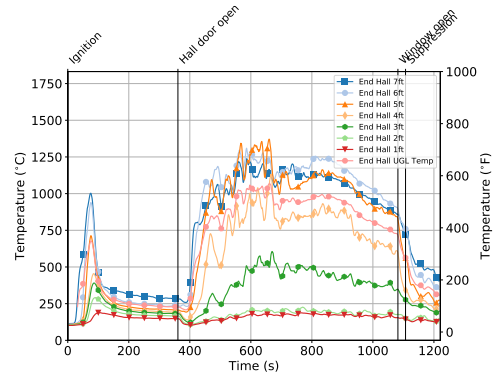


Figure B.159: Experiment 25  
End Hall Temperature

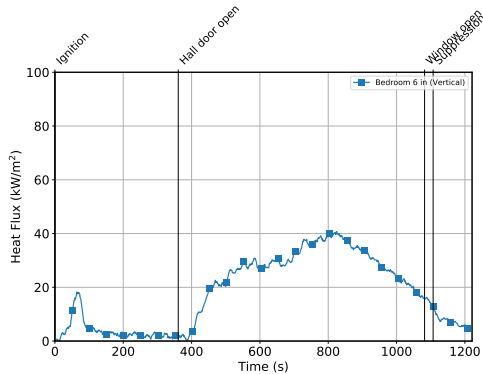


Figure B.160: Experiment 25  
Bedroom Heat Flux

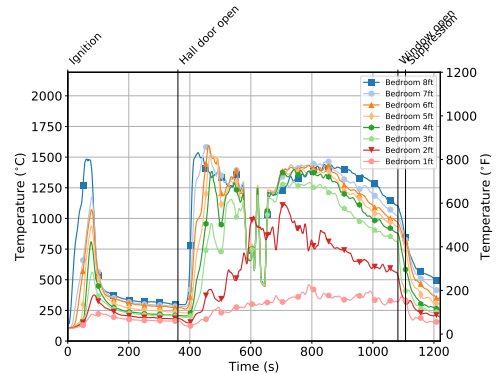


Figure B.161: Experiment 25  
Bedroom Temperature

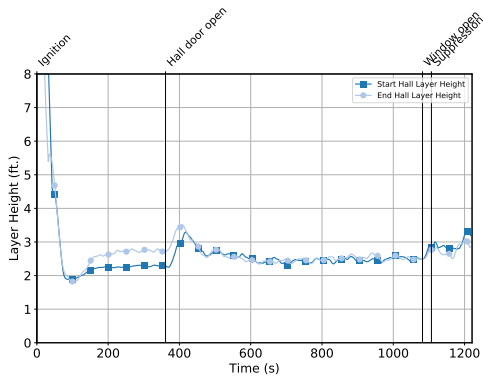


Figure B.162: Experiment 25  
Layer Height

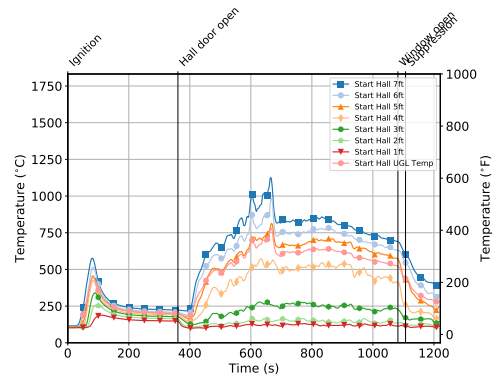


Figure B.163: Experiment 25  
Start Hall Temperature